Estimation and Control of Dynamical Systems with Unknown Inputs toward Renewable Sources

Joel Abraham Gonzalez Vieyra

N° d'ordre : 384

CENTRALE LILLE

THESE

Présentée en vue
d'obtenir le grade de

DOCTEUR

En

Automatique, Génie Informatique, Traitement du Signal et des Images

Par

Joel-Abraham GONZALEZ-VIEYRA

DOCTORAT DELIVRE PAR CENTRALE LILLE

Titre de la thèse :

Estimation et Contrôle des Systèmes Dynamiques à Entrées Inconnues et Energies Renouvelables

Estimation and Control of Dynamical Systems with Unknown Inputs toward Renewable Sources

Soutenue le 02 Décembre 2019 devant le jury d'examen :

Président	*Mme. Isabelle FANTONI, Directeur de Recherche, Ecole Centrale de Nantes*
Rapporteur	*M. Frédéric HAMELIN, Professeur, Université de Lorraine*
Rapporteur	*M. Noureddine MANAMANNI, Professeur, Université de Reims Champagne-Ardenne*
Examinateur	*M. Rochdi MERZOUKI, Professeur, Polytech Lille*
Examinateur	*M. Patrick DUPONT, Maître de conférences HDR, Ecole Centrale de Lille*
Invitée	*Mme. Geneviève DAUPHIN-TANGUY, Professeur, Ecole Centrale de Lille*
Directeur de thèse	*M. Christophe Sueur, Professeur, Ecole Centrale de Lille*

Thèse préparée au **Centre de Recherche en Informatique, Signal et Automatique de Lille**
CRIStAL CNRS UMR 9189

Ecole Doctorale Régionale SPI 072

Keywords: disturbance rejection, bond graph, derivative state feedback, unknown input observer, pole placement, structural approach, torsion-bar system, pelton turbine.

Mots clés : rejet de perturbations, bond graph, retour d'état dérivé, observateur à entrées inconnues, placement de pôles, approche structurelle, système de barre de torsion, turbine pelton.

"We lay down a fundamental principle of generalization by abstraction:
The existence of analogies between central features of various theories implies the existence of a general theory which underlies the particular theories and unifies them with respect to those central features..."

Eliakim Hastings Moore

"The ideals that have lighted my way, and time after time have given me new courage to face life cheerfully, have been Kindness, Beauty, and Truth."

Albert Einstein

Résumé

De nos jours, d'importants problèmes auxquels ont à faire face les industries et la société concernent la réduction des gaz à effet de serre, ainsi que le problème de consommation d'énergie (énergie fossile, fabrication de produits, etc.), et la recherche d'énergies renouvelables. Actuellement, chez les industriels ou laboratoires de recherche, les études pour la commande de systèmes à énergie renouvelable deviennent très pertinentes. Dans la plupart de ces systèmes, des phénomènes de perturbation sont présents. Ils diminuent l'efficacité, la qualité de service ou réduisent même la durée de vie des processus. Les lois de commandes doivent prendre en compte la nécessité d'améliorer les performances des nouveaux composants, machines ou systèmes complexes tels que les systèmes à énergie renouvelable.

Notre travail a pour objectif d'améliorer l'efficacité des processus dans la production et/ou consommation d'énergie en analysant l'influence des perturbations (ou influences équivalentes) sur le comportement du système complet en concevant un contrôleur/observateur efficace, ceci dans une démarche de conception intégrée. Nous utilisons une démarche physique basée sur la représentation bond graph. Nous parlons de Rejet de Perturbation (atténuation) à l'aide d'un Observateur à Entrée Inconnue. Des développements théoriques sont proposés et appliqués sur un système réel de type Barre de Torsion, qui est le cas d'étude tout au long du travail de recherche. Dans un même temps, nous comparons notre approche avec d'autres approches dites "approches modernes" pour le rejet de perturbation dans la littérature scientifique. Nous proposons aussi dans un même esprit une solution alternative au problème d'estimation à entrée inconnue. L'étude est limitée aux systèmes linéaires.

L'expression "rejet de perturbation" utilisée dans le contexte classique de la théorie de la commande fait référence à comment les perturbations externes sont atténuées et se propagent dans le processus, en affectant éventuellement les grandeurs de sortie. La mesure concerne l'amplitude des réponses fréquentielles représentant les relations perturbation-sortie. De cette manière, le terme "rejet" est synonyme d'atténuation ou compensation, et la mesure s'exprime par un pourcentage d'atténuation. L'association des deux termes "rejet" et "perturbation" veut dire littéralement aucune interruption.

Pour la plupart des systèmes pilotés, il est difficile de choisir/trouver un modèle mathématique précis permettant de décrire fidèlement le comportement. De plus, de nombreux paramètres ne sont pas connus explicitement dans les équations mathématiques. De la même manière, des

phénomènes internes ou externes tels que les perturbations liées à l'environnement existent. C'est probablement la raison pour laquelle en pratique, la commande de type PID est exploitée de manière intensive dans l'industrie, car la commande par PID ne nécessite que très peu la connaissance d'un modèle.

Dans l'industrie, l'objectif principal est en général d'atteindre un régime permanent, souvent fixé et indépendant des perturbations, ceci pendant de longues périodes. Deux techniques sont souvent mises en œuvre, à savoir essayer de limiter l'amplitude de la perturbation ou alors son effet, et dans le meilleur des cas "la rejeter". Dans le premier cas, la commande est synthétisée de manière à être "tolérante" aux perturbations. Nous parlons en général de commande robuste. La commande permet de fonctionner en situation normale et si des perturbations apparaissent, la performance de la commande doit être suffisante pour que le processus continue à respecter le cahier des charges. De nombreux travaux existent sur ce sujet dans la littérature scientifique et ne seront pas traités dans ce travail.

La commande prédictive permet aussi d'éliminer l'effet des perturbations sous certaines conditions : 1) la perturbation peut être mesurée, 2) son effet sur le processus peut être évaluée, dans ce cas un modèle précis doit être élaboré, 3) les variables de commande peuvent générer l'effet opposé sur les variables de perturbation. La dernière condition est très restrictive et exige en général de trouver un modèle inverse. A l'aide d'une connaissance partielle de la perturbation ou du modèle, il est possible de trouver une contre réaction partielle.

Pour d'autres approches, la perturbation est mesurée directement ou indirectement par estimation en mesurant ses effets sur le processus. Dans ces cas, l'effet de la perturbation peut être totalement ou en partie éliminé. Nous étudions deux approches dans cette thèse. Dans un premier temps, la méthode dite DOBC (Disturbance Observed-Based Control) pouvant être appliquée dans diverses situations (systèmes non linéaires, régulation tolérante aux fautes...) et une seconde technique dite ARDC (Active Disturbance Rejection Control). Ces techniques de commande dites "modernes" se basent sur une estimation des variables de perturbation. Elles sont comparées dans le chapitre trois de cette thèse à une technique développée pour ce travail basée sur une commande par retour d'état dérivé.

Le second sujet d'étude dans ce travail de recherche concerne le concept "d'Observateur à Entrée Inconnue". Comme évoqué précédemment, dans de nombreuses situations l'expression de la loi de commande peut faire apparaitre explicitement les variables de perturbation. Dans ce cas, ces variables doivent être au minimum estimées. Pour les modèles linéaires, de nombreuses techniques constructives existent. Elles concernent des observateurs d'ordre réduit ou complet. Les approches sont de type algébrique, géométrique ou basées sur des matrices à inverse généralisée. La connaissance de la structure à l'infini du modèle est alors nécessaire et une condition restrictive appelée "Observer Matching condition" s'applique pour certaines techniques. Si cette condition n'est pas respectée, différentes alternatives existent, comme la technique d'observateur à modes glissants, qui peut aussi être étendue aux modèles non linéaires.

Plusieurs de ces approches sont comparées dans le chapitre 2, avec de nouveaux développements basés sur l'estimation des variables d'état dérivées et des variables de perturbation. Les chapitres 3 et 4 sont dédiés à l'évaluation du concept de variable d'état dérivée pour la commande et l'observation avec une application réelle de type barre de torsion. Une comparaison est faite entre les trois approches étudiées dont les techniques DOBC et ADRC.

Notre recherche est décomposée de la manière suivante :

- Chapitre 1 : Historique sur le problème du rejet de perturbation et analyse de quelques techniques classiques, i.e la technique de type PID, commande par retour d'état et par retour d'état dérivé. Nous incluons quelques éléments théoriques pour l'analyse de la structure des modèles linéaires (structure finie et structure à l'infini). Le système de barre de torsion est décrit et son modèle bond graph est validé par expérimentation. La commande par retour d'état dérivé pour le rejet de perturbation est aussi validée.

- Chapitre 2 : Ce chapitre a pour premier objectif de comparer différents types d'observateurs à entrée inconnue. Ces différents observateurs sont testés sur le système de barre de torsion. Nous proposons de nouvelles solutions dans le cas multivariable, avec une approche semblable dans sa conception à celle développée pour le problème de commande par rejet de perturbation. En effet, les techniques d'analyse structurelle et de synthèse basées sur la représentation bond graph permettent de proposer une base théorique similaire. C'est une contribution théorique de ce travail de thèse.

- Chapitre 3 : Dans ce chapitre, nous comparons par simulation les performances de trois techniques de commande pour le rejet de perturbation (DOBC, ADRC, DSF) sur l'exemple de barre de torsion. Nous prouvons l'efficacité de la technique basée sur le retour d'état dérivé avec estimation de la perturbation, d'un point de vue méthodologique, de l'analyse structurelle à la synthèse de la loi de commande, mais aussi d'un point de vue performance, efficacité à rejeter à perturbation. Étant donné les similarités de la résolution des problèmes de rejet de perturbation et du problème de découplage entrée-sortie, nous en profitons pour proposer une solution au problème de découplage entrée-sortie avec une commande de type retour d'état dérivé. C'est la deuxième contribution théorique de ce travail.

- Chapitre 4 : Finalement nous testons la loi de commande par retour d'état dérivé sur la maquette barre de torsion et comparons les performances aux deux autres techniques, i.e, DOBC et ADRC.

- Chaptitre 5 : Dans ce dernier chapitre, sachant que l'objectif affiché est d'améliorer les performances des systèmes industriels, nous développons un modèle très simplifié d'une centrale hydraulique avec objectif d'appliquer les techniques de commande développées. Après une brève discussion sur les énergies renouvelables, un modèle bond graph simplifié d'un système hydroélectrique est proposé à partir d'un "mot bond-graph" représentant les échanges de puissances entre les différents constituants du système (approche intégrée). Les premières simulations permettent de valider le modèle simplifié en première approximation.

Acknowledgements

First and foremost, I offer my most sincere gratitude to my supervisor, Mr. Christophe Sueur for his support, guidance and patience. I'm really thankful to him for the motivation and confidence in all the aspects related to this research.

I'm very grateful with the jury members, Mme. Geneviève Dauphin-Tanguy, M. Patrick Dupont, Rochdi Merzouki, Mme. Isabelle Fantoni, M. Noureddine Manamanni, M. Fédéric Hamelin. For their time, suggestions and recommendations to improve this thesis.

I would like to thank Bénédicte Fievet, Dominique Deremetz, Martine Mouvaux, Christine Yvoz, Thi Nguyen, Malika Debuysschere, Vanessa Fleury, Brigitte Foncez and others who helped us with the administrative matters.

My gratitude goes to my professors who showed me the French language and culture. My knowledge and interest in the French culture is inspired by their work and talks, they taught me traditions, art, history, food, etc.

I am also grateful to all my partners and dear friends who made this journey different and it would not have been the same without them. To mention a few: Gerardo, Noe, Triolo, Joëlle, Adel, Mahdi, Mohamed, Marlyn, Nicolas, Jaime, Elvira, Cynthia, Claudia, Romain, Andreina, Carla, Monica, Paola, Jeremy, Cesar, Anilu, Valentin, Binh, Wei, David, Houria, Ibrahim, Quentin, Nouha, The Gordos, and many others. I would like to thank them all their time, company, support, advices, help, etc.

My PhD studies were supported by the cooperation between the CONACyT and the SENER that bring me the financial support. So, I would like to thank all of the people who have built this relationship and contributed to select candidates for interesting research projects. I am extremely grateful to CONACyT-SENER who financed me.

In the end, I convey special acknowledgement to my whole family, my parents, Joel, Silvia, my sisters and especially to my lovely wife Marlene and my handsome son Zeruel Sesshōmaru for their love, patience, effort, sacrifice, bravery, etc.

Villeneuve D'Ascq, France
11th December, 2019

GONZALEZ-VIEYRA Joel-Abraham

List of Abbreviations

A | **B** | **D** | **E** | **F** | **H** | **I** | **L** | **M** | **P** | **R** | **S** | **T** | **U**

A

ADRC Active Disturbance Rejection Control. xvi, xvii, 2–4, 58, 61, 62, 77, 78, 88, 99–101

B

BG Bond Graph. xvi, xvii, xix, xxii, 1, 3, 7, 8, 14, 19, 30, 35, 42, 48, 49, 51–53, 58, 62, 63, 72, 75, 77, 78, 83, 88, 91, 92, 94, 96, 98, 100–102, 104, 106, 108, 140, 147
BGD Bond Graph model with Derivative causality. xxi, xxii, 28, 37, 51, 72, 73, 83, 86, 87, 89, 140
BGI Bond Graph model with Integral causality. xxi, xxii, 25, 64, 74, 86, 92, 103, 140

D

DC Direct Current. 18, 113, 116
DOBC Disturbance Observed-Based Control. xvi, xvii, xxii, 2–4, 58–60, 65, 77, 78, 88, 97
DR Disturbance Rejection. xv, xvii, xxii, 1, 11, 15, 16, 25, 26, 30, 48, 57, 58, 63, 75, 77, 78, 91, 92, 94, 96, 98, 100–102, 104, 106, 108, 147
DRP Disturbance Rejection Problem. 1, 4, 7, 8, 15–17, 30, 31, 57, 58, 72, 88, 89
DSF Derivative State Feedback. xv–xvii, xxi, xxii, 3, 4, 7, 14–17, 25, 28–30, 58, 62, 63, 72, 74, 75, 77–83, 85, 87–89, 91, 92, 94, 96, 98, 100–104, 106–108, 147

E

e.g. exempli gratia. 7, 78, 94, 119
ESO Extended State Observer. 61, 99

F

FDI Fault Detection Isolation. 32, 47

H

HIL Hardware-in-the-loop. xxii, 94, 95

I

i.e. id est. 3, 4, 11, 14, 16, 17, 74, 80, 82, 91, 103, 119, 144

L

LFT Linear Fractional Transformations. 47
LTI Linear Time-Invariant. 3, 32, 35, 140

M

MIMO Multiple Input - Multiple Output. xvi, xvii, 4, 14, 48, 49, 51, 52, 72, 84, 87, 101, 119, 144, 145

P

PI Proportional-Integral. xvi, xxi, 7, 10, 14, 26, 32, 33, 42
PID Proportional-Integral-Derivative. xvi, xvii, 2, 4, 7, 10, 11, 26, 61, 94
PWM Pulse-Width Modulation. 93

R

RSSF Regular Static State Feedback. xvi, 78, 79, 82

S

SISO Single Input - Single Output. xvi, xix, 13, 14, 26, 31, 35–40, 49, 50, 53, 72, 80, 82, 84, 86, 101, 143
SSF Static State Feedback. xv, 7, 11, 13, 17, 25, 26, 48, 58, 83, 88

T

T-B Torsion-Bar. xv, xxi, cl, 1, 3, 7, 17–21, 25, 27, 29, 30, 32, 37, 47, 52, 58, 61, 63, 73, 74, 78, 83, 88, 89, 91, 94, 99, 101, 103

U

UIO Unknown Input Observer. xvi, xvii, xix, xxii, 1, 3, 4, 10, 17, 25, 30–32, 34–36, 38–40, 42, 44, 46, 48–56, 58, 62, 63, 72–75, 77, 78, 88, 91, 92, 94, 96, 98, 100–104, 106–108, 141, 147

Table of Contents

List of Tables

List of Figures

General Introduction

Nowadays, some of the important problems that industries and the society prioritise are more related to the reduction of the greenhouse gas emission that are related to the consumption of energy (fossil fuels, manufacture and fabrication of products, etc.), and the research of renewable sources. Actually, in the industry or research laboratories, studies for controlling renewal energy systems become relevant. In most of these systems, different perturbations are present. They decrease the efficiency, quality of service, or reduce the life span (duration). New controls have been studied or modified to satisfy the necessities of performance for the new devices, machinery, or complex systems such as renewal systems.

Due to the physical approach used in this thesis (Bond Graph Modelling), our work aims to improve the efficiency (or energy expenditure) of the associated processes in the energy production (consumption) by means of analysing influence of the disturbances (or equivalent influences) on the behaviour of the whole system by designing efficient control/observer in an integrated approach. We will speak of Disturbance Rejection (DR) (attenuation) with the aid of Unknown Input Observer (UIO). Some theoretical developments are proposed and applied to a real Torsion-Bar (T-B) system that is the case study all along this report. At the same time, we compare the proposed approach with so-called some modern approaches for the Disturbance Rejection Problem (DRP) and in the same way we study some observers and we propose some alternative solutions. The study is limited to linear systems (models).

Most of the dynamical systems developed in real life are affected by disturbances. The disturbance is defined by the Oxford English Dictionary (OED) as *"The interruption of a settled and peaceful condition"*. If engineering is understood as the process of creating an apparatus to serve the human needs, the "settled and peaceful condition" of such an apparatus is the primary concern and the subject of study in the field of automatic control, [Gao, 2014].

The term "disturbance rejection" used in the context of classical and modern control theory refers to how the external disturbance is attenuated as it is propagated through the process, eventually affecting the output. It is measured as the magnitude of the frequency response that defines the disturbance–output relationship. It is specified, usually, in terms of the amount of attenuation and the corresponding frequency range required. Used in such a manner, "rejection" is synonymous to attenuation, or mitigation, or compensation. Shaping system response, in frequency domain, to external disturbances is what it really means by "disturbance rejection" in the current textbooks on control.

The word “reject” comes from Latin, meaning “throw back”, and it has a derivative, rejector. The word “reject” projects a sense of totality and finality, regarding the object of concern. Putting the two words together “disturbance rejection” should, and therefore does from now on, means literally “no” interruptions, whatsoever, of “a peaceful and settled condition”. If, the problem of automatic control is the problem of disturbance, then disturbance rejection is absolutely central. In an ideal control system, the disturbance, the sum total of the internal dynamics and the external forces, should have absolutely no effect on the operation of the system as designed [Gao, 2014].

In most control applications, it is difficult to establish *precise mathematical models* to describe accurately systems. In addition, there are some terms that are not explicitly known in mathematical equations and, on the other hand, some unknown external (or internal) disturbances exist around (inside) the system environment. The uncertainty, which includes internal uncertainties and external disturbances, is ubiquitous in practical control systems. This is perhaps the main reason why the Proportional-Integral-Derivative (PID) control approach has dominated the control industry for almost a century because PID control does not utilize any mathematical model for system control [Guo and Zhao, 2016].

In process industries, more than set-point tracking disturbance rejection is the principal goal, as most industrial processes operate with a fixed set-point during long periods of time, but they are subject to disturbances coming from the outside world or generated by the process model uncertainties. When considering any of these disturbances, two approaches are mainly taken: to bound the disturbance magnitude or to try to reduce its effect and, in the best case, reject it. In the first approach, the control is designed to be tolerant to these disturbances. It is generally known as robust control [Morari and Manfred, 1989]. The control is computed to operate under “normal” conditions and if some bounded disturbances appear in the process the resulting performance of the controlled plant should be good enough, according to the requirements. A lot of literature has been devoted to this topic and it will not be considered for the actual research work.

Feed-forward is also a classical approach to counteract the effect of external disturbances if some conditions apply: 1) the disturbance can be measured, 2) its effect on the plant can be estimated, that is, there is a perfect model of the disturbance dynamics and also of its effect on the controlled variables, and 3) the control variables can generate the opposite effect on these variables. The last condition is very restrictive, as it implies in most cases the inversion of the disturbance effect model. Approximate disturbance counteraction can be achieved if a partial knowledge of this model is available (for instance, the steady-state behaviour), or if the control action is bounded.

In another approach, some information about the actual disturbance is collected either directly, by measuring the disturbance, or indirectly, by estimating it looking at its effects on the plant. In this case, the disturbance is counteracted, and its effects can be reduced and, in some cases, fully eliminated. We study two approaches in this thesis. First, the Disturbance Observed-Based Control (DOBC) [Visioli and Zhong, 2011] which is applied to non-linear systems [Chen, 2004], or a fault tolerant tracking control [Baldini et al., 2018] and other applications [Tang et al., 2018]. An overview is in [Chen et al., 2016]. Secondly, the Active Disturbance Rejection Control (ADRC) [Han, 2009] with works on non-linear systems [Guo et al., 2016, Zhao and Guo, 2016, Xue et al., 2015] or real applications [Wang et al., 2018, Cui et al., 2018, Wang et al., 2017, Albertos et al., 2015]. These so-called new modern approaches based on the

estimation of the state variables and on estimation of the disturbance variables are compared in chapter 3, with new developments based on the Bond Graph (BG)bond graph representation with a Derivative State Feedback (DSF) control. Since we prove the effectiveness of this approach with simulations, we propose also in this chapter the application of Derivative State Feedback control for solving the Input-Output decoupling problem from a theoretical framework.

Actually, there are also many other methods in control theory that work in disturbance rejection control. Principles are different that the mentioned before; some of them are for instance: adaptive control [Nikiforuk and Tamura, 1988], sliding-mode control [Riachy and Fliess, 2011], [Guo and Jin, 2013], control based on Conditional Integrators [Seshagiri and Khalil, 2005], [Singh and Khalil, 2005], [Burger, 2011], etc. Due to the huge quantity of references, we will not recall all the works.

The second subject of this research work is about the concept of Unknown Input Observer. In the context of the Disturbance Rejection Problem, in many cases the control law is expressed as a function of the disturbance variable, and thus this one must be at least estimated. For LTI models, constructive solutions with reduced order observers are first proposed with the geometric approach [Guidorzi and Marro, 1971, Bhattacharyya, 1978, Basile and Marro, 1973]. Constructive solutions based on generalized inverse matrices are given in [Kudva et al., 1980, Miller and Mukunden, 1982, Hou and Muller, 1992]. Full order observers are then proposed in a similar way (based on generalized inverse matrices) in [Darouach et al., 1994, Darouach, 2009], but with some restriction on the infinite structure of the model, known as *Observer Matching condition*, which is a rather restrictive condition. When the previous conditions are not satisfied, [Floquet and Barbot, 2006] proposed unknown input sliding mode observers after implementing a procedure to get a canonical observable form of the model. This method can also be extended in the non-linear case.

The algebraic approach is proposed in [Trentelman et al., 2001] and in [Daafouz et al., 2006] for continuous and discrete time systems, without restriction on the infinite structure of the model. Sliding mode observers combined with a High-Gain approach are often proposed [Kalsi et al., 2010]. New developments are also proposed with an observer-based approach for some classes of non-linear systems with a fuzzy approach [Xu et al., 2012], fuzzy systems with time delays [Tong and Yang, 2011] or with uncertain systems [Chen et al., 2011].

Some of these approaches are compared in chapter 2, with new developments based on the Bond Graph representation with a *Derivative State Estimation* associated to the estimation of the disturbance variable.

Chapters 3 and 4 are thus dedicated to the evaluation of the use of the concept of derivative state at the same time for control and estimation with simulations in chapter 3 and real application on the Torsion-Bar system in chapter 4. A comparison is carried out with two other approaches, *i.e.* DOBC and ADRC approaches.

Thesis Layout and Summary of Thesis

This document aims to present the research in a structure in order to locate relevant information. The research is presented as follows:

- Chapter 1: Background about the Disturbance Rejection Problem that clarifies some classical existing approaches, *i.e.* PID, state space and derivative state space controls are presented. We include some theoretical bases about model properties (finite and infinite structure) and the description of the case study (Torsion-Bar System) and the validation of our Bond Graph model. The Derivative State Feedback control law is also validated.

- Chapter 2: This chapter aims firstly to compare different observers, for disturbance variables and state variables estimation. The different observers are tested on the model of the Torsion Bar system. Secondly, we propose new solutions for the UIO observer in the linear Multiple Input - Multiple Output (MIMO) case. A theoretical framework close to the one used for the Disturbance Rejection Problem is developed, from analysis to synthesis, based on the structural properties of the bond graph model. It is one of the main theoretical contributions of the thesis.

- Chapter 3: In this chapter, we firstly compare from a numerical point of view (simulations) the performances of three approaches (DOBC, ADRC, DSF) for the Disturbance Rejection Problem on the model of the Torsion-Bar system. We prove the efficiency of the Derivative State Feedback control law and the methodology from analysis to synthesis in order to obtain the control law. Due to the similarity to the state-space approach for solving simultaneously two classical problems, *i.e.* Disturbance Rejection and Input-Output decoupling problems, we take the opportunity to propose a solution for the Input-Output Decoupling Problem based on a Derivative State Feedback control law. It is the second theoretical contribution of our work.

- Chapter 4: Finally, we aim to prove that the Derivative State Feedback control strategy is effective, with a physical approach especially, by applying it from a practical point of view on the real Torsion-Bar system. Results are analysed and compared with the two others control strategies (DOBC and ADRC).

- Chapter 5: In this last chapter, since we claimed before that this work aims to develop solutions for improving the efficiency of industrial plants, we develop a very simplified model of an industrial hydraulic power plant in order to apply the previous concepts. First a brief discussion about renewable power technologies is proposed, information obtained from recent literature which is not exhaustive. A Word Bond Graph model is then drawn following the power exchange between the different elements of the system (integrated approach). With a detailed bond graph model, some simulations are issued in order to validate with a first approximation the model and our assumptions.

Contributions of the Thesis

The results obtained during the development of this work have been the subject of following publications:

Journals

- *Unknown Input Observer with Stability: A Structural Analysis Approach in Bond Graph*. European Journal of Control, ELSEVIER (Published). [Gonzalez and Sueur, 2018b]
- *Disturbance Rejection with Derivative State Feedback Theory and application*. Advanced Engineering Informations, ELSEVIER (Submitted).
- *Input-output decoupling with derivative state feedback: a bond graph approach*. Advances in Mechanical Engineering, SAGE (Submitted).

International conferences

- *Unknown Input Observer for MIMO Systems with Stability*. International Conference on "Integrated Modeling and Analysis in Applied Control and Automation" (IMAACA), 2017, International Conference part of the I3M conference, September, Barcelona, Spain. (Accepted). [Gonzalez and Sueur, 2017]
- *Comparison of control strategies for a real bar system in the presence of disturbances: a bond graph approach*. ICBGM'18 International Conference on Bond Graph Modeling, July, Bordeaux, France. (Accepted). [Gonzalez et al., 2018]
- *Bond Graph Approach for Disturbance Rejection with Derivative State Feedback*. IMAACA'18, International Conference part of the I3M conference, September, Budapest, Hungary. (Accepted). [Gonzalez and Sueur, 2018a]
- *Comparison of Disturbance Rejection with Derivative State Feedback and Active Disturbance Rejection Control: Case Study*. International Conference on Control, Decision and Information Technologies (CODIT), 2019, April, Paris, France. (Accepted). [Gonzalez, Joel and Sueur, Christophe, 2019]
- *Approach of dynamic modelling of a hydraulic System*. International Conference. Which models for extreme situations and crisis management? SimHydro, 2019, June, Nice, France. (Accepted). [Ratolojanahary et al., 2019]

Chapter 1

Disturbance Rejection Problem

1.1 Introduction

In this chapter, the Disturbance Rejection Problem (DRP) will be recalled from different approaches, and a comparison between these approaches is carried out on a real Torsion-Bar (T-B) system, whose model is first validated while comparing simulations and experiments.

From a general point of view, we consider linear time-invariant perturbed systems described by a state-space representation (1.1).

$$\begin{cases} \dot{x}(t) = Ax(t) + Bu(t) + Fd(t) \\ y(t) = Cx(t) \end{cases} \tag{1.1}$$

where, $x(t) \in \mathbb{R}^n$ describes the state vector, $y(t) \in \mathbb{R}^p$ is the vector of measurable variables (outputs). The vector $u(t) \in \mathbb{R}^m$ represents the known input variables, whereas $d(t) \in \mathbb{R}^q$ is the vector which represents the *unknown input variables*.

Assumption 1. *A, B, F, C are known constant matrices of appropriate dimensions.*

Most of the approaches require the analysis of the structural invariants of the model which play an essential role in this problem. The infinite structure of the model is also related to solvability conditions. The knowledge of zeros (*finite structure*) is an important issue because these zeros are directly related to stability conditions of the controlled system. The concepts of poles and zeros are briefly recalled in section 1.2, see also appendix A for more details and notations used in this document.

In section 1.3, some classic control strategies to solve this problem will be recalled and some of these will be developed, *e.g.* Proportional-Integral-Derivative (PID) (PI) control, Static State Feedback (SSF) control. The next section contains the Derivative State Feedback (DSF) approach which is based on the Bond Graph (BG) methodology. Previous works are recalled.

At least, two sections are dedicated to simulations. The T-B system is used as case study and the model is validated with experiments. Then, different control strategies for the disturbance rejection problem are compared and some characteristics are highlighted.

1.2 Poles and Zeros: Theoretical framework

Before developing any methodology to solve the Disturbance Rejection Problem, modelling, analysis and observer/control synthesis of the dynamical system is required (Integrated Design Approach). These are necessary steps in the design phase of the observer as well as for the synthesis of control laws.

The selected representation (Transfer Function, Space-State representation, BG, ...) must allow us to understand the studied physical phenomena with an accurate mathematical model. First of all, in order to study the structure of systems, a model must be chosen.

System dynamics are here represented through a differential equation of order n. This differential equation can be written in matrix form and this representation is called State-Variables Model or State-Space Representation. A State-Space representation is also a particular type of Rosenbrock representation [Bourlès, 2010, Fliess, 1990].

Consider the system described by the state-space equation (1.2).

$$\begin{cases} \dot{x}(t) = Ax(t) + Bu(t) \\ y(t) = Cx(t) + Du(t) \end{cases} \tag{1.2}$$

where $x(t)$ is the vector for the system states, $u(t)$ is the vector for the system inputs and $y(t)$ is the vector for the system outputs. Taking the single-sided Laplace transforms, the following set of equations (1.3) is obtained.

$$\begin{cases} sx(s) - x(0) = Ax(s) + Bu(s) \\ y(s) = Cx(s) + Du(s) \end{cases} \tag{1.3}$$

where B can contain the known and/or unknown inputs. Considered the initial conditions $x(0) = 0$, then the Input-Output relation is expressed in equation (1.4).

$$y(s) = [C(sI - A)^{-1}B + D]u(s) \tag{1.4}$$

where the matrix $G(s) = [C(sI - A)^{-1}B + D]$ is called *transfer-function matrix*.

The equations in (1.3) may be rewritten in the form (1.5).

$$\begin{bmatrix} sI - A & -B \\ C & D \end{bmatrix} \begin{bmatrix} x(s) \\ u(s) \end{bmatrix} = \begin{bmatrix} x(0) \\ y(s) \end{bmatrix} \tag{1.5}$$

This is a particular type of Rosenbrock representation [Bourlès, 2010, Fliess, 1990]. The matrix $P(s) = \begin{bmatrix} sI - A & -B \\ C & D \end{bmatrix}$ plays a key role for the study of the zeros associated with the system.

The matrix $G(s)$ gives a description of the way in which the system appears to its environment and can be thought of as an *external form* of description. $P(s)$ exhibits the internal structure associated with the State-Space model and can be thought as an *internal form* of description.

$P(s)$ conveys more information about the system then $G(s)$, which represents only the completely controllable/observable subsystem associated with the system defined in (1.2). In general, a larger set of zeros is defined from $P(s)$; if the system is completely controllable and observable, then the set of zeros are the same [Macfarlane and Karcanias, 1976].

The concept of the poles and zeros for the general matrix transfer-function case is done using a standard form for transfer-function matrices called *Smith-McMillan form* that is an extension of the *Smith form* for polynomial matrices.

Assume that all the elements of a real-coefficient rational-function matrix $H(s)$ are polynomials (*polynomial matrix*). The polynomial matrices can be put into a standard form (*Smith form*) by a series of elementary row and column operations. If $H(s)$ is a polynomial Matrix of *rank* r, then $H(s)$ may be transformed into the matrix $S(s)$ defined in equation (1.6).

$$S(s) = \begin{bmatrix} S^*(s)_{r,r} & 0_{r,l-r} \\ 0_{m-r,r} & 0_{m-r,l-r} \end{bmatrix} \tag{1.6}$$

where $S^*(s) = diag\{s_1(s), s_2(s), \cdots, s_r(s)\}$. The row and column operations involved in transforming $H(s)$ to Smith form may be represented by suitable polynomial matrices, then the transformation to the Smith form can be represented by

$$S(s) = L(s)H(s)R(s)$$

where both the matrix $L(s)$ and the matrix $R(s)$ must be *uni-modular polynomial matrices*. A direct consequence of the existence of the Smith form is a canonical form for rational function matrices, the *Smith-McMillan form*.

In addition, any transfer matrix $G(s)$ of dimension $\mathbb{R}^{m\times l}$ and *rank r* can be factorized as

$$G(s) = L(s)M(s)R(s) \tag{1.7}$$

where $L(s)$ and $R(s)$ are the same matrices that the one mentioned before. Matrix $M(s)$ is described by equation (1.8).

$$M(s) = \begin{bmatrix} M^*(s) & 0 \\ 0 & 0 \end{bmatrix} \tag{1.8}$$

with

$$M^*(s) = diag\left[\frac{\varepsilon_1(s)}{\psi_1(s)} \quad \frac{\varepsilon_2(s)}{\psi_2(s)} \quad \cdots \quad \frac{\varepsilon_r(s)}{\psi_r(s)}\right] \tag{1.9}$$

where the elements ε_i and ψ_i are monic polynomials such that:

(i) each $\varepsilon_i(s)$ divides all $\varepsilon_{i+1}(s)$ so that $\varepsilon_1(s)|\varepsilon_2(s)|\cdots\varepsilon_r(s)$.

(ii) each $\psi_i(s)$ divides all $\psi_{i+1}(s)$ so that $\psi_1(s)|\psi_2(s)|\cdots\psi_r(s)$.

$M(s)$ is unique and called the *Smith-McMillan form* of $G(s)$.

Defining $\Delta(s) = \det[sI - A]$ as the *least common denominator* of all the elements of $G(s)$. The Smith-MacMillan form can be obtained from $G(s)$ as follows: Let $G(s) = \frac{N(s)}{\Delta(s)}$, where $N(s)$ is a polynomial matrix and has a Smith form $S(s)$, then $N(s) = L^{-1}(s)S(s)R^{-1}(s)$, where $L^{-1}(s)$ and $R^{-1}(s)$ are appropriate uni-modular matrices. The Smith-McMillan form of $G(s)$ is then defined as

$$M(s) = \frac{S(s)}{\Delta(s)} = L(s)G(s)R(s) \tag{1.10}$$

- Poles and zeros of transfer-function matrix: Let $G(s)$ a matrix of normal rank r with a Smith-McMillan decomposition described by (1.7) [Macfarlane and Karcanias, 1976]. The poles and zeros of $G(s)$ are defined to be respectively the roots of the polynomials $\psi_i(s), i = 1, \cdots, r$ and $\varepsilon_i(s), i = 1, \cdots, r$ of the Smith-McMillan form given previously.

- Invariant zeros: Consider the Smith form of the polynomial matrix $P(s)$ and let it be such that

$$P(s) = L(s) \begin{bmatrix} f_1(s) & \cdots & \cdots & 0 \\ \vdots & f_2(s) & & \vdots \\ \vdots & & \ddots & \vdots \\ \vdots & & & f_{m+n}(s) \\ \cdots & \cdots & \cdots & \cdots \\ 0 & \cdots & \cdots & 0 \end{bmatrix} R(s)$$

  where $f_i(s)$ are the invariant factors of $P(s)$ and the set of zeros of these invariant polynomials will be called the set of the invariant zeros of the system. The null invariant zeros are the common null roots of the transfer matrix numerator.

The invariant zeros can be viewed as the system poles of the inverse system (when it exists). One of the basic assumptions of the well-known Glover-Doyle algorithm in the H_∞ theory is that two subsystems have no invariant zeros on the imaginary axis ([Glover and Doyle, 1988]); see also [Schrader and Sain, 1989] and [Wonham, 1985] for other uses of invariant zeros.

1.3 Control System: Disturbance rejection problem

Some classical control approaches are recalled in the following sections in order to compare them with the *Derivative State Feedback - Bond Graph* one. This last approach is then the methodology developed in this thesis. One important feature is that a structural analysis of the model must be achieved before control synthesis. We will show that very similar concepts developed for Unknown Input Observer (UIO) property analysis are as well expressed in chapter 2 in term of finite and infinite structures of the model.

1.3.1 PID (PI) Control

The birth and large-scale deployment of the PID control technology can be traced back to the period of the 1920*s*-1940*s* in response to the demands of industrial automation before World War II. Its dominance is evident even today across various sectors of the entire industry. In process control applications, more than 95% of the controllers are of the PID type, [Åmström and Hägglund, 1995, Guo and Zhao, 2016, Guo and Zhao, 2016].

The PI and PID controllers have been studied since many years and they are the most common control strategies. The Proportional-Integral (PI) Controllers have different expressions and they have the ability to eliminate steady state offsets through the integral action. Their technology has greatly changed, from analogue to digital electronics, with digital versions (*discrete time*)

and the possibility to use micro-controllers [Chen and Seborg, 2002]. There are many methods for tuning PID controllers, most of these methods are based on the classical Ziegler-Nichols methods, [Cominos and Munro, 2002].

The classical PID control is defined in (1.11), where $e(t)$ is the error variable, difference between the reference input signal $v(t)$ and the output variable $y(t)$. It is rewritten in Laplace domain as a transfer function described in (1.12). The PID controller is described by three parameters (K_p-Proportional Gain, T_i-Integral Gain and T_d- Derivative Gain). With proportional control, there is normally a control error in the steady state behaviour. The main action of the integral function is to make sure that the process output agrees with the set-point in the steady state behaviour. With an integral action, a small positive error will always lead to an increasing control signal, and a negative error will give a decreasing control signal no matter how small the error is. The purpose of the derivative action is to improve the closed-loop stability. Several properties of the PID control are well studied and analysis are shown in many books in the literature as [Åmström and Hägglund, 1995].

$$u(t) = K_p e(t) + \frac{K_p}{T_i}\int_0^t e(t)dt + K_p T_d \dot{e}(t) \tag{1.11}$$

$$G(s) = K_p\left[1 + \frac{1}{s\,T_i} + sT_d\right] \tag{1.12}$$

Some works related to perturbation rejection with PI or PID controllers are [Tavakoli et al., 2005, Tidke et al., 2018, Krohling, 1997, Chen and Seborg, 2002, Vrančić et al., 2004]. It is known that only constant perturbation can be rejected (attenuated) following some rather restrictive conditions; see references for more details.

1.3.2 Static State Feedback (SSF) control

The state-space formalism is very useful in providing both a simple and complete system representation. This type of representation is indeed simpler than "Rosenbrock representation": see [Bourlès, 2010]. On the other hand, within this formalism, a complete description of the system is possible (if the latter's "structure at infinity" is left aside [Bourlès and Marinescu, 2011]).

We recall the study of control by an "elementary" state feedback that is well studied and applied in different fields. Some of these works and historical research of the feedback control are in [Mayr, 1970, Chen, 1998, WilliamsII and Lawrence, 2007]. We will then extend the state feedback knowledge to the (derivative) state feedback control (next section) in order to solve the Disturbance Rejection (DR) control problem.

The connection between the ability to arbitrarily place the closed-loop eigenvalues by proper choice of the state feedback gain matrix K and controllability property of the open-loop state equation, *i.e.*, the pair (A,B) of the system $\Sigma(C,A,B)$ is well established for systems without disturbance. In that case we can speak of non-controllable modes (poles) or as well as input decoupling zeros. This problem has received also much attention when a disturbance exists. In that case, when the disturbance rejection problem has a solution with static state feedback, the ability to arbitrarily place the closed-loop eigenvalues is related to non-controllable modes but also to some of the invariant zeros. Finite structures of models $\Sigma(C,A,B)$ and $\Sigma(C,A,B,F)$ must

be compared. A structural approach from the bond graph representation has been proposed in case of control with state feedback. The algebraic approach is also well-known. When the disturbance rejection problem with state feedback has no solution, an alternative control with derivative state feedback can be proposed. We show in the following that the pole placement with the disturbance rejection problem is similar to the state feedback problem in its formulation. A similar approach is developed in terms of structural analysis and then in terms of control synthesis.

The state-space system described in (1.1) rewriting without disturbance in equation (1.13) is the open-loop model to be controlled.

$$\begin{cases} \dot{x}(t) = Ax(t) + Bu(t) \\ y(t) = Cx(t) \end{cases} \tag{1.13}$$

The state feedback control law without disturbance rejection has the form (1.14).

$$u(t) = -Kx(t) + Lv(t) \tag{1.14}$$

where each parameter of feedback gain K is a real constant. If equation (1.14) is substituted in (1.13), the closed-loop state equation is (1.15).

$$\begin{cases} \dot{x}(t) = (A - BK)x(t) + BLv(t) \\ y(t) = Cx(t) \end{cases} \tag{1.15}$$

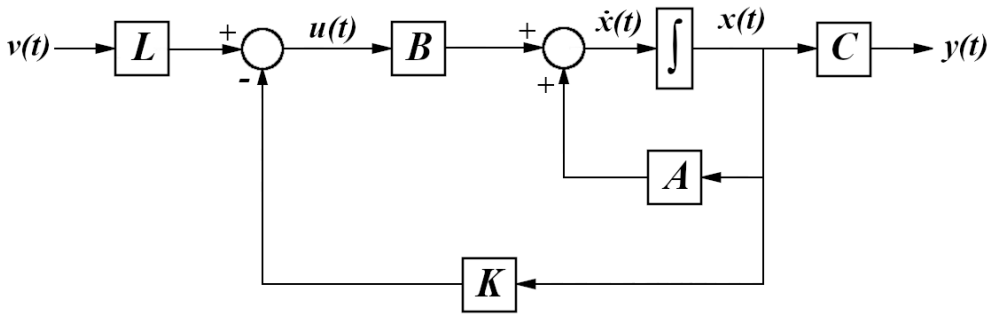

Figure 1.1 – State Feedback Control block diagram.

The block diagram shown in Fig. 1.1 describes the structure of the system. The state feedback control law (1.14) features a constant state feedback gain matrix K of dimension $m \times n$ and a new external reference input $v(t)$ necessarily having the same dimension $m \times 1$ as the open-loop input $u(t)$, as well as the same physical units.

For the Single Input - Single Output (SISO) case, the feedback gain K is a $1 \times n$ row vector, the reference input $v(t)$ is a scalar signal, and the state feedback control law has the form (1.16).

$$\begin{aligned} u(t) = & -\begin{bmatrix} k_1 & k_2 & \cdots & k_n \end{bmatrix} \begin{bmatrix} x_1(t) \\ x_2(t) \\ \vdots \\ x_n(t) \end{bmatrix} + lv(t) \\ = & -k_1x_1(t) - k_2x_2(t) - \cdots - k_nx_n(t) + lv(t) \end{aligned} \tag{1.16}$$

If the external reference input $v(t)$ is absent, the state feedback control law is called a "regulator" that is designed to deliver desirable transient response for non-zero initial conditions and/or attenuate disturbances to maintain the equilibrium state.

Theorem 1. *[WilliamsII and Lawrence, 2007] For any symmetric set of n complex numbers* $\{\mu_1, \mu_2, \cdots, \mu_n\}$*, there exists a state feedback gain matrix K such that* $\sigma(A - BK) = \{\mu_1, \mu_2, \cdots, \mu_n\}$ *if and only if the pair* (A, B) *is controllable.*

In the following, it will be supposed that the studied model is state controllable/observable. In that situation, non-assigned modes with a state feedback control law for the Disturbance Rejection problem are one part or all the invariant zeros

1.3.3 Static State Feedback (SSF) Control with disturbance rejection

The state-space system described in (1.1) is rewriting in equation (1.17). It is supposed that the model is state controllable/observable and invertible.

$$\begin{cases} \dot{x}(t) = Ax(t) + Bu(t) + Fd(t) \\ y(t) = Cx(t) \end{cases} \tag{1.17}$$

In order to study the disturbance rejection problem, the structure of the model $\Sigma(C, A, B, F)$ must be highlighted. The different transfer functions are $T_{yu}(s) = C(sI - A)^{-1}B$ and $T_{yd}(s) = C(sI - A)^{-1}F$.

The disturbance rejection problem for the system described by equation (1.17) has a solution by a state feedback control law (without measurement of the disturbance variables) $u(t) = F_c x(t) + Gv(t)$ iff the infinite structure of matrix $s^{-1}T_{yu}(s)$ is equal to the infinite structure of matrix $[s^{-1}T_{yu}(s) \quad T_{yd}(s)]$. With the measurement of the disturbance variables, the condition is on matrices $T_{yu}(s)$ and $[T_{yu}(s) \quad T_{yd}(s)]$.

At most, the disturbance rejection problem for the system described by equation (1.17) has a solution with stability iff the invariant zeros of model $\Sigma(C, A, B)$ which are not invariant zeros of model $\Sigma(C, A, B, F)$ are strictly stable [Malabre and Martínez-García, 1993] (for invertible and controllable models).

Consider now a SISO system and n_c and n_p the infinite zero orders of systems $\Sigma(C, A, B)$ and $\Sigma(C, A, F)$, respectively, Appendix A. If $n_p < n_c$, the disturbance rejection problem is not solvable with static state feedback. From a causal point of view on the bond graph representation, the causal path length between the disturbance input and the output detector is shorter than the causal

path length between the control input source and the output detector. In that case a Derivative State Feedback is proposed as an alternative solution (next section).

Remark 1. *The state feedback control law expression for the disturbance rejection problem is not recalled here, since it will not be used in this work.*

1.4 Disturbance Rejection with Derivative State Feedback (DSF)

Recently, the DSF control of linear systems has been studied, mainly in order to solve the pole placement problem, with or without robust performance criteria. Procedures consider for instance, the pole placement problem for SISO systems in [Abdelaziz and Valášek, 2004] and Multiple Input - Multiple Output (MIMO) systems [Abdelaziz, 2008, Abdelaziz and Valášek, 2005, Cardim et al., 2007] as well with a robust criterion [Duan et al., 2005]. A geometric theory of derivative state feedback is given in [Lewis and Symons, 1991]. In the control of mechanical systems, there are many applications, as the suppression of vibration, where the concept of Derivative State Feedback is used. In these problems, because of their low cost, the main sensors used, are accelerometers. In that case, from the signals of the accelerometers it is possible to reconstruct the velocities with a good precision but not the displacements. [Kwak et al., 2002], [Reithmeier and Leitmann, 2003] and [Duan et al., 2005]. More generally, there exist some practical problems where the derivative state signals are easier to be obtained than the state signals.

There are different applications in the literature, where the design of the control law depends on the approach and assumptions of it, *i.e.*, when the state vector $x(t)$ is the same for state-derivative feedback and state feedback [Cardim et al., 2007]; the state-derivative $\dot{x}(t)$ and the disturbance-derivative $\dot{d}(t)$ are easy to measure [Cheng et al., 2015]; PI control design with state-derivative feedback [Korosi and Veselý, 2018]; etc.

In this section, the Derivative State Feedback approach is focused on the Bond Graph methodology [Paynter, 1960, Karnopp et al., 1975, Karnopp, 1979, Rosenberg and Karnopp, 1983, Dauphin-Tanguy, 2000] for the SISO case. A Bond Graph is composed of elements and lines which identify the power flow. Main elements are sources of effort and flow $\{Se, Sf\}$, sensors represented by flow and effort detectors $\{Df, De\}$, physical phenomena (resistive R, capacitive C and inertial I), junctions (zero for common effort and one for common flow) and two power conservative transformer elements : Transformer (TF) and Gyrator (GY). Elements are connected by power bonds represented by a half arrow labelled by two conjugated variables (effort e and flow f) where the product is the exchanged power between elements, and information signals (such as detectors and controllers) generally modelled by an arrow. Indeed, firstly for structural analysis of the model properties, the bond graph representation is well adapted. Secondly, the design of the control law is made from the state-space representation. Properties of the control law and of the controlled model can be also achieved as well from the bond graph representation. Through the bond graph approach, it has been proved that solutions to the Disturbance Rejection problem with Derivative State Feedback can be provided. A Derivative State Feedback control law has been proposed in [Sueur, 2016].

Consider system $\Sigma(C, A, B, F)$ as defined in equation (1.17). Non-restrictive assumptions that can be verified graphically from the bond graph representation are written, studied here in the SISO case.

- System $\Sigma(C,A,B)$ is state controllable/observable and the state matrix A is invertible
- The invariant zeros of $\Sigma(C,A,B)$ are strictly stable and $CA^{-1}B \neq 0$
- $n_p < n_c$, the Disturbance Rejection problem is not solvable with Static State Feedback

n_c and n_p are the infinite zero orders of systems $\Sigma(C,A,B)$ and $\Sigma(C,A,F)$, respectively, Appendix A.

Consider the system $\Sigma(C,A,B,F)$, and the Derivative State Feedback control law with disturbance defined as (1.18), where $v(t)$ is the new control input variable.

$$u(t) = F_c\dot{x}(t) + Gv(t) + F_p d(t), \tag{1.18}$$

Property 1. *The Disturbance Rejection Problem DRP with a DSF defined in (1.18) has a solution with pole placement iff $n_p \leq n_c$.*

The controlled system is written in equation (1.19).

$$\begin{cases} (I - BF_c)\dot{x}(t) = Ax(t) + BGv(t) + (BF_p + F)d(t) \\ y(t) = Cx(t) \end{cases} \tag{1.19}$$

If matrix $(I - BF_c)$ is not invertible, the state equation in (1.19) is called "generalized state-space system" or "singular system" [Verghese, 1978], [Coob, 1984, Verghese and Kailath, 1979, Verghese et al., 1981, Yip and Sincovec, 1981]. The characteristic equation of the closed loop system (1.19) is defined as (1.20). The degree γ of the characteristic polynomial in equation (1.20) is the number of system's finite eigenvalues, while $n - \gamma$ is the number of system's eigenvalues at infinity [Fahmy and O'Reilly, 1989].

$$\det(sI - sBF_c - A) = 0 \tag{1.20}$$

1.4.1 DR-DSF without pole placement

If a preferential derivative causality assignment is chosen for the bond graph model, the new state-space representation is in equation (1.21).

$$\begin{cases} x(t) = A^{-1}\dot{x}(t) - A^{-1}Bu(t) - A^{-1}Fd(t) \\ y(t) = CA^{-1}\dot{x}(t) - CA^{-1}Bu(t) - CA^{-1}Fd(t) \end{cases} \tag{1.21}$$

With the control law equation (1.18), the equations (1.21) can be written as equations (1.22).

$$\begin{cases} x(t) = (A^{-1} - A^{-1}BF_c)\dot{x}(t) - (A^{-1}BG)v(t) - (A^{-1}BF_p + A^{-1}F)d(t) \\ y(t) = (CA^{-1} - CA^{-1}BF_c)\dot{x}(t) - CA^{-1}BGv(t) - (CA^{-1}BF_p + CA^{-1}F)d(t) \end{cases} \tag{1.22}$$

If $(CA^{-1} - CA^{-1}BF_c) = 0$ and $(CA^{-1}BF_p + CA^{-1}F) = 0$ then $y(t) = -CA^{-1}BGv(t)$ and the rejection of the disturbance is achieved. There is a direct transmission between the new input

variable $v(t)$ and the output variable $y(t)$. The matrices F_c, G and F_p, solution of the disturbance rejection problem are defined in equation (1.23), with condition $CA^{-1}B \neq 0$, and the input-output relation is $y(t) = v(t)$.

$$\begin{cases} G = -(CA^{-1}B)^{-1} \\ F_c = (CA^{-1}B)^{-1}CA^{-1} \\ F_p = -(CA^{-1}B)^{-1}CA^{-1}F \end{cases} \tag{1.23}$$

With the control law defined by the equation (1.18), the invariant zeros of the controlled system $\Sigma(C,A,B)$ (without disturbance) are the same as the invariant zeros of the model $\Sigma(C,A,B)$ without control. At most, without pole placement, the controlled system $\Sigma(C,A,B)$ is an implicit model [Rosenbrock, 1970].

Property 2. *The degree γ of the characteristic polynomial $\det(sI - sBF_c - A)$ of the controlled system $\Sigma(C,A,B)$ with a DSF control law (1.18) with matrices defined in (1.23) is equal to the number of invariant zeros of $\Sigma(C,A,B)$, i.e. $\gamma = n - n_c$. The new model contains only $n - n_c$ finite modes (invariant zeros of $\Sigma(C,A,B)$).*

The output decoupling zeros (non-observable modes) are the zeros of matrix $[sI - A^t \quad C^t]^t$. For an observable model, this matrix doesn't contain any zero, but with the DSF control law, the new model can become non-observable.

Property 3. *The zeros of matrix $[sI - s(BF_c)^t - A^t \quad C^t]^t$ of the controlled system $\Sigma(C,A,B)$ with a DSF control law (1.18) with matrices defined in (1.23) are the invariant zeros of the model $\Sigma(C,A,B)$. They are the finite non-assigned modes of the controlled system.*

1.4.2 DR-DSF with pole placement

Property 4. *The DRP (Disturbance Rejection Problem) with a DSF of type defined in (1.18) with matrices G and F_p defined in (1.23) and matrix F_c in (1.24) has a solution with pole placement iff $n_p \leq n_c$.*

The solution for the DR-DSF with pole placement is obtained with the matrices G and F_p defined in (1.23) and with a new matrix F_c defined in equation (1.24), where the set $\{\alpha_1; \alpha_2; \cdots; \alpha_{n_p}\}$ is a set of n_p free parameters used for pole placement.

$$F_c = (CA^{-1}B)^{-1}[CA^{-1} + \alpha_1 C + \alpha_2 CA + \cdots + \alpha_{n_p} CA^{n_p - 1}] \tag{1.24}$$

Property 5. *The differential equation verified by the output variable $y(t)$ with a derivative state feedback control law defined by equation (1.18), with matrices G and F_p defined in (1.23) and matrix F_c in (1.24) is written in equation (1.25).*

$$\alpha_{n_p} y^{(n_p)} + \cdots \alpha_2 \ddot{y} + \alpha_1 \dot{y} + y = v(t) \tag{1.25}$$

Property 6. *The degree of the characteristic polynomial* $\det(sI - sBF_c - A)$ *of the controlled system* $\Sigma(C,A,B)$ *with a* DSF *control law defined in (1.18), with matrices G and* F_p *defined in (1.23) and matrix* F_c *in (1.24) is equal to* $(n-n_c)+n_p$ *(number of invariant zeros of* $\Sigma(C,A,B)$*, id est (i.e.)* $(n-n_c)$ *+ infinite zero order of* $\Sigma(C,A,F)$*, i.e.* n_p*).*

Since the properties of the controlled model are known, a final property can be written.

Property 7. *The* DRP *(Disturbance Rejection Problem) with a* DSF *of type defined in (1.18) with matrices G and* F_p *defined in (1.23) and matrix* F_c *in (1.24) has a stable solution with pole placement if* $n_p \leq n_c$ *and the invariant zeros of model* $\Sigma(C,A,B)$ *are strictly stable.*

It is worth noting that if the disturbance rejection problem is solvable either by a Static State Feedback (SSF) control law or a Derivative State Feedback (DSF) control law, in most situations it is not possible to measure all the state (or derivative) variables directly: they must be estimated by an observer. Since the disturbance variables are unknown input variables, an Unknown Input Observer (UIO) is added in order to estimate different variables: (derivative) state variables, as well as the disturbances variables. For linear Bond Graph models, solutions dealing with the finite structure of the model $\Sigma(C,A,B,F)$ for stability conditions of the observer and dealing with the infinite structure of the model $\Sigma(C,A,B,F)$ are in [Gonzalez and Sueur, 2018b] and presented in the following chapters. An observer bond graph model similar to the bond graph model of the physical system is synthesized.

1.5 Experimental System

In this section, a Mechatronics Experimental System is described which consists of a DC power source, a DC motor, a gear mechanism and two disks connected by a flexible shaft (see Fig. 1.2).

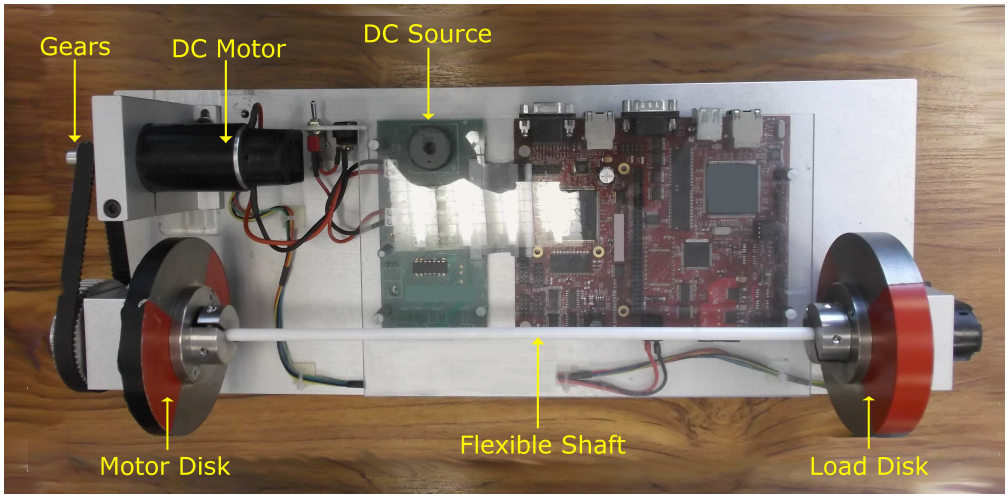

Figure 1.2 – Real Torsion-Bar system.

1.5.1 System description

In Fig. 1.2, the real Torsion-Bar (T-B) system is shown with its main parts. A functional schematic model of the T-B system is presented in Figure 1.3, schematic representation given by *20-Sim*®. According to Fig. 1.3, the system consists of the following components: a DC Power Source, a classical DC Motor which is modelled by an electrical part (Inductance L_a and Resistance R_a) and a mechanical part (Inertia J_m is supposed negligible), a transmission element which transfers the rotation from the motor to the motor disk with a transmission ratio (k_b), a first rotational disk (Motor Disk) with an inertial parameter J_1 and a friction coefficient R_1, a flexible shaft modelled as a spring-damper element (Spring C_{fs} and Damper R_{fs}), and a second rotational disk (Load Disk) with an inertial parameter J_2 and a friction coefficient R_2.

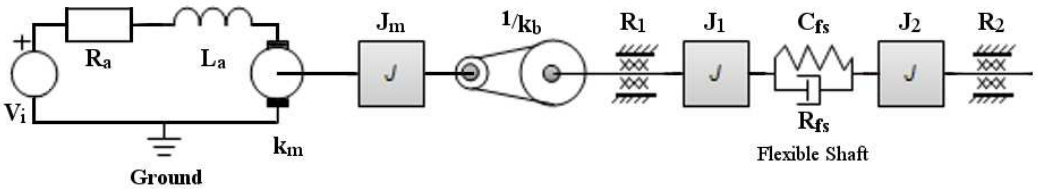

Figure 1.3 – Schematic model of the real Torsion-Bar system.

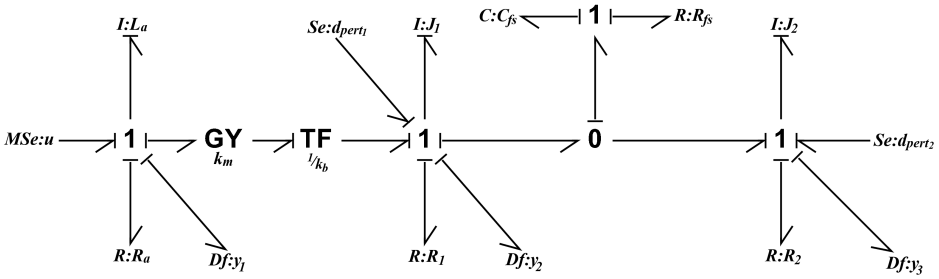

Figure 1.4 – Simplified Bond Graph of the Torsion-Bar system.

The simplified Bond Graph model of the system is shown in the Fig. 1.4. For the experimental system in Fig. 1.4, the controlled input voltage is represented by a modulated effort source $MSe : u$. Moreover, y_2 and y_3 are speed rotational variables represented in the Bond Graph model by flow output detectors $Df : y_2$ and $Df : y_3$ respectively. The current output detector $Df : y_1$ is associated to y_1 which is a current variable. These sensors are used to estimate the state variables and to estimate the unknown input vector $d(t)$ modelled by the source $Se : d_{pert1}$, unknown torque applied to the motor disk, and the source $Se : d_{pert2}$ which represents a torque applied to the second rotational disk(J_2). The numerical values for each element of the system are given in Table 1.1.

Element	Symbol	Value
Inductance	L_a	1.34×10^{-3} H
Inertia of motor disk	J_1	9.07×10^{-4} kg m^2 rad^{-1}
Inertia of load disk	J_2	1.37×10^{-3} kg m^2 rad^{-1}
Spring compliance	C_{fs}	0.56 N m rad^{-1}
Resistance	R_a	1.23 Ω
Motor disk friction	R_1	5.025×10^{-3} N m s rad^{-1}
Load disk friction	R_2	25×10^{-6} N m s rad^{-1}
Damping spring	R_{fs}	5×10^{-4} N s rad^{-1}
Motor constant	k_m	38.9×10^{-3} N m A^{-1}
Transmission ratio	k_b	3.75

Table 1.1 – Parameters of experimentation for the Torsion-Bar system model.

1.5.2 State-Space Equation

A state model or a transfer matrix representation can be directly deducted from the Linear Bond Graph model without the need to do complex numerical calculations, [Karnopp et al., 1975], [Rosenberg and Karnopp, 1983]. Two features of Bond Graph modelling are the causality and causal paths that are used in the analysis stage but also in order to derive models.

According to the Bond Graph model, a state-space representation is performed as described in the form (1.1). The state vector $x = [x_1, x_2, x_3, x_4,]^t$ is composed of energy storage variables: $x_1 = q_c = q_{c_{shaft}}$ (represents the angular displacement), $x_2 = p_{J_2}$, $x_3 = p_{J_1}$ (represent the angular momentums), and $x_4 = p_{L_a}$ (representing the flux linkage). The outputs described by flow output detectors are y_1, y_2 and y_3 which represent a current and two angular velocities. Then, the output matrix C can be also written as $C = [{C_1}^t, {C_2}^t, {C_3}^t]^t$. The disturbance vector is composed of two variables $d(t) = [d_{pert2}, d_{pert1}]^t$ and thus matrix F is $F = [{F_1}^t, {F_2}^t]^t$. The state equations are written as (1.26). The poles of the model (eigenvalues of matrix A) are equal to $-898.33, -7.834 \pm 55.68\,j, -10.379$.

$$\begin{cases} \dot{x}_1 = -\frac{1}{J_2}x_2 + \frac{1}{J_1}x_3 \\ \dot{x}_2 = \frac{1}{C_{fs}}x_1 - (\frac{R_2+R_{fs}}{J_2})x_2 + \frac{R_{fs}}{J_1}x_3 + d_{pert2} \\ \dot{x}_3 = -\frac{1}{C_{fs}}x_1 + \frac{R_{fs}}{J_2}x_2 - (\frac{R_1+R_{fs}}{J_1})x_3 + \frac{k_m}{L_a.k_b}x_4 + d_{pert1} \\ \dot{x}_4 = -\frac{k_m}{J_1.k_b}x_3 - \frac{R_a}{L_a}x_4 + u \\ y_1 = \frac{1}{L_a}x_4 \quad y_2 = \frac{1}{J_1}x_3 \quad y_3 = \frac{1}{J_2}x_2 \end{cases} \tag{1.26}$$

1.5.3 Model Validation

In this part, we compare some simulations obtained from the model developed by the Bond Graph methodology and the schematic given by *20-Sim*® and finally the data acquired from the real Torsion-Bar system. This study allows us to present the proximity between the models and the real system from some temporal responses.

1.5.3.1 Step signal response

The first entry is a step signal and the results of the simulation are shown below. In Fig. 1.5, the three output variables defined in the state-space representation (eq. 2.1) are displayed. They are obtained from the *20-Sim*® platform.

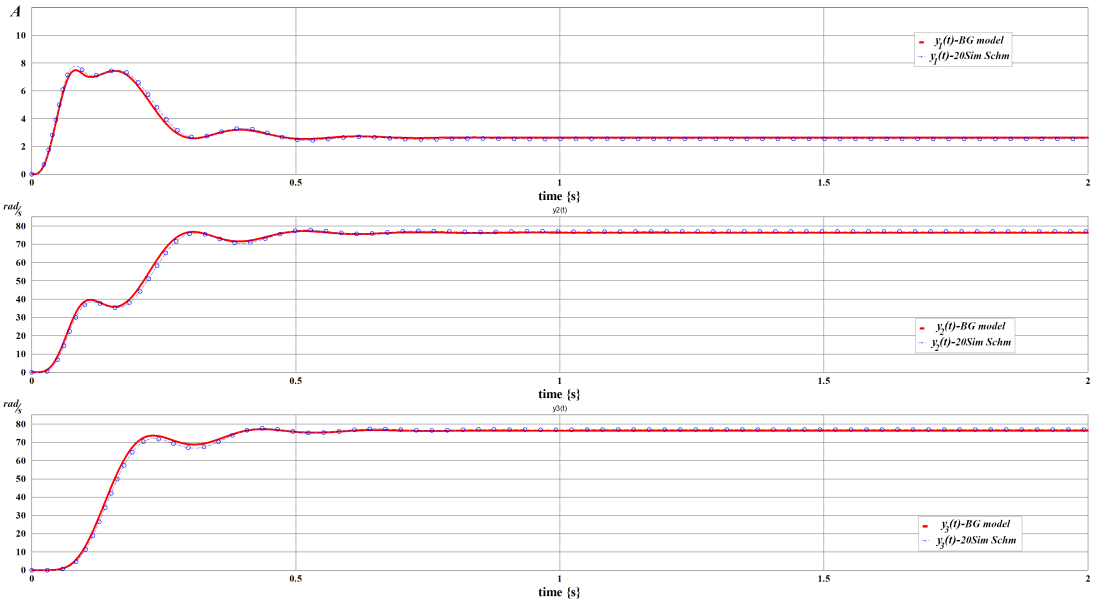

Figure 1.5 – Outputs from the Schematic given by *20-Sim*® (blue) and bond graph model (red).

The outputs $y_1(t)$, $y_2(t)$ and $y_3(t)$ derived from the bond graph model and from the schematic model of the Torsion-Bar system are compared. The dynamics of the schematic model is almost equal to the bond graph model; thus, the bond graph model of the T-B system can be used for the next applications and simulations in this thesis.

For the Real Torsion-Bar system, the direct measurement of $y_1(t)$ is not possible. Then, only the output $y_2(t)$ and $y_3(t)$ are presented in the Fig. 1.6 which are the data acquired by the *20-Sim 4C*® platform. Also, variables $y_2(t)$ and $y_3(t)$ obtained from the bond graph representation are shown simultaneously in order to compare simulated variables and measured data from the Torsion-Bar system.

In Fig 1.6, a) one output represents the motor disk velocity, b) and the other, the load disk velocity. The responses in the steady state phase are almost the same ($\approx$76 rad s^{-1}). Also, some differences could be caused by neglected dynamics in the model or the equipment features to the control and/or measurement (see the section 2.2.4).

In the following, comparisons are displayed in the same order for other input variables (ramp, sine function).

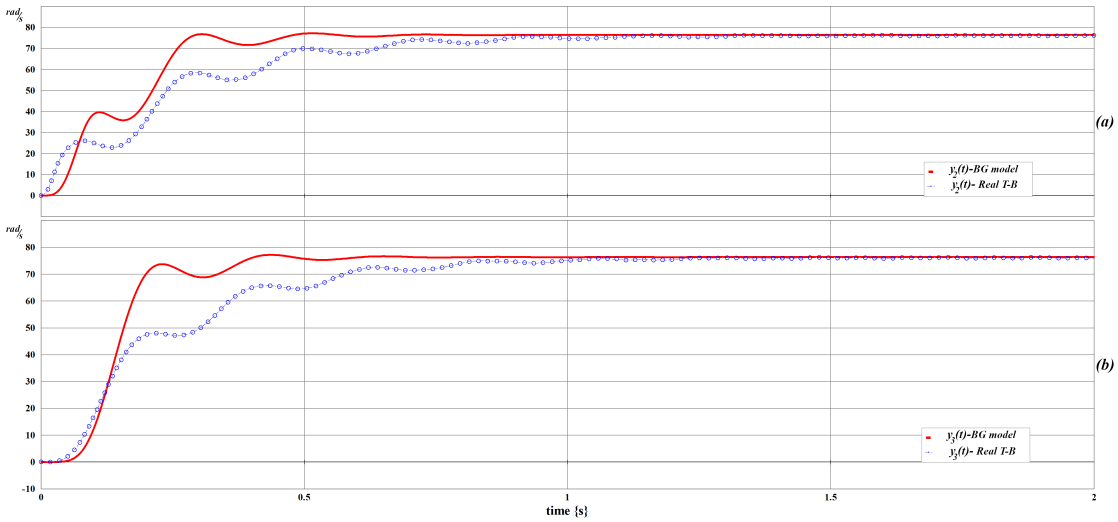

Figure 1.6 – Data from the outputs of real T-B system (blue) compared with outputs from BG model (red).

1.5.3.2 Temporal response for a ramp signal

This entry is a Ramp signal and the results are shown below. In the following figures, a characteristic of the T-B system, the limit (saturation) at the input is due to the protection for the real torsion-bar system (entry limit ±12 V). Fig. 1.7 shows the behaviour of the outputs $y_1(t)$, $y_2(t)$ and $y_3(t)$ of bond graph model and of the schematic model. After, the output signals (disks velocities) from the bond graph model and the data obtained from the real torsion-bar system ($y_2(t)$ and $y_3(t)$) are compared in Fig. 1.8.

1.5.3.3 Temporal response for a Sine type signal

Now the entry is a sine type signal and some graphics are shown below. Fig. 1.9 shows simulations of the outputs variables $y_1(t)$, $y_2(t)$ and $y_3(t)$. It compares the output signals from the bond graph model (1.4) and the schematic model (1.3). The output signals (disks velocities) from the bond graph model and the data from the real torsion-bar system ($y_2(t)$ and $y_3(t)$) are compared in Fig. 1.10.

1.5.3.4 Pulse signal response

Finally, a pulse signal is applied, and its graphics are shown below, as for previous inputs, Fig. 1.11 show simulations of the outputs variables $y_1(t)$, $y_2(t)$ and $y_3(t)$ and Fig. 1.12 presents the output signals (disks velocities) from the bond graph model and the data from the real torsion-bar system.

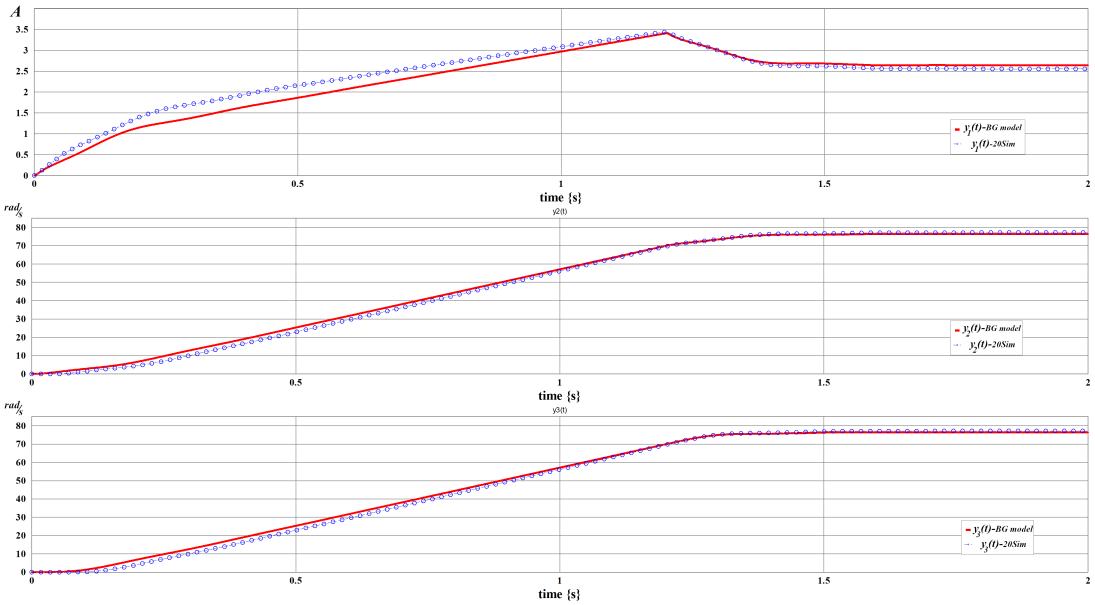

Figure 1.7 – Outputs from the Schematic given by *20-Sim*® (blue) and bond graph model (red).

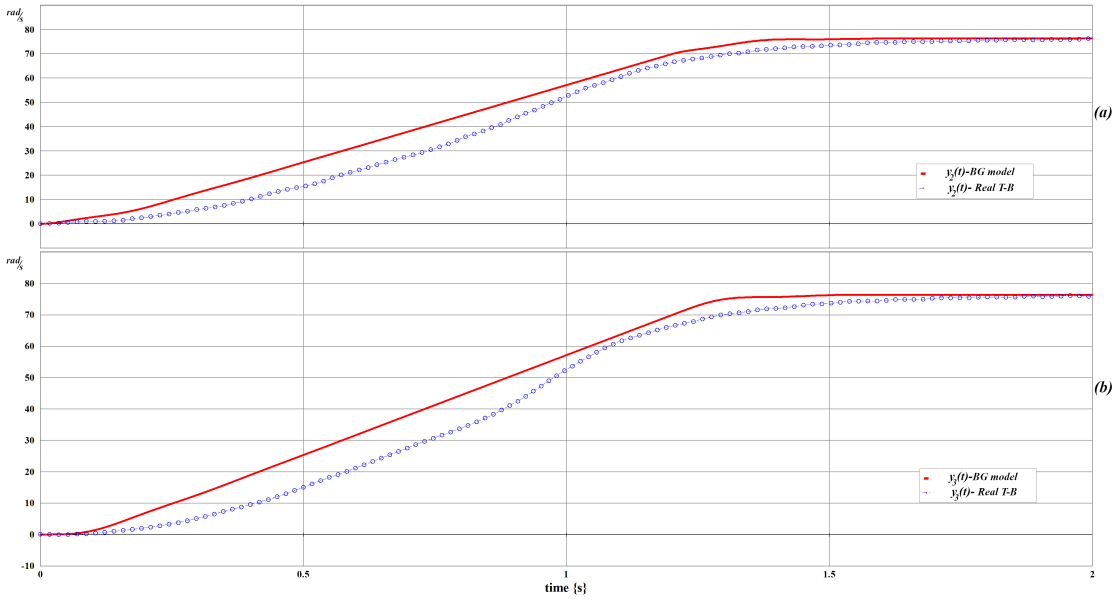

Figure 1.8 – Data from the outputs of real T-B system (blue) compared with outputs from BG model (red).

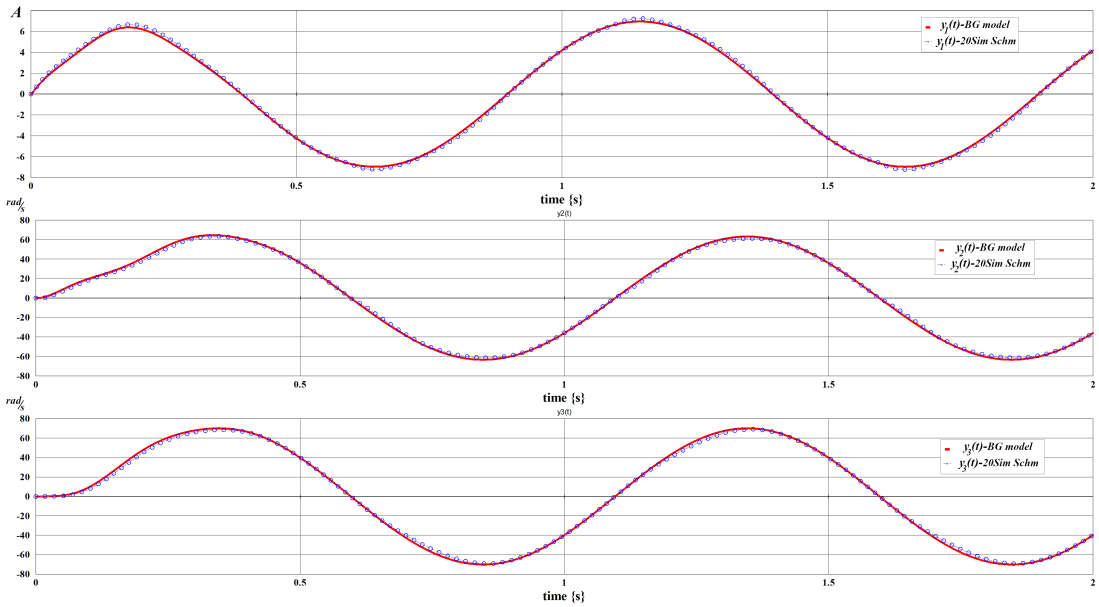

Figure 1.9 – Outputs from the Schematic given by *20-Sim*® (blue) and bond graph model (red).

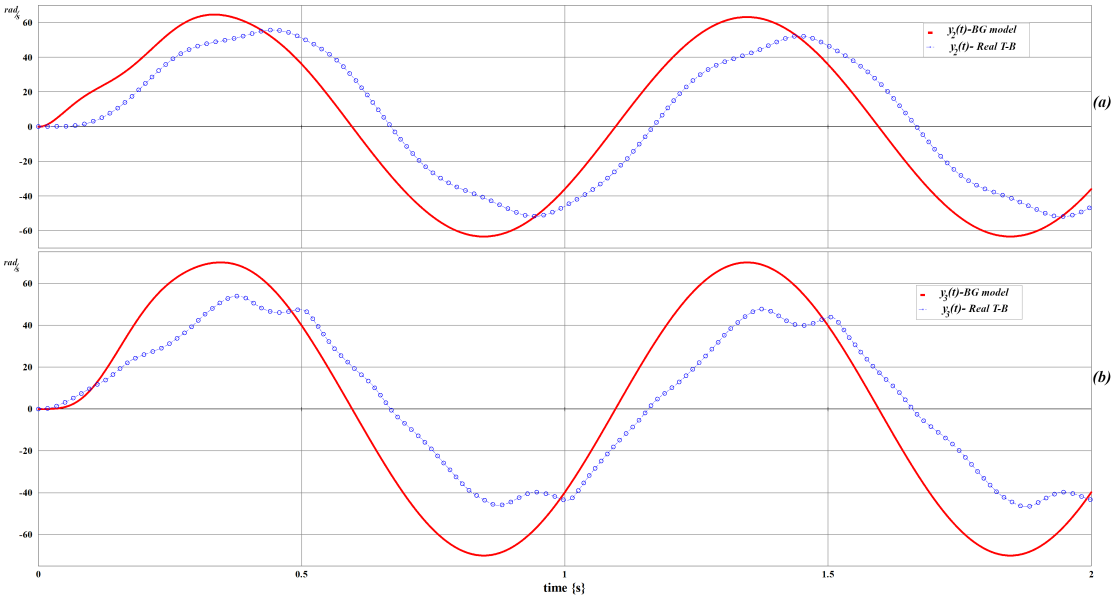

Figure 1.10 – Data from the outputs of real T-B system (blue) compared with outputs from BG model (red).

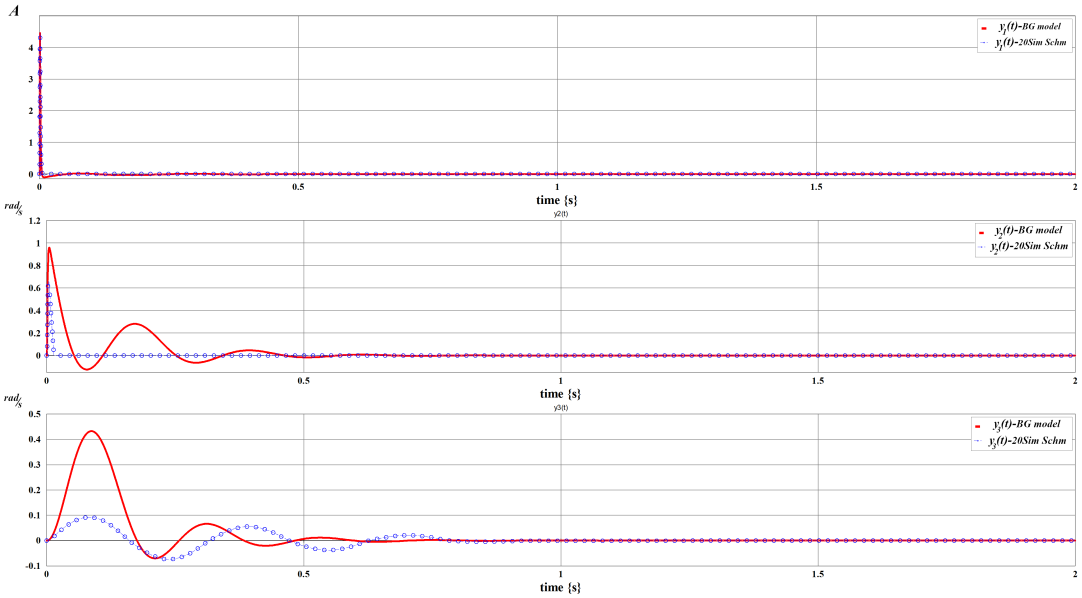

Figure 1.11 – Outputs from the Schematic given by *20-Sim*® (blue) and bond graph model (red).

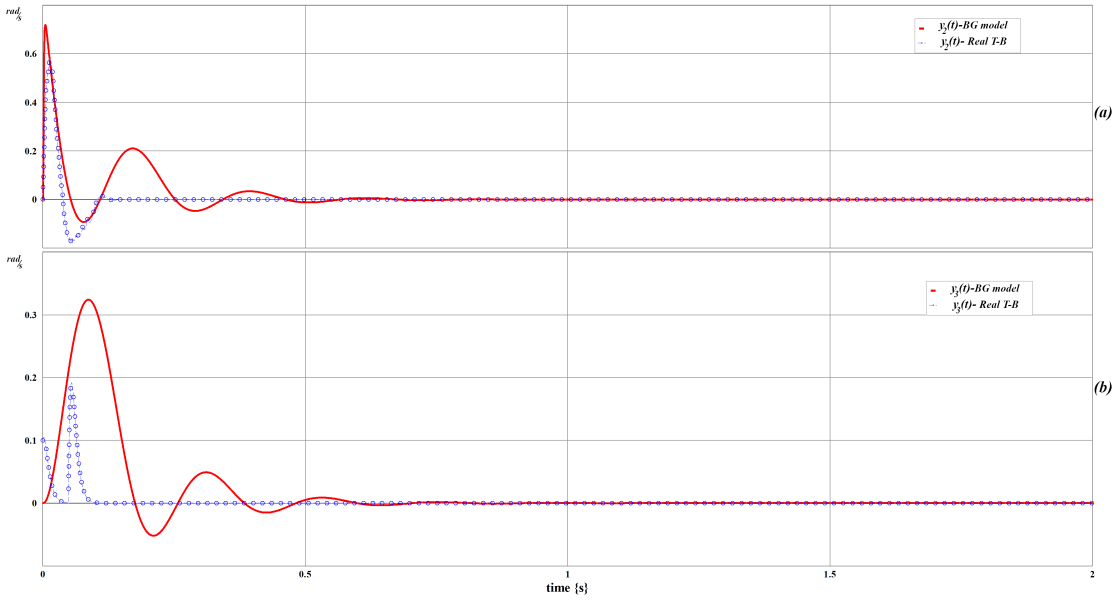

Figure 1.12 – Data from the outputs of real T-B system (blue) compared with outputs from BG model (red).

1.6 Disturbance Rejection for the T-B System

In the previous section, the model of the real torsion bar system developed in bond graph representation is validated. It can then be used in this thesis for the UIO synthesis and Disturbance Rejection with the concept of Derivative State Feedback.

The previous approaches presented in sections 1.3 and 1.4 for the Disturbance Rejection problem are now applied to the Torsion-Bar system presented in section 1.5. A slightly modified bond graph model and its state-space representation (1.27) are presented below.

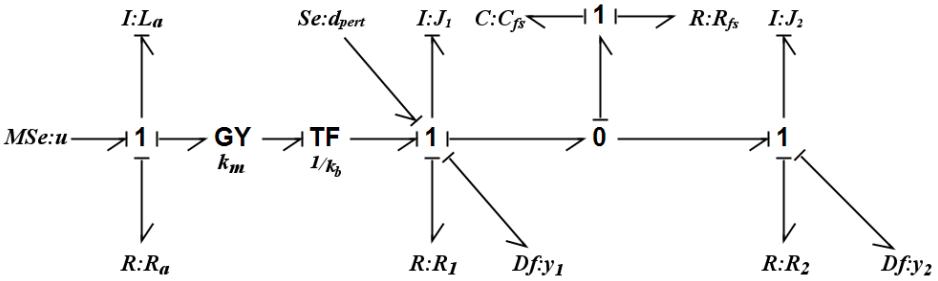

Figure 1.13 – Modified T-B bond graph model with integral causality assignment: BGI.

$$\begin{cases} \dot{x}_1 = -\frac{1}{J_2}x_2 + \frac{1}{J_1}x_3 \ , \\ \dot{x}_2 = \frac{1}{C_{fs}}x_1 - (\frac{R_2+R_{fs}}{J_2})x_2 + \frac{R_{fs}}{J_1}x_3 \ , \\ \dot{x}_3 = -\frac{1}{C_{fs}}x_1 + \frac{R_{fs}}{J_2}x_2 - (\frac{R_1+R_{fs}}{J_1})x_3 + \frac{k_m \cdot k_b}{L_a}x_4 + d_{pert} \ , \\ \dot{x}_4 = -\frac{k_m \cdot k_b}{J_1}x_3 - \frac{R_a}{L_a}x_4 + u \ , \\ y_1 = \frac{1}{J_1}x_3 \ ; \ y_2 = \frac{1}{J_2}x_2 \ . \end{cases} \tag{1.27}$$

Only the second output $y_2(t)$ will be controlled. The new control variable $v(t)$ is defined as a step function in rad s^{-1} and its action begins at 0.5 s with a value of 20 rad s^{-1}. At $t = 2$s the input is incremented to 40 rad s^{-1} and maintained until the end. The unknown input is defined as $d_{pert}(t) = -0\,3$Nm with time action between 5s and 15s.

1.6.1 Structural properties of the BG model: Disturbance Rejection problem

We consider the classical Disturbance Rejection problem by a Static State Feedback control (DR-SSF). A structural approach is used due to the structural properties of the bond graph model. Structural properties of bond graph models, such as the *infinite structure* and *finite structure* are recalled in Appendix A. These structures are generally defined for system $\Sigma(C,A,B)$. Since the Torsion-Bar system contains one input control variable, one input disturbance variable, one output variable to be controlled and two measured output variables, different finite and infinite structures of models must be highlighted, with a particular notation for each infinite zero order. Only the row infinite structure of the models is studied in this part. We denote $\{n_{ci}\}$ the set of

row infinite zero orders of the row sub-systems $\Sigma(C_i,A,B)$ and $\{n_{pi}\}$ the set of row infinite zero orders of the row sub-systems $\Sigma(C_i,A,F)$, (*index* $\boldsymbol{c}$ for control and *index* $\boldsymbol{p}$ for perturbation).

The disturbance rejection problem for the system $\Sigma(C,A,B,F)$ described by equation (1.1) has a solution by a state feedback control law $u(t) = F_c x(t) + Gv(t)$ (without measurement of the disturbance variables) iff the infinite structure of matrix $\left[s^{-1}(C(sI-A)^{-1}B)\right]$ is equal to the infinite structure of matrix $\left[\begin{array}{cc} s^{-1}(C(sI-A)^{-1}B) & C(sI-A)^{-1}F \end{array}\right]$. With the estimation of the disturbance variables, the condition is on matrices $[C(sI-A)^{-1}B]$ and $\left[\begin{array}{cc} C(sI-A)^{-1}B & C(sI-A)^{-1}F \end{array}\right]$. At most, the disturbance rejection problem for the system described by equation (1.1) has a solution with stability iff the zeros of model $\Sigma(C,A,B)$ which are not zeros of model $\Sigma(C,A,B,F)$ are strictly stable [Malabre and Martínez-García, 1993]. From a bond graph approach, in the SISO case, the condition for DR-SSF is: the causal path length between the input control $MSe : u$ and the output to be controlled $Df : y$ is shorter than the causal path length between the disturbance input $Se : d$ and the output to be controlled $Df : y$.

First, properties of the submodels $\Sigma(C_2,A,B)$ and $\Sigma(C_2,A,F)$ are studied since only the second output variable must be controlled. The shortest causal path between the output variable to be controlled and the control input $MSe : u$ is:

$$Df : y_2 \rightarrow I : J_2 \rightarrow R : R_{fs} \rightarrow I : J_1 \rightarrow TF : 1/k_b \rightarrow GY : k_m \rightarrow I : L_a \rightarrow MSe : u \; .$$

The length of this causal path is equal to 3, then $n_{c2} = 3$. The shortest causal path between the output variable to be controlled and the disturbance input $Se : d_{pert}$ is:

$$Df : y_2 \rightarrow I : J_2 \rightarrow R : R_{fs} \rightarrow I : J_1 \rightarrow Se : d_{pert} \; .$$

The length of this causal path is equal to 2, then $n_{p2} = 2$ and $n_{p2} < n_{c2}$.

The causal path length between the disturbance input $Se : d_{pert}$ and the output to be controlled $Df : y_2$ is shorter than the causal path length between the input control $MSe : u$ and the output to be controlled $Df : y_2$: The *Disturbance Rejection problem with Static State Feedback is not possible*. For this reason, simulations when using state-feedback control are not presented in this section.

An open loop control is first proposed in order to analyse the influence of the disturbance on the output variable, Fig. 1.14. Each simulation is proposed with a white Gaussian noise, as it is usual for realistic systems.

1.6.2 PID (PI) Control

The classical PID control is defined in (1.11), where $e(t)$ is the error variable, difference between the reference input signal $v(t)$ and the output variable $y_2(t)$. The PID controller is described by three parameters (K_p-Proportional Gain, T_i-Integral Gain and T_d-Derivative Gain).

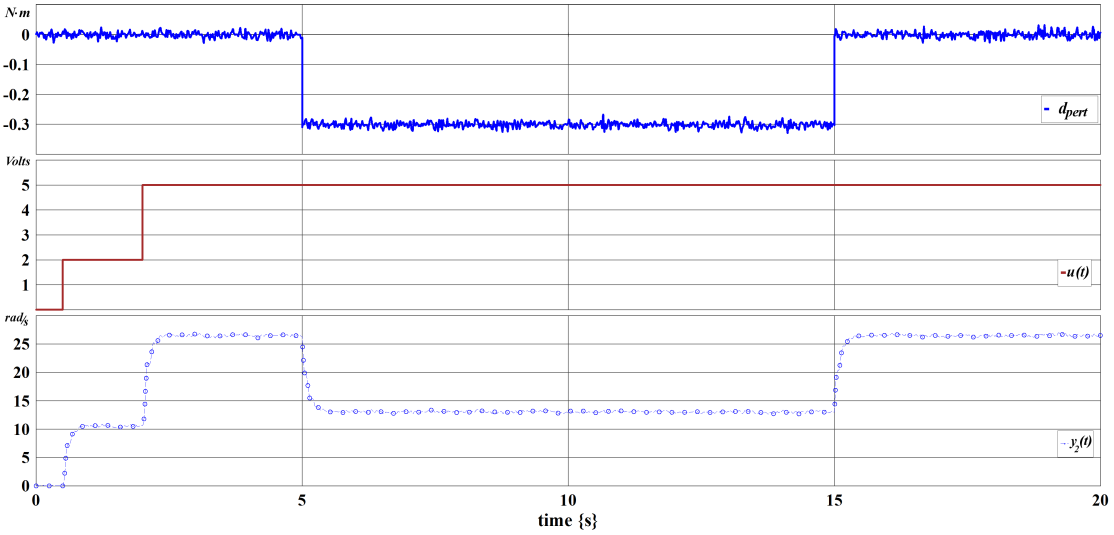

Figure 1.14 – Open loop control, without disturbance rejection.

After probing different tuning methods in order to define the parameters for the PID controller, we get parameters $K_p = 0.1$, $T_i = 0.09s^{-1}$ and $T_d = 0.009s$. Since the model is linear, it is also possible to calculate the gains on beforehand. The PID Controller for disturbance attenuation is applied to the equipment and variables behaviours (output variable $y_2(t)$ and control signal $u(t)$) are presented in Fig. 1.15. The output variable $y_2(t)$ varies around its steady-state behaviour which could be reached without any disturbance or with a constant one.

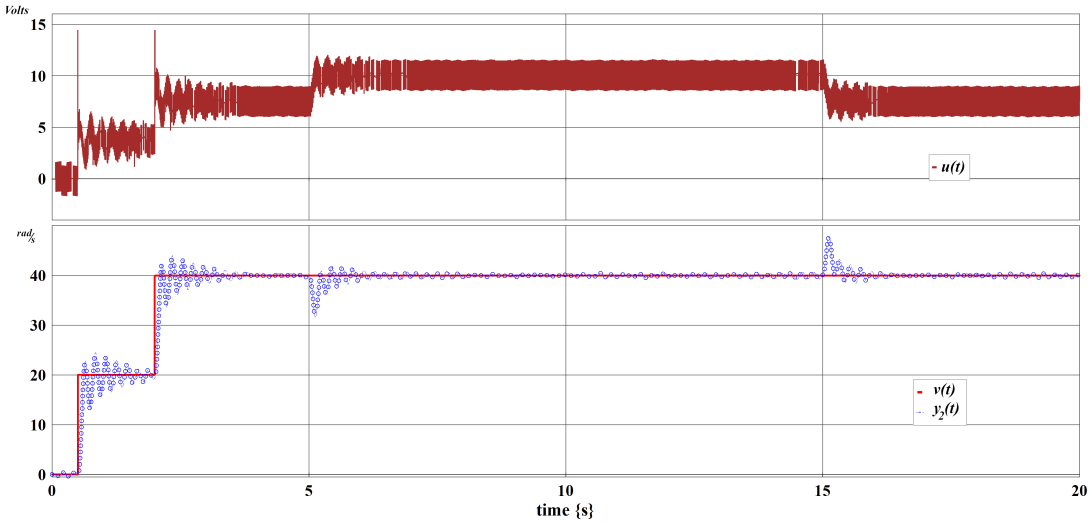

Figure 1.15 – Response of output y_2 and the signal control $u(t)$ for PID control.

1.6.3 Disturbance Rejection with DSF

Model $\Sigma(C,A,B)$ is structurally controllable/observable and the state matrix A is invertible, a derivative causality assignment can be applied to the bond graph model, as proved in the Bond Graph model with Derivative causality (BGD) model, Fig. 1.16. As studied in section 1.6.1, $n_{c2} = 3$ and $n_{p2} = 2$. Since $n_{p2} < n_{c2}$, from properties 4 and 6 the DSF has a solution with $n - n_{c2} = 1$ finite non-assigned mode that is the invariant zero of model $\Sigma(C_2,A,B)$ and $n_{p2} = 2$ finite modes which can be chosen freely with matrix F_c.

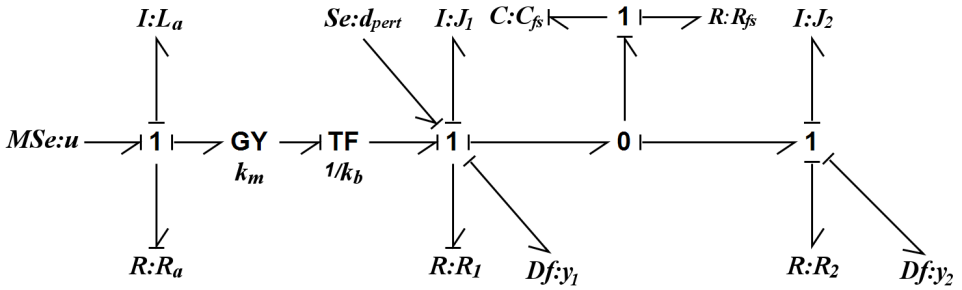

Figure 1.16 – Derivative causality assignment of the bond graph model: BGD.

From the BGD model of Fig. 1.16, the causal path lengths between the output y_2 and the different inputs (known and unknown input variables) are equal to 0, thus $C_2A^{-1}B \neq 0$ and $C_2A^{-1}F \neq 0$. The system $\Sigma(C_2,A,B)$ has one invariant zero since $n_{c2} = 3$ which is not equal to zero (property of the BGD model). Its value is $I_z = -\frac{1}{C_{fs}\cdot R_{fs}} = -3571.42$. Some coefficients can be derived from a causal analysis (causal path gains), but here they are directly obtained from formal calculus, equation (1.28) for matrices without pole placement.

$$\begin{array}{lll} G &= \frac{(R_1\cdot R_a + R_2\cdot R_a + k_m^2\cdot k_b^2)}{(k_m\cdot k_b)} & = 188.456\cdot 10^{-3} \\ F_p &= \frac{R_a}{k_m\cdot k_b} & = 8.4319 \\ F_c &= \left[\begin{array}{cccc} \frac{R_1\cdot R_a + k_m^2\cdot k_b^2}{k_m\cdot k_b} & \frac{R_a}{k_m\cdot k_b} & \frac{R_a}{k_m\cdot k_b} & 1 \end{array}\right] & = \left[\begin{array}{cccc} 188.245\cdot 10^{-3} & 8.432 & 8.432 & 1 \end{array}\right] \end{array} \tag{1.28}$$

Without pole placement, $Y_2(s) = V(s)$. The degree of the characteristic polynomial is 1, with root equal to the invariant zero (fixed finite mode) and $\det(sI - sBF_c - A) = \frac{R_1\cdot R_a + R_2\cdot R_a + k_m^2\cdot k_b^2}{C_{fs}\cdot J_2\cdot L_a\cdot J_1}\cdot(C_{fs}\cdot R_{fs}\cdot s + 1)$.

With pole placement, matrix F_c is defined in equation (1.29), with numerical values in equation (1.30), and $Y_2(s) = \frac{1}{1+\alpha_1 s+\alpha_2 s^2}V(s)$ (two poles can be chosen because $n_{p2} = 2$). In that case, $\det(sI - A - sBF_c) = \frac{R_1\cdot R_a + R_2\cdot R_a + k_m^2\cdot k_b^2}{C_{fs}\cdot J_2\cdot L_a\cdot J_1}\cdot(C_{fs}\cdot R_{fs}\cdot s + 1)\cdot(\alpha_2\cdot s^2 + \alpha_1\cdot s + 1) = 2.9483\cdot 10^7\cdot(2.8\cdot 10^{-4}\cdot s + 1)\cdot(\alpha_2\cdot s^2 + \alpha_1\cdot s + 1)$.

$$F_c = (C_2A^{-1}B)^{-1}[C_2A^{-1} + \alpha_1 C_2 + \alpha_2 C_2 A] \tag{1.29}$$

$$F_c = \begin{bmatrix} 0.18824 - 245.6413\alpha_2 & 8.4319 + 52.7143\alpha_2 - 137.559\alpha_1 & 8.4319 - 75.8319\alpha_2 & 1 \end{bmatrix} \tag{1.30}$$

The differential equation verified by the output variable $y_2(t)$ with the Derivative State Feedback control law defined by equation (1.18), with matrices G and F_p defined in (1.23) and matrix F_c in (1.29) is written in equation (1.31). Parameters α_1 and α_2 can be arbitrarily chosen, according to the poles of the closed loop model.

$$\alpha_2 \ddot{y}_2(t) + \alpha_1 \dot{y}_2(t) + y_2(t) = v(t) \tag{1.31}$$

Then, the two DSF control laws are applied, Fig. 1.17 and Fig. 1.18. The simulations are proposed in two ways: at first for DSF without pole placement using matrices G, F_p and F_c in (1.28) and then for DSF control with pole placement where matrix F_c is defined in (1.30). Parameters have been chosen as $\alpha_1 = 15/50$ and $\alpha_2 = 1/50$, poles are arbitrarily chosen equal to -5 and -10. In both cases, the Disturbance Rejection is achieved, with best results for the second case because the model has only one infinite mode and two modes which are assigned. It can be noticed that in the last case, the control input variable $u(t)$ is must efficient (no oscillation with hard value) and that the output variable $y_2(t)$ is equal to the input variable $v(t)$ in less than 2 s without oscillation.

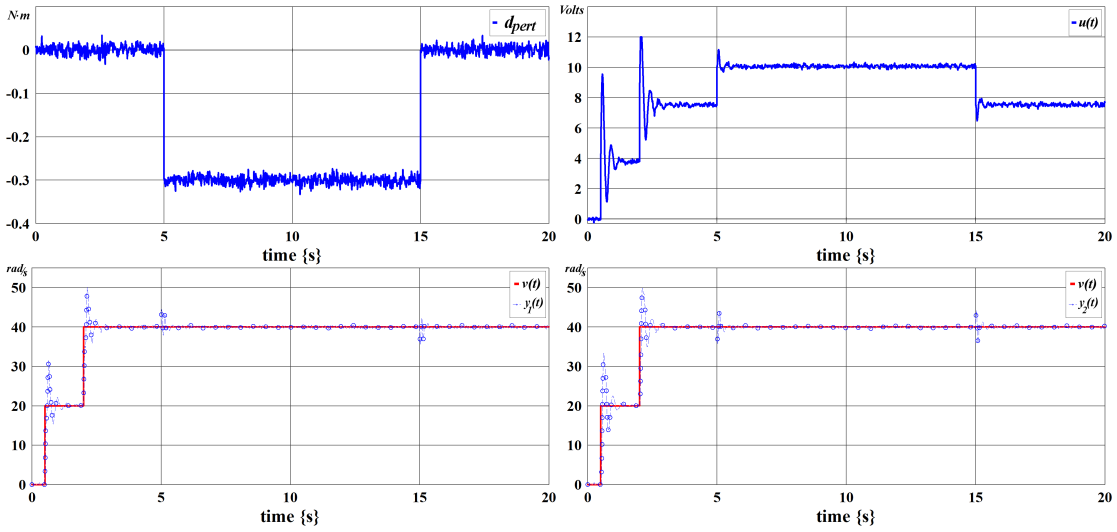

Figure 1.17 – Disturbance Rejection with DSF without pole placement.

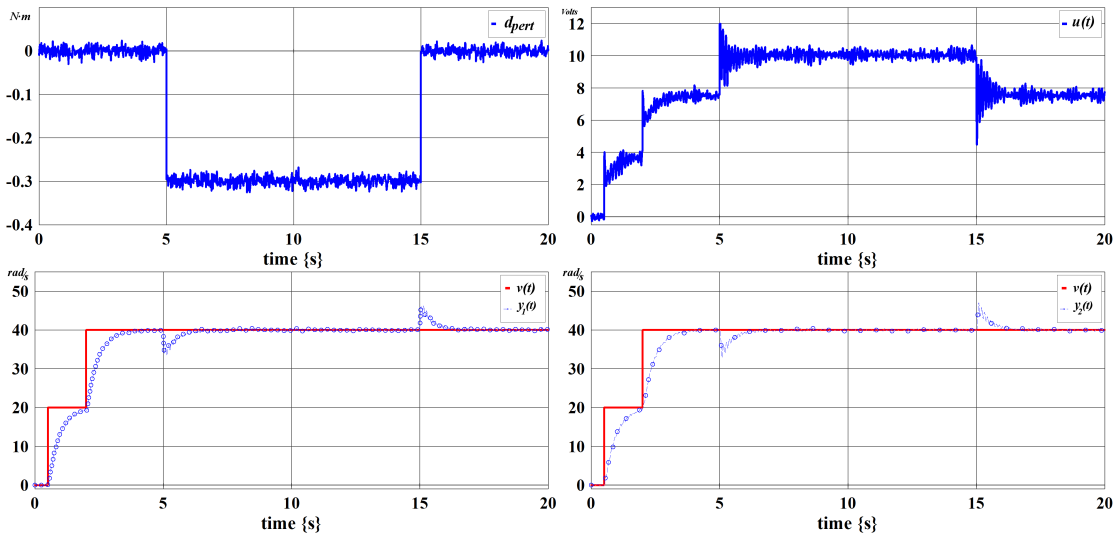

Figure 1.18 – Disturbance Rejection with DSF with pole placement.

1.7 Conclusion

In this chapter, different controllers have been recalled in order to solve the Disturbance Rejection problem. The Torsion-Bar system is used as a case study. We proved the validity of the Bond Graph model and a structural approach is used as a basis for the study of the model properties before the synthesis of the control law. A solution via Derivative State Feedback (DSF) control for the Disturbance Rejection Problem is recalled. The aim is to propose some contributions in this way, first with the concept of Unknown Input Observer (UIO) which is the object of the next chapter.

Chapter 2

Unknown Input Observer (UIO): Background and new developments

2.1 Introduction

In this chapter, we consider linear time-invariant perturbed systems described by a state-space representation (2.1), where $x(t) \in \mathbb{R}^n$ describes the state vector, $y(t) \in \mathbb{R}^p$ is the vector of measurable variables (outputs). The vector $u(t) \in \mathbb{R}^m$ represents the known input variables, whereas $d(t) \in \mathbb{R}^q$ is the vector which represents the *unknown input variables*.

$$\begin{cases} \dot{x}(t) = Ax(t) + Bu(t) + Fd(t) \\ y(t) = Cx(t) \end{cases} \tag{2.1}$$

Assumption 2. *A, B, F, C are known constant matrices of appropriate dimensions.*

Generally, most of the state variables cannot be measured. At most, they are often subject to the effects of unknown inputs. We can speak of perturbed systems, or systems with unknown inputs.

This chapter is addressing the presentation of some works dealing with the estimation of unknown inputs, but also state variables. An unknown input can represent different effects in a system such as disturbances, perturbations, failures, modelling error, noise or non-linearities. The unknown input estimation and state observability problem (UIO) is a well-known problem and different approaches give solvability conditions and constructive solutions for this problem.

As for the Disturbance Rejection Problem (DRP), most of the UIO approaches require the analysis of the structural invariants of the model which play an essential role in this problem. In a similar manner, the infinite structure of the model is related to solvability conditions and the finite zeros (finite structure) are directly related to stability conditions of the observer. The concepts of poles and zeros are recalled in section 1.2, see also appendix A.

In this chapter, for an easy understanding, the UIO observer is first developed for the SISO case from a mathematical point of view. Three classical approaches are first recalled, namely the PI approach, the approach based on inverted matrices and finally an algebraic approach.

Moreover, since the developed work in this research is mainly based on the bond graph representation, a section is dedicated to UIO with bond graphs. Finally, since we compare the efficiency of different approaches from theoretical and practical point of view, the experimental system presented in Section 1.5 is worked out as a specific application. Different simulations are compared, mainly from the bond graph model and the schematic diagram given by *20-Sim®*. Finally, simulation results are compared with data acquired from the real Torsion-Bar (T-B) system.

In the end of this chapter, section 2.3 , new specific developments are proposed.

2.2 Comparison between UIO approaches

Many of the issues and associated problems of Linear Time-Invariant (LTI) systems have been studied for a long time. This section is dedicated to the presentation of different backgrounds. We recall previous works for observer analysis and synthesis for LTI systems with unknown inputs, thus with different methodologies. In the literature, many works have been proposed for modelling dynamical systems, while studying system properties for control design and estimation (stability, controllability, observability, Input-Output decoupling, etc.), Fault Detection Isolation (FDI) analysis, and many other problems.

2.2.1 Some classical approaches

In order to solve the UIO problem for systems defined in equation (2.1), some conditions are often necessary, depending on the proposed approach. A well-known one, which is a necessary condition for the existence of an observer is called *observer matching condition* [Kudva et al., 1980, Darouach et al., 1994]. This condition is expression as rank condition for some matrices: $\mathbf{rank}[CF] = \mathbf{rank}[F]$.

Another condition is related to the concepts of *strong* detectability* and *strong observability*, proposed in [Hautus, 1983]. The strong detectability of system with only the unknown input vector $d(t)$ corresponds to the minimum-phase condition, directly related to the zeros of a system $\Sigma(C,A,F)$ (finite structure, see Appendix A). The system $\Sigma(C,A,F)$ in (2.1) is strongly detectable iff all its zeros s satisfies $\mathbb{R}e(s) < 0$.

In [Floquet and Barbot, 2006], a solution is proposed when the previous conditions are not satisfied: after implementing a procedure to get a canonical observable form of the model, an unknown input sliding mode observer is designed. This method can also be extended in the non-linear case. Necessary and sufficient conditions are that system $\Sigma(C,A,F)$ is left invertible and minimum phase.

All these conditions are related to the concept of poles of zeros (finite or not) of the system, concepts recalled above.

2.2.1.1 Proportional-Integral (PI) Observer

This observer was reformulated as a High-Order Observer to obtain a robust estimation of output. The representation for the PI observer was given for [Niemann et al., 1995]. Then, it is possible to create the structure shown in Fig. 2.1 and the equation (2.1) is rewritten as (2.2).

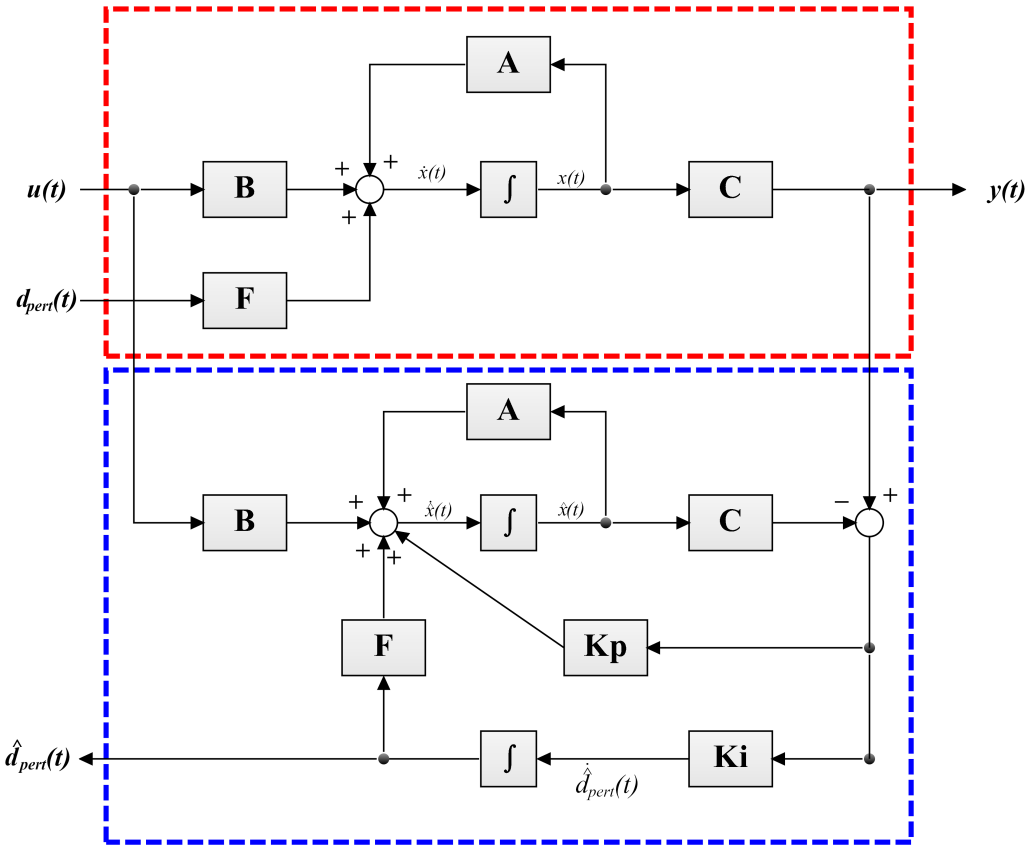

Figure 2.1 – Structure of the PI observer (blue).

$$\begin{cases} \dot{\hat{x}}(t) = A\hat{x}(t) + K_p(y(t) - C\hat{x}(t)) + Bu(t) + F\hat{d}(t) \\ \dot{\hat{d}}(t) = K_I(y(t) - C\hat{x}(t)) \end{cases} \tag{2.2}$$

where, K_p and K_I are the Proportional an Integral gains respectively. These gains cannot be obtained independently, and this complicates the observer's design because there is not a direct method to obtain the gain values.

Applying the PI observer at the system (2.1) and defining the estimation error as $e = x - \hat{x}$ and the estimation perturbation error $\varepsilon = d - \hat{d}$, the next equation (2.3) is obtained.

$$\begin{bmatrix} \dot{e}(t) \\ \dot{\varepsilon}(t) \end{bmatrix} = \begin{bmatrix} A - K_P C & F \\ -K_I C & 0 \end{bmatrix} \begin{bmatrix} e(t) \\ \varepsilon(t) \end{bmatrix} \tag{2.3}$$

With $\xi = \begin{bmatrix} e(t) & \varepsilon(t) \end{bmatrix}^T$, it is easy to write $\dot{\xi} = R\xi$.

The stability condition for the PI observer are associated directly with the eigenvalues of the matrix R. The PI observer is stable if and only if all the eigenvalues (λ) of R are stable ($\mathbb{R}e(\lambda) < 0$). Then, $e(t)$ will be close to zero asymptotically ($\hat{x}(t) \to x(t)$).

2.2.1.2 UIO: Inverted matrices

In [Darouach et al., 1994] and [Darouach, 2009], an observer is proposed with the concept of inverted matrices. State variables as well as unknown inputs can be estimated under some model conditions related to the concept of *strong* detectability* defined in [Hautus, 1983].

Consider the following equations (2.4).

$$\begin{cases} \dot{\xi}(t) = N\xi(t) + Jy(t) + Hu(t) \\ \hat{x}(t) = \xi(t) - Ey(t) \end{cases} \tag{2.4}$$

where $\hat{x} \in \mathbb{R}^n$ is the estimate of x. Matrices N, J, H and E are constant matrices of appropriate dimensions which must be determined such that $\hat{x}$ will asymptotically converge to x.

From the state equation (2.1) and the observer (2.4), it is possible to define the estimation error as equation (2.5), with $P = I + EC$.

$$e(t) = x(t) - \hat{x}(t) = Px(t) - \xi(t) \tag{2.5}$$

The dynamic of the error variable is defined in equation (2.6).

$$\dot{e}(t) = Ne(t) + (PA - NP - JC)x(t) + (PB - H)u(t) + PFd(t) \tag{2.6}$$

The following proposition provides conditions such that equation (2.4) to be a full order observer for the system (2.1).

Proposition 1 ([Darouach, 2009]). *The full-order observer (2.4) will estimate $x(t)$ if the following conditions are verified:*

- *N is a Hurwitz Matrix $\mathbb{R}e(\lambda(N)) < 0$*
- *$PA - NP - JC = 0$*
- *$PF = 0$*
- *$H = PB$*

If all the conditions given in the proposition 1 have been accomplished, then $\lim_{t\to\infty} e(t) = 0$ for any $x(0)$, $\hat{x}(0)$, $d(t)$, and $u(t)$. Therefore $\hat{x}(t)$ is an estimate of $x(t)$.

In [Darouach, 2009], a procedure to obtain an estimation of the perturbation has been proposed and it is related with the existence of the inverse of matrix F from the system (2.1).

Matrix F has an inverse matrix defined as F^+ such that $F^+F = I_q$. The next expression is obtained rewriting the equation (2.1).

$$\begin{cases} d = F^+(\dot{x}(t) - Ax(t) - Bu(t)) \\ \hat{d} = F^+(\dot{\hat{x}}(t) - A\hat{x}(t) - Bu(t)) \end{cases} \tag{2.7}$$

where $\hat{x}(t)$ and $\hat{d}(t)$ are the estimation of $x(t)$ and $d(t)$. The estimation error for the unknown input is written below.

$$e_d(t) = d(t) - \hat{d}(t) = F^+(N-A)e_x(t) \tag{2.8}$$

2.2.1.3 UIO: Algebraic Approach

The observer proposed in [Daafouz et al., 2006] is now recalled for the case Single Input - Single Output (SISO). The observer proposed in [Daafouz et al., 2006] is written in (2.9).

$$\begin{cases} \dot{\hat{x}} = (PA-LC)\hat{x} + Q(y^{(r)} - U) + Ly + Bu \\ \hat{d}(t) = (CA^{r-1}F)^{-1}(y^{(r)} - CA^r\hat{x} - U) \end{cases} \tag{2.9}$$

where, $\hat{d}(t)$ represents the estimation of the perturbation $d(t)$. Matrices Q, U and P are defined as: $Q = F(CA^{r-1}F)^{-1}$, $U = \sum_{i=0}^{r-1} CA^iBu^{(r-1-i)}$ and $P = I_n - QCA^{r-1}$. The order of the zero at infinity of system $\Sigma(C,A,F)$ is defined by r, d is the unknown input variable and y the output variable.

The estimation error for the state variables is given in equation (2.10).

$$\dot{e_x} = \dot{x} - \dot{\hat{x}} = (PA-LC)(x-\hat{x}) \tag{2.10}$$

Assuming that $\lim_{t\to\infty} e_x(t) = 0$ for all $x(0)$, $\hat{x}(0)$, $d(t)$ thus $\hat{x}(t)$ define an estimation of $x(t)$. The estimation error of the unknown input is written as $e_d = d - \hat{d} = (CA^{r-1}F)^{-1}CA^r(x-\hat{x})$.

Then, this observer is stable if the finite structure for system $\Sigma(C,A,F)$ is stable. The necessary and sufficient conditions for the existence of the observer (2.9) for the system (2.1) are given by the following theorem.

Theorem 2 ([Daafouz et al., 2006])**.** *The state $x(t)$ in (2.1) can be estimated (asymptotically) by the full-order observer (2.9) if the next points are accomplished.*

- *The perturbed system (2.1) is observable asymptotically if, and only if, it is left invertible.*
- *The perturbed system (2.1) is* strongly detectable* *(condition of minimal phase).*

The Unknown Input Observer (UIO) performed by the algebraic approach is intrinsic, and the computational complexity is lower than in the case of observer based on inverted matrix calculus, presented in the previous section. The conditions are less restrictive, since the order of zero to infinity can be arbitrary (in particular $CF \neq 0$ is not necessary).

2.2.2 UIO: Bond Graph (BG) Approach

Model $\Sigma(C,A,F)$ is supposed to be a SISO Linear Time-Invariant model. If a somewhat physical approach is proposed, some assumptions are also possible for the state model deduced from a Bond Graph representation.

Assumption 3. *It is supposed that the SISO system $\Sigma(C,A,F)$ defined in equation (2.1) is* Controllable and Observable*, and the state matrix A is invertible.*

For physical systems described with a Bond Graph representation, the assumption 3 is not a restrictive (see Appendix A.2 or [Sueur and Dauphin-Tanguy, 1991]) in particular due to the choice of energy variables for the state-space representation (generalized momentum $p(t)$ and generalized displacement $q(t)$). Moreover, a *derivative causality* assignment is possible for Bond Graph models with the assumption 3 (physical model without null pole).

For many physical systems modelled by (2.1), the observer matching condition is not satisfied. To overcome the restriction imposed by this condition, an observer has been proposed in [Floquet and Barbot, 2006] using the infinite structure of model $\Sigma(C,A,F)$, and the derivatives of input and output variables.

An alternative solution is proposed in this work, where state and unknown input estimation procedures are recalled without the observer matching condition in the SISO case. Note that only some derivatives of the output variables are needed for this observer. Note that the Bond Graph model is thus used as a multidisciplinary tool for this research.

2.2.2.1 UIO:synthesis

The state equation (2.1) can be written as (2.11).

$$\begin{cases} x(t) = A^{-1}\dot{x}(t) - A^{-1}Bu(t) - A^{-1}Fd(t) \\ y(t) = CA^{-1}\dot{x}(t) - CA^{-1}Bu(t) - CA^{-1}Fd(t) \end{cases} \tag{2.11}$$

The disturbance variable and the estimation of the disturbance variable can be written in equation (2.12) if $CA^{-1}F \neq 0$ (model $\Sigma(C,A,F)$ has no null invariant zero).

$$\begin{cases} d(t) = -(CA^{-1}F)^{-1}\left[y(t) - CA^{-1}\dot{x}(t) + CA^{-1}Bu(t)\right] \\ \hat{d}(t) = -(CA^{-1}F)^{-1}\left[y(t) - CA^{-1}\dot{\hat{x}}(t) + CA^{-1}Bu(t)\right] \end{cases} \tag{2.12}$$

The disturbance estimation error is written in equation (2.13).

$$d(t) - \hat{d}(t) = -(CA^{-1}F)^{-1}CA^{-1}[\dot{x}(t) - \dot{\hat{x}}(t)] \tag{2.13}$$

Let r be the infinite zero order for the SISO model $\Sigma(C,A,F)$. This is the smallest positive integer such that $(CA^{r-1}F) \neq 0$. The estimation of the state vector is written as (2.14). The r^{th} output variable derivative is multiplied by matrix K which is used for pole placement.

$$\dot{\hat{x}}(t) = A\hat{x}(t) + Bu(t) + F\hat{d}(t) - AK(y^r(t) - \hat{y}^r(t)) \tag{2.14}$$

If $e(t) = x(t) - \hat{x}(t)$ is the state vector error, from (2.11), (2.12) and (2.14), the state error estimation equation is given by (2.15), where matrix N_{CL_r} is defined in equation (2.16).

$$e(t) = N_{CL_r}\dot{e}(t) \tag{2.15}$$

The matrix N_{OL} is written without matrix K (Open Loop estimation).

$$\begin{cases} N_{OL} = A^{-1} - A^{-1}F(CA^{-1}F)^{-1}CA^{-1} \\ N_{CL_r} = A^{-1} - A^{-1}F(CA^{-1}F)^{-1}CA^{-1} - KCA^{r-1} \end{cases} \tag{2.16}$$

Equations (2.15) and (2.16) are proved for $r = 2$. The extension for any integer r is simple and straight. First, write $y = Cx$. A first order derivative is $\dot{y} = C\dot{x} = C(Ax + Bu + Fd) = CAx + CBu$ with $CF = 0$. Thus $\ddot{y} = C\ddot{x} = CA\dot{x} + CB\dot{u}$. The same equation is written for $\hat{y}$, thus $\ddot{\hat{y}} = C\ddot{\hat{x}} = CA\dot{\hat{x}} + CB\dot{u}$. From these two expressions, a new one is written: $\ddot{y} - \ddot{\hat{y}} = CA\dot{x} + CB\dot{u} - (CA\dot{\hat{x}} + CB\dot{u}) = CA(\dot{x} - \dot{\hat{x}})$. With an easy extension, it is proved that $y^{(r)} - \hat{y}^{(r)} = CA^{r-1}(\dot{x} - \dot{\hat{x}})$, which proves equations (2.15) and (2.16).

The design from a practical point of view of the UIO for a linear SISO Bond Graph model is recalled. Some works related with this issue are [Yang et al., 2013, Tarasov et al., 2013, Tarasov et al., 2014b, Tarasov et al., 2014a, Pichardo-Almarza et al., 2005] where some examples and the Torsion-Bar (T-B) system are treated.

If the state equation (2.1) is written from a Bond Graph model, it is possible to design a Bond Graph model for the state estimation defined in (2.14) because the equation (2.14) is very close to the initial state-space representation in (2.1). Some signal bonds must be added for the disturbance equation defined in (2.12). A block structure for the observer is proposed in Fig. 2.2, where BG_{SYS} is the Bond Graph model of perturbed systems defined by the equation (2.1) and BG_{OBS} is for the observer Bond Graph model based in equation (2.14). This block diagram represented in Fig. 2.2 is also the structure of simulation to estimate variables (unknown inputs and state variables). Note that in the literature, almost none of the UIO models are close to the initial model. With this particular approach, the properties can be studied from a structural point of view, as well from a symbolic point of view for parameters associated to physical elements.

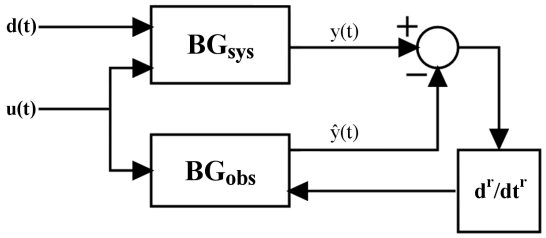

Figure 2.2 – Structure of the simulation to estimate unknown variables.

The *20-Sim*® software is dedicated to simulating Bond Graph models and is used here as well as the *MATLAB*® software for some examples. Some simulation results for the real bar system were proposed in [Tarasov et al., 2014b] as a SISO model with a flat control.

2.2.2.2 Properties of the Observer

Conditions for pole placement in equation (2.15), are studied. Note that the classical error equation is written as $\dot{e}(t) = Me(t)$, with M a matrix to be studied. In our approach, properties of matrix N_{CL_r} are first studied due to the *derivative causality* assignment applied to the Bond Graph model, (BGD), but for simulation and estimation of the experimental system, the classical equation is used. If matrix N_{CL_r} is invertible, a classical pole placement is studied, and the error vector $e(t) = x(t) - \hat{x}(t)$ does not depend on the disturbance variable. The conditions for (2.15)

to be an asymptotic state observer of $x(t)$ is that N_{CL_r} must be a *Hurwitz* matrix, i.e., has all its eigenvalues in the left-hand side of the complex plane. A necessary condition for the existence of the state estimator is in Proposition 2.

Proposition 2. *A necessary condition for the matrix N_{CL_r} defined in (2.16) to be invertible is $CA^{r-1}F \neq 0$.*

Proof. Matrix $N_{CL_r}F$ is equal to $[A^{-1} - A^{-1}F(CA^{-1}F)^{-1}CA^{-1} - KCA^{r-1}]F$, thus it can be rewritten as $N_{CL_r}F = A^{-1}F - A^{-1}F(CA^{-1}F)^{-1}CA^{-1}F - KCA^{r-1}F = -KCA^{r-1}F$. If condition $CA^{r-1}F \neq 0$ is not satisfied, the Kernel of matrix N_{CL_r} is not empty, which means that matrix N_{CL_r} is not invertible and that this matrix contains at least one null mode, thus pole placement is not possible (all its eigenvalues are not in the left-hand side of the complex plane). □

Condition defined in proposition 2 is an extension of the well-known *matching condition* defined in [Hautus, 1983, Darouach, 2009]. It means that the infinite zero order (relative degree) between the disturbance variable $d(t)$ and the measured variable $y(t)$ can be greater than 1, equal to r with this observer. Some other properties are recalled: with matrix N_{CL_r}, r poles can be assigned and the other poles (fixed poles) are the inverse of the invariant zeros of system $\Sigma(C,A,F)$, invariant zeros for the classical error equation $(\dot{e}(t) = N_{CL_r}^{-1}e(t))$.

Proposition 3. *For matrix N_{CL_r} defined in (2.16), r poles can be chosen with matrix K.*

Proof. Appendix B.1 □

Proposition 4. *The eigenvalues of matrix N_{OL} defined in (2.16) are the inverse of the invariant zeros of the system $\Sigma(C,A,F)$ $(n-r$ modes) plus r eigenvalues equal to 0.*

Proof. Appendix B.2 □

Proposition 5. *The fixed poles of the estimation equation error defined in (2.15) are the invariant zeros of the system $\Sigma(C,A,F)$.*

Proof. From proposition 4, the eigenvalues of matrix N_{OL} are the inverse of the invariant zeros of the system $\Sigma(C,A,F)$ with r eigenvalues equal to 0, and since N_{CL_r} is invertible and only r poles can be chosen, all the fixed poles are the non-null eigenvalues. □

2.2.3 UIO SISO case: Simulations

In this section, the Torsion-Bar system is considered as the case study with its bond graph model presented in the figure 1.4. In order to simplify the study, only the disturbance d_{pert_1} is considered. As well, each output variable is considered independently in order to present theoretically the SISO case. Only one example is considered for simulation and for comparison between the different approaches recalled before. Since only one disturbance variable is considered, the infinite zero order is denoted as r, but as well n_{p_i} in oreder to consider the i^{th} output variable $y_i(t)$. To realize the simulations and/or to compute the different parameter for UIO synthesis, the following platforms are used: *MATLAB®*, *Maple* and *20-Sim®*.

UIO: Bond Graph Approach

The poles of matrix N_{CL_r} are placed according to the number of fixed modes. The properties are studied according to the choice of the output variable:

- Study of $\Sigma(C_1, A, F_2)$

  First, properties of the SISO model $\Sigma(C_1, A, F_2)$ are studied (finite and infinite structures). The causal path between the output variable $y_1(t)$ and the disturbance input $Se : d_{pert_1}(t)$ is $Df : y_1 \rightarrow I : L_a \rightarrow GY : k_b \rightarrow TF : k_m \rightarrow I : J_1 \rightarrow Se : d_{pert_1}$. The length of the causal path is equal to 2, then $r = n_{p_1} = 2$. Thus model $\Sigma(C_1, A, F_2)$ has two invariant zeros which can be directly pointed out from the reduced Bond Graph model obtained by removing elements of the causal path between the unknown input and the output detector. The two invariant zeros are stable. They are the fixed modes of the error equation (2.15) of the UIO.

  The estimation of the unknown input variable is defined in equation (2.12) with the appropriate output variable $y_1(t)$ and the matrix C_1. The estimation of the state vector $\dot{\hat{x}}(t) = A\hat{x}(t) + Bu(t) + F\hat{d}(t) - AK(\ddot{y}_1(t) - \ddot{\hat{y}}_1(t))$. For pole placement with matrix $K = \begin{bmatrix} k_1 & k_2 & k_3 & k_4 \end{bmatrix}$, only one pole can be chosen.

- Study for $\Sigma(C_2, A, F_2)$

  Properties of the SISO model $\Sigma(C_2, A, F_2)$ are studied. The causal path between the output variable $y_2(t)$ and the disturbance input $Se : d_{pert_1}(t)$ is $Df : y_2 \rightarrow I : J_1 \rightarrow Se : d_{pert_1}$. The length of the causal path is equal to one, then $r = n_{p_2} = 1$. Thus model $\Sigma(C_2, A, F_2)$ has three invariant zeros. The three invariant zeros are stable and can be directly deduced from the reduced Bond Graph model. They are the fixed modes of the error equation (2.15) of the UIO.

  The estimation of the unknown input variable is defined in equation (2.12) with the appropriate output variable $y_2(t)$ and the matrix C_2. The estimation of the state vector is $\dot{\hat{x}}(t) = A\hat{x}(t) + Bu(t) + F\hat{d}(t) - AK(\dot{y}_2(t) - \dot{\hat{y}}_2(t))$. For pole placement with matrix $K = \begin{bmatrix} k_1 & k_2 & k_3 & k_4 \end{bmatrix}$, one pole can be chosen.

- Study for $\Sigma(C_3, A, F_2)$

  Properties of the SISO model $\Sigma(C_3, A, F_2)$ are studied. The causal path between the output variable $y_3(t)$ and the disturbance input $Se : d_{pert_1}(t)$ is $Df : y_3 \rightarrow I : J_2 \rightarrow R : R_{sf} \rightarrow I : J_1 \rightarrow Se : d_{pert_1}$. The length of the causal path is equal to two, then $r = n_{p_3} = 2$.
  Thus model $\Sigma(C_3, A, F_2)$ has two invariant zeros. The two invariant zeros are stable and can be directly deduced from the reduced Bond Graph model. In that case, a formal expression is $s = -\frac{R_a}{L_a}$ and $s = -\frac{1}{R_{fs} \cdot C_{fs}}$. They are the fixed modes of the error equation (2.15) of the UIO.

  The estimation of the unknown input variable is defined in equation (2.12) with the appropriate output variable $y_3(t)$ and the matrix C_3. The estimation of the state vector is $\dot{\hat{x}}(t) = A\hat{x}(t) + Bu(t) + F\hat{d}(t) - AK(\ddot{y}_3(t) - \ddot{\hat{y}}_3(t))$. For pole placement with matrix $K = \begin{bmatrix} k_1 & k_2 & k_3 & k_4 \end{bmatrix}$, two poles can be chosen.

From the SISO case of the system $\Sigma(C_3, A, F_2)$ some significant parameters and matrices will be presented in order to achieve the simulation.

The input variable $u(t)$ is defined as a step function which is defined in *volts* and its action begins at $0.5\,\mathrm{s}$ with a value of $2\,\mathrm{V}$. At $t = 2\,\mathrm{s}$ the input is incremented at $5\,\mathrm{V}$ and maintained until the end. The unknown input defined as $d_{pert_1}(t) = -0.3\,\mathrm{N\,m}$ with time action between $5\,\mathrm{s}$ and $15\,\mathrm{s}$ and in addition to a Gaussian noise.

For the system $\Sigma(C_3, A, F_2)$ the principal matrices of the UIO are written below.

$$\Omega_d = C_3 A^{-1} F_2 = -44.74189 \neq 0$$

$$\Omega = C_3 A^{r-1} F_2 = C_3 A^{n_{p_3}-1} F_2 = C_3 A F_2 = 402.38534 \neq 0$$

For pole placement the *matrix K* is obtained. The four poles are chosen as $-\frac{1}{R_a/L_a}$, $-1/1500$, $-1/2000$ and $-C_{fs}R_{fs}$ for matrix N_{CL}, but they are the inverse of the classical estimation error equation. Thus:

$$N_{OL} = \begin{bmatrix} -280 \cdot 10^{-6} & 560 \cdot 10^{-3} & -108.4202 \cdot 10^{-21} & 0 \\ 0 & 0 & 0 & 0 \\ 907 \cdot 10^{-6} & 0 & 0 & -867.3617 \cdot 10^{-21} \\ -158.9207 \cdot 10^{-6} & 867.3617 \cdot 10^{-21} & 867.3617 \cdot 10^{-21} & -1.0894 \cdot 10^{-3} \end{bmatrix} \tag{2.17}$$

$$K = \begin{bmatrix} 939.866 \cdot 10^{-9} & 685 \cdot 10^{-12} & 683.752 \cdot 10^{-9} & -123.877 \cdot 10^{-9} \end{bmatrix}^t \tag{2.18}$$

The results are shown in the next three graphics, in Fig. 2.3 the system state variables and their estimations are shown.

In Fig. 2.4, the output variables and estimated output variables are shown. It is possible to observe the accuracy of the estimation even during the action of the unknown input ($d_{pert_1}(t)$).

Finally, the estimation of the unknown input variable $d_{pert_1}(t)$ is displayed in the Fig. 2.5. The unknown input applied to the system was added to the graphic to compare it with its estimation. This is only possible in simulation but it brings the possibility to see the accuracy of the unknown input estimation.

Remark 2. *The simulation takes into account some discrete elements and parameters given by the equipment manufacturer.*

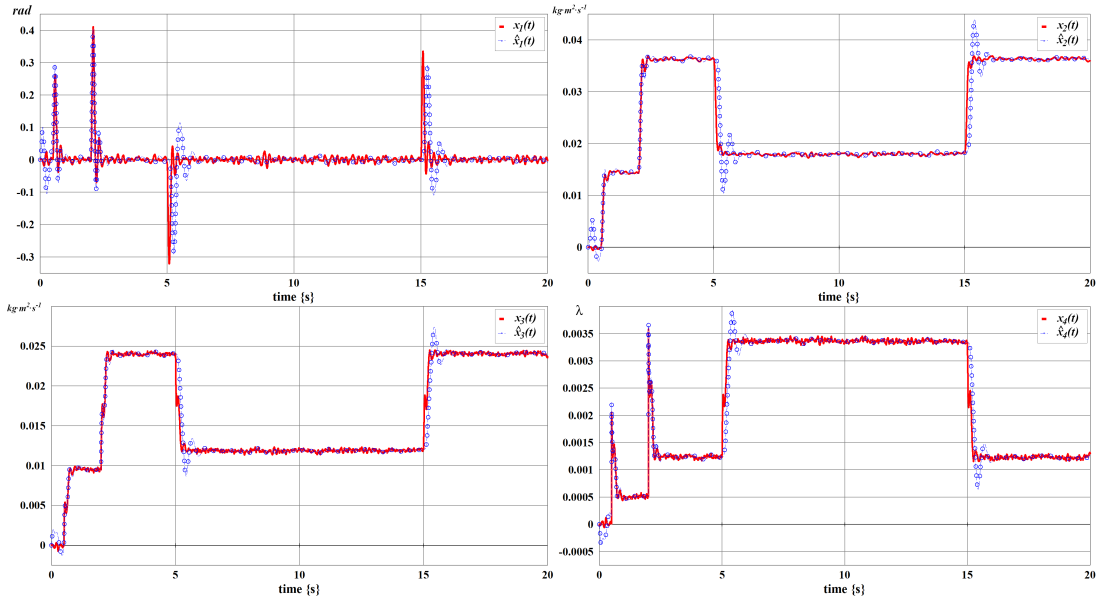

Figure 2.3 – State variables $x(t)$ and their estimations $\hat{x}(t)$.

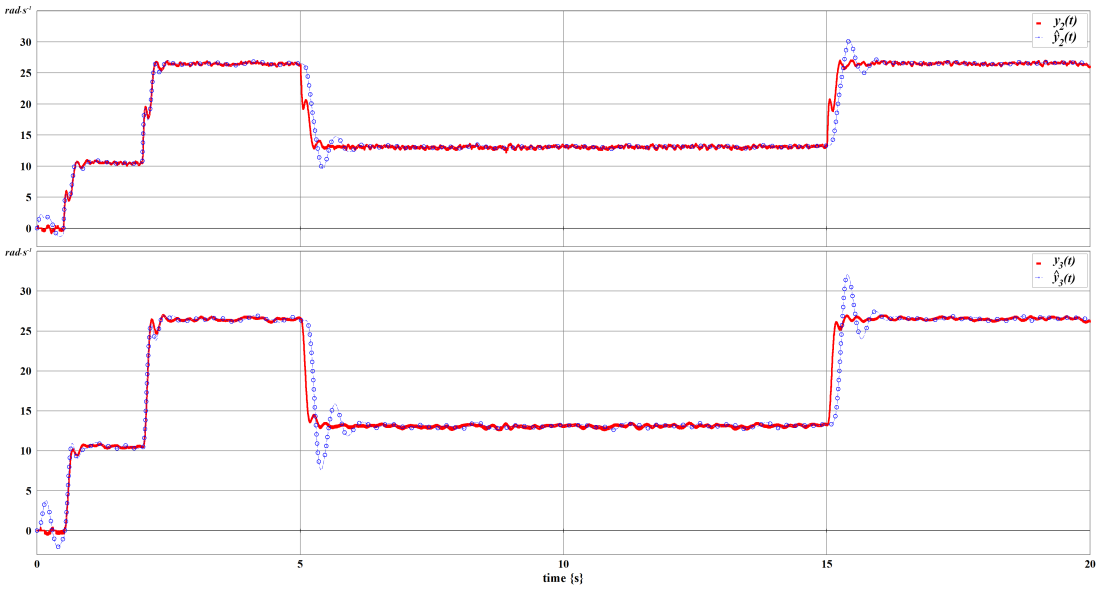

Figure 2.4 – Output variables $y_2(t)$ and $y_3(t)$ and their estimations.

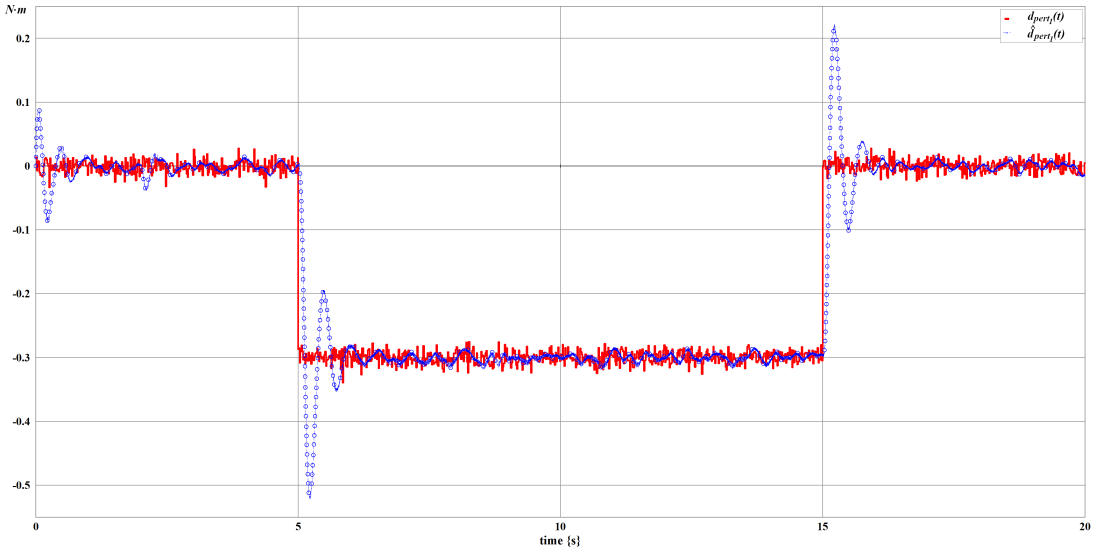

Figure 2.5 – Unknown input $d_{pert_1}(t)$ and its estimation for the SISO case $\Sigma(C_3, A, F_2)$.

PI Observer

This observer is presented in section 2.2.1.1. The equation of the observer is (2.2) while the error equation is (2.3) as $\dot{\xi} = R\xi$, where

$$R = \begin{bmatrix} A - K_P C & F \\ -K_I C & 0 \end{bmatrix}$$

Recalling that the PI observer is stable if and only if all the eigenvalues λ of matrix R are stable ($\mathbb{R}e(\lambda) < 0$), thus $e(t)$ will be close to zero asymptotically ($\hat{x}(t) \to x(t)$).

The eigenvalues selected for matrix R and that achieve the stability property for the PI observer are close to the selected one for the UIO-BG, $\{-\frac{Ra}{L_a}, -\frac{1}{C_{fs}R_{fs}}, -1500, -2000, -2500\}$. Thus, the values for K_P gain and K_I are defined as $K_P = [16422.97, 13.10, 29061.36, -2020.3]^t$ and $K_I = 1.864 \cdot 10^7$. Remarking that the way to obtain the values for the gains is complex and take a lot of time. Different program platforms are used to solve this problem.

Some simulation results are presented in the next graphics. Fig. 2.6 shows the system state variables and their estimations. In Fig. 2.7, the output variables and the estimated outputs are shown. The accuracy of this estimation is good for the different variables (state and output) even during the effect of the unknown input variable $d_{pert_1}(t)$.

In the Fig. 2.8, the estimation of d_{pert_1} (blue) is shown in this simulation, and this estimation is capable to estimate also the added noise. The graphics prove that the PI observer is capable of producing an accurate estimation of the different variables. Remarking that the simulation was done in *Simulink* from *MATLAB*® and some characteristics of the system were ignored in this simulation. They will be taking into account in some next simulations.

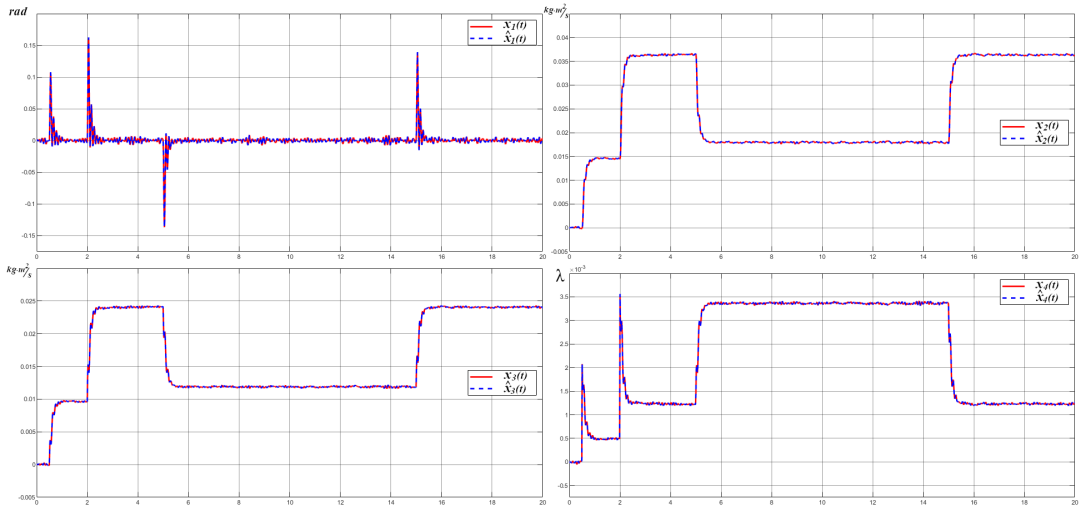

Figure 2.6 – State variables $x(t)$ and their estimations $\hat{x}(t)$.

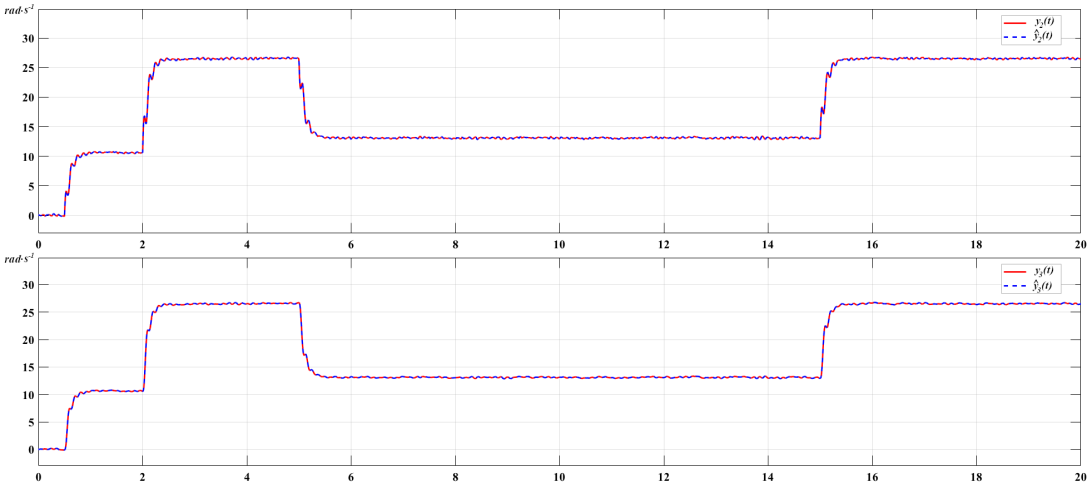

Figure 2.7 – Output variables $y_2(t)$ and $y_3(t)$ and their estimations.

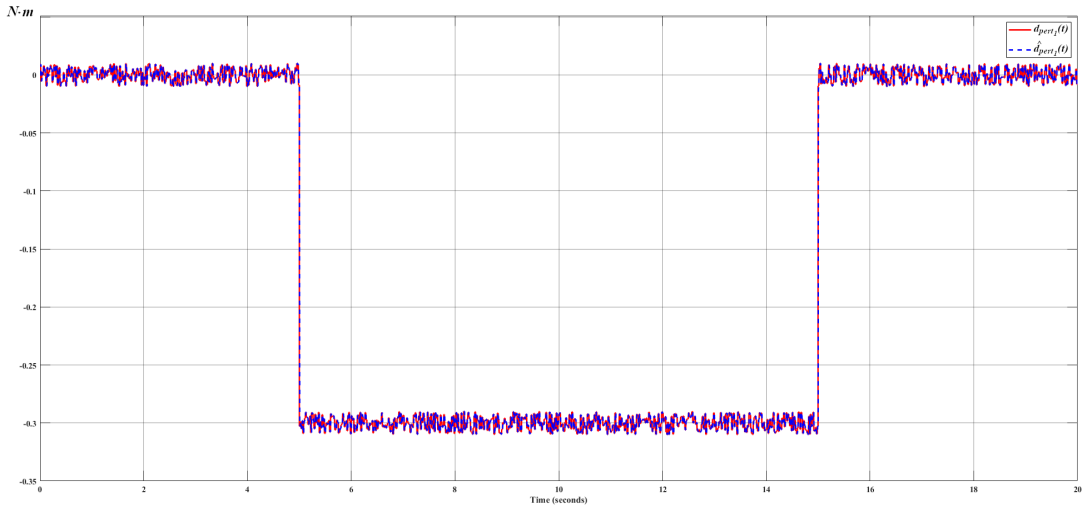

Figure 2.8 – Unknown input variable $d_{pert_1}(t)$ and its estimation for model $\Sigma(C_3, A, F_2)$.

UIO: Inverted Matrices

The observer applying the concept of inverted matrices presented in section 2.2.1.2 has some conditions to be verified. These conditions are related the *Strong* detectability* property [Hautus, 1983], and more precisely one of this condition is the *observer matching condition* that is defined as $\text{rank}[CF] = \text{rank}[F]$.

Rewriting the *observer matching condition* for system $\Sigma(C_3, A, F_2)$, it comes $\text{rank}[C_3F_2] \neq \text{rank}[F_2]$, thus the condition is *not satisfied*. Moreover, conditions given in the proposition 1 are not fulfilled at all. For example, the condition $P * F_2 = 0$ with $P = I + EC_3$ is not verified. In conclusion, the observer cannot be developed for this example.

UIO: Algebraic Approach

Equation (2.9) for this observer is rewritten for the case study, system $\Sigma(C_3, A, F_2)$ and equation (2.19), as for main matrices.

$$\begin{cases} \dot{\hat{x}} = (PA - LC_3)\hat{x} + Q\ddot{y} + Ly + Bu \\ \hat{d}(t) = (C_3AF_2)^{-1}(\ddot{y} - C_3A^2\hat{x}) \end{cases} \tag{2.19}$$

where

$$Q = F_2(C_3AF_2)^{-1} = [0,\ 0,\ 2.48 \cdot 10^{-3},\ 0]^t$$

$$P = I_{4\times4} - QC_3A = \begin{bmatrix} 1 & 0 & 0 & 0 \\ 0 & 1 & 0 & 0 \\ -3.24 & 695.146 & 0 & 0 \\ 0 & 0 & 0 & 1 \end{bmatrix}$$

and $L = [14110.36322,\ 4.794589,\ 53168.4357,\ 0]^t$. The poles for the matrix $(PA - LC)$ are selected as $\{-\frac{Ra}{L_a},\ -\frac{1}{C_{fs}R_{fs}},\ -1500,\ -2000\}$.

Some results are presented in the next graphics. Fig. 2.9 shows the system state variables and their estimations. With this observer, the output variable is not directly estimated, except if it is a state variable. In Fig. 2.10, the estimation of d_{pert_1} (blue) is shown. An error is existing due to some variable derivations and the way to obtain numerical differentiation, (see following remarks, section 2.2.4.1). Some specific filters are added in order to proceed this simulation.

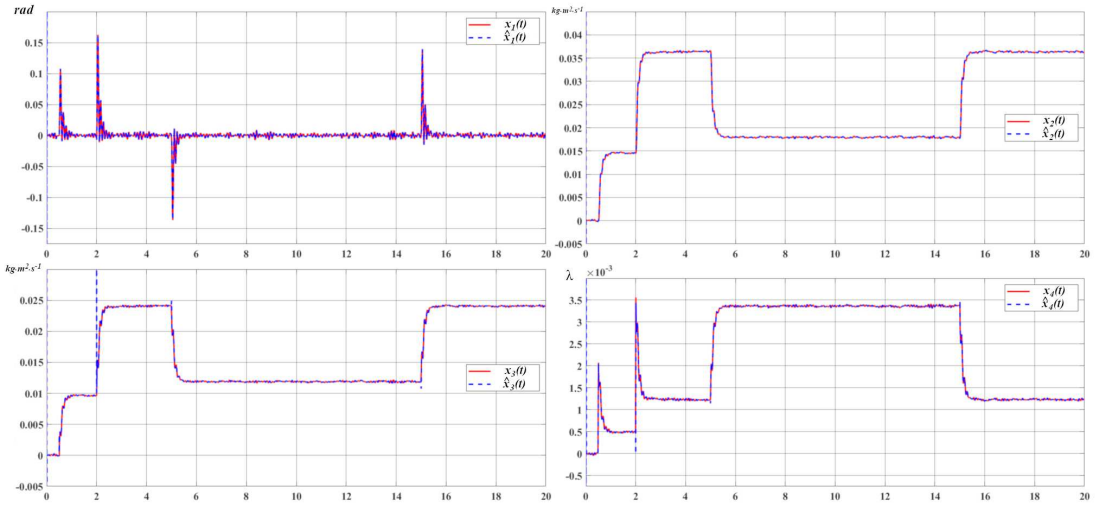

Figure 2.9 – State variables $x(t)$ and their estimations $\hat{x}(t)$.

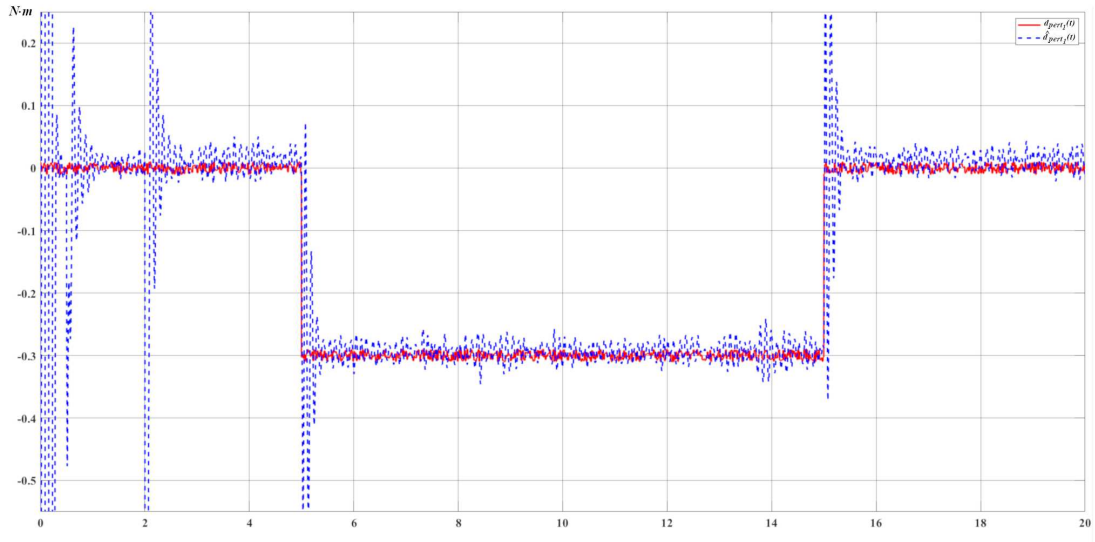

Figure 2.10 – Unknown input variable $d_{pert_1}(t)$ and its estimation for model $\Sigma(C_3, A, F_2)$.

2.2.4 Remarks

2.2.4.1 Output Differentiation and Noise

In order to estimate the state vector $x(t)$ and the disturbance variable $d(t)$, output differentiation with order r (relative degree of model $\Sigma(C,A,F)$) is necessary for the measured output variables as for their estimations. It is a classical practice for control and estimation, as in [Floquet and Barbot, 2006], where differentiation of input variables is also necessary. Literature offers many ways for solving the output or input differentiation problem. Numerical differentiation of signals that come from measures is thus a classical problem in signal processing and automation, and many problems have been solved by creating algorithms for approximation of derivatives (*forward-difference formula, backward-difference formula, automatic (algorithmic) differentiation, etc.*) [Griewank and Walther, 2008, Burden and Faires, 2011].

The numerical methods for approximation of derivatives of measurable signals can be used to obtain signals which are not possible through measurements and reconstruct the missing system data.

There exist many ways in the literature to derivate signals. Some common features are the precision between derivative estimation and noise sensibility and perturbations. Noise or perturbations are the principal troubles for developing derivation algorithms. Most of them assume some features of derivate signal and noise (perturbation) of this derivation.

Different approaches are used for different situations such as Linear Systems [Luenberger, 1971, Pei and Shyu, 1989, Carlsson et al., 1991, Diop et al., 1994, Al-Alaoui, 1993, Dabroom and Khalil, 1997, Levant, 1998, Bartolini et al., 2000, Levant, 2003, Mehdi, 2010], Non-Linear Systems [Mboup et al., 2007], Linear Time-Variant Systems [Chitour, 2002] or Discrete Systems [Dabroom and Khalil, 1999]. These approaches can be classified by two principal classes: a) Model Approach or b) Signal Approach.

In our work, simulations and applications of control laws and estimation algorithms are performed using *MATLAB® 20-Sim®* and *20-Sim 4C®* software, [Kleijn, 2013]. Good approximations have been obtained.

Moreover, for the real Torsion-Bar system, the sensors are incremental encoders with a maximum counting frequency, [Kleijn, 2008]. The outputs variables are subject to a loss of data or incorrect information because of the treatment of the signal from the encoders, or due to vibrations on the entire model. The noise is a fundamental aspect of many systems which use communication methods. At the signal abstraction, the additive white Gaussian noise is often a good noise model or in other words it is a decent noise approximation of many systems. An advantage to use this Gaussian noise is that it's very easy to deal with mathematically (and translate into discrete algorithms), making it an attractive model to be used [Balakrishnan and Verghese, 2012]. For the Torsion-Bar system, many realizations of the signal noise associated to the estimated variable $\hat{d}_{pert}$ have been considered. The distribution of frequency (or frequency spectrum) of d_{pert} has a Gaussian form ("Bell form") and for this reason the Gaussian noise block in *20-Sim®*.

The robustness is an attribute given to controllers when the controlled system works under effects of perturbations, incertitude, parameter changing, etc., and guarantee a good performance

in the results. There are some works related to the Bond Graph methodology for analysis and modelling of almost linear systems, e.g. the estimation of non-linear parameters of dynamical systems using the concept of unknown input observer dedicated to linear systems [Tarasov et al., 2014a], the robust Fault Detection Isolation (FDI) with respect to uncertainties given into a bond graph representation in Linear Fractional Transformations (LFT) configuration [Djeziri et al., 2007, Djeziri et al., 2006, Kam and Dauphin-Tanguy, 2005] or approaches in order to know whether a system will still operate as intended when some system parameters vary slightly [Borutzky and Dauphin-Tanguy, 2004, Borutzky and Granda, 2002].

In a way, the robustness of our approach will be proved by comparison of theoretical results applied on the real Torsion-Bar system (simulations) and results on the real plant. It will be proved to be efficient in the next chapters where differentiation is used for estimation as well for control synthesis using real measured signals and their derivatives.

2.2.4.2 Summary

Some important features from previous sections are summarized in different tables. There are many works that give different points of view for analysing and developing different observers. Some works are in [Bakhshande and Söffker, 2015, Hidayat et al., 2011, Al-Bayati and Skaf, 2010, Radke and Zhiqiang Gao, 2006].

Features / Observer	Unknown Input Estimation	State Estimation	Robustness performance and Stability improvement	Requires noise information	Requires accurate system model	Based on disturbance model	Complexity	Graphic approach
Kalman Filter		⋆	⋆	⋆	⋆		⋆	
Extended Kalman Filter		⋆	⋆	⋆	⋆		⋆	
Luenberger Observer		⋆			⋆			
PI observer	⋆	⋆	⋆					⋆
UIO:inverse Matrix	⋆	⋆	⋆			⋆	⋆	
UIO algebraic approach	⋆	⋆	⋆			⋆	⋆	
UIO-BG approach	⋆	⋆	⋆			⋆		⋆

Table 2.1 – Table to compare different observers

Properties in table 2.1 had been selected for the importance in the present thesis. The Kalman filter and the observer mentioned in table 2.1 were taken from different bibliographies, some are [Kalman et al., 1969, Luenberger, 1971]. Note that the PI-observer is one of the more complex, due to the way to design its gain matrix, [Bakhshande and Söffker, 2015], but it gives good results.

Table 2.2 shows some properties of the UIO presented in this previous section with the bond graph approach. In the next section, we propose new developments of the observer for the MIMO case.

2.3 UIO-BG: Multiple Input - Multiple Output (MIMO) case

In this section, three specific types of MIMO models are studied: non-square models with only one disturbance input, square models without null invariant zeros and square models with one null invariant zero. Theoretical developments can be easily achieved from these three specific cases.

2.3.1 Non-Square Model

In order to simplify the presentation and proofs, first a non-square model with one unknown input variable ($q = 1$) and p output detectors is studied, then a square model with two unknown input variables and two output detectors is studied ($p = q = 2$) in the next section.

The concept of row and global infinite zero order of the model $\Sigma(C,A,F)$ (recalled in appendix A.1) is used in this part. Usually, this concept is proposed for control purposes (row by row input-output decoupling problem with a regular Static State Feedback (SSF) law, or Disturbance Rejection (DR)), and thus for the model $\Sigma(C,A,B)$. In this work, the order of the infinite zero for the row sub-system $\Sigma(C_i,A,F)$ is denoted as n_{p_i}.

2.3.1.1 UIO: Synthesis

It is supposed without restriction that $n_{p_1} \leq n_{p_i}\,; i = 2,\cdots,p$. The state equation (1.1) is now rewritten as (2.20), with $y_1 = C_1 x(t)$ the first output variable and $\bar{y}_1 = \bar{C}_1 x(t)$ is the set of $p-1$ output variables (except $y_1(t)$).

$$\begin{cases} x(t) = A^{-1}\dot{x}(t) - A^{-1}Bu(t) - A^{-1}Fd(t)\,, \\ y_1(t) = C_1A^{-1}\dot{x}(t) - C_1A^{-1}Bu(t) - C_1A^{-1}Fd(t)\,, \\ \bar{y}_1(t) = \bar{C}_1A^{-1}\dot{x}(t) - \bar{C}_1A^{-1}Bu(t) - \bar{C}_1A^{-1}Fd(t)\,. \end{cases} \tag{2.20}$$

If $C_1A^{-1}F \neq 0$ (Model $\Sigma(C_1,A,F)$ has no null invariant zero), variable $d(t)$ and its estimation $\hat{d}(t)$ can be written in equation (2.21), and the estimation error for the disturbance written in (2.22).

$$\begin{cases} d(t) = -(C_1A^{-1}F)^{-1}[y_1(t) - C_1A^{-1}\dot{x}(t) + C_1A^{-1}Bu(t)]\,, \\ \hat{d(t)} = -(C_1A^{-1}F)^{-1}[y_1(t) - C_1A^{-1}\dot{\hat{x}}(t) + C_1A^{-1}Bu(t)]\,. \end{cases} \tag{2.21}$$

$$\left\{ d(t) - \hat{d}(t) = (C_1A^{-1}F)^{-1}C_1A^{-1}(\dot{x}(t) - \dot{\hat{x}}(t))\,. \right. \tag{2.22}$$

The estimation of the state vector is written as (2.23). Matrix K, used for pole placement, is multiplied by the $n_{p_1}^{th}$ derivative of the first output variable, and with the other output variables, with a first order derivation.

$$\dot{\hat{x}}(t) = A\hat{x}(t) + Bu(t) + F\hat{d}(t) - AK \begin{bmatrix} y_1^{(n_{p_1})}(t) - \hat{y}_1^{(n_{p_1})}(t) \\ \dot{y}_1(t) - \dot{\hat{y}}_1(t) \end{bmatrix} \tag{2.23}$$

If $e(t) = x(t) - \hat{x}(t)$ is the state vector error, from (2.20), (2.21) and (2.23), the state error estimation equation is given by (2.24), where N_{CL} is defined in (2.25). Matrix N_{OL} is written without matrix K (Open Loop Estimation).

$$e(t) = N_{CL} \cdot \dot{e}(t) \tag{2.24}$$

$$\begin{cases} N_{OL} = A^{-1} - A^{-1}F(C_1A^{-1}F)^{-1}C_1A^{-1} \\ N_{CL} = A^{-1} - A^{-1}F(C_1A^{-1}F)^{-1}C_1A^{-1} - K \begin{bmatrix} C_1A^{n_{p_1}-1} \\ \bar{C}_1 \end{bmatrix} \end{cases} \tag{2.25}$$

2.3.1.2 Properties of the Observer

Condition for pole placement in equation (2.24) are similar to the SISO case. N_{CL} must be invertible, and also a *Hurwitz matrix*. Properties of the observer are studied. A necessary condition for the existence of the state estimator is proposed in Proposition 6.

Proposition 6. *A necessary condition for matrix N_{CL} defined in (2.25) to be invertible is that $C_1A^{n_{p_1}-1}F \neq 0$ if $n_{p_1} > 1$ or $CF \neq 0$ if $n_{p_1} = 1$.*

Proof. Matrix $N_{CL}F$ is equal to $\left[A^{-1} - A^{-1}F(C_1A^{-1}F)^{-1}C_1A^{-1} - K \begin{bmatrix} C_1A^{n_{p_1}-1} \\ \bar{C}_1 \end{bmatrix}\right] F$, thus it can be rewritten as $N_{CL}F = K \begin{bmatrix} C_1A^{n_{p_1}-1} \\ \bar{C}_1 \end{bmatrix} F$.

If condition $K \begin{bmatrix} C_1A^{n_{p_1}-1} \\ \bar{C}_1 \end{bmatrix} F \neq 0$ is not satisfied, the Kernel of matrix N_{CL} is not empty, then matrix N_{CL} is not invertible and this matrix contains at least one non null mode, thus pole placement is not possible (all its eigenvalues are not in the left-hand side of the complex plane). □

If $n_{p_1} > 1$, then $\bar{C}_1F = 0$ and condition in proposition 6 is equivalent to condition in proposition 2. Some other properties are proved: with matrix N_{CL}, the fixed poles are the inverse of the invariant zeros of system $\Sigma(C,A,F)$. Denote n_{IZ} the number of invariant zeros of system $\Sigma(C,A,F)$.

Proposition 7. *The eigenvalues of matrix N_{OL} defined in (2.25) are the inverse of the invariant zeros of system $\Sigma(C_1,A,F)$ $(n - n_{p_1}$ modes$)$ plus n_{p_1} eigenvalues equal to 0.*

Proof. SISO case. □

Proposition 8. *The fixed poles of the estimation equation error defined in (2.24) are the n_{ZI} invariant zeros of system $\Sigma(C,A,F)$.*

Proof. Appendix B.3 □

2.3.2 Square Model: UIO without Null Invariant Zeros

The UIO problem is studied for the multi-variable case with two unknown input variables and two measured outputs variables $p = q = 2$. It can easily be extended to any square model with $p = q$. It is supposed that system $\Sigma(C,A,F)$ is controllable, observable and invertible. Suppose that $\{n_{p_1}, n_{p_2}\}$ and $\{n'_{p_1}, n'_{p_2}\}$ are the set of row infinite zero orders and global infinite zero orders respectively, of system $\Sigma(C,A,F)$. In the classical Input-Output decoupling problem, the decoupling matrix Ω defined in equation (2.26) is used with matrix B instead of matrix F (with the control input variables). It is proved that the matrix is necessary in this estimation problem.

$$\Omega = \begin{bmatrix} C_1 A^{n_{p_1}-1} F \\ C_2 A^{n_{p_2}-1} F \end{bmatrix}. \tag{2.26}$$

The disturbance vector $d(t)$ and its estimation $\hat{d}(t)$ are written as in the SISO case, equation (2.12), and the disturbance equation error as in equation (2.13), if matrix $CA^{-1}F$ is invertible (model $\Sigma(C,A,F)$ has no null invariant zeros). The estimation of the state vector is written in equation (2.27).

$$\dot{\hat{x}}(t) = A\hat{x}(t) + Bu(t) + F\hat{d}(t) - AK \begin{bmatrix} y_1^{(n_{p_1})}(t) - \hat{y}_1^{(n_{p_1})}(t) \\ y_2^{(n_{p_2})}(t) - \hat{y}_2^{(n_{p_2})}(t) \end{bmatrix}. \tag{2.27}$$

Matrix N_{CL} in this multivariable problem is thus written as (2.28).

$$N_{CL} = A^{-1} - A^{-1}F\left(CA^{-1}F\right)^{-1}CA^{-1} - K \begin{bmatrix} C_1 A^{n_{p_1}-1} \\ C_2 A^{n_{p_2}-1} \end{bmatrix}. \tag{2.28}$$

Condition for pole placement in equation (2.28) are studied. If matrix N_{CL} is invertible, a classical pole placement is studied, and the equation defined in (2.16) for the error vector $e(t) = x(t) - \hat{x}(t)$ is still valid, it does not depend on the disturbance variable. A necessary condition for the existence of the state estimator is proposed in Proposition 9.

Proposition 9. *A necessary condition for matrix N_{CL} to be invertible is that matrix Ω is invertible.*

Proof. Appendix B.4. □

Proposition 10. *In matrix N_{CL} defined in (2.28), $n_{p_1} + n_{p_2}$ poles can be chosen with matrix K.*

Proof. Appendix B.5. □

Proposition 11. *The eigenvalues of matrix N_{OL} defined in (2.16) are the inverse of the invariant zeros of system $\Sigma(C,A,F)$ $(n - (n_{p_1} + n_{p_2}))$ modes) plus $n_{p_1} + n_{p_2}$ eigenvalues equal to 0.*

Proof. Appendix B.5. □

Proposition 12. *The fixed poles of the estimation equation error defined in (2.15) are the invariant zeros of system $\Sigma(C,A,F)$.*

Proof. From proposition 11, the eigenvalues of matrix N_{OL} are the inverse of the invariant zeros of system $\Sigma(C,A,F)$ with $n_{p_1} + n_{p_2}$ eigenvalues equal zero, and since N_{CL} is invertible and since only $n_{p_1} + n_{p_2}$ poles can be chosen, all the fixed poles are non-null eigenvalues. □

2.3.3 Square Model: UIO with Null Invariant Zeros

In this section, an UIO observer is proposed for square models with $p = q = 2$ (two unknown inputs and two measured outputs) with null invariant zeros. The case with only one null invariant zero is considered, it can be easily extended to more general situations.

Equation (2.1) can be written as (2.29).

$$\begin{cases} x(t) = A^{-1}\dot{x}(t) - A^{-1}Bu(t) - A^{-1}Fd(t), \\ y_1(t) = C_1A^{-1}\dot{x}(t) - C_1A^{-1}Bu(t) - C_1A^{-1}Fd(t), \\ y_2(t) = C_2A^{-1}\dot{x}(t) - C_2A^{-1}Bu(t) - C_2A^{-1}Fd(t). \end{cases} \tag{2.29}$$

Consider, without restriction, that $C_1A^{-1}F = 0$. In that case, in the BGD, the causal path length between the output detector associated to variable $y_1(t)$ and the two disturbance inputs is at least equal to 1 (it is supposed to be equal to 1 in order to simplify the theoretical development). In (2.29), the mathematical expression of $y_1(t)$ and of its primitive is then (2.30).

$$\begin{cases} y_1(t) = C_1A^{-1}\dot{x}(t) - C_1A^{-1}Bu(t), \\ \int y_1(t)dt = C_1A^{-1}x(t) - C_1A^{-1}B\int u(t)dt. \end{cases} \tag{2.30}$$

Thus

$$\int y_1(t)dt = C_1A^{-2}\dot{x}(t) - C_1A^{-2}Bu(t) - C_1A^{-1}B\int u(t)dt - C_1A^{-2}Fd(t). \tag{2.31}$$

If model $\Sigma(C,A,F)$ has only one null invariant zero, matrix $C_1A^{-2}F \neq 0$ and matrix $\Omega_d = [(C_1A^{-2}F)^t, (C_2A^{-1}F)^t]^t$ is invertible. A new expression of vector $d(t)$ can be written, as well for $\hat{d}(t)$ from equation (2.31) in the same manner as in the classical case and the error equation is written in (2.34).

$$d(t) = -\Omega_d^{-1}\begin{bmatrix} \int y_1(t)dt - C_1A^{-2}\dot{x}(t) + \delta(u) \\ y_2(t) - C_2A^{-1}\dot{x}(t) + C_2A^{-1}Bu(t) \end{bmatrix}. \tag{2.32}$$

$$\hat{d}(t) = -\Omega_d^{-1}\begin{bmatrix} \int y_1(t)dt - C_1A^{-2}\dot{\hat{x}}(t) + \delta(u) \\ y_2(t) - C_2A^{-1}\dot{\hat{x}}(t) + C_2A^{-1}Bu(t) \end{bmatrix}. \tag{2.33}$$

Where $\delta(u) = C_1A^{-2}Bu(t) + C_1A^{-1}B\int u(t)dt$ and then

$$d(t) - \hat{d}(t) = \Omega_d^{-1}\begin{bmatrix} C_1A^{-2} \\ C_2A^{-1} \end{bmatrix}(\dot{x}(t) - \dot{\hat{x}}(t)). \tag{2.34}$$

The estimation of the state vector $x(t)$ is the same as in equation (2.27) as well as for the state estimation error equation defined in (2.24). Nevertheless, expressions of matrices N_{OL} and N_{CL} have changed since the model has one null invariant zero and thus matrix N_{OL} contains $(n_{p_1}+n_{p_2}+1)$ null eigenvalues. New expressions are written in (2.35).

$$\begin{cases} N_{OL} = A^{-1} - A^{-1}F\Omega_d^{-1}\begin{bmatrix} C_1A^{-2} \\ C_2A^{-1} \end{bmatrix} \\ \\ N_{CL} = A^{-1} - A^{-1}F\Omega_d^{-1}\begin{bmatrix} C_1A^{-2} \\ C_2A^{-1} \end{bmatrix} - K\begin{bmatrix} C_1A^{n_{p_1}-1} \\ C_2A^{n_{p_2}-1} \end{bmatrix} \end{cases} \tag{2.35}$$

A new proposition can be written.

Proposition 13. *The fixed poles of the estimation equation error defined in (2.24) with matrix N_{CL} in equation (2.35) are the strictly stable invariant zeros of system $\Sigma(C,A,F)$. $(n-(n_{p_1}+n_{p_2}+1))$ fixed poles.*

Proof. See appendix B.6 □

As said before, this approach can be easily extended to MIMO models with several null invariant zeros. The idea consists in applying integration on the output variables. Once again, the approach is very similar to the concepts used for the input-output decoupling problem solved with the concept of invariant subspaces calculated for the control synthesis.

Tables 2.3 and 2.4 synthesize properties of the new UIO.

2.4 Conclusion

This chapter is first dedicated to conceptual issues regarding the estimation of state variables as well as disturbances variables for linear perturbed systems described mainly with a state-space representation. In section 2.2, four approaches are briefly recalled and then a comparison is performed thanks to a case study, the Torsion-Bar system.

As well, section 2.3 is dedicated to new conceptual issues regarding the UIO observer in case of some kinds of MIMO linear models, but this time with an approach based on the Bond Graph representation. Note that a state-space approach only could be employed, but thanks to its graphical and causal properties, the analysis of the UIO properties as well as its synthesis can be achieved from a structural point of view, and the mathematical expressions of the UIO can be obtained formally. A distinctive characteristic of this UIO is that it is a so-called BG-observer, because the observer can also be described by a Bond Graph representation.

Assumption and Notation	Structural property of $\Sigma(C,A,F)$	UIO property	Expression for Estimation
Matrix $[A]$ invertible	$\Sigma(C,A,F)$ Structurally Controllable and Observable; No null poles		$\Omega_d = (CA^{-1}F) \neq 0$
Infinite zero order of $\Sigma(C,A,F)$: r	$\Sigma(C,A,F)$ has $n-r$ invariant zeros	$n_{IZ} = n-r$ fixed poles; r poles can be chosen	$\Omega = (CA^{r-1}F) \neq 0$
$n-r$ invariant zeros of $\Sigma(C,A,F)$ are stable		Estimation with stability	$N_{CL} = A^{-1} - A^{-1}\Omega_d^{-1}CA^{-1} - KCA^{r-1}$

Table 2.2 – Table: Assumptions and properties of the UIO-BG (SISO case)

SYSTEM		Ω	N_{CL}
MIMO *No Null IZ* $p>1\,;q=1$ $Non-squareModel$.	$\Omega_d=(C_1A^{-1}F)\neq 0$	*non restrictive condition* $n_{p_1}\leq n_{p_i};i=2,\cdots,p$ $\begin{bmatrix} C_1A^{n_1-1}F \\ \bar{C}_1F \end{bmatrix}\neq 0$	$A^{-1}-A^{-1}\Omega_d^{-1}C_1A^{-1}-K\begin{bmatrix} C_1A^{n_{p_1}-1} \\ \bar{C}_1 \end{bmatrix}$ $n_{IZ}\ \ (fixed\ poles)$ $\bar{C}_1=(C_2^t,C_3^t,\cdots,C_p^t)^t$
MIMO *No Null IZ* $p=q$ *SquareModel* .	$\Omega_d=\begin{bmatrix} C_1A^{-1}F \\ C_2A^{-1}F \\ \vdots \\ C_pA^{-1}F \end{bmatrix}$ $\Omega_d-invertible$	$\Omega=\begin{bmatrix} C_1A^{n_{p_1}-1}F \\ C_2A^{n_{p_2}-1}F \\ \vdots \\ C_pA^{n_{pp}-1}F \end{bmatrix}$ $\Omega-invertible$	$A^{-1}-A^{-1}\Omega_d^{-1}CA^{-1}-K\begin{bmatrix} C_1A^{n_{p_1}-1} \\ C_2A^{n_{p_2}-1} \\ \vdots \\ C_pA^{n_{pp}-1} \end{bmatrix}$ $n_{IZ}=n-\Sigma n_{p_i}\ \ (fixed\ poles)$

Table 2.3 – Main equations and properties when solving the UIO problem (without null invariant zeros)

SYSTEM		Ω	N_{CL}
SISO *With Null IZ* $p = q = 1$.	$\Omega_d^* = (CA^{-(n_{IZ_0}+1)}F) \neq 0$	$(CA^{r-1}F) \neq 0$ $r = relative\ degree$	$A^{-1} - A^{-1}\Omega_d^{-1}CA^{-(n_{IZ_0}+1)} - KCA^{r-1}$ $n - r - n_{IZ_0}\ \ (fixed\ poles)$
MIMO *With* n_{IZ_0} *Null IZ* *Associated to* y_1 $p = q$ *SquareModel* .	$\Omega_d^* = \begin{bmatrix} C_1A^{-(n_{IZ_0}+1)}F \\ C_2A^{-1}F \\ \vdots \\ C_pA^{-1}F \end{bmatrix}$ $\Omega_d^* - invertible$	$\Omega = \begin{bmatrix} C_1A^{n_{p_1}-1}F \\ C_2A^{n_{p_2}-1}F \\ \vdots \\ C_pA^{n_{pp}-1}F \end{bmatrix}$ $\Omega - invertible$	$A^{-1} - A^{-1}\Omega_d^{-1} \begin{bmatrix} C_1A^{-(n_{IZ_0}+1)} \\ C_2A^{-1} \\ \vdots \\ C_pA^{-1} \end{bmatrix} - K \begin{bmatrix} C_1A^{n_{p_1}-1} \\ C_2A^{n_{p_2}-1} \\ \vdots \\ C_pA^{n_{pp}-1} \end{bmatrix}$ $n - \Sigma n_{p_i} - n_{IZ_0}\ \ (fixed\ poles)$

Table 2.4 – Main equations and properties when solving the UIO problem (with null invariant zeros)

Chapter 3

Disturbance Rejection with estimation and Input-Output Decoupling with Derivative State Feedback: Theory and simulations

3.1 Introduction

In the last decades, the Disturbance Rejection Problem (DRP) has received a great deal of attention. The Disturbance Rejection Problem can be considered in multiple ways, depending for example on the full knowledge or not of the physical phenomena, and thus of the availability of a model.

The disturbance rejection problem is presented in chapter 1 as a well-known problem with many real applications and many control strategies that have been designed in order to solve it, guaranteeing stability property. Well established solutions for this problem are proposed in state-space and frequency domain formulations [Hautus, 1979, Wonham, 1985] with stability conditions and also in terms of the unstable zero structure through algebraic treatments in [Verghese, 1978, Malabre and Martínez-García, 1993, Martínez-García et al., 1995] or in [Basile and Marro, 1992] through the geometric approach with structural conditions.

When a state-space model or a transfer function is available, solutions are thus frequently defined in terms of infinite zero structure and in terms of the unstable zero structure, with a static state feedback control law. Structural invariants play an important role in the DR problem, [Hautus, 1980, Wonham, 1985, Morse, 1973, Brunovsky, 1970, Rosenbrock, 1970, Kailath, 1980].

Nevertheless, there is not always a solution through a static state feedback control law for the DRP and an alternative solution based on a Derivative State Feedback (DSF) control law is given in [Moreira et al., 2010] for a particular case. We propose to compare three methodologies in this chapter: The Disturbance Observed-Based Control (DOBC) approach [Li et al., 2014, Mita et al., 1998, Chen et al., 2016], the Active Disturbance Rejection Control (ADRC) [Han, 2009] and the Derivative State Feedback (DSF) proposed in chapter 1. It is applied on the Torsion-Bar (T-B) case study. The simulation results are compared and analysed.

An extension to the Disturbance Rejection (DR) problem is the so-called Input-Output Decoupling problem. As for the DR problem, the Input-Output decoupling problem is not always solvable by regular Static State Feedback (SSF) control laws. The Input-Output decoupling problem are available in the literature since many years [Morgan, 1964, Falb and Wolovich, 1967, Gilbert, 1969]. More complete answers to questions such as the stability property of the controlled system and the intrinsic relation between the finite and infinite structures of the model [Brunovsky, 1970] and decoupling properties are in [Descusse and Dion, 1982], [Dion and Commault, 1993]. The geometric approach is also an alternative way that made clear relations between subspaces and the decoupling properties, [Wonham and Morse, 1970, Basile and Marro, 1992, Commault and Dion, 1982, Martínez-García et al., 1993].

In section 3.4, we present a new solution for the well-known Input-Output decoupling problem of linear square invertible multivariable systems with a derivative state feedback control law. This solution can be addressed particularly if the classical Regular Static State Feedback does not offer any solution. A simple solution to the pole placement problem with a structural analysis of the model properties is achieved with application to a mechanical system.

3.2 Disturbance Rejection - Three approaches

We begin by introducing two of the most recent works that are presented as solutions for the disturbance rejection problem. First, the Disturbance Observed-Based Control (DOBC) [Visioli and Zhong, 2011] on non-linear systems [Chen, 2004], fault tolerant tracking control [Baldini et al., 2018] or other kinds of applications [Tang et al., 2018]. In [Chen et al., 2016], a summary on the existing disturbance uncertainty estimation and attenuation techniques is given, and some applications of these methods were reviewed. Secondly, the Active Disturbance Rejection Control (ADRC) [Han, 2009] with works on non-linear systems [Guo et al., 2016, Zhao and Guo, 2016, Xue et al., 2015] or real applications [Wang et al., 2018, Cui et al., 2018, Wang et al., 2017]. Finally, the Derivative State Feedback (DSF) control law in Bond Graph (BG) approach is developed when the Disturbance Rejection Problem (DRP) is not solvable with a classical Static State Feedback control law. A first development is proposed in chapter 1, [Sueur, 2016]. In this approach, the state vector, its derivative and the disturbance input variables are estimated with the aid of an Unknown Input Observer (UIO) [Tarasov et al., 2014a, Gonzalez and Sueur, 2017, Gonzalez and Sueur, 2018b].

Some simulations of these controllers are applied to the T-B system. Performances are compared and analysed.

3.2.1 Disturbance Observed-Based Control (DOBC)

Disturbance Observer-Based Control (DOBC) has been regarded as one of the widely accepted disturbance-attenuation approaches, also it is easy to understand, to implement and quite intuitive, [Li et al., 2014, Mita et al., 1998, Chen et al., 2016].

In some works, the DOBC is considering as a solution for controllers that need to improve their stability property and tracking performance but usually, they have unsatisfactory disturbance attenuation. For this kind of control, the influence of the disturbances is estimated by a disturbance observer and it is then compensated on the basis of the estimation. The DOBC has its antecedents in many mechatronic applications in the last decades, [Huang and Messner, 1998, Ishikawa and Tomizuka, 1998, Kempf and Kobayashi, 1999, Baldini et al., 2018, Tang et al., 2018], in particular for linear systems.

A basic structure of the Disturbance Observed-Based Control is shown in the Fig. 3.1. In this figure, it is possible to see that the controller consists of two parts: a feedback control part and a feed-forward control part based on a disturbance observer. The feedback control is generally employed for tracking and stabilization of the dynamics of the controlled system. The disturbances and uncertainties on controlled plants are estimated by a disturbance observer and then compensated by a feed-forward control, [Visioli and Zhong, 2011, Li et al., 2014, Chen et al., 2016].

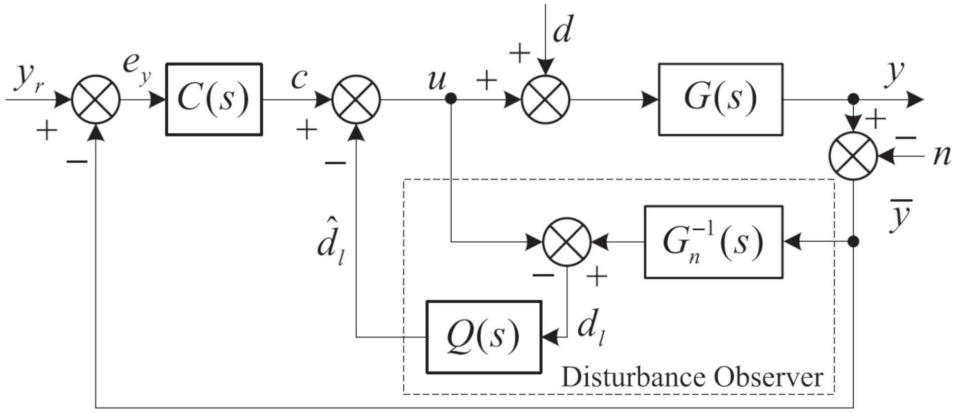

Figure 3.1 – Original structure of DOBC.

From the Fig. 3.1, $G(s)$ represents the real physical plant, $G_n(s)$ is the nominal model used for the controller design, $Q(s)$ is a stable filter, $C(s)$ is the feedback controller output, u is the control input, y is the system output, y_r is the reference signal, $\bar{y}$ is the measured output, n is the measurement noise, d is the external disturbance, d_l is the accumulated disturbance, and $\hat{d}_l$ is the estimate of the accumulated disturbance.

There are many ways to create the DOBC structure while satisfying the performance specifications and stability property for the feedback control part, while the disturbance observer part is designed to reject (or attenuate) disturbance. A way to express the DOBC controller is by

its state-space representation as shown below with the disturbance observer and the feedback control, [Li et al., 2014]. This approach supposes that the perturbation d and its derivatives are bounded. Considering that the system can be represented by the eq. (3.1), and the disturbance observer is written as eq. (3.2), where z is an internal variable of the observer and L is the matrix gain of the observer to be designed.

$$\begin{cases} \dot{x} = Ax + B(u+d) \\ y = Cx \end{cases} \tag{3.1}$$

$$\begin{cases} \dot{z} = -LB(z+Lx) - L(Ax+Bu) \\ \hat{d}_l = z + Lx \end{cases} \tag{3.2}$$

The controller of the DOBC is described by the control law designed in eq. (3.3), where K is the control gain to be designed. The block diagram for this scheme is given by Fig. 3.2.

$$u = Kx - \hat{d}_l \tag{3.3}$$

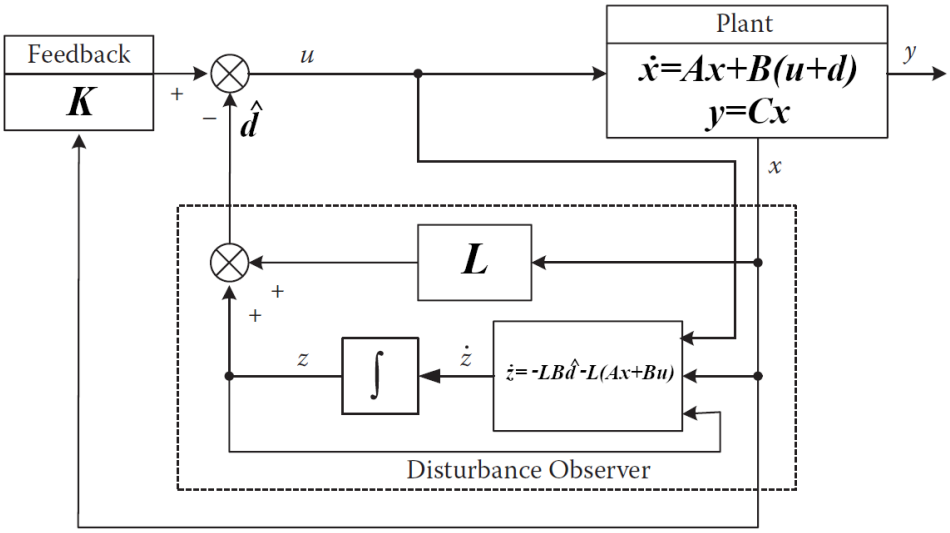

Figure 3.2 – Block diagram of DOBC under the time domain formulation.

If the disturbance estimation error is defined as $e_d = \hat{d}_l - d$, with the disturbance observer (3.2) and the control law (3.3), the closed-loop model is written in equation (3.4).

$$\begin{cases} \dot{x} = (A+BK)x - Be_d \\ \dot{e_d} = -LBe_d - \dot{d} \end{cases} \tag{3.4}$$

It can be shown that closed-loop system is stable if the feedback control gain is selected such that $A+BK$ is *Hurwitz*, and the observer gain matrix is selected such that $-LB$ is *Hurwitz*.

3.2.2 Active Disturbance Rejection Control (ADRC)

When the system cannot be described by a precise analytical model, an alternative solution to the DRP can be the Active Disturbance Rejection Control (ADRC) that is now well-known in modern control theory [Han, 2009]. As for the PID approach, it is an error-based control with a state observer. It is based on an extension of the system model with an additional and fictitious state variable, representing everything that is not included in the mathematical description of the plant. The total disturbance is the sum of internal and external disturbances, usually denoted as a total disturbance. It is estimated online with a state observer and used in the control signal in order to decouple the system from the actual perturbation acting on the plant. For recent mathematical analysis of this design approach designed for practical applications, the readers are referred to [Miklosovic and Gao, 2004, Zhao and Gao, 2010, Wicher and Nowopolski, 2017, Wicher, 2018].

The main idea of ADRC is to treat any unknown dynamics of the system together with external disturbance as a total disturbance and to use an Extended State Observer (ESO) to estimate this total disturbance in real time, and then cancel it in the control law [Han, 2009, Zhao and Gao, 2010]. A precise analytical description of the system is not needed. The unknown parts of dynamics can be considered as the internal disturbance in the plant. In this manner, the exact knowledge of the system model is not needed in order to control it, and particularly in this application, the resonance can be treated, no matter what the frequency is, as part of the total disturbance.

The ADRC control system consists of three basic blocks, [Han, 2009]: The Extended State Observer (ESO), the Rejector block and the Controller. The classical block diagram is shown in Fig. 3.3. Notations applied in this figure are given according to the principal case study (Torsion-Bar System) of this thesis, in order to avoid repetition.

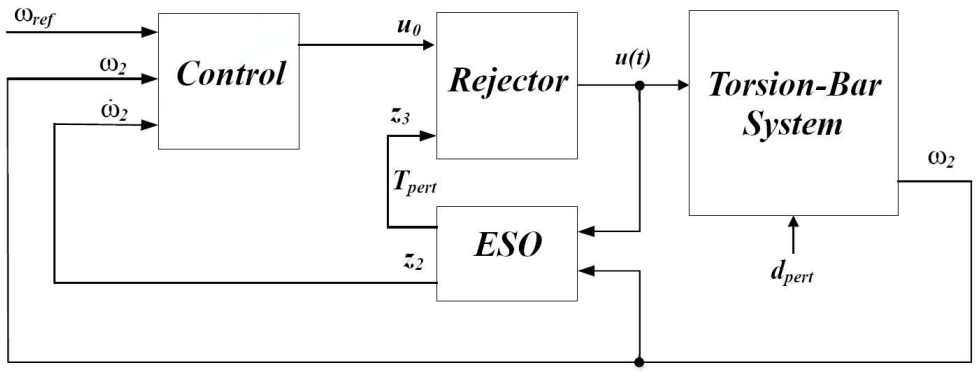

Figure 3.3 – ADRC block diagram.

All the main functional blocks are derived in the following case study, such as the Extended State Observer (ESO), the rejector block and the controller.

For an n^{th} order linear system, the linear ADRC allows us to write the canonical form (3.5), see [Miklosovic and Gao, 2004]. $y^{(n)}$ denotes the n^{th} derivative of the output $y(t)$, $u(t)$ and d_{pert} denote the control input variable and the disturbance variable respectively.

$$y^{(n)}(t) = bu(t) + f(y(t), \dot{y}(t), \cdots, y^{(n-1)}(t), d_{pert}(t), t) \tag{3.5}$$

The extended state observer can be written as equation (3.6). $z_1(t)$ is the estimation of the output variable $y(t)$ and $z_j(t)$ is the estimation of $y^{(j-1)}(t)$, $(j-1)^{th}$ derivate of $y(t)$. At most, $z_{n+1} = f(\cdot)$.

$$\begin{cases} \dot{z}_1 = z_2 + \beta_1(y - z_1) \\ \vdots \\ \dot{z}_{n-1} = z_n + \beta_{n-1}(y - z_1) \\ \dot{z}_n = z_{n+1} + \beta_n(y - z_1) + bu \\ \dot{z}_{n+1} = \beta_{n+1}(y - z_1) \end{cases} \tag{3.6}$$

The observer gains $(\beta_1, \ldots, \beta_{n+1})$ can be calculated by expressions (3.7), where coefficient α_j denotes the binary coefficients of Pascal's Triangle and ω_0 is the cut-off frequency of the extended state observer [Miklosovic and Gao, 2004].

$$\left\{ \beta_j = \alpha_j \omega_0^j = \begin{pmatrix} n+1 \\ j \end{pmatrix} \omega_0^j \right\}_{j=1,2,\ldots,n+1} \tag{3.7}$$

The control law is described by the equation (3.8), where the gains of the controller are calculated in equations (3.9), where ω_c is the controller cut-off frequency.

$$u_c = k_0(r - z_1) - k_1 z_2 - \cdots - k_{n-1} z_n - k_n z_{n+1} \tag{3.8}$$

$$\left\{ K_j = \begin{pmatrix} n \\ j \end{pmatrix} \omega_c^{n-j} \right\}_{j=1,2,\ldots,n+1} \tag{3.9}$$

The so-called rejector in the ADRC control is defined from the combination of the decoupling signal of the total disturbance estimate ($f(\cdot) = z_{n+1}$) and of the controller output u_c, equation (3.10). $u(t)$ is the input signal for the system.

$$u(t) = \frac{u_c(t) - z_{n+1}(t)}{b} \tag{3.10}$$

3.2.3 DSF-UIO-BG

It is known from classical control theory that feedback control with derivatives can be very useful, and even in some cases essential for achieving a desired performance or control objectives. The output feedback, state feedback or the derivative state feedback are used in many works, with robust control performances, [Armentano, 1985], [Kawamura et al., 1988], [Chang et al., 1991], [Le, 1992, Estrada and Malabre, 1997, Bonilla Estrada and Malabre, 2000, Kim et al., 2015].

Some basic principles of the Disturbance Rejection with Derivative State feedback (chapter 1, section 1.4) as well as the ones for the Unknown Input Observer (chapter 2, section 2.3) developed with the Bond graph approach are used in the following section.

It is worth noting that if the disturbance rejection problem is solvable either by a static state feedback control law or a derivative state feedback control law, in most situations it is not possible to measure all the state (or derivative) variables directly: they must be estimated by an observer. Since the disturbance variables are unknown input variables, an Unknown Input Observer (UIO) is added in order to estimate different variables: (derivative) state variables, as well as the disturbances variables.

For linear Bond Graph models, solutions dealing with the finite structure of the model $\Sigma(C,A,B,F)$ for stability conditions of the controlled model and dealing with the infinite structure of the model $\Sigma(C,A,B,F)$, [Gonzalez and Sueur, 2018b] for solvability conditions.

Remark 3. *The solution presented in the present thesis for the disturbance rejection problem is based on the concept of Derivative State Feedback on bond graph models and this solution involves the use of disturbance measurements. The disturbances are considered as unknown inputs and thus the Bond graph-based Unknown Input Observer is synthesized in order to solve the Disturbance Rejection Problem. Thus, the comprehensive solution for the Disturbance Rejection Problem presented in this thesis, from analysis to synthesis of the solutions (controller and observer) is based on the bond graph representation, even if a state-space representation can be exploited for the mathematical point of view. The complete solution can be called* ***Disturbance Rejection via Derivative State Feedback with Unknown Input Observer on Bond Graph approach (DR-DSF-UIO-BG).***

The general structure for the DR-DSF-UIO-BG is described in Fig. 3.4. This structure is used as well for simulation as for application to the real systems. In this figure, block BG_{sys} is the system itself or its bond graph model, block BG_{obs} is for the bond graph model of the observer which is used for the estimation of the state variables, their derivatives and the estimation of the disturbances and at least block BG_{ctrl} is for the calculation of the control law (here with the estimation of the state variables derivatives).

3.3 Disturbance Rejection: Simulations

The previous approaches are applied in this section to the Torsion-Bar system presented in section 1.5 where parameters and features are described, also the Bond Graph model in Fig. 1.4 and the state-space representation in eq. (1.26). A modified bond graph model and its state-space representation (3.11) are presented below, while considering specific measured output and disturbance input variables. Properties of the controllers or observers mentioned in previous chapters are considered in this section.

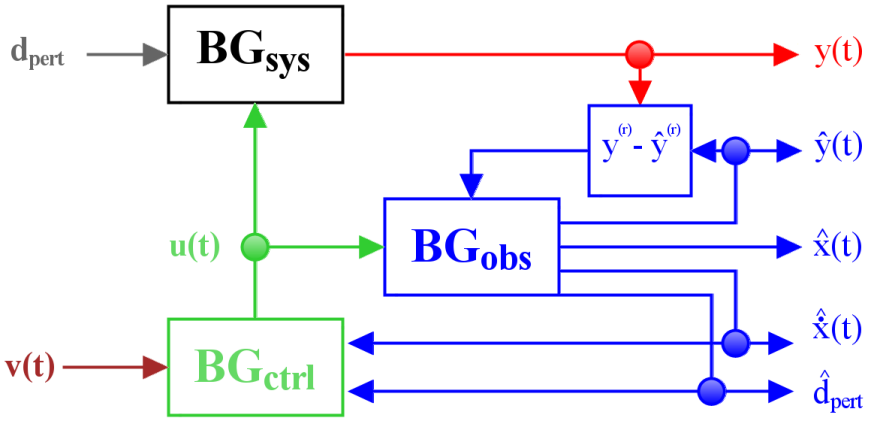

Figure 3.4 – General control structure with system (or model) and observer

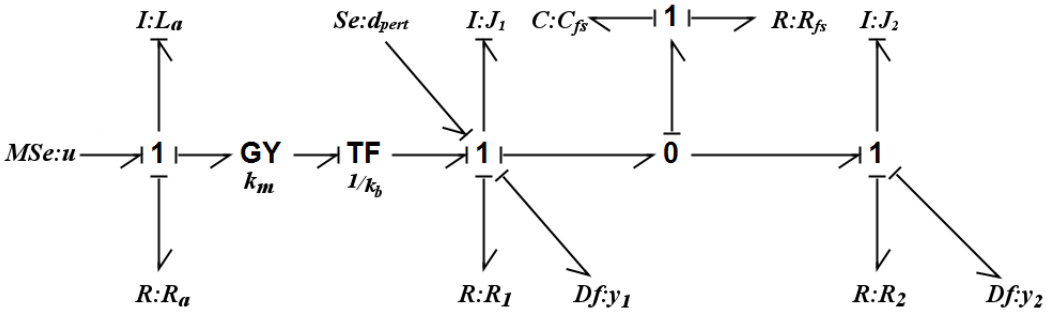

Figure 3.5 – Modified T-B bond graph model with integral causality assignment: BGI.

$$\begin{cases} \dot{x}_1 = -\frac{1}{J_2}x_2 + \frac{1}{J_1}x_3 \\ \dot{x}_2 = \frac{1}{C_{fs}}x_1 - (\frac{R_2+R_{fs}}{J_2})x_2 + \frac{R_{fs}}{J_1}x_3 \\ \dot{x}_3 = -\frac{1}{C_{fs}}x_1 + \frac{R_{fs}}{J_2}x_2 - (\frac{R_1+R_{fs}}{J_1})x_3 + \frac{k_m \cdot k_b}{L_a}x_4 + d_{pert} \\ \dot{x}_4 = -\frac{k_m \cdot k_b}{J_1}x_3 - \frac{R_a}{L_a}x_4 + u \\ y_1 = \frac{1}{J_1}x_3 \; ; \; y_2 = \frac{1}{J_2}x_2 \end{cases} \tag{3.11}$$

Only the variable output $y_2(t)$ is controlled and the measured output variables are $y_1(t)$ and $y_2(t)$. The control input variable $v(t)$ is defined as a step function in rad s^{-1} and its action begins at 0.5 s with a value of 20 rad s^{-1}. At $t = 2$s the input is incremented at 40 rad s^{-1} and maintained until the end. The unknown input is defined as $d_{pert}(t) = -0.3\,\mathrm{N\,m}$ with time action between $5s$ and $15s$. Finally, an important characteristic of the T-B system is adding in these simulations, the *voltage supply limits* to the system that are $\pm 12\,\mathrm{V}$.

The simulation results are displayed in three figures. The input reference $v(t)$, the output variable $y_2(t)$ and its estimation $\hat{y}_2(t)$ in the first figure. The second figure shows the output variable error $e_y(t) = y_2(t) - \hat{y}_2(t)$ and the estimation of the perturbation $\hat{d}_{pert}(t)$ if possible. Finally, the control signal $u(t)$ and the energy consumption J(t) are displayed.

3.3.1 Disturbance Observer-Based Control

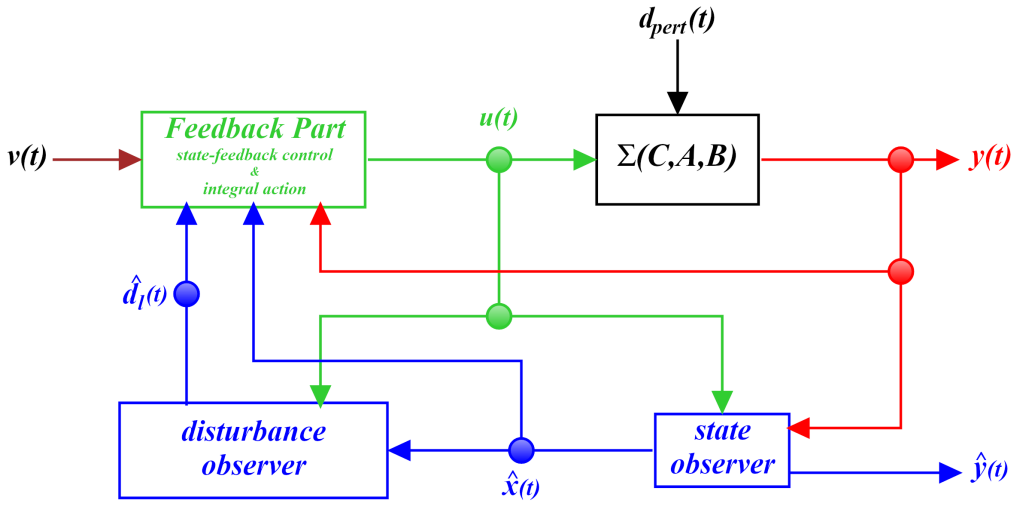

Figure 3.6 – DOBC block diagram, the feedback control part in green and disturbance observer part in blue.

Some structures are analysed in order to achieve a DOBC controller applied to Torsion-Bar System. Block diagram Fig. 3.6 has the same structure that the one mentioned in the DOBC methodology. Two important parts of the DOBC are highlighted in this figure. The *feedback part* contains the state-feedback control with integral action and for the *disturbance observer part* is

divided in two observers. The first is the Disturbance Observer defined in the eq. 3.2 and the second corresponds to the State Observer. This state observer is necessary for the disturbance observer part and feedback part.The state observer is defined as the well-known Luenberger observer, [Swonder and Swonder, 1971, WilliamsII and Lawrence, 2007, Gonzalez et al., 2018]. The integral action has bias and offset handling functionalities. Thus, it is added for attenuation of constant disturbance and set point tracking ($y_2(t)$), [Edwards and Spurgeon, 1996].

Using the separation principle for linear systems, it is possible to analyse separately the controller and observer properties (pole placement).

Consider system description $\Sigma(C,A,B)$ and the adding of integral action in the Fig. 3.7. The state-space representation is rewritten in equation (3.12).

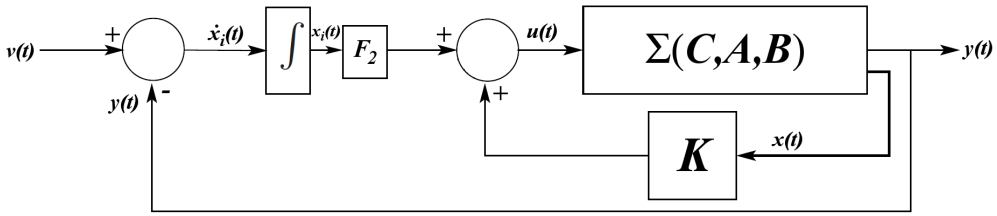

Figure 3.7 – State feedback control with integral action.

$$\begin{cases} \dot{x}(t) = Ax(t) + Bu(t) \\ \dot{x}_i(t) = v(t) - y(t) \\ y(t) = Cx(t) \end{cases} \tag{3.12}$$

The control law is given by $u(t) = Kx(t) + F_2 x_i(t)$ and the augmented system is described below, equations (3.13) and (3.14). The controller matrix gains $F_{aug} = [F_c \; | F_2]$ is chosen such that the eigenvalues of the closed loop state matrix of system (3.14) are all in the left half complex plane. The magnitude of the poles is generally related to physical limitations and to the convergence rate of the system and of the control law. The gains in the control law are calculated based on mathematical functions in *MATLAB®*.

$$\begin{bmatrix} \dot{x}(t) \\ \dot{x}_i(t) \end{bmatrix} = \begin{bmatrix} A & 0 \\ -C & 0 \end{bmatrix} \begin{bmatrix} x(t) \\ x_i(t) \end{bmatrix} + \begin{bmatrix} B \\ 0 \end{bmatrix} u(t) + \begin{bmatrix} 0 \\ 1 \end{bmatrix} v(t) \tag{3.13}$$

$$\begin{bmatrix} \dot{x}(t) \\ \dot{x}_i(t) \end{bmatrix} = \begin{bmatrix} (A+BK) & BF_2 \\ -C & 0 \end{bmatrix} \begin{bmatrix} x(t) \\ x_i(t) \end{bmatrix} + \begin{bmatrix} 0 \\ 1 \end{bmatrix} v(t) \tag{3.14}$$

Considering system $\Sigma(C,A,B)$, the state-space representation for the well-known Luenberger observer is written as $\dot{\hat{x}} = A\hat{x} + Bu + L_S[y - C\hat{x}]$ and the block diagram representation is shown in Fig. 3.8. The observer matrix gain L_S is chosen such that the dynamics of the observer are faster than the observed system, hence, the magnitude of the poles must be larger than the magnitude of the poles in the observed system. The eigenvalues of $(A - L_S C)$ are all in the left-half complex plane.

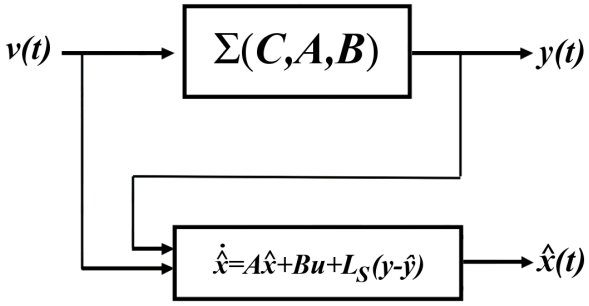

Figure 3.8 – Representation of the Luenberger observer.

Thus, applying this controller to the T-B system and for the control design, the poles are placed at $[-5,-10,-15,-20\ ,-2]$. Values obtained for the control are such $F_{aug} = [-1.2347,\ 14.376,\ -184.66,\ -872.39,\ 1]$. The eigenvalues of $(A - L_S C)$ for the observer are placed at $[-25,\ -20,-15,\ -10]$. Matrix L_S is given in equation (3.15).

$$L_S = \begin{bmatrix} 1 & -0.866 \\ 0.45 \cdot 10^{-3} & 38.57 \cdot 10^{-3} \\ -0.8 & -0.825 \\ 6.56 & 6.707 \end{bmatrix} \tag{3.15}$$

And finally, for the disturbance estimator described in (3.2) is rewritten in (3.16) to be applied on the Torsion-Bar system and the values for the gain matrix $L_d = [l1, l2, l3, l4]$ are defined as $L_d = [100, 100, 100, 70]$.

$$\begin{cases} \dot{z} = -L_d B(z + L\hat{x}) - L_d(A\hat{x} + Bu) \\ \hat{d}_l = z + L_d\hat{x} \end{cases} \tag{3.16}$$

The simulation results are displayed below. In Fig. 3.9, the output and its estimation are shown. The estimated variable $\hat{y}_2(t)$ is different of the output $y_2(t)$. As well, the perturbation variable is attenuated in the output y_2 but not completely rejected.

The cumulated perturbation $\hat{d}_l$ and the error definition $e_y = y_2 - \hat{y}_2$ are shown in the Fig. 3.10.

In the Fig. 3.11, two important information are displayed: the control signal (up) that have a smooth dynamic and the Energy consumption (down) with a value of 432 J after 20 s.

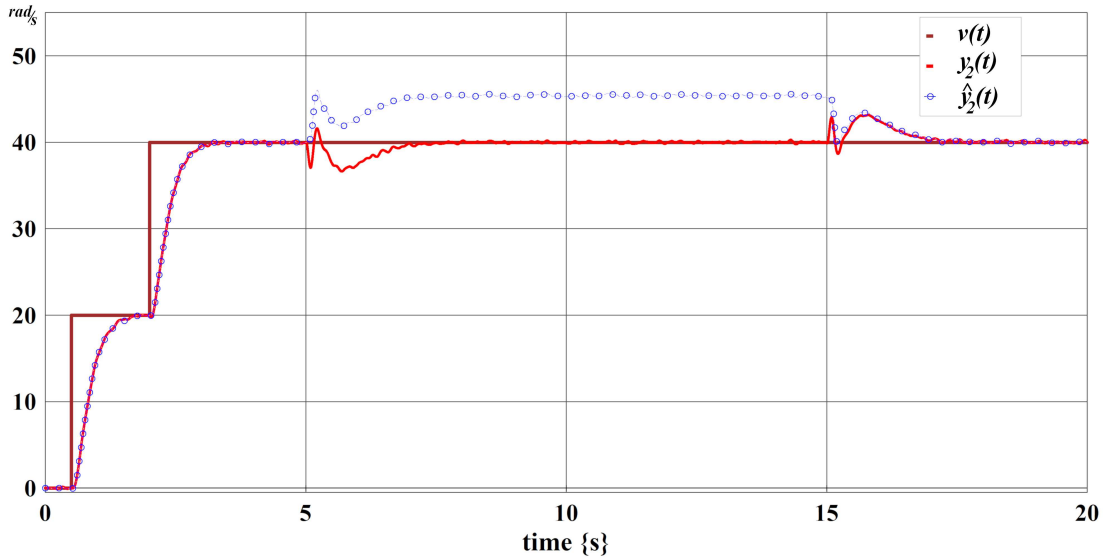

Figure 3.9 – DOBC: controlled output and its estimation.

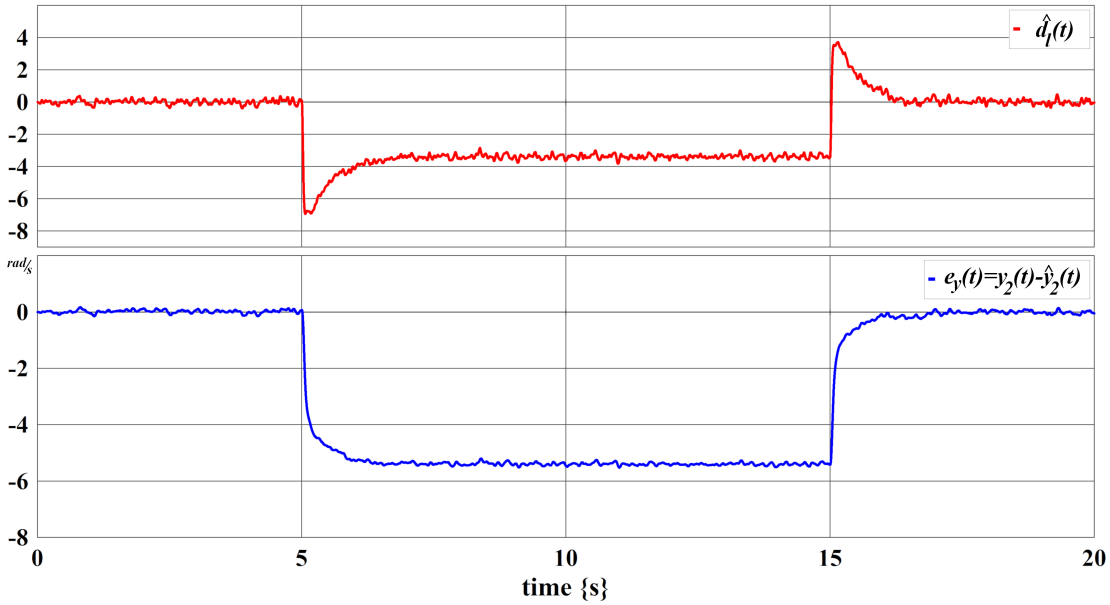

Figure 3.10 – DOBC:Cumulative perturbation $\hat{d}_l$ and the error e_y

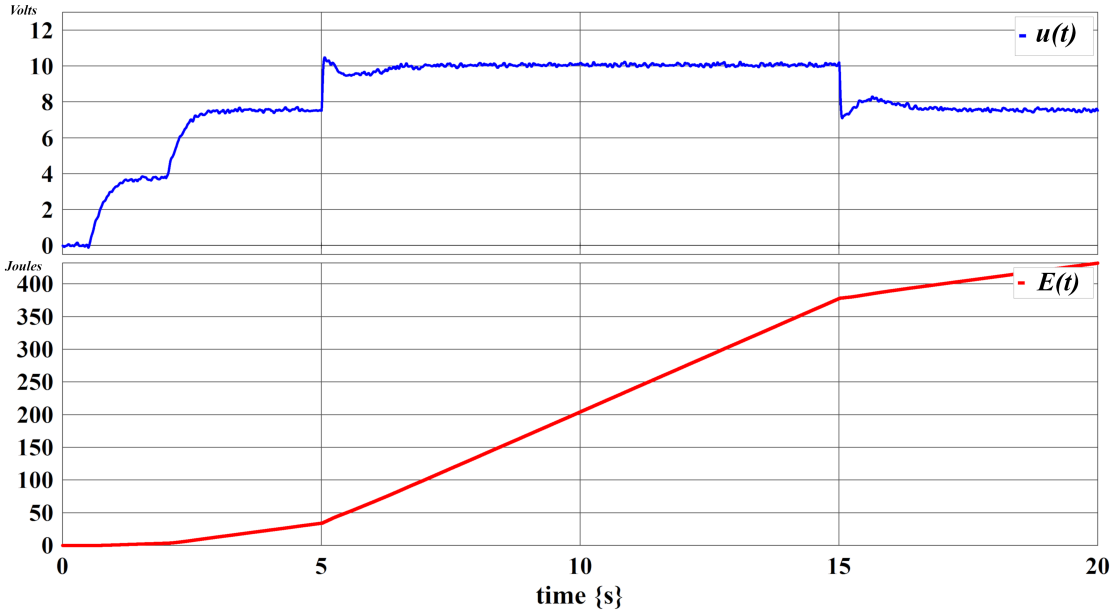

Figure 3.11 – DOBC: control signal $u(t)$ (blue) and energy consumption

3.3.2 Active Disturbance Rejection Control

From the Torsion-Bar state-space representation (3.11), it is possible to obtain the mathematical input-output representation (3.17), where $y_2(t)$ is the load velocity, $u(t)$ is the voltage variable applied to the motor and d_{pert} is the unknown perturbation variable.

$$\dddot{y}_2 + nm_3\ddot{y}_2 + nm_2\dot{y}_2 + nm_1 y_2 + nm_0 y_2 = dn_1\dot{u} + dn_0 u + d_{pert} \tag{3.17}$$

Integrating equation (3.17) one time on both sides, the forth-order system with relative degree 3 becomes a three-order system, where function $f(\ddot{y},\dot{y},y,\int y,\int u,d_{pert})$ includes the external disturbance d_{pert} and internal dynamics. This function represents the total disturbance to be estimated and dn_1 is a constant that have to be calculated or known.

$$\begin{aligned}\dddot{y} &= dn_1 u + (-nm_3\ddot{y}_2 - nm_2\dot{y}_2 - nm_1 y_2 - nm_0\int y + dn_0\int u + \int d_{pert}) \\ &= dn_1 u + f(\ddot{y},\dot{y},y,\int y,\int u,d_{pert})\end{aligned} \tag{3.18}$$

3.3.2.1 Extended State Observer

Rewriting equation (3.18) with a state-space representation, with control variable $u(t)$, output variable $y_2(t)$ and with an additional (extended) state $x_4(t)$, it comes equation (3.19), where $x_1 = y_2$, $x_2 = \dot{y}_2$, $x_3 = \ddot{y}_2$, $x_4 = f(\cdot)$.

$$\begin{cases} \dot{x}_1 = x_2 \\ \dot{x}_2 = x_3 \\ \dot{x}_3 = dn_1 u(t) + x_4 \\ \dot{x}_4 = \dot{f}(\cdot) \end{cases} \tag{3.19}$$

From equation (3.19), the state of the ESO can be designed as equation (3.20), where the estimation error is given as $e_0 = y_2 - z_2$, z_1 is the estimation of y_2 and z_4 estimates the total disturbance $f(\cdot)$.

$$\begin{cases} \dot{z}_1 = z_2 + \beta_1 e_0 \\ \dot{z}_2 = z_3 + \beta_2 e_0 \\ \dot{z}_3 = dn_1 u(t) + z_4 + \beta_3 e_0 \\ \dot{z}_4 = \beta_4 e_0 \end{cases} \tag{3.20}$$

Parameters $\beta_1, \beta_2, \beta_3, \beta_4$ are the observer gains calculated following [Wicher and Nowopolski, 2017, Miklosovic and Gao, 2004]

3.3.2.2 Rejector Block

The rejector is a part of the system where the decoupling signal of the total disturbance estimates z_4 and the virtual control signal u_0 are combined. The output signal of the rejector u_i is the input signal for the plant. This block can be described by (3.21).

$$u_i = \frac{u_0 - z_4}{dn_1} \tag{3.21}$$

3.3.2.3 Controller

The controller is described by equation (3.22), where only the control error is taken from direct velocity measurement of variable $y_2(t)$ while the derivative $\dot{y}_2(t) = z_2(t)$ is estimated by the ESO. The gains of the controller were calculated according to formula [Miklosovic and Gao, 2004, Wicher, 2018].

$$u_0 = K_p(v_{ref} - y_2) - K_{D_1} z_2 - K_{D_2} z_3 \tag{3.22}$$

In regard to ADRC: if ω_0 is the cut-off frequency of the observer with $\omega_0 = 100Hz$, thus parameter values for the ADRC controller are $\beta_1 = 4 \cdot \omega_0$, $\beta_2 = 6 \cdot {\omega_0}^2$, $\beta_3 = 4 \cdot {\omega_0}^3$, $\beta_4 = {\omega_0}^4$, $K_p = 1 \cdot 10^6$, $K_1 = 3 \cdot 10^4$, $K_2 = 300$ and $dn_1 = 43804.58$. The simulation for the ADRC with these parameters is shown below.

In Fig. 3.12, the output and its estimation are shown. The disturbance is rejected, but the output and its estimation overstep the reference signal.

The error $e_0 = y_2 - z_1$ (down) and the total disturbance estimated $f(\cdot)$ (up) are shown in the Fig. 3.13. In this figure, it is possible see the value of the total perturbation $f(\cdot)$ and the error that is close to zero except for changes when the output is under changes (input changes or significant perturbations).

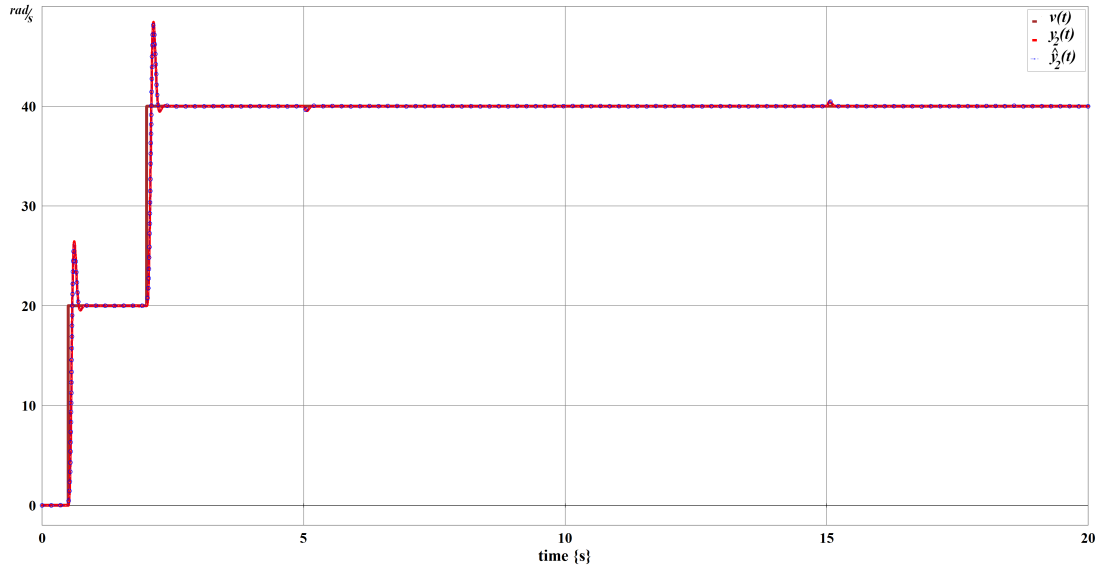

Figure 3.12 – ADRC: controlled output variable $y_2(t)$ and its estimation $z_1(t)$

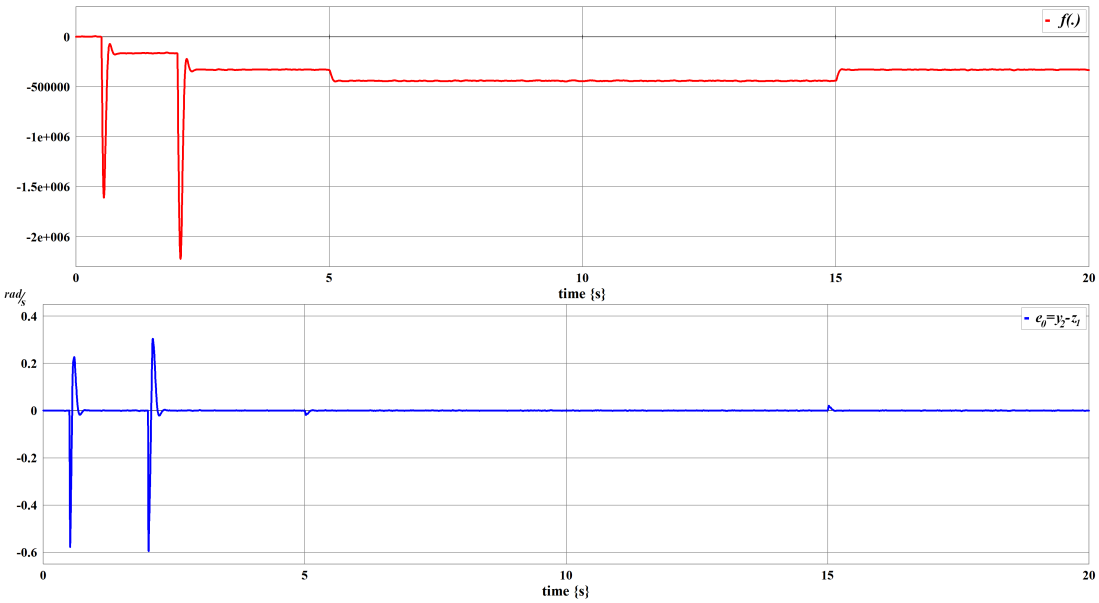

Figure 3.13 – ADRC: Cumulative perturbation $f(\cdot)$ and the error $e_0 = y_2 - z_1$.

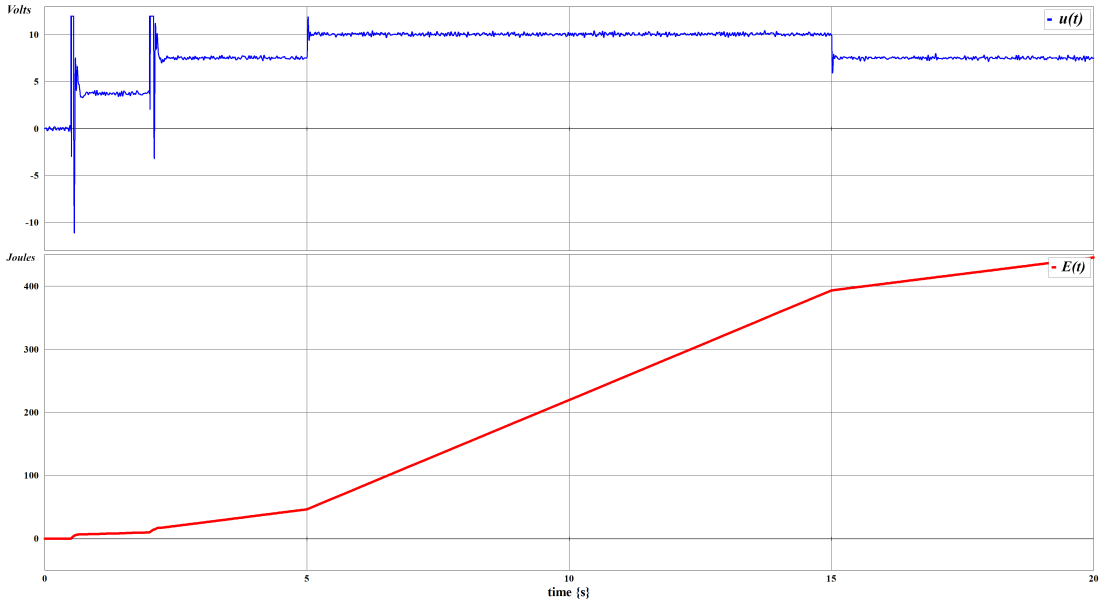

Figure 3.14 – ADRC: input control signal $u(t)$ (blue) and the energy consumption (red)

In the Fig. 3.14, two important pieces of information are displayed: the control signal (up) that have some peak voltages in the dynamic (limited in simulation at ±12 V) and the Energy consumption (down) with a value of around 445 J after 20 s.

3.3.3 Disturbance Rejection by Derivative State Feedback using UIO

The alternative strategy proposed in this thesis is applied now: The Derivative State Feedback (DSF) using Unknown Input Observer (UIO) to reject disturbances developed by Bond Graph approach.

The model $\Sigma(C,A,B)$ associated to the torsion bar system is structurally controllable/observable, a derivative causality assignment can be applied to the bond graph model, as proved in Fig. 3.15 for the bond graph model with preferential derivative causality assignment (BGD). As well, the state matrix A is invertible. The Disturbance Rejection with Derivative State Feedback is applied in the Single Input - Single Output (SISO) case, see chapter 2, and an Unknown Input Observer is used in the Multiple Input - Multiple Output (MIMO) case since two variables are measured, see section 3.2.3 or [Sueur, 2016, Gonzalez and Sueur, 2018b, Gonzalez et al., 2018].

In property 1, we recall the condition for disturbance rejection with DSF. Note that if $n_p \leq n_c$ and the invariant zeros of model $\Sigma(C,A,B)$ are strictly stable, then the DRP with the previous DSF has a stable solution with pole placement.

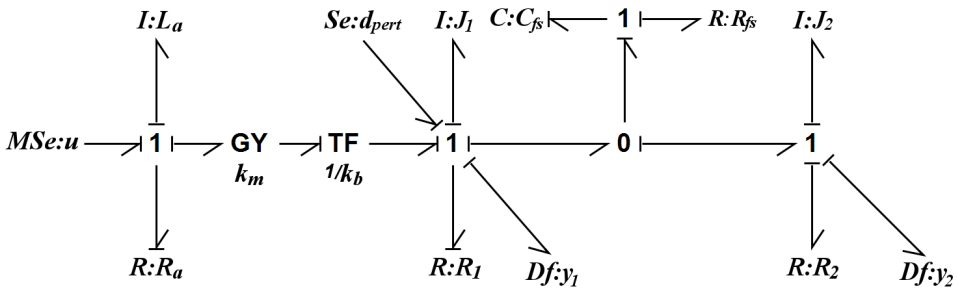

Figure 3.15 – Derivative causality assignment of the bond graph model: BGD.

3.3.3.1 Unknown Input Observer applied to the T-B system

The Unknown Input Observer for this Bond Graph model is now designed, see chapter 2, section 3.2.3. For system $\Sigma(C,A,B,F)$ defined in equation (1.1), $m=1$ (one input control), $q=1$ (one unknown input variable, disturbance) and $p=2$ (two measured variables $y_1(t)$ and $y_2(t)$).

The UIO synthesis is thus proposed with the two output detectors $Df:y_1$ and $Df:y_2$. It is a non-square model. Structural properties of the model $\Sigma\left([C_1^t,C_2^t]^t,A,F\right)$ are studied. The causal path with the first output detector is $Df:y_1 \rightarrow I:J_1 \rightarrow Se:d_{pert}$ and the causal path with the second output detector is $Df:y_2 \rightarrow I:J_2 \rightarrow R:R_{fs} \rightarrow I:J_1 \rightarrow Se:d_{pert}$. The length of these causal paths is equal to $n_{p1}=1$ and $n_{p2}=2$ for $y_1(t)$ and $y_2(t)$ respectively. Since $n_{p1}<n_{p2}$, the estimation of the state vector is written in equation (3.23) and the estimation of the unknown input variable is still defined in equation (2.21). Matrix N_{CL} is written in equations (3.24).

$$\dot{\hat{x}}(t)=A\hat{x}(t)+Bu(t)+F\hat{d}(t)-AK\begin{pmatrix} y_1^{(1)}(t)-\hat{y}_1^{(1)}(t) \\ y_2^{(1)}(t)-\hat{y}_2^{(1)}(t) \end{pmatrix} \tag{3.23}$$

$$N_{CL}=A^{-1}-A^{-1}F(C_1A^{-1}F)^{-1}C_1A^{-1}-K\begin{bmatrix} C_1 \\ C_2 \end{bmatrix} \tag{3.24}$$

Matrix $K=(k_{ij})$ is a 4 by 2 matrix with eight unknown parameters and matrix N_{CL} can be numerically rewritten as:

$$N_{CL}=\begin{bmatrix} -294\cdot10^{-6} & 560\cdot10^{-3}-729.927\cdot k_{21} & -100\cdot10^{-15}-1102.54\cdot k_{11} & -10\cdot10^{-15} \\ -1.37\cdot10^{-3} & -729.927\cdot k_{22} & -1102.54\cdot k_{12} & -1\cdot10^{-12} \\ 0 & -729.927\cdot k_{23} & -1102.54\cdot k_{13} & 0 \\ 100\cdot10^{-18} & -2\cdot10^{-12}-729.927\cdot k_{24} & -2\cdot10^{-12}-1102.54\cdot k_{14} & -1.09\cdot10^{-3} \end{bmatrix} \tag{3.25}$$

From a structural analysis, it can be proved that model $\Sigma\left([C_1^t,C_2^t]^t,A,F\right)$ has one invariant zero, which is the common invariant zero of submodels (C_1,A,F) and (C_2,A,F).

The invariant zero is equal to $z_I = -{}^{R_a}/_{L_a} = -917.91$. The inverse of this invariant zero is a fixed mode for the estimation error equation, *i.e.*, for matrix N_{CL}. If the four poles of matrix N_{CL} are $-{}^{1}/_{917.91}$, $-{}^{1}/_{1000}$, $-{}^{1}/_{2000}$ and $-{}^{1}/_{3401.4}$, matrix K is thus as expressed as:

$$K = \begin{bmatrix} -9.07 \cdot 10^{-17} & 7.672 \cdot 10^{-4} \\ 0 & 1.37 \cdot 10^{-6} \\ 4.535 \cdot 10^{-7} & 0 \\ -1.814 \cdot 10^{-15} & -2.74 \cdot 10^{-15} \end{bmatrix}$$

3.3.3.2 Disturbance Rejection with DSF applied to the T-B system

The infinite structure of models $\Sigma(C_2, A, B)$ and $\Sigma(C_2, A, F)$ are first studied with a structural approach. The shortest causal path between the output variable to be controlled $Df : y_2(t)$ and the control input $MSe : u(t)$ in the BGI model of Fig. 3.5 is

$$Df : y_2 \to I : J_2 \to R : R_{fs} \to I : J_1 \to TF : 1/k_b \to GY : k_m \to I : L_a \to MSe : u \, .$$

The length of this causal path is equal to 3, then $n_{c2} = 3$. The shortest causal path between the output variable to be controlled $Df : y_2(t)$ and the disturbance input $Se : d_{pert}$ is

$$Df : y_2 \to I : J_2 \to R : R_{fs} \to I : J_1 \to Se : d_{pert} \, .$$

The length of this causal path is equal to 2, then $n_{p2} = 2$. Since $n_{p2} < n_{c2}$, from property 1 the DSF has a solution with $n - n_{c2} = 1$ finite fixed mode which is the invariant zero of model $\Sigma(C_2, A, B)$ and $n_{p2} = 2$ finite modes which can be freely chosen with matrix F_c (property 6). Its value is $I_z = -{}^{1}/_{C_{fs} \cdot R_{fs}} = -3571.42$. Some coefficients can be derived from a causal analysis (causal path gains), but here they are directly obtained from formal calculus. With pole placement, matrix F_c is defined in equation (1.29), with numerical values in equation (1.30). Two poles can be chosen because $n_{p2} = 2$. In that case,

$$\begin{aligned} \det(sI - A - sBF_c) = & \\ & = \frac{R_1 \cdot R_a + R_2 \cdot R_a + k_m^2 \cdot k_b^2}{C_{fs} \cdot J_2 \cdot L_a \cdot J_1} \cdot (C_{fs} \cdot R_{fs} \cdot s + 1) \cdot (\alpha_2 \cdot s^2 + \alpha_1 \cdot s + 1) \\ & = 2.9483 \cdot 10^7 \cdot (2.8 \cdot 10^{-4} \cdot s + 1) \cdot (\alpha_2 \cdot s^2 + \alpha_1 \cdot s + 1) \, . \end{aligned}$$

The differential equation verified by the output variable $y_2(t)$ with the derivative state feedback control law with pole placement is $\alpha_2 \ddot{y}_2(t) + \alpha_1 \dot{y}_2(t) + y_2(t) = v(t)$. Parameters α_1 and α_2 can be arbitrarily chosen, according to the poles of the closed loop model.

The DSF control applied to T-B system with the UIO with general structure is shown in Fig. 3.4. This structure is used as well for simulation as for application to the real system (see chapter 4). BG_{obs} is the bond graph model of the physical system with some signal bonds, and in order to obtain the estimation of the state variables derivatives, it is sufficient to add effort sensors (elements I) or flow sensors (elements C) on the dynamical elements of the bond graph observer, without any use of mathematical derivation.

With the parameters obtained before, the results are shown below in different graphics. The studied variables are the previous ones in order to compare the different methods.

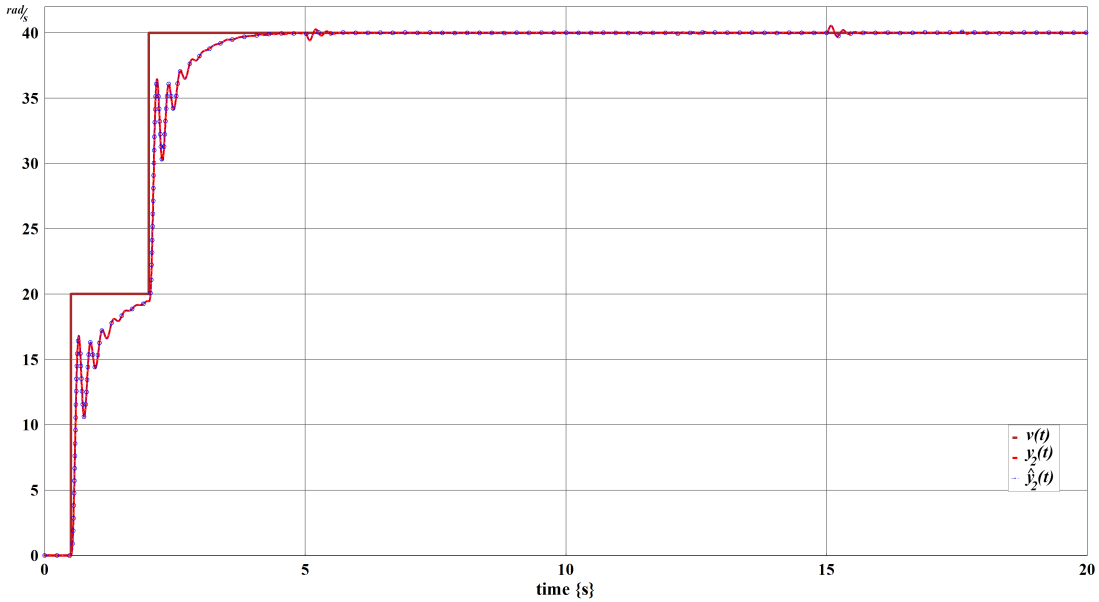

Figure 3.16 – DR-DSF-UIO-BG: output controlled $y_2(t)$ and its estimation $\hat{y}_2(t)$

In Fig. 3.16, the output and its estimation are shown. The disturbance rejection is achieved. Signal $y_2(t)$ and its estimation $\hat{y}_2(t)$ are smooth signals and the set-tracking of the reference is well done. The disturbance variable and its estimation are shown in the Fig. 3.17. In this figure, it is proved that the estimation for the perturbation is well accomplished.

The error variables $e_1(t) = y_1(t) - y_1(t)$ and $e_2(t) = y_2(t) - y_2(t)$ are shown in Fig. 3.18. They prove the efficiency of the control law as well as the estimation of the disturbance variable that is used in the expression of this control law.

In Fig. 3.19, two pieces of information are displayed, the control signal (up) applied to the system and the Energy consumption (down) with a value of around 433 J after 20 s.

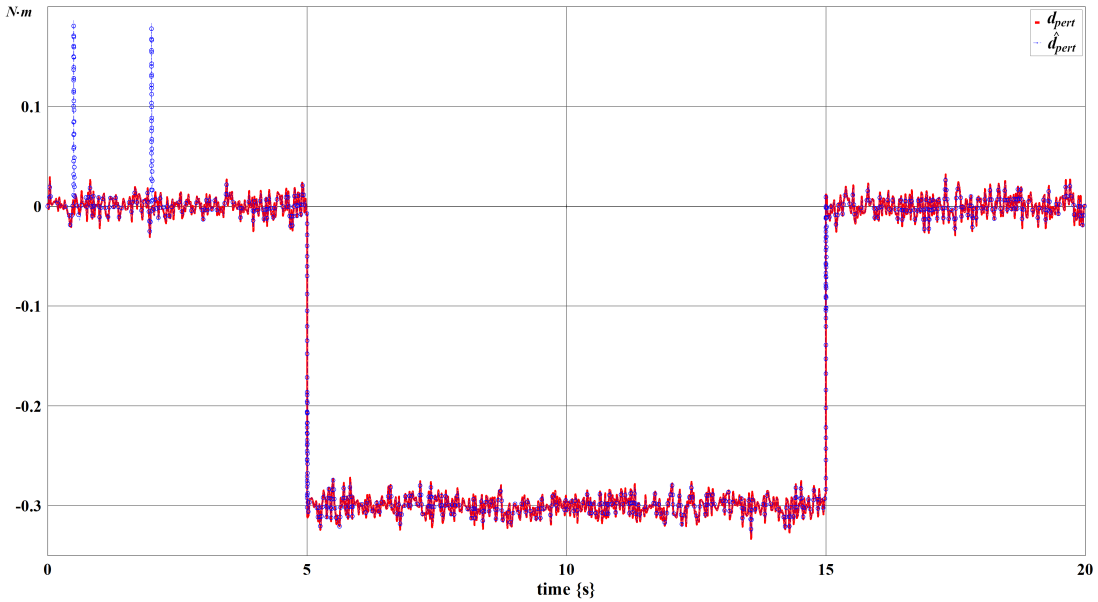

Figure 3.17 – DR-DSF-UIO-BG: disturbance variable d_{pert} and its estimation $\hat{d}_{pert}$.

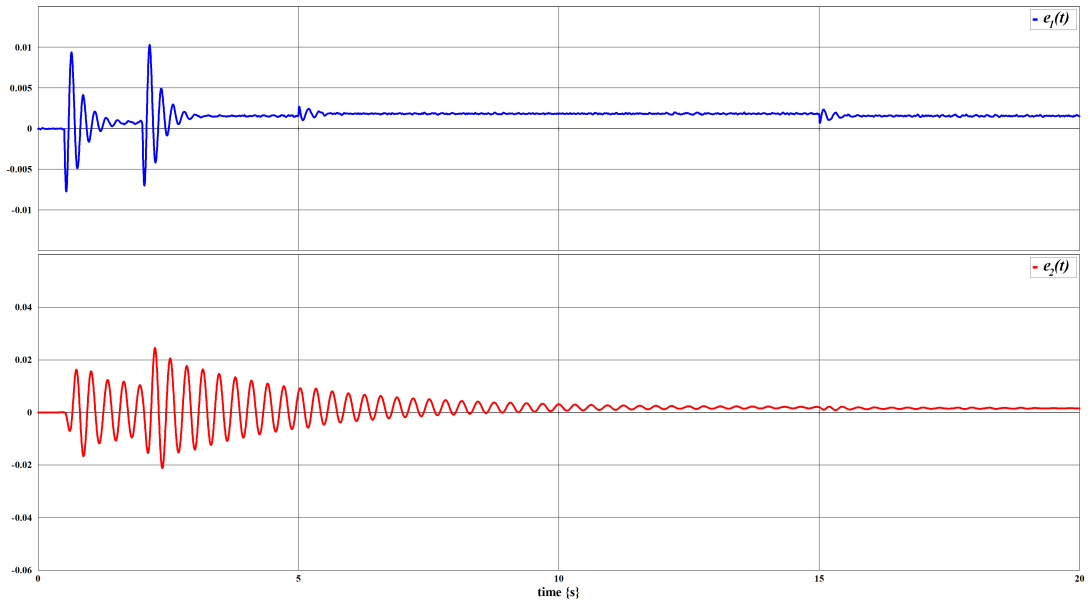

Figure 3.18 – DR-DSF-UIO-BG: Errors $e_1 = y_1 - \hat{y}_1$ (up) and $e_2 = y_2 - \hat{y}_2$ (down).

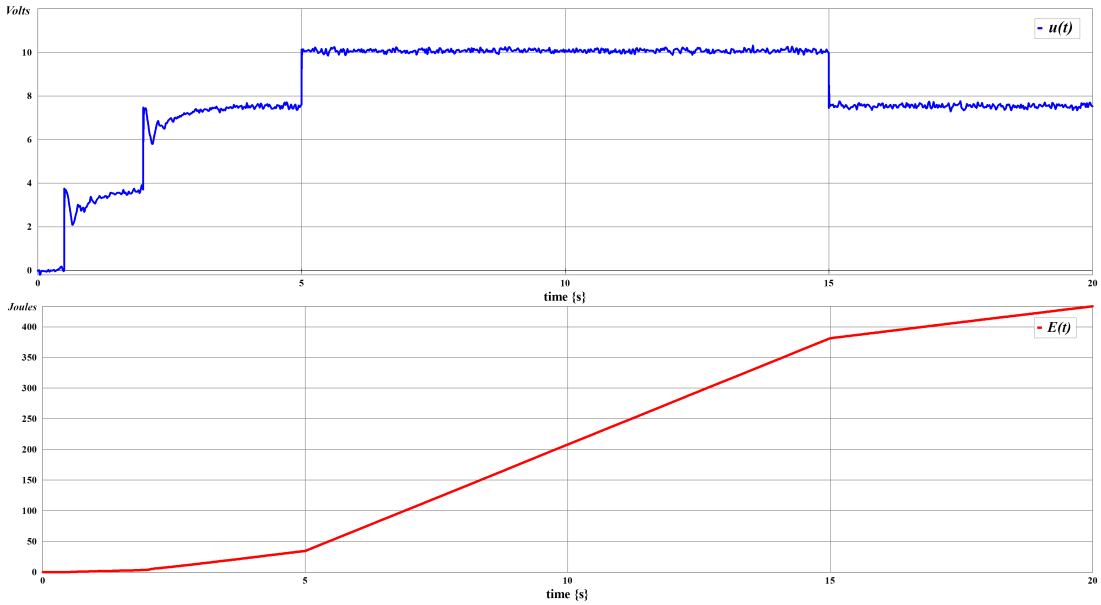

Figure 3.19 – Control signal $u(t)$ (blue) and the energy waste (red) for this control.

3.3.4 Analysis of the results

Among other tasks, disturbance rejection is the main control objective. It is achieved with different solutions that are now compared.

For each approach, the control aim is achieved. Results are in Figures (3.9), (3.12) and (3.16) for the output controlled. From these figures, it is possible to check the output estimation. This estimation is realised for each solution but only in the output estimation by DOBC appear the effect of the control signal when the perturbation affect the system. This effect in the output estimation can be modified if the method used in the *Observer part* of DOBC is modified. Also, these figures shown if the main objective is accomplished. The disturbance rejection is *achieved* for each solution with some different responses when the perturbation appears. It is also possible to analyse the state estimations (not included in this work), except for the ADRC approach because the state variables are not estimated in that case.

Another characteristic of these solutions is the capacity of estimating the Unknown Input (perturbation) in different ways. The unknown input estimation for the DOBC (Fig. 3.10) and the ADRC (Fig. 3.13) is based in the idea of estimating the cumulated perturbation in the whole system. In the solution proposed in this work (DR-DSF-UIO-BG), the estimated perturbation is associated to a real phenomena in a certain defined part of the system and with the possibility to study the constitution of this perturbation (Fig. 3.17).

From the solutions presented in this chapter, only the DR-DSF-UIO-BG uses the derivative state estimation to achieve the main objective. Using DSF represents an advantage when the Regular Static State Feedback (RSSF) cannot be applicable or when the sensors in the real system make measurements of energy variables (*e.g.*. force, torque, (angular) velocity, electric potential, current, pressure, flow rate, etc.).

Finally, the solution proposed in this research work is based on the bond graph approach (Graphical approach) and one of the notorious characteristic is that the Bond Graph model used for DSF-UIO-BG is the same Bond Graph model of the one of the system to be controlled.

In addition, the energy required is also shown in each solution. The energy consumption in the DOBC and DSF-UIO-BG methods are lower that the ADRC one. Also, the quantity of information from the DSF-UIO-BG is different in comparison of DOBC or ADRC. This information can be useful for system behaviour analysis.

These approaches will be used and analysed in chapter 4 on the real Torsion-Bar system.

3.4 Input-Output decoupling with DSF

This section presents a new solution for the well-known input-output decoupling problem of linear square invertible multivariable systems with a Derivative State Feedback (DSF) control law.

We first present some properties of the classical Regular Static State Feedback (RSSF) control law in order to compare it with the new one. It is shown that the methodology is very similar in term of structural analysis (same invariants) and also in term of the synthesis of the control law.

We consider linear square invertible systems $\Sigma(C,A,B)$ described by the classical state-space representation written in (3.26), with $x \in \Re^n$ the state vector, $u \in \Re^m$ the input vector and $y \in \Re^m$ the vector of output variables to be controlled.

$$\begin{cases} \dot{x}(t) = Ax(t) + Bu(t) \\ y(t) = Cx(t) \end{cases} \tag{3.26}$$

3.4.1 RSSF: some properties

System $\Sigma(C,A,B)$ in equation (3.26) is supposed to be state controllable and observable. We recall here some simple necessary and sufficient conditions for the model to be decouplable by a Regular Static State Feedback control law with stability, with a control law $u(t)$ defined as $u(t) = Fx(t) + Gv(t)$, where $v(t)$ is the new control law, for the closed loop system. Ω is the decoupling matrix defined in equation (3.27), with C_i the i^{th} row of matrix C.

$$\Omega = \begin{pmatrix} C_1 A^{n_1 - 1} B \\ : \\ C_m A^{n_m - 1} B \end{pmatrix} \tag{3.27}$$

System $\Sigma(C,A,B)$ is decouplable by a regular static state feedback control law $u(t) = Fx(t) + Gv(t)$ iff matrix Ω is invertible, or equivalently iff $\{n_i\} = \{n_i'\}$ [Morse and Wonham, 1973].

Suppose $\{Z(C,A,B)\}$ the set of invariant zeros of model $\Sigma(C,A,B)$ and $\{Z_i(C_i,A,B)\}$ the set of invariant zeros of submodels $\Sigma(C_i,A,B)$. It is well known that the fixed poles of the controlled model are the invariant zeros of the global model (open loop model) which are not invariant zeros of one of the submodels, see [Morse and Wonham, 1973, Icart et al., 1989] for a geometric domain approach characterization or [Koussiouris, 1980] for a frequency domain approach characterization. The fixed modes are thus one part of the invariant zeros of model $\Sigma(C,A,B)$. If $\bigcup_i\{Z_i(C_i,A,B)\}$ is the union set with multiplicity of the invariant zeros of subsystems $\Sigma(C_i,A,B)$, the set $\{Z_{fixed}\}$ of fixed modes is defined as $\{Z(C,A,B)\}-\bigcup_i\{Z_i(C_i,A,B)\}$ and it number n_{fixed} is defined as $n_{fixed}=card\{Z_{fixed}\}$.

If the model is decouplable with a regular static state feedback control law, matrix F defined in equation (3.28) and $G=\Omega^{-1}$ are solutions of the problem if all the invariant zeros are the non-assigned modes. Parameters α_{ij} are used for pole placement. If $n_{fixed}\neq n_{IZ}$, matrix F is different of the previous one. Its expression is more difficult to be designed. Generally, the geometric approach is employed in that situation.

$$F=F_1=-\Omega^{-1}\begin{bmatrix} C_1A^{n_1}+\alpha_{11}C_1+\cdots+\alpha_{1n_1}C_1A^{n_1-1} \\ \vdots \\ C_mA^{n_m}+\alpha_{m1}C_m+\cdots+\alpha_{mn_m}C_mA^{n_m-1}\end{bmatrix} \tag{3.28}$$

3.4.2 DSF for Input-Output decoupling

A simplified version for the Input-Output decoupling problem with stability is given for $m=2$. It can be easily extended to any linear square invertible models. Some non-restrictive assumptions for physical models are written.

- System $\Sigma(C,A,B)$ is state *controllable/observable* and the state matrix A is *invertible*
- The state variable derivatives are measured or estimated
- The invariant zeros of $\Sigma(C,A,B)$ are strictly stable

For system $\Sigma(C,A,B)$, if $\{n_i\}\neq\{n_i'\}$, the input-output decoupling problem with the classical regular static state feedback control (RSSF) is not possible, or equivalently the decoupling matrix Ω defined in equation (3.29) is not invertible. Otherwise, the problem has a solution with RSSF. In the sequel, the proposed procedure can be applied equivalently in both cases.

$$\Omega=\begin{pmatrix} C_1A^{n_1-1}B \\ C_2A^{n_2-1}B\end{pmatrix} \tag{3.29}$$

A Derivative State Feedback control defined in (3.30) is applied. $v(t)$ is the new input vector (new control).

$$u(t)=F\dot{x}(t)+Gv(t) \tag{3.30}$$

The controlled system can be written as (3.31).

$$\begin{cases} (I-BF)\dot{x}(t) = Ax(t)+BGv(t) \\ y(t) = Cx(t) \end{cases} \tag{3.31}$$

The state equation in (3.31) is called "generalized state-space form" or "descriptor form", as for the DSF solution proposed in section 1.4. The controlled model contains poles at infinity. The characteristic equation of the closed loop system (3.31) is defined as (3.32).

$$det(sI - sBF - A) = 0 \tag{3.32}$$

The degree γ of the characteristic polynomial in equation (3.32) is the number of system's finite eigenvalues, while $n-\gamma$ is the number of system's eigenvalues at infinity [Fahmy and O'Reilly, 1989]. If matrix $(I-BF)$ is not invertible, the system has thus poles at infinity and properties such as controllability/observability properties must be studied in a different way [Cobb, 1984, Verghese et al., 1981, Yip and Sincovec, 1981].

A different state-space representation (3.33) can be written if vector $x(t)$ is expressed as a function of $\dot{x}(t)$.

$$\begin{cases} x(t) = (A^{-1}-A^{-1}BF)\dot{x}(t) - A^{-1}BGv(t) \\ y(t) = (CA^{-1}-CA^{-1}BF)\dot{x}(t) - CA^{-1}BGv(t) \end{cases} \tag{3.33}$$

If the model defined by equation (3.26) does not have any null invariant zero, thus matrix $\Omega_d = CA^{-1}B$ is invertible and the control law defined by equation (3.30) with matrices F and G defined in (3.34) leads to a simple decoupled singular model with direct transmission between the new input variables and the output variables as described in equation (3.35).

$$\begin{cases} F = (CA^{-1}B)^{-1}CA^{-1} = \Omega_d^{-1}CA^{-1} \\ G = -(CA^{-1}B)^{-1} = -\Omega_d^{-1} \end{cases} \tag{3.34}$$

$$\begin{cases} y_1(t) = v_1(t) \\ y_2(t) = v_2(t) \end{cases} \tag{3.35}$$

With the control law defined in equation (3.30), the invariant zeros of the controlled system are the zeros of matrix $S_{CL}(s)$ defined in equation (3.36). As proved for the SISO case in [Sueur, 2016], the invariant zeros of the model $\Sigma(C,A,B)$ are the same ones as the controlled system with a DSF control law defined in (3.30) and (3.34). It is also an implicit model [Rosenbrock, 1970] of the type $E\dot{x} = Ax+Bu$, with matrix E non-invertible.

$$S_{CL}(s) = \begin{pmatrix} sI-A-sBF & -BG \\ C & 0 \end{pmatrix} \tag{3.36}$$

The degree γ of the characteristic polynomial $\det(sI-sBF-A)$ of the controlled system $\Sigma(C,A,B)$ with a DSF control law defined in equations (3.30) and (3.34) is equal to the number of invariant zeros of $\Sigma(C,A,B)$, *i.e.* $\gamma = n-\Sigma n_i'$. The new model contains only $n-\Sigma n_i'$ (and not $n-\Sigma n_i$) finite modes, the invariant zeros of $\Sigma(C,A,B)$.

With the DSF control law, it can be easily proved that matrix $[sI - A - sBF \quad -BG]$ is equivalent to matrix $[sI - A \quad -B]$ and thus this matrix doesn't contain any zero. With the DSF control law, the new model can become non observable. It is a classical property when applying a static state feedback control the input-output decoupling problem. It is well known that the non-observable modes are all or one part of the invariant zeros. The zeros of matrix $[sI - s(BF)^t - A^t \quad C^t]^t$ of the controlled system $\Sigma(C,A,B)$ with a DSF control law defined in equations (3.30) and (3.34) are the invariant zeros of the model $\Sigma(C,A,B)$.

3.4.3 Properties of the controlled model with pole placement

The solution for the input-output decoupling problem with pole placement is obtained with $G = -\Omega_d^{-1}$ and with the new matrix F defined in equation (3.37). The set $\{\alpha_1, \alpha_2, \cdots, \alpha_{n_1}\}$ is a set of n_1 free parameters used for pole placement for the first submodel and $\{\beta_1, \beta_2, \cdots, \beta_{n_2}\}$ is a set of n_2 free parameters used for pole placement for the second submodel.

$$F = \Omega_d^{-1} \begin{bmatrix} C_1A^{-1} + \alpha_1 C_1 + \cdots + \alpha_{n_1} C_1 A^{n_1-1} \\ C_2A^{-1} + \beta_1 C_2 + \cdots + \beta_{n_2} C_2 A^{n_2-1} \end{bmatrix} \tag{3.37}$$

The differential equations satisfied by the two output variables $y_1(t)$ and $y_2(t)$ with a derivative state feedback control law defined in (3.30) with matrix G in (3.34) and matrix F in (3.37) is written in (3.38).

$$\begin{cases} \alpha_{n_1} y_1^{(n_1)}(t) + \cdots + \alpha_2 \ddot{y}_1(t) + \alpha_1 \dot{y}_1(t) + y_1(t) = v_1(t) \\ \beta_{n_2} y_2^{(n_2)}(t) + \cdots + \beta_2 \ddot{y}_2(t) + \beta_1 \dot{y}_2(t) + y_2(t) = v_2(t) \end{cases} \tag{3.38}$$

Proof. From equation (3.33), with matrix $G = -\Omega_d^{-1}$, the output vector can be written as (3.39) and thus, with matrix F defined in equation (3.37), the output vector $y(t)$ is now after a first quite simple simplification in (3.40).

$$y(t) = [CA^{-1} - CA^{-1}BF]\dot{x}(t) + v(t) \tag{3.39}$$

$$\begin{cases} y_1(t) = -\{\alpha_1 C_1 + \alpha_2 C_1 A + \cdots + \alpha_{n_1} C_1 A^{n_1-1}\}\dot{x}(t) + v_1(t) \\ y_2(t) = -\{\beta_1 C_2 + \beta_2 C_2 A + \cdots + \beta_{n_2} C_2 A^{n_2-1}\}\dot{x}(t) + v_2(t) \end{cases} \tag{3.40}$$

But $C_1\dot{x}(t) = \dot{y}(t)$ and $C_1Ax(t) = C_1A[(A^{-1} - A^{-1}BF)\dot{x}(t) - A^{-1}BGv(t)] = C_1[(I - BF)\dot{x}(t) - BGv(t)]$. Since $C_1B = 0$, it comes $C_1Ax(t) = C_1\dot{x}(t)$ and thus $C_1A\dot{x}(t) = \ddot{y}(t)$. With a similar calculus, it comes $C_1A^{(k-1)}\dot{x}(t) = y^{(k)}$ for $k \leq n_1$ and thus relation (3.38), and the same conclusion for the output variable $y_2(t)$.

□

The degree of the characteristic polynomial $\det(sI - sBF - A)$ of the controlled system $\Sigma(C,A,B)$ with a DSF control law defined in equations (3.30), matrix G in equation (3.34) and matrix F in (3.37) is equal to $(n - \Sigma n_i') + \Sigma n_i$ (number of invariant zeros of $\Sigma(C,A,B)$ + sum of row infinite zero orders of submodels $\Sigma(C_i,A,B)$).

Proof. Since Matrices $S(s)$ (equation (A.2)) and $S_{CL}(s)$ are equivalent, $\det S(s) = \det S_{CL}(s)$, which is a polynomial of degree $n - \Sigma n_i'$, (number of invariant zeros). Moreover, $\det S_{CL}(s) = \det(sI - A - sBF) \cdot \det(C(sI - A - sBF)^{-1}BG)$, and since the new diagonal transfer matrix is such that $\det(C(sI - A - sBF)^{-1}BG)$ is of order Σn_i with a constant numerator, $\det(sI - A - sBF)$ is a polynomial of degree $(n - \Sigma n_i') + \Sigma n_i$. □

With this control law, the controlled system is thus an implicit model, *i.e.*, matrix $(I - BF)$ is not invertible, with $\Sigma n_i' - \Sigma n_i$ poles at infinity, due to the difference between the two sets $\{n_i'\}$ and $\{n_i\}$. Theoretical developments must still be achieved. A future research challenge is also to compare the set of non-assigned modes with the set of fixed modes, among the invariant zeros. It is worth noting that in the SISO case, with pole placement, the degree of the characteristic polynomial $\det(sI - sBF - A)$ of the controlled system $\Sigma(C,A,B)$ is equal to $(n-r)+r = n$ ($n-r$ is the number of invariant zeros of $\Sigma(C,A,B)$ and r is the infinite zero order of $\Sigma(C,A,B)$). In that case, the controlled system is never an implicit model.

3.4.4 Comparison between RSSF and DSF

In this subsection, to address new challenges in the Derivative State Feedback control type, a comparison study is proposed between the Regular Static State Feedback control (RSSF) and the Derivative State Feedback control (DSF) in table 3.1. This table considers some conditions for the capability of decoupling with, if relevant, the control law expressions and some properties of the decoupled model. The feedback control matrix F in its general expression for the DSF control law is defined in equation 3.41.

$$F = F_2 = \Omega_d^{-1} \begin{bmatrix} C_1A^{-1} + \alpha_{11}C_1 + \cdots + \alpha_{1n_1}C_1A^{n_1-1} \\ \vdots \\ C_mA^{-1} + \alpha_{m1}C_m + \cdots + \alpha_{mn_m}C_mA^{n_m-1} \end{bmatrix} \tag{3.41}$$

If matrix $\Omega_d = CA^{-1}B$ is not invertible, model $\Sigma(C,A,B)$ has at least one null invariant zero. This case is not considered here, but a simple extension is possible. If n_{id} is the number of null invariant zeros of the row subsystem $\Sigma(C_i,A,B)$, then matrix Ω_d is rewritten in the general case as equation (3.42). If matrix Ω_d is invertible, Σn_{id} is equal to the number of null invariant zeros of $\Sigma(C,A,B)$ and the input-output decoupling problem with DSF has a solution with $n - \Sigma n_i - \Sigma n_{id}$ non-assigned modes (not developed here).

$$\Omega_d = \begin{pmatrix} C_1A^{-n_{1d}-1}B \\ \vdots \\ C_mA^{-n_{md}-1}B \end{pmatrix} \tag{3.42}$$

<table>
<tr><td colspan="3">Controllable/Observable and invertible linear square model $\Sigma(C,A,B)$; $m=p$</td></tr>
<tr><td></td><td>Regular Static State Feedback
$RSSF$: $u=Fx+Gv$
Notations and properties : see appendix A</td><td>Derivative State Feedback
DSF : $u=F\dot{x}+Gv$
Assumptions: A invertible; Ω_d invertible</td></tr>
<tr><td rowspan="2">$\sum n_i=\sum n_i'$
$n_{IZ}=n-\sum n_i$</td><td>Non assigned modes: $\{Z(C,A,B)\}$
n_{IZ} non assigned modes
$F=F_1$ (equation (3.28)); $G=\Omega^{-1}$</td><td>Non assigned modes: $\{Z(C,A,B)\}$
n_{IZ} non assigned modes
$F=F_2$ (equation (3.41)); $G=-\Omega_d^{-1}$
not any infinite (impulsive) modes</td></tr>
<tr><td>Best solution
Fixed modes: $\{Z(C,A,B)\}-\bigcup_i\{Z_i(C_i,A,B)\}$
n_f fixed modes
F no simple expression ; $G=\Omega^{-1}$</td><td>Best solution
Study of fixed modes : to be developed</td></tr>
<tr><td rowspan="2">$\sum n_i\neq\sum n_i'$
$n_{IZ}=n-\sum n_i'$</td><td rowspan="2">No solution with RSSF
$\Sigma(C,A,B)$: not decouplable by RSSF</td><td>Non assigned modes: $\{Z(C,A,B)\}$
n_{IZ} non assigned modes
$F=F_2$ (equation 3.41); $G=-\Omega_d^{-1}$
$\sum n_i'-\sum n_i$ infinite (impulsive) modes</td></tr>
<tr><td>Best solution
Study of fixed modes : to be developed</td></tr>
</table>

Table 3.1 – Comparison between applicability conditions and properties of RSSF and DSF

Some remarks about robustness

Before developing the case study, some remarks are made about the robustness of the control law, particularly for the steady state behaviour. It is well-known that classical control laws such as Static State Feedback (SSF) type may not be able to suppress the disturbance and track the set point in the presence of model mismatch. Few methods achieving simultaneous decoupling and set-point tracking have been proposed in the literature. From the classical control law $u(t)=Fx(t)+Gv(t)$, the closed loop transfer matrix is $Y(s)=C(sI-A-BF)^{-1}BGV(s)=M_{CL}(s)V(s)$. In the steady state behaviour with $s=0$, it comes $M_{CL}(0)=C(A-BF)^{-1}BG$ which is diagonal matrix containing the static gains. Clearly, these static gains can vary in the presence of model mismatch with a difficult evaluation. Consider now equation (3.31). The closed loop transfer matrix is $Y(s)=C(sI-sBF-A)^{-1}BGV(s)=M_{CL}(s)V(s)$. In the steady state behaviour with $s=0$, it comes $M_{CL}(0)=CA^{-1}BG$. Matrix $CA^{-1}B$ is only a function of some well-identified parameters and model mismatch has few influences on the steady state behaviour. Matrix $CA^{-1}B$ contains the causal path gains for paths of length 0 between the input variables and the output variables in the Bond Graph model with Derivative causality (BGD). It is independent of matrix F, thus of the control matrix gain, only of some parameters which are well identified, since contained in the causal paths. Concerning impulsive modes, a fundamental aspect associated with Derivative State Feedback, from a theoretical point of views, discontinuity in the state trajectory and thus unbounded values of the control law, [Verghese et al., 1981]. Indeed, an impulsive mode can cause a jump at time $t=0$ for some state variables and thus impulses for the control law for some initial conditions. In our approach, derivative state variables are estimated from the Bond Graph model without applying any derivation for the state variables. Even if values can change strongly and rapidly, the effectiveness of the approach is proved in ([Gonzalez et al., 2018]), with application of this control type applied to a real Torsion-Bar

system for disturbance rejection purpose.

3.4.5 Case study: simple mechanical system

The studied mechanical system is presented in Fig. 3.20. The system consists of the following components (names and parameters are identical): two masses M and m that can move without friction on the ground, a damper R and a spring $C_a = {}^1/_{k_a}$ between the two masses, a spring $C_r = {}^1/_{k_r}$ that acts on the mass m, and two actuators imposing a speed on the spring C_r and a force between the two masses, respectively. In a vertical representation, this simple mechanical system is the classical car shock absorber.

This system is studied first in the SISO case (without null invariant zero) and then in the MIMO case, only in order to illustrate the different theoretical properties developed in the previous section. The proposed procedures can be easily applied to more complex models.

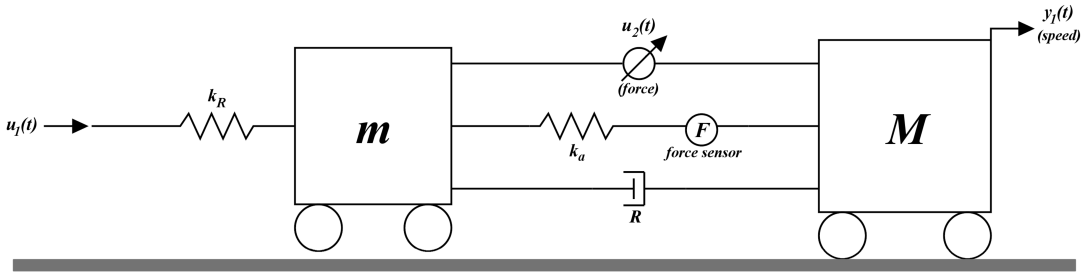

Figure 3.20 – Schematic representation of the mechanical system

The bond graph model of the system (drawn with *20-Sim*®) is shown in Fig. 3.21. $MSf : u_1$ one of the two control inputs, is a flow source and $MSe : u_2$ is an effort source. There are two output variables associated to output detectors which can be used to estimate the derivatives of the state variables that are used in the different control laws. These output variables are considered here as output variables to be controlled. $y_1(t)$ is a speed variable associated to a flow output detector $Df : y_1$ and $y_2(t)$ is an effort variable associated the force applied on the spring C_a and denoted as $De : y_2$.

The state equations (3.43) are directly obtained from the bond graph model of Fig. 3.21. The state vector is chosen as $x = (x_1, x_2, x_3, x_4)^t$, with generalized energy variables: $x_1 = p_M$ and $x_2 = p_m$ (representing the momenta of the two masses), and $x_3 = q_{C_a}$ and $x_4 = q_{C_r}$ (representing the generalized displacements of the two springs). The output matrix C can be written as $C = [C_1^t, C_2^t]^t$ and the control matrix B as $B = [B_1, B_2]$ The state equations are written in equation (3.43).

The study is first proposed for the row model $\Sigma(C_1, A, B_1)$ and thus for model $\Sigma(C, A, B)$. The Bond graph model is controllable/observable and the state matrix is invertible, a derivative causality can be assigned to each dynamical element, Fig. 3.22.

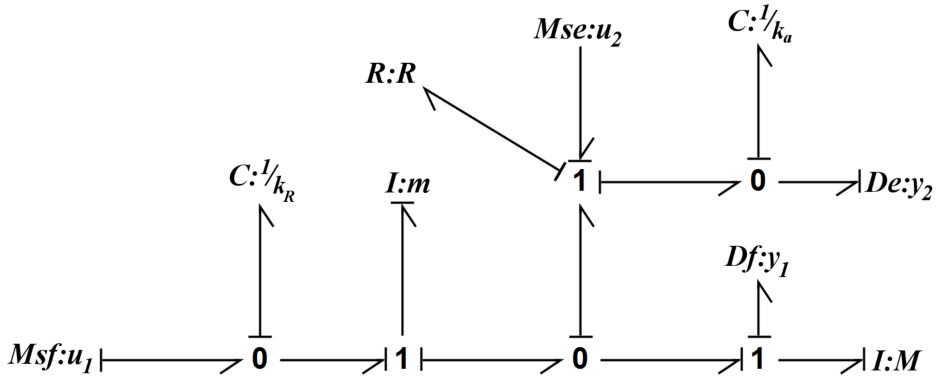

Figure 3.21 – Bond graph model of the mechanical system: BGI

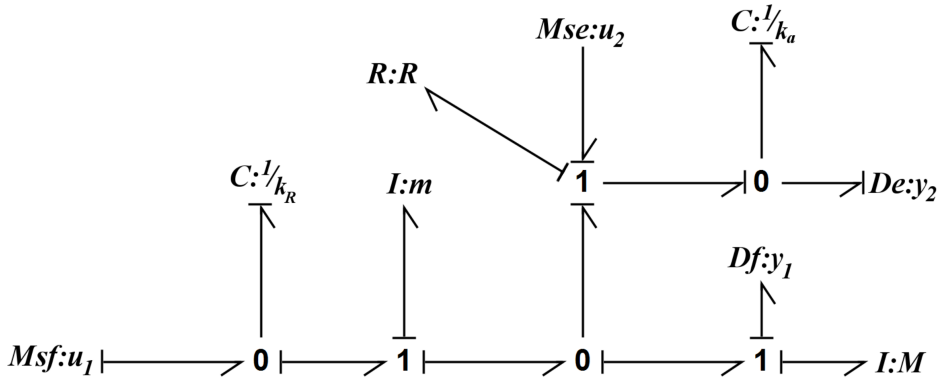

Figure 3.22 – BG model with derivative causality assignment: BGD

$$\begin{cases} \dot{x}_1 = -\frac{R}{M}x_1 + \frac{R}{m}x_2 + \frac{1}{C_a}x_3 - u_2(t) \\ \dot{x}_2 = \frac{R}{M}x_1 - \frac{R}{m}x_2 - \frac{1}{C_a}x_3 + \frac{1}{C_r}x_4 + u_2(t) \\ \dot{x}_3 = -\frac{1}{M}x_1 + \frac{1}{m}x_2 \\ \dot{x}_4 = -\frac{1}{m}x_2 + u_1(t) \\ y_1(t) = \frac{1}{M}x_1 \quad y_2(t) = \frac{1}{C_a}x_3 \end{cases} \tag{3.43}$$

3.4.5.1 Structural analysis and control of submodel $\Sigma(C_1,A,B_1)$: SISO case

Model $\Sigma(C_1,A,B_1)$ is controllable/observable and the state matrix is invertible. The infinite zero order for the output variable $y_1(t)$, denoted n_1, is equal to the shortest causal path length between the input source $MSf : u_1$ and the output detector $Det : y_1$ on the BGI in Fig. 3.21. The causal path is $Df : y_1 \to I : M \to R : R \to I : m \to C : C_r \to MSf : u_1$ with length $n_1 = 3$. We can conclude that $C_1B_1 = C_1AB_1 = 0$ and $C_1A^2B_1 \neq 0$, and that the submodel $\Sigma(C_1,A,B_1)$ has one invariant zero.

For the BGD in Fig. 3.22, the infinite zero order for the output variable $y_1(t)$, denoted n_{1d}, is equal to the shortest causal path length between the input source $MSf : u_1(t)$ and the output detector $Df : y_1$. The causal path is $Df : y_1 \to MSf : u_1$ with length $n_{1d} = 0$. We can conclude that $C_1A^{-1}B_1 \neq 0$ and that the submodel $\Sigma(C_1,A,B_1)$ doesn't have any null invariant zero. The invariant zero is $s = -1/RC_a$.

Consider matrices G and F defined respectively in equations (3.34) and (3.37). There is a set $\{\alpha_1,\alpha_2,\alpha_3\}$ of 3 free parameters for pole placement. $G = -\Omega_{d11}^{-1} = -(C_1A^{-1}B_1)^{-1} = 1$ and matrix F is in equation (3.44).

$$F = \Omega_{d11}^{-1}[C_1A^{-1} + \alpha_1C_1 + \alpha_2C_1A + \alpha_3C_1A^2] \tag{3.44}$$

The Input-Output relation with pole placement is $\alpha_3\dddot{y}_1(t) + \alpha_2\ddot{y}_1(t) + \alpha_1\dot{y}_1(t) + y_1(t) = v(t)$. Matrix $(I - B_1F)$ is invertible, the controlled model is not singular, and the fixed pole is the invariant zero (strictly stable for this example). The characteristic polynomial of matrix $(sI - sB_1F - A)$ is $(\alpha_3s^3 + \alpha_2s^2 + \alpha_1s + 1)(RC_as + 1)/(MmC_rC_a)$. It is worth noting that since $(C_1A^{-1}B_1)^{-1} = -1$, the static gain of the closed loop model is theoretically always equal to 1 even with model mismatch.

3.4.5.2 Structural analysis and control of submodel $\Sigma(C_1,A,B_2)$: $C_1A^{-1}B_2 = 0$

The infinite zero order of submodel $\Sigma(C_1,A,B_2)$ is equal to the shortest causal path length between the input source $MSf : u_2(t)$ and the output detector $Det : y_1$ on the BGI in Fig. 3.21. The causal path is $Df : y_1 \to I : M \to MSe : u_2$, thus $n_1 = 1$. We can conclude that $C_1B_2 \neq 0$ and that the submodel $\Sigma(C_1,A,B_2)$ has 3 invariant zeros.

For the BGD in Fig. 3.22, the shortest causal path length between the input sources $MSe : u_2$ and the output detector $Det : y_1$ is $Df : y_1 \rightarrow C : C_a \rightarrow MSe : u_2$ thus $n_{1d} = 1$ and $C_1A^{-1}B_2 = 0$, but $C_1A^{-2}B_2 \neq 0$. This submodel has one null invariant zero. The 3 invariant zeros are solution of the polynomial $s(s^2 + {}^1/_{C_rm})$.

Consider matrices G and F defined respectively in equations (3.34) and (3.37). There is a set $\{\alpha_1, \alpha_2\}$ of 2 free parameters for pole placement. $G = -(C_1A^{-2}B_2)^{-1} = ({}^{-1}/_{C_a})$ and matrix F is in equation (3.45), with $F(1,1) = \beta = [-M(C_a + C_r) + \alpha_2]/(M \cdot C_a)$.

$$\begin{cases} F = (C_1A^{-2}B_2)^{-1}[C_1A^{-2} + \alpha_1 C_1A^{-1} + \alpha_2 C_1] \\ F = [\beta \quad -C_r/C_a \quad R - \alpha_1/C_a \quad -\alpha_1/C_a] \end{cases} \tag{3.45}$$

The Input-Output relation with pole placement is $\alpha_2\ddot{y}_1(t) + \alpha_1\dot{y}_1(t) + y_1(t) = \dot{v}(t)$.

Matrix $(I - B_2F)$ is invertible, the controlled model is not singular, and the two fixed poles are the non-null invariant zeros (not strictly stable for this example). The characteristic polynomial of matrix $(sI - sB_2F - A)$ is $(\alpha_2 s^2 + \alpha_1 s + 1)(C_rms^2 + 1)/(MmC_rC_a)$. It is worth noting that since $(C_1A^{-1}B_1)^{-1} = ({}^{-1}/_{C_a})$, the static gain of the closed loop model is only sensible to parameter C_a.

3.4.5.3 Structural analysis and control of model $\Sigma(C,A,B)$: MIMO case

The infinite zero orders for each output variable $y_i(t)$, denoted n_i, are equal to the shortest causal path length between the two input sources $MSf : u_1(t)$ and $MSe : u_2(t)$ and the output detector $Det : y_i$, $i = 1,2$ on the bond graph model with an integral causality assignment drawn in Fig. 3.21. The shortest causal path length is $Df : y_1 \rightarrow I : M \rightarrow MSe : u_2$ for the first output variable thus $n_1 = 1$. For the second output detector, the causal paths are $De : y_2 \rightarrow C : C_a \rightarrow I : M \rightarrow MSe : u_2$ or with the same length $De : y_2 \rightarrow C : C_a \rightarrow I : m \rightarrow MSe : u_2$ thus $n_2 = 2$. Since these two paths are not disjoint (same input variable), the model is not decouplable with a regular static state feedback control law. The decoupling matrix $\Omega = [(C_1B)^t \ (C_2AB)^t]^t$ is not invertible. Two disjoint causal paths are $Df : y_1 \rightarrow I : M \rightarrow MSe : u_2$ and $De : y_2 \rightarrow C : C_a \rightarrow I : m \rightarrow C : C_r \rightarrow MSf : u_1$.

The global infinite zero structure of model $\Sigma(C,A,B)$ is associated to the two global infinite zero orders that are equal to $n'_1 = 1$ and $n'_2 = 3$. The model doesn't have any invariant zero since its number is equal to $n - \Sigma n'_i = 0$. The infinite zero structure of the BGD could be analysed, but it is not required here since the model doesn't have any invariant zero, and thus matrix $\Omega_d = [(C_1A^{-1}B)^t \ (C_2A^{-1}B)^t]^t = CA^{-1}B$ is invertible.

An Input-Output decoupling can be achieved with the derivative state feedback control law defined in equation (3.30), with matrices F and G defined in equation (3.34) for control without pole placement, and matrix F in equation (3.46) for a solution with pole placement.

$$F = (CA^{-1}B)^{-1} \begin{bmatrix} C_1A^{-1} + \alpha_1 C_1 \\ C_2A^{-1} + \beta_1 C_2 + \beta_2 C_2A \end{bmatrix} \tag{3.46}$$

The differential equations verified by the two output variables $y_1(t)$ and $y_2(t)$ with this derivative state feedback control law are written in equation (3.47).

$$\begin{cases} \alpha_1 \dot{y}_1(t) + y_1(t) = v_1(t) \\ \beta_2 \ddot{y}_2(t) + \beta_1 \dot{y}_2(t) + y_2(t) = v_2(t) \end{cases} \tag{3.47}$$

The matrices for the control law are $G = I_2$ (the identity matrix) and F defined in equation (3.48).

$$F = \begin{bmatrix} -\alpha_1/M & 0 & 0 & 1 \\ -1+\beta_2/(MCa) & -\beta_2/(mCa) & R-\beta_1/Ca & 0 \end{bmatrix} \tag{3.48}$$

The characteristic polynomial of matrix $(sI - sBF - A)$ is $(\beta_2 s^2 + \beta_1 s + 1)(\alpha_1 s + 1)/(M m C_r C_a)$. Matrix $(I - BF)$ is not invertible, the controlled model is singular since $\Sigma n'_i - \Sigma n_i \neq 0$, and there is one pole at infinity.

3.4.6 Concluding remarks on Input-Output decoupling with DSF

The main contribution of this approach is the development of Derivative State Feedback control laws for the Input-Output decoupling design with pole placement. It is proved to be accurate and can be applied when the problem is not solvable with classical techniques based on Static State Feedback control. Structural properties of the open loop system are first achieved in order to highlight properties of the controlled model.

In the future, we aim at clarifying the link between the stability property of the controlled system with its finite structure, particularly the link between the set of invariant zeros of the different submodels and the composition of the set of fixed modes associated with the Derivative State Feedback control. Theoretical developments will also be proposed for the study of infinite modes of the controlled model.

3.5 Conclusion

This chapter had two main objectives. First, we compared three solutions for the disturbance rejection problem. These relatively modern solutions are compared with simulations applied to a Torsion-Bar system. Even if the three approaches DOBC, ADRC and the solution developed in this research work DSF-UIO-BG are relatively different in their concept, the idea is to use an estimation of the perturbation in the control law, even if this estimation is not an exact value of the disturbance itself. We prove that the DSF is a good solution for this problem. The multivariable solution is not presented in this thesis, but a simple extension is possible.

Secondly, we proposed a solution for the Input-Output decoupling problem with DSF. In some way, it is a simple extension of the disturbance rejection problem with DSF. The same concepts are used: a structural analysis is implemented with the Bond Graph approach for a solution with stability, and the synthesis of the control law is proposed formally. As for the Disturbance Rejection Problem developed more than two decades ago with the Bond Graph approach, it is possible to express properties of the control law with a geometric approach based on (A,B)-invariant subspaces. The formal expression of the control law is quite similar, but it is

obtained with the bond graph model in a derivative causality assignment (BGD) for the so-called decoupling matrix, whether for the I/O-decoupling problem or for the DRP. A somewhat duality exists between the two approaches: State Feedback and Derivative State Feedback.

Future work must allow us to clarify the link between the stability property of the controlled system with its finite structure, particularly the link between the set of invariant zeros of the different submodels and the composition of the set of fixed modes associated with the Derivative State Feedback control for the two problems. Theoretical developments are also necessary in order to the study of infinite modes of the controlled model. As well, the jointly problems of DRP and I/O-decoupling could be in that way easily studied.

The case study (Torsion-Bar system) is presented in the next chapter, that time in a practical way. We prove the very good performances of the control law.

Chapter 4

Disturbance Rejection (DR) - Derivative State Feedback (DSF) - Unknown Input Observer (UIO) - Bond Graph (BG): Study case

4.1 Introduction

In this fourth chapter, the application of different methods for the disturbance estimation, and its rejection (attenuation) will be performed for the real study case, *i.e.*, the Torsion-Bar system. Thus, this chapter is only dedicated to the application, and we don't provide any additional theoretical development.

This case study is introduced in the previous chapters where some simulations were developed to show the effectiveness of the developed methodology in this research work and as well to compare it with relatively known and modern methodologies proposed in the current literature.

First, we begin with the description of the Torsion-Bar (T-B) system with more details and characteristics given by the factory owner (*Controllab Products*©). After, each controller is synthesised associated to an observer, if this applies. We propose to compare the performance of each one by displaying some temporal responses and by analysing the results.

Finally, some conclusions and remarks about the application are provided.

4.2 Real Torsion-Bar Description

The Torsion-Bar system described in chapter 1, section 1.5, is redrawn in Fig. 4.1 with a new mechanical part allowing us to apply a torque (disturbance) on the first rotating disk (motor disk).

The Bond Graph model for the T-B system is show again in Fig. 4.2 and the state-space representation obtained from this representation is rewritten in (4.1).

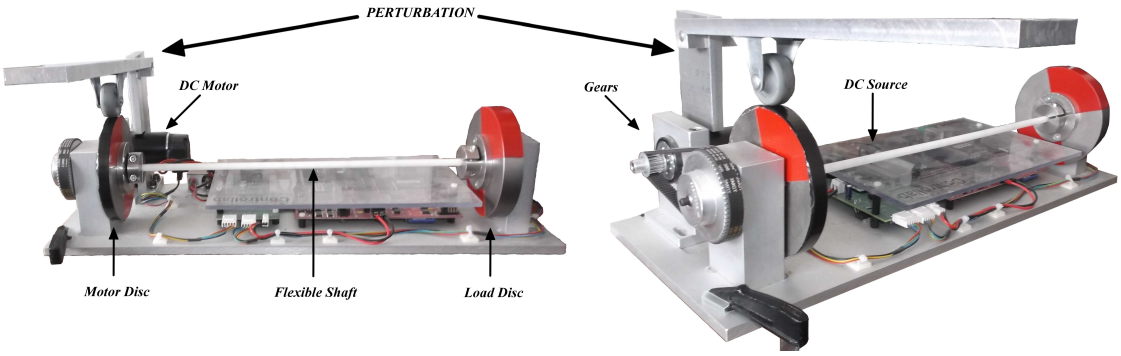

Figure 4.1 – Real Torsion-Bar system with mechanical perturbation.

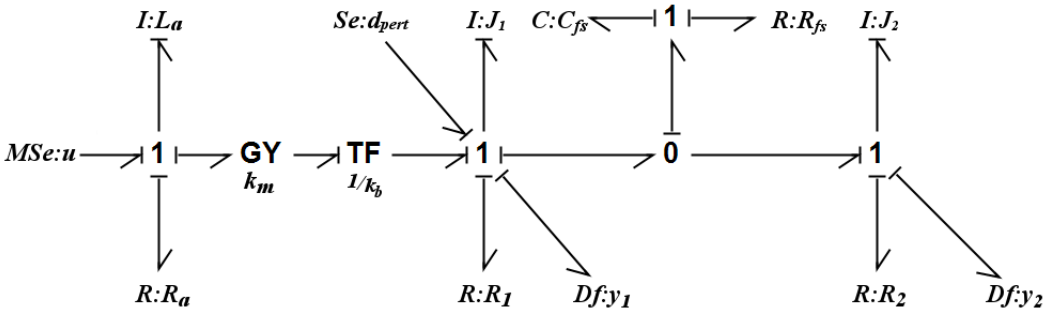

Figure 4.2 – Modified T-B bond graph model with integral causality assignment: BGI.

$$\begin{cases} \dot{x}_1 = -\frac{1}{J_2}x_2 + \frac{1}{J_1}x_3 \\ \dot{x}_2 = \frac{1}{C_{fs}}x_1 - (\frac{R_2+R_{fs}}{J_2})x_2 + \frac{R_{fs}}{J_1}x_3 \\ \dot{x}_3 = -\frac{1}{C_{fs}}x_1 + \frac{R_{fs}}{J_2}x_2 - (\frac{R_1+R_{fs}}{J_1})x_3 + \frac{k_m \cdot k_b}{L_a}x_4 + d_{pert} \\ \dot{x}_4 = -\frac{k_m \cdot k_b}{J_1}x_3 - \frac{R_a}{L_a}x_4 + u \\ y_1 = \frac{1}{J_1}x_3 \; ; \; y_2 = \frac{1}{J_2}x_2 \end{cases} \tag{4.1}$$

The numerical values for each element mentioned in the bond graph model and state-space representation are listed in table 4.1.

Element	Symbol	Value
Inductance	L_a	1.34×10^{-3} H
Inertia of motor disk	J_1	9.07×10^{-4} kg m^2 rad^{-1}
Inertia of load disk	J_2	1.37×10^{-3} kg m^2 rad^{-1}
Spring compliance	C_{fs}	0.56 N m rad^{-1}
Resistance	R_a	1.23 Ω
Motor disk friction	R_1	5.025×10^{-3} N m s rad^{-1}
Load disk friction	R_2	25×10^{-6} N m s rad^{-1}
Damping spring	R_{fs}	5×10^{-4} N s rad^{-1}
Motor constant	k_m	38.9×10^{-3} N m A^{-1}
Transmission ratio	k_b	3.75

Table 4.1 – Parameters of experimentation for the Torsion-Bar system model.

In the practical side, two software are necessary to apply the disturbance rejection methods: *20-Sim*® software used for modelling and simulation of dynamical systems, and *20-Sim 4C*® used to export and load the *C-code* and to run it on the hardware.

Before applying the Disturbance rejection methods, some features of the *20-Sim 4C*® are expressed, [Kleijn, 2013]. From *20-Sim 4C*®, the *C-code* can be created automatically or directly from *20-Sim*®. With the software *20-Sim 4C*®, it is also possible to start and to stop the control law applied to the system in real time and also to change the parameters during the run-time. Implementing code is also possible from *20-Sim*®.

In the previous Chapter, simulations proved the effectiveness of each disturbance rejection methodology. These are now proved on the real Torsion-Bar system. For this, it is necessary to take into account some characteristics given by the manufacturer (*Controllab Products*). These characteristics are important to model the whole real system. It is important to emphasize that the machine only has two velocity sensors (two incremental encoders) and one actuator of PWM type. There is also a current limit at the entry for equipment protection, [Kleijn, 2008].

Only the variable output $y_2(t)$ is controlled and the measured output variables are $y_1(t)$ and $y_2(t)$. The control input variable $v(t)$ is defined as a step function in rad s^{-1} and its action begins at 0.5 s with a value of 20 rad s^{-1}. At $t = 2$s the input is incremented at 40 rad s^{-1} and maintained until the end. The unknown input that is defined as $d_{pert}(t)$(N m) could have time action between 5s and 15s. This perturbation is not applied automatically but manually, and its value is not known. Finally, an important characteristic of the T-B system must be taken into account: the *voltage supply limits* to the system that are ± 12 V. It is also linked to the current limit at entry.

The results are displayed in different figures. The first figure for each method have the same information, the input reference $v(t)$, the output variable $y_2(t)$ and its estimation $\hat{y}_2(t)$ (if possible). The next figures could contain the output variable error $e_{y_2}(t) = y_2(t) - \hat{y}_2$(t) and the estimation of the (total, cumulated or estimated) perturbation if possible. Finally, the control signal $u_c(t)$ and the supplied energy.

4.3 Disturbance Rejection: Applications

A simplified description of the Hardware-in-the-loop (HIL) with this real time plant application is proposed in Fig. 4.3. The connection between the real system and the control part is highlighted. The control law is exported to a *C-code* from a model developed in the *20-Sim*® platform. The model requires some adaptations before to be applied to the T-B system because the sensor entries and the control signal outputs are given in discrete time, thus, the model needs be redefined for discrete time.

With this idea, signal treatment on the data output from the control $u_c(t)$ and the data entries $y_1(t)$ and $y_2(t)$ are necessary. An D/A converter associated to $u_c(t)$ and two *counts to velocity* converters associated to $y_1(t)$ and $y_2(t)$ are used. As well, the dynamical elements in Bond Graph modelling (*e.g.*, elements I, C, etc.) are adapted to be used in discrete time.

We will prove that all the studied controllers are able to achieve the DR but in different manners and performances.

4.3.1 PID control

The classical Proportional-Integral-Derivative (PID) control described in the first chapter, section 1.3.1 and equation (1.11), where only the error variable $e(t)$, difference between the reference input signal $v(t)$ and the output variable $y_2(t)$, is used as information for the controller. The PID controller is described by three parameters (K_p-Proportional Gain, T_i-Integral Gain and T_d-Derivative Gain).

After probing different tuning methods in order to define the parameters for the PID controller, we get parameters $K_p = 0.1$, $T_i = 0.09s^{-1}$ and $T_d = 0.009s$. Since the model is linear, it is also possible to calculate the gains on beforehand. The PID Controller for disturbance attenuation is applied to the system and some variables are presented in the next figures. Note that the disturbance variable must be constant and that it is not estimated with this approach. The data of the output variable $y_2(t)$ and the reference $v(t)$ are presented in Fig. 4.4 and the control signal $u(t)$ apply to the T-B system in Fig. 4.5.

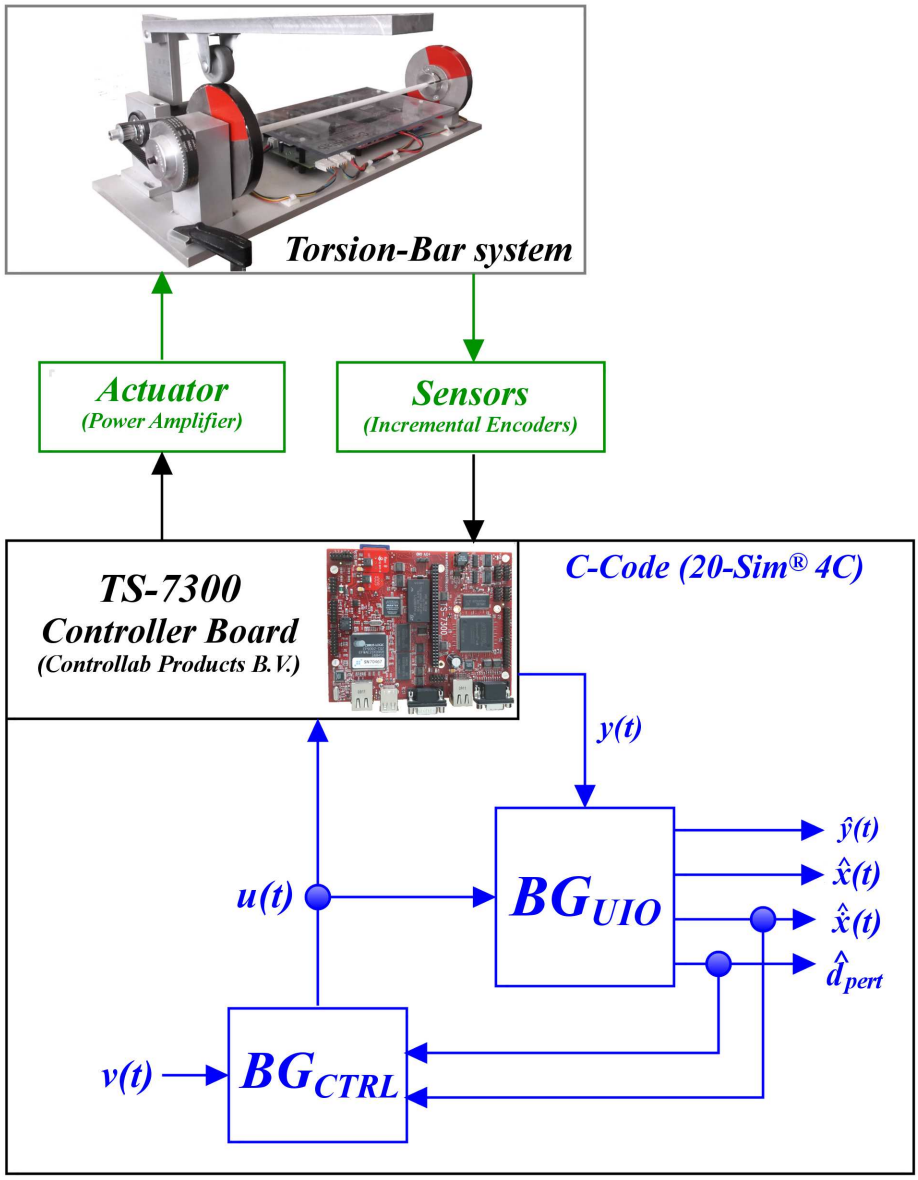

Figure 4.3 – Real time plant application with HIL description.

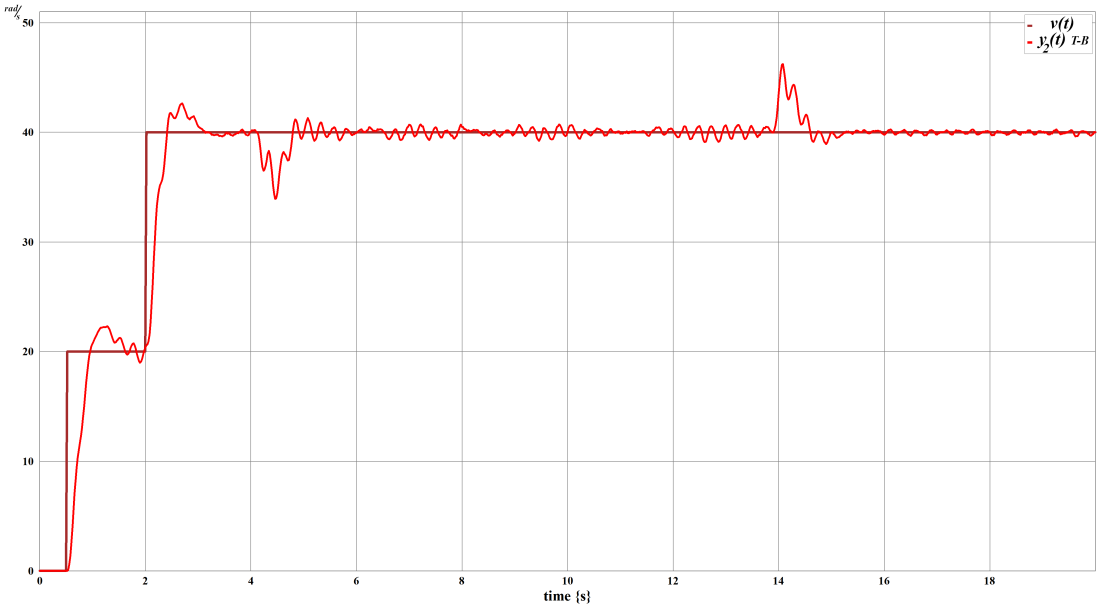

Figure 4.4 – PID: output variable $y_2(t)$ and the reference speed $v(t)$

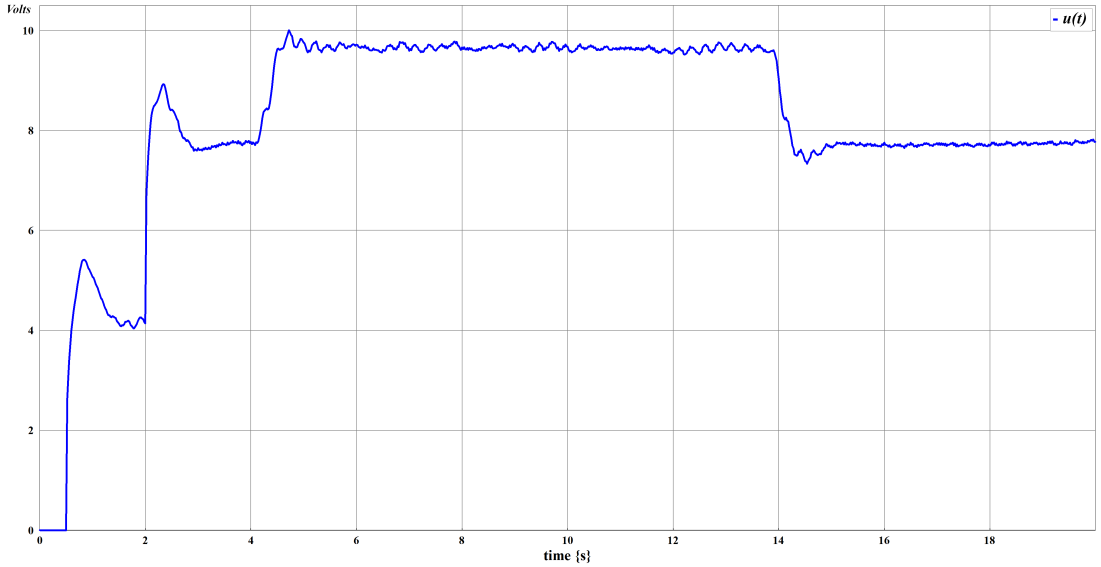

Figure 4.5 – PID: Control signal input $u(t)$

4.3.2 Disturbance Observed-Based Control (DOBC)

The description of the DOBC methodology is in section 3.2.1 and the simulations in section 3.3.1. The schematic structure is displayed in Fig. 3.6 and is applied to the real T-B system. Note that the DOBC structure is divided in two parts: *the feedback part* state-feedback control with integral action defined in equation (4.2), in addition with the disturbance rejection $\hat{d}_l$, the *Disturbance Observer Part*, Disturbance observer equation (4.4) and a state observer (Luenberger)).

The integral action is added for attenuation of constant disturbance and set point tracking of the signal output $y_2(t)$.

$$\begin{bmatrix} \dot{x}(t) \\ \dot{x}_i(t) \end{bmatrix} = \begin{bmatrix} (A+BK) & BF_2 \\ -C & 0 \end{bmatrix} \begin{bmatrix} x(t) \\ x_i(t) \end{bmatrix} + \begin{bmatrix} 0 \\ 1 \end{bmatrix} v(t) \tag{4.2}$$

Thus, for the *feedback part* that contains the state feedback control with the integral action, the poles are placed at $[-5, -10, -15, -20, -2]$. The values obtained for this part are such $F_{aug} = [K\,|F_2] = [-1.2347,\ 14.376,\ -184.66,\ -872.39,\ 1]$.

For the *Disturbance observer part*, considering the state-space representation for the well-known Luenberger observer as $\dot{\hat{x}} = A\hat{x} + Bu + L_S[y - C\hat{x}]$. The observer matrix gain L_S is chosen such that the eigenvalues of $(A - L_S C)$ are all in the left-half complex plane. The eigenvalues of $(A - L_S C)$ for the observer are placed at $[-25,\ -20, -15,\ -10]$. Matrix L_S is given in equation (4.3).

$$L_S = \begin{bmatrix} 1 & -0.866 \\ 0.45 \cdot 10^{-3} & 38.57 \cdot 10^{-3} \\ -0.8 & -0.825 \\ 6.56 & 6.707 \end{bmatrix} \tag{4.3}$$

And finally, the disturbance estimator described in equation (4.4) is applied on the T-B system and the values for the gain matrix $L_d = [l1, l2, l3, l4]$ are defined as $L_d = [100, 100, 100, 70]$.

$$\begin{cases} \dot{z} = -L_d B(z + L\hat{x}) - L_d(A\hat{x} + Bu) \\ \hat{d}_l = z + L_d\hat{x} \end{cases} \tag{4.4}$$

The results and the data obtained from the application of this method with these parameters are shown in the figures below.

Fig. 4.6 contains the data of the signal output $y_2(t)$ obtained from the real system, its estimation $\hat{y}_2(t)$ and the reference described by $v(t)$. $\hat{y}_2(t)$ is computed from the state-estimator that doesn't contain information about the perturbation. It can be observed that the output variable is not at all well estimated. Nevertheless, the disturbance is rather well rejected. In Fig. 4.7, the total perturbation variable is displayed and also $e_{y_2} = y_2(t) - \hat{y}_2(t)$. In comparison with other approaches, the disturbance effect seems to be rather well estimated. Finally, the control signal input $u(t)$ applied to the T-B system is displayed in the Fig. 4.8. As well, it is similar to other control laws.

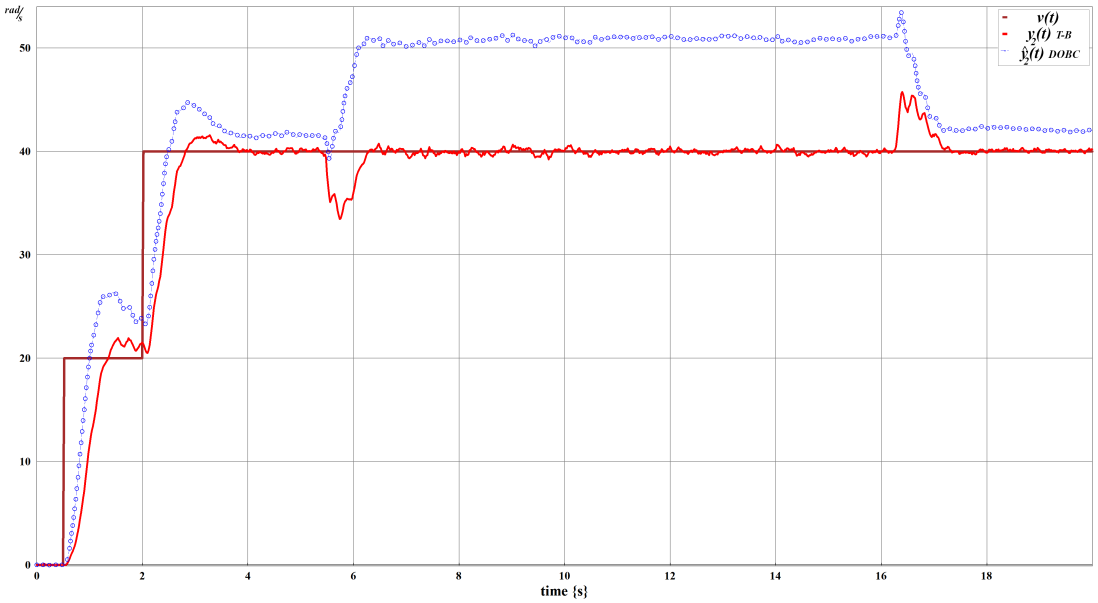

Figure 4.6 – DOBC: output signal $y_2(t)$ and its estimation $\hat{y}_2(t)$ and the reference speed $v(t)$

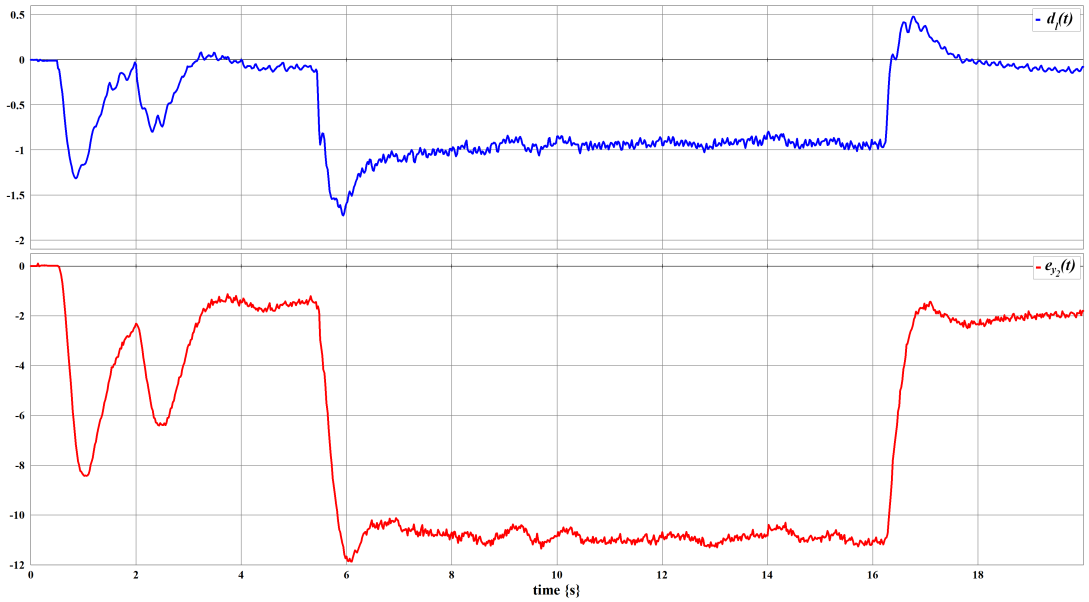

Figure 4.7 – DOBC: Estimated disturbance variable $\hat{d}_l$ (up) and the error $e_{y_2}(t) = y_2 - \hat{y}_2$

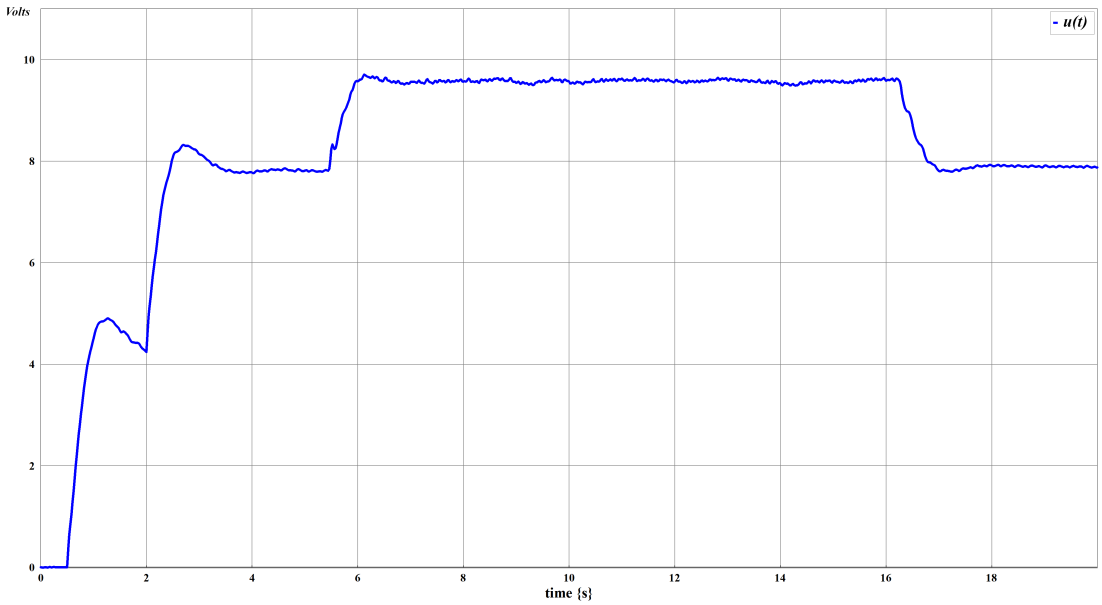

Figure 4.8 – DOBC: control signal $u(t)$ applied to the T-B system

4.3.3 Active Disturbance Rejection Control (ADRC)

This method is presented in chapter 3, sections 3.2.2 and 3.3.2, the three parts are rewriting hereafter with the parameters for the application to the T-B system.

- Extended State Observer (ESO)

  A state-space representation, with control variable $u(t)$, output variable $y_2(t)$ and with an additional (extended) state $x_4(t)$, is described in equation (4.5), where $x_1 = y_2$, $x_2 = \dot{y}_2$, $x_3 = \ddot{y}_2$, $x_4 = f(\cdot)$. The function $f(\cdot)$ represents the total disturbance to be estimated and dn_1 is a calculated constant.

$$\begin{cases} \dot{x}_1 = x_2 \\ \dot{x}_2 = x_3 \\ \dot{x}_3 = dn_1 u(t) + x_4 \\ \dot{x}_4 = \dot{f}(\cdot) \end{cases} \tag{4.5}$$

  From equation (4.5), the ESO can be designed as (4.6), where the estimation error is given as $e_0 = y_2 - z_1$, z_1 is the estimation of y_2 and z_4 estimates the total disturbance $f(\cdot)$.

$$\begin{cases} \dot{z}_1 = z_2 + \beta_1 e_0 \\ \dot{z}_2 = z_3 + \beta_2 e_0 \\ \dot{z}_3 = dn_1 u(t) + z_4 + \beta_3 e_0 \\ \dot{z}_4 = \beta_4 e_0 \end{cases} \tag{4.6}$$

Parameters $\beta_1, \beta_2, \beta_3, \beta_4$ are the observer gains calculated following chapter 3 and references [Wicher and Nowopolski, 2017, Miklosovic and Gao, 2004]. The parameter values for the ADRC are $\beta_1 = 40$, $\beta_2 = 600$, $\beta_3 = 4000$, $\beta_4 = 10000$ and $dn_1 = 43804.58$.

- Controller

  The controller is described in (4.7). The gains of the controller were calculated according to formula, [Miklosovic and Gao, 2004, Wicher, 2018]. The values computed are $K_p = 1 \cdot 10^6$, $K_1 = 3 \cdot 10^4$, $K_2 = 300$

$$u_0 = K_p(v_{ref} - y_2) - K_{D_1} z_2 - K_{D_2} z_3 \tag{4.7}$$

- Rejector Block

  The rejector block deals with the total disturbance estimation z_4 and with the virtual control signal u_0. The output signal of the rejector u_i is the control signal applied to the system and is a combination of the two previous signals. This block is described by equation (4.8).

$$u_i = \frac{u_0 - z_4}{dn_1} \tag{4.8}$$

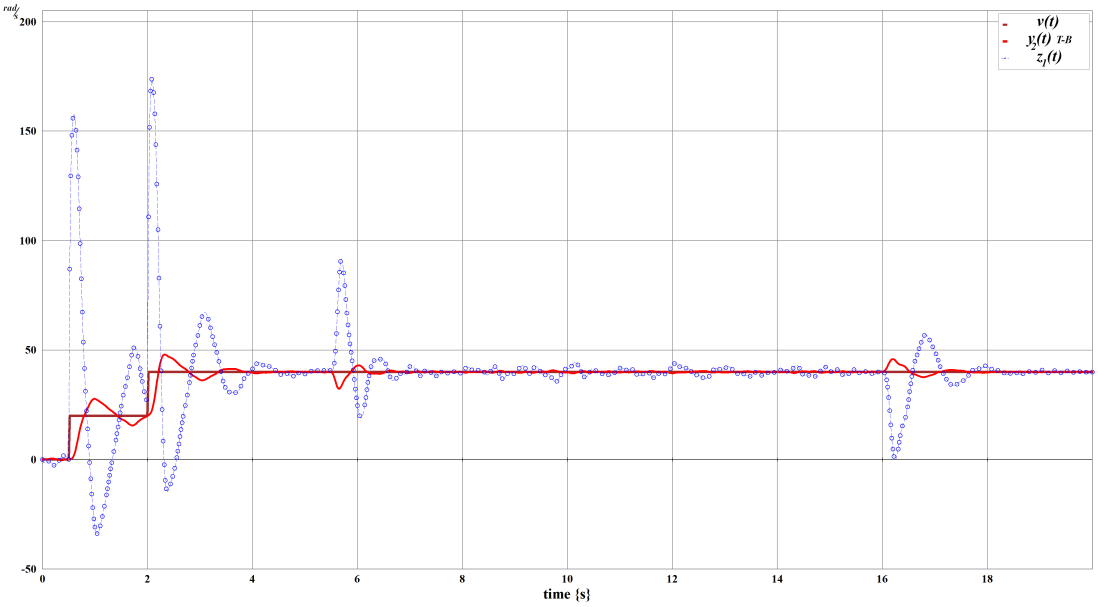

Figure 4.9 – ADRC: output variable $y_2(t)$ (red) and its estimation $z_1(t)$ (blue)

The behaviour of the T-B system with the ADRC control is now displayed following different graphical representations. In Fig. 4.9, the output variable $y_2(t)$ and its estimation are shown. It can be observed that the estimated variable contains high values. A focus on the output variable is made in Fig. 4.10 with the reference speed variable. The error $e_0 = y_2 - z_1$ and the total disturbance estimated $f(\cdot)$ are shown in Fig. 4.11. In this figure, it is possible to observe the value of the total perturbation $f(\cdot)$ and the dynamic for the error e_0, but as stated in the theoretical part, it is not the exact estimation of the disturbance (real torque) applied to the T-B system. The control signal is displayed in Fig. 4.12. We remark that some peak voltages are close to the limits given by the T-B system.

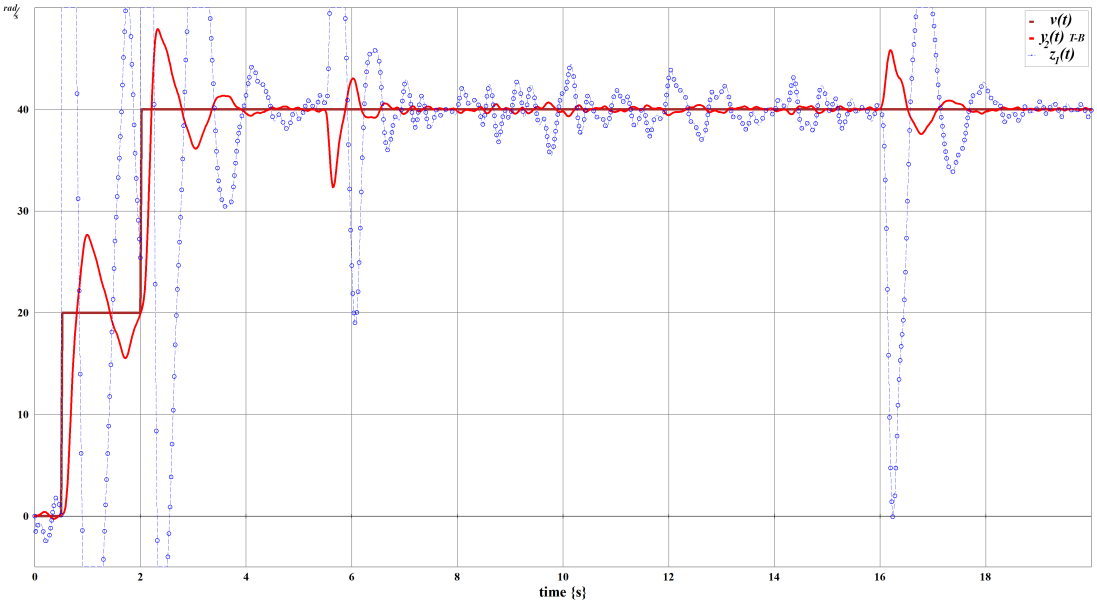

Figure 4.10 – ADRC: output variable $y_2(t)$ and the reference $v(t)$

4.3.4 DSF-UIO-BG

In chapter 3 and section 3.3.3, the Derivative State Feedback (DSF) control law associated to an Unknown Input Observer (UIO) is applied to the T-B system. Structural analysis is implemented with a bond graph approach and a Disturbance Rejection (DR) solution is provided and then evaluated by simulation. We recall some properties of the model and expressions of the control law as well as the observer. Then, the control law is applied to the T-B system.

The model $\Sigma(C,A,B)$ associated to the torsion bar system is structurally *controllable/observable*, a derivative causality assignment can be applied to the bond graph model, see Fig. 3.15. As well, the state matrix A is invertible. The Disturbance Rejection with Derivative State Feedback is applied in the Single Input - Single Output (SISO) case, see chapter 1, and an Unknown Input Observer is used in the Multiple Input - Multiple Output (MIMO) case since two variables are measured, see section 2.3 or [Sueur, 2016, Gonzalez and Sueur, 2018b, Gonzalez et al., 2018].

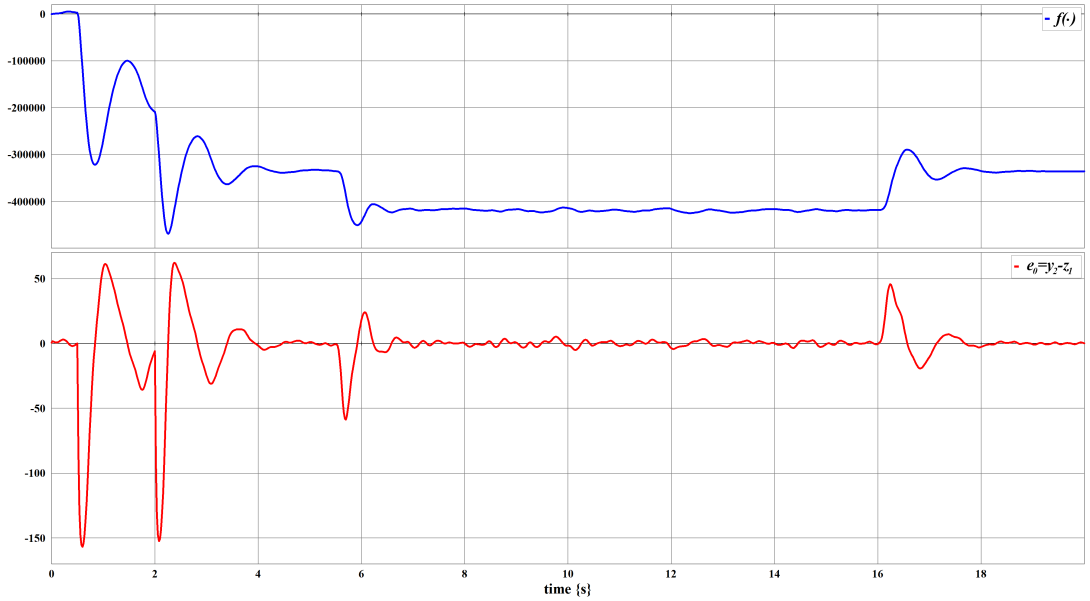

Figure 4.11 – ADRC: cumulative perturbation $f(\cdot)$ (up) and the error $e_0(t) = y_2(t) - z_1(t)$ (down)

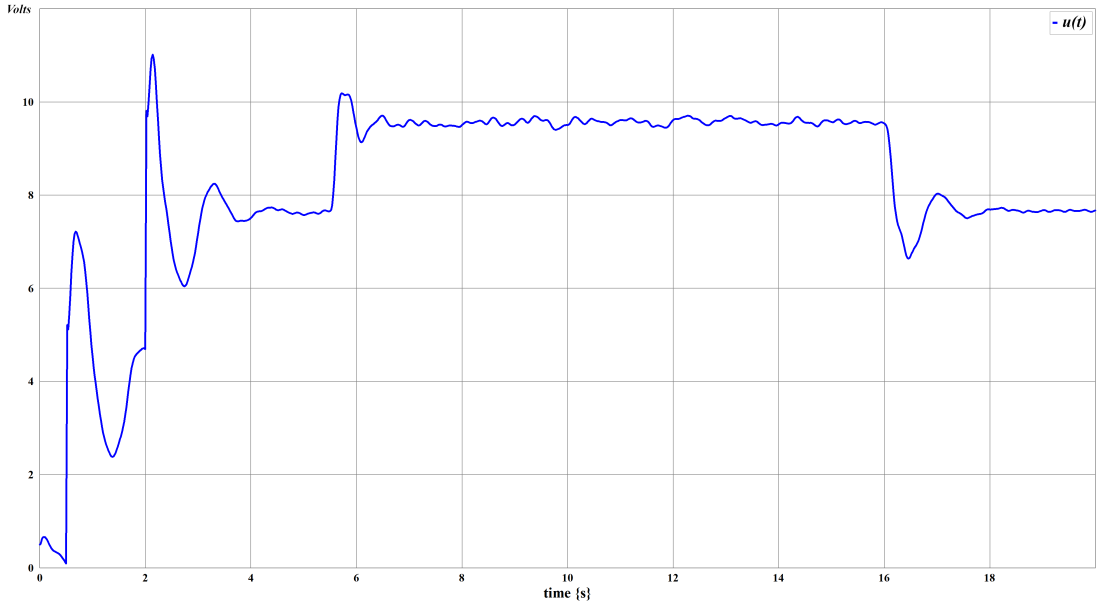

Figure 4.12 – ADRC: input control signal $u(t)$

4.3.4.1 Unknown Input Observer applied to the T-B system

The Unknown Input Observer for this Bond Graph model is now designed, see chapter 2, section 3.2.3. For system $\Sigma(C,A,B,F)$ defined in equation (1.1), $m=1$ (one input control), $q=1$ (one unknown input variable, disturbance) and $p=2$ (two measured variables $y_1(t)$ and $y_2(t)$).

The UIO synthesis is thus proposed with the two output detectors $Df:y_1$ and $Df:y_2$. It is a non-square model. Structural properties of the model $\Sigma\left([C_1^t,C_2^t]^t,A,F\right)$ are studied. The causal path with the first output detector is $Df:y_1 \rightarrow I:J_1 \rightarrow Se:d_{pert}$ and the causal path with the second output detector is $Df:y_2 \rightarrow I:J_2 \rightarrow R:R_{fs} \rightarrow I:J_1 \rightarrow Se:d_{pert}$. The length of these causal paths are equal to $n_{p1}=1$ and $n_{p2}=2$ for y_1 and y_2 respectively. Since $n_{p1}<n_{p2}$, the estimation of the state vector is written in equation (4.9) and the estimation of the unknown input variable is still defined in equation (2.21). Matrix N_{CL} is written in equations (4.10).

$$\dot{\hat{x}}(t)=A\hat{x}(t)+Bu(t)+F\dot{\hat{d}}(t)-AK\begin{pmatrix} y_1^{(1)}(t)-\hat{y}_1^{(1)}(t) \\ y_2^{(1)}(t)-\hat{y}_2^{(1)}(t) \end{pmatrix} \tag{4.9}$$

$$N_{CL}=A^{-1}-A^{-1}F(C_1A^{-1}F)^{-1}C_1A^{-1}-K\begin{bmatrix} C_1 \\ C_2 \end{bmatrix} \tag{4.10}$$

From a structural analysis, it can be proved that model $\Sigma\left([C_1^t,C_2^t]^t,A,F\right)$ has one invariant zero, which is the common invariant zero of submodels (C_1,A,F) and (C_2,A,F). The invariant zero is equal to $z_I=-{}^{R_a}/_{L_a}=-917.91$. The inverse of this invariant zero is a fixed mode for the estimation error equation, *i.e.* for matrix N_{CL}. If the four poles of matrix N_{CL} are ${}^{-1}/_{917.91}$, ${}^{-1}/_{1000}$, ${}^{-1}/_{1000}$ and ${}^{-1}/_{3401.4}$, matrix K is thus as expressed as:

$$K=\begin{bmatrix} -9.07\cdot10^{-17} & 7.672\cdot10^{-4} \\ 0 & 1.37\cdot10^{-6} \\ 4.535\cdot10^{-7} & 0 \\ -1.814\cdot10^{-15} & -2.74\cdot10^{-15} \end{bmatrix}$$

4.3.4.2 Disturbance Rejection with DSF applied to the T-B system

The infinite structure of models $\Sigma(C_2,A,B)$ and $\Sigma(C_2,A,F)$ are first studied with a structural approach. The shortest causal path between the output variable to be controlled $Df:y_2(t)$ and the control input $MSe:u(t)$ in the Bond Graph model with Integral causality (BGI) of Fig. 3.5 is

$$Df:y_2 \rightarrow I:J_2 \rightarrow R:R_{fs} \rightarrow I:J_1 \rightarrow TF:1/k_b \rightarrow GY:k_m \rightarrow I:L_a \rightarrow MSe:u\ .$$

The length of this causal path is equal to 3, then $n_{c2}=3$. The shortest causal path between the output variable to be controlled $Df:y_2(t)$ and the disturbance input $Se:d_{pert}$ is

$$Df:y_2 \rightarrow I:J_2 \rightarrow R:R_{fs} \rightarrow I:J_1 \rightarrow Se:d_{pert}\ .$$

The length of this causal path is equal to 2, then $n_{p2} = 2$. Since $n_{p2} < n_{c2}$, from property 1 the DSF has a solution with $n - n_{c2} = 1$ finite fixed mode which is the invariant zero of model $\Sigma(C_2, A, B)$ and $n_{p2} = 2$ finite modes which can be freely chosen with matrix F_c (property 6). Its value is $I_z = -1/C_{fs} \cdot R_{fs} = -3571.42$. Some coefficients can be derived from a causal analysis (causal path gains), but here they are directly obtained from formal calculus. With pole placement, matrix F_c is defined in equation (1.29), with numerical values in equation (1.30). Two poles can be chosen because $n_{p2} = 2$. In that case,

$$\begin{aligned}\det(sI - A - sBF_c) = \\ &= \frac{R_1 \cdot R_a + R_2 \cdot R_a + k_m^2 \cdot k_b^2}{C_{fs} \cdot J_2 \cdot L_a \cdot J_1} \cdot (C_{fs} \cdot R_{fs} \cdot s + 1) \cdot (\alpha_2 \cdot s^2 + \alpha_1 \cdot s + 1) \\ &= 2.9483 \cdot 10^7 \cdot (2.8 \cdot 10^{-4} \cdot s + 1) \cdot (\alpha_2 \cdot s^2 + \alpha_1 \cdot s + 1)\,.\end{aligned}$$

The differential equation verified by the output variable $y_2(t)$ with the Derivative State Feedback control law with pole placement is $\alpha_2 \ddot{y}_2(t) + \alpha_1 \dot{y}_2(t) + y_2(t) = v(t)$. Parameters α_1 and α_2 can be arbitrarily chosen, according to the poles of the closed loop model.

The DSF control applied to T-B system with the UIO with general structure is shown in Fig. 3.4. This structure is used as well for simulation as for application to the real system (see chapter 3). BG_{obs} is the bond graph model of the physical system with some signal bonds, and in order to obtain the estimation of the state variables derivatives, it is sufficient to add effort sensors (elements I) or flow sensors (elements C) on the dynamical elements of the bond graph observer, without any use of mathematical derivation.

With the parameters computed for this method, the results are shown below in different graphics.

In Fig. 4.13, the output and its estimation are shown. The disturbance rejection is achieved. Signal $y_2(t)$ and its estimation $\hat{y}_2(t)$ are smooth signals and the set-tracking of the reference is well done. The estimation of the disturbance variable is displayed in the Fig. 4.14. Note that this variable is not known at all, because it is a torque applied manually to the motor disk. Since this estimated variable is explicitly used in the expression of the control law, we can consider that it is well estimated.

The error variables $e_1(t) = y_1(t) - y_1(t)$ and $e_2(t) = y_2(t) - y_2(t)$ are shown in Fig. 4.15. They prove the efficiency of the control law.

The control signal $u(t)$ apply to the T-B system is presented in the Fig. 4.16. This control signal doesn't have any peak of voltage over the limits.

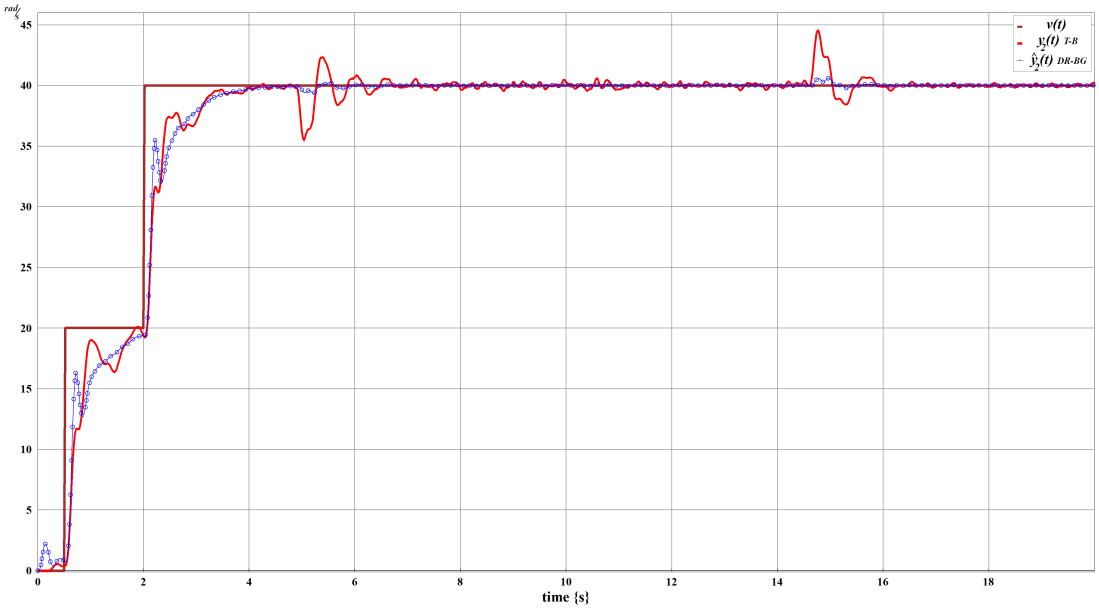

Figure 4.13 – DR-DSF-UIO-BG: output variable $y_2(t)$ and its estimation $\hat{y}_2(t)$

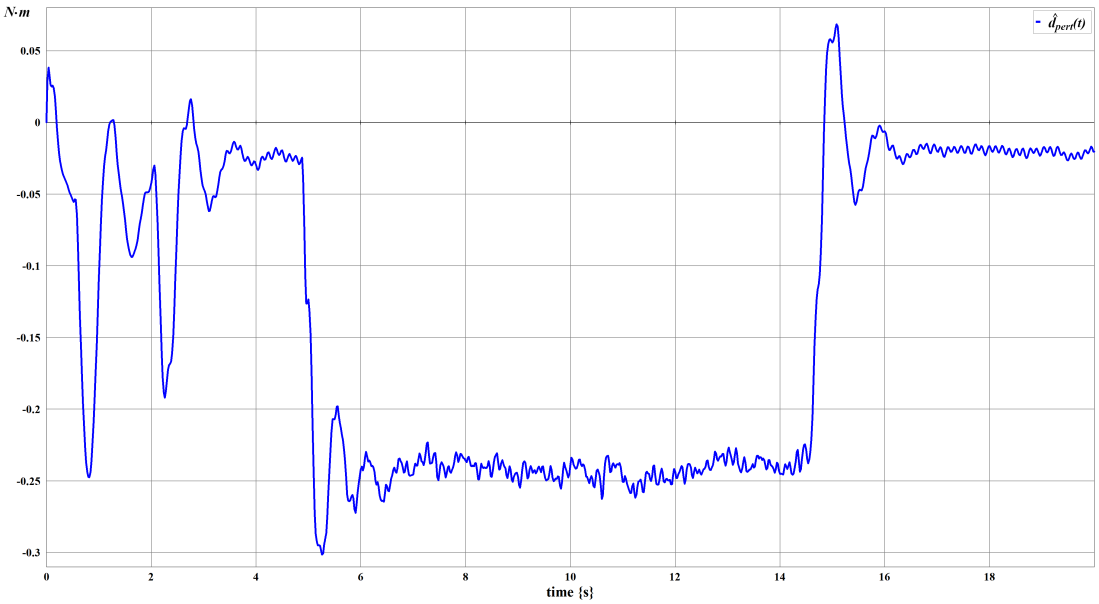

Figure 4.14 – DR-DSF-UIO-BG: estimation of the disturbance variable $\hat{d}_{pert}$.

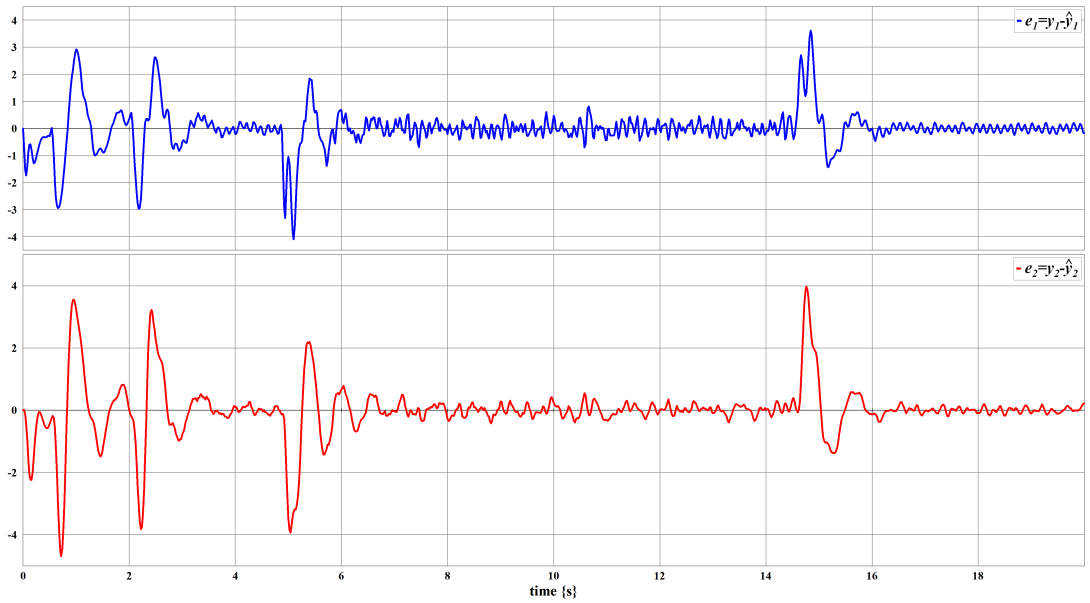

Figure 4.15 – DR-DSF-UIO-BG: errors $e_1(t) = y_1(t) - \hat{y}_1(t)$ (up) and $e_2(t) = y_2(t) - \hat{y}_2(t)$ (down).

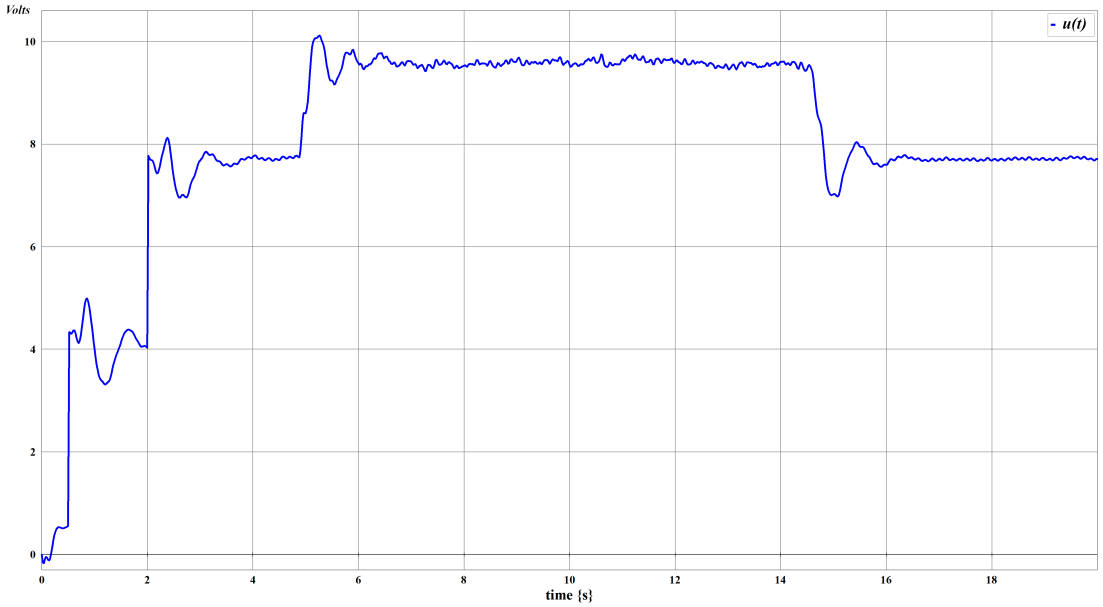

Figure 4.16 – DR-DSF-UIO-BG: control signal $u(t)$.

4.4 Concluding remarks

Numerous approaches for solving the disturbance rejection problem are available in the scientific literature. In chapter 3, we recalled some of them and we made a comparative study, first from a theoretical point of view in order to highlight the outstanding features such as conditions for application (solvability conditions) and thus some features about the control law synthesis and some properties of the controlled system. This enabled us to compare their performances with some simulations.

This chapter aims to compare some of the control laws on the real torsion bar system used as a case study. Each of the tested approach seems to be capable of achieving the objectives, namely rejecting the disturbance, but with some different conclusions. Even if a constant disturbance is each time rejected, the new approach based on the bond graph approach (DSF-UIO) is capable of given a good estimation of this disturbance, and we even prove practically that this unknown input can be of various nature. In particular, it could be easy to extend this approach to estimation of parameter uncertainty or variation and thus adapting the control law accordingly. For that reason, we strongly believe that this control strategy can be applied to power plant systems in order to improve their performance by estimating some unknown phenomena and by elaborating performant control law. This idea is the object of the next concluding chapter.

Chapter 5

Future Works: Renewal energy

5.1 Introduction

In this chapter, we present briefly a possible application of the present research work and we direct it towards the improvement of renewable sources. We begin with a brief summary about the climate change and the renewable energy and how it affects the research and investment in the renewable power technologies, information from recent literature.

In a second step, we present a simplified model of a hydroelectric plant that could be a case study for us. Indeed, some future works could be developed in respect to this subject. Some points are highlighted to show the usefulness of this research work, first using the integrated approach based on the bond graph representation, with the concept of "Word-Bond Graph". Secondly, a detailed bond graph model is displayed in order to proceed some simulations. As for the previous case study, i.e. the torsion bar system, we aim to be able to characterize properties of the model (system) and be able to synthesize robust control laws with a complex system under the influence of external phenomena, such as disturbances, failures or parameter variations.

Notice that this project under development is made in collaboration with researchers from the fluid mechanics laboratory of Ecole Centrale de Lille. To conclude, we formulate some future perspectives for this project.

5.2 Renewable sources: Brief summary

Global demand for energy continues to rise, led by developing countries, reflecting an expanding global economy, rapid industrialization, population growth, urbanisation and improved energy access, [IRENA, 2017].

The decrease in fossil sources, excessive environmental pollution and high prices are some of the most reported problems of traditional energy resources. Energy and climate change are related each other. This is why a fundamental change in current energy systems is necessary to successfully confront climate change, [IRENA, 2019a].

Governments around the world are rethinking their energy sector strategy and embracing renewable energy technologies. Then, the global energy transformation is happening, driven by the dual imperatives of limiting climate change and fostering sustainable growth.

The increasing energy demand is one of the key factors that manipulates the energy research trends. As a result of the search for new resources, renewable energy resources have been confirmed as an adequate alternative to traditional generation of fossil fuel energy [Habibi et al., 2019].

An unprecedented decline in renewable energy costs, new opportunities in energy efficiency, digitalisation, smart technologies and electrification solutions are some of the key enablers behind this trend. Renewable power technologies are often the first choice for expanding, upgrading and modernising electricity infrastructure around the world, [IRENA, 2019c].

In most parts of the world today, renewable sources are the lowest-cost source of new power generation. As costs for solar and wind technologies continue falling, this will become the case in even more countries. The cost of electricity from bioenergy, hydro-power, geothermal, onshore and offshore wind was within the range of fossil fuel-fired power generation costs between 2010 and 2018. Since 2014, the global-weighted average cost of electricity of solar photovoltaics (PV) has also fallen into the fossil-fuel cost range. For the vast majority of renewable energy technologies, capacity and output continue to grow as renewable energies in the power sector far outpace growth in conventional technologies.

During 2018, the contribution of all renewable energy sources to the global energy mix grew by largest increment yet, particularly in the electricity sector, [IRENA, 2017, IRENA, 2019a]. Renewable power capacity represented 61% of all new power generating capacity added worldwide.

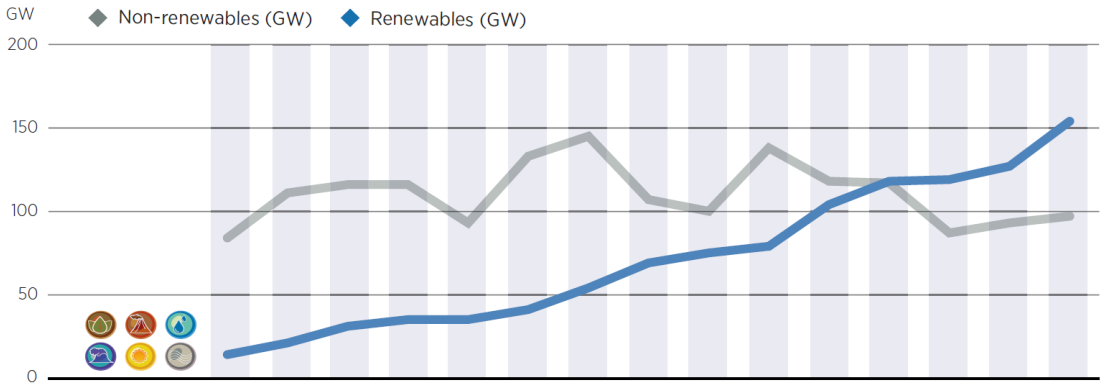

Figure 5.1 – Renewable and Non-renewable power capacity additions between 2001-2015.

In Fig. 5.1, [IRENA, 2017], we observe the moment when the additions on renewable power capacity exceeds the non-renewable, and Fig 5.2 shows the global power generating capacity until 2018, [REN21, 2019].

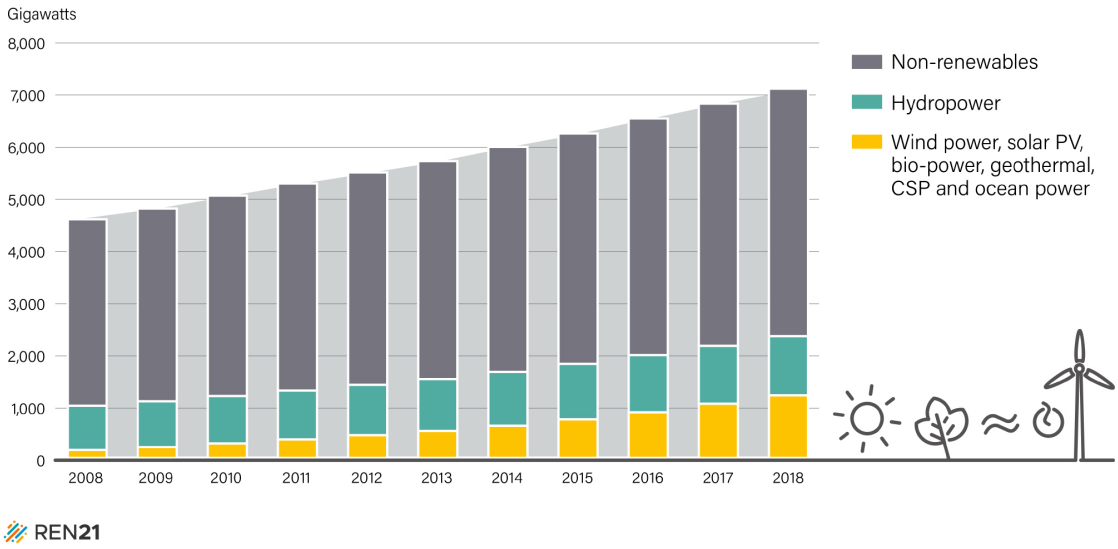

Figure 5.2 – Global Power Generating capacity, 2008-2018.

Each year, more electricity is generated from renewable energy then in the previous year. Renewable energies provided an estimated 23.5% of all electricity generated in 2015 - 5660 TW h, [IRENA, 2019b, IRENA, 2017]. In Fig. 5.3, in "Rethinking energy 2017", the different sources of energy are shown for generation of electricity in 2015.

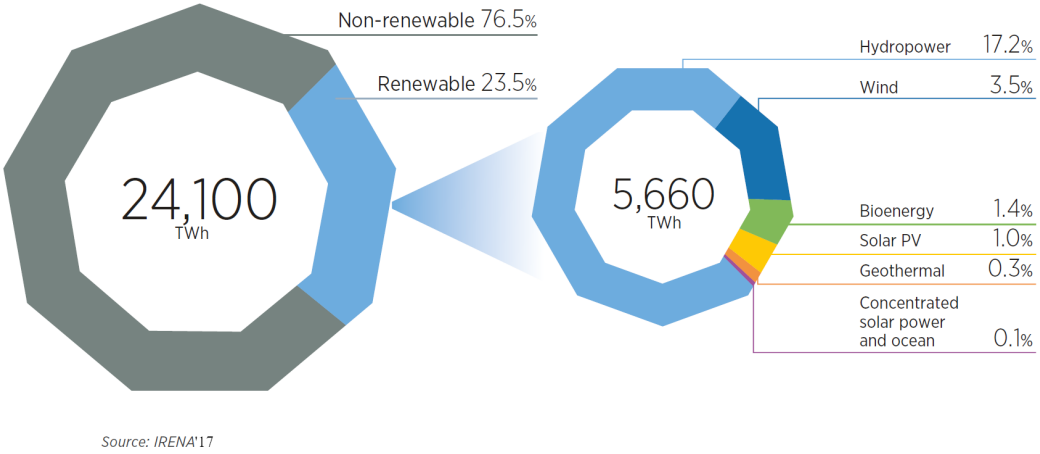

Figure 5.3 – Global electricity generation by source, 2015.

In 2018, the rates are: wind power (21%), solar 59% and bio-power (8%). Overall, the installed renewable power capacity at year's end was enough to supply around 26.02% of global electricity production (see Fig. 5.4), [REN21, 2019]. Hydro-power still accounted for some 60% of the renewable electricity production followed by wind power, bioenergy and solar PV.

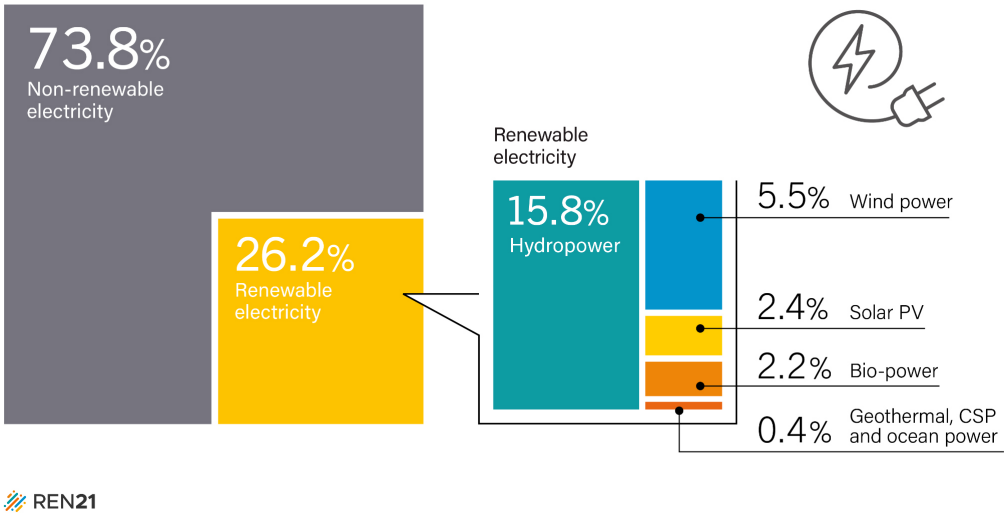

Figure 5.4 – Global electricity production by source, End-2018

Renewable energies overall are struggling to increase their share of the global energy mix for three main reasons: **1)** the traditional use of biomass is in decline as more people gain access to modern energy; **2)** Total final energy use continues to rise; **3)** The technologies that have grown the fastest have done so from a very low base (Solar PV and Wind power).

Despite a second consecutive year of rising global energy related CO_2 emissions, some regions have achieved significant reductions in the electricity generation emissions due in part to deployment of renewable power capacity. *European* emissions related to electricity production reportedly fell 5% in 2018 as a result of renewable energies. *US* CO_2 emissions from power generation fell nearly 30% between 2005 and 2018, due in part to slower demand growth (*improvements in energy efficiency*) and growing renewable electricity production, especially from wind energy, [REN21, 2019].

There are more sectors that have been benefited by the renewable energies as the cost of electricity production, sources of employment, heating and cooling, transport, etc. ([REN21, 2019, IRENA, 2019a, IRENA, 2019c, IRENA, 2017]).

5.3 Hydroelectric plant

This case study and project is inspired for the previous summary and the previous chapters. In addition, a collaboration with researchers from the fluid mechanics field bright to this research a possibility to investigate, analyse and modelling a hydroelectric system. This hydroelectric system, its model and modelling tools can be useful for related researches in hydraulic domain or energy storage development, [Ratolojanahary et al., 2019, Ortego Sampedro, 2013].

In the next figure, Fig.5.5, the representation of the study case is presented. According to this representation the model can consist of different parts: an opened tank linked to a pipe, a kink, a needle valve (with conical bearing surface), a nozzle, a Pelton turbine and a Direct Current (DC) generator.

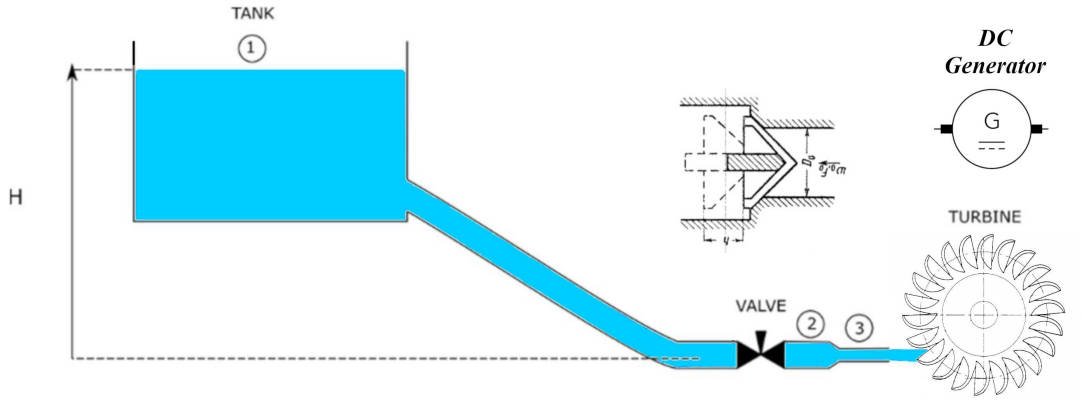

Figure 5.5 – Hydro-electric system representation

A series of power interchange is also observed through the system. The flow at the tank outlet is directed in the pipe and kink, it goes through the needle valve and it is accelerated in the nozzle. The water jet is out of the nozzle at the atmospheric pressure level. The power from the water jet exerts a force on the Pelton impeller bucket and starts spinning the impeller. A generator coupled with the turbine is also driven rotationally to convert the mechanical energy into electrical energy.

5.3.1 Hydroelectric model: Word Bond Graph

The Bond Graph modelling process of the hydroelectric system described above is shown in Fig. 5.6 where the transmission of power between each block is observed. This block diagram, name Word-Bond Graph, is based in the power interchange in the bond graph approach. There is an electromechanical part (red) that represents the generator and its load, a mechanical part (purple) representing the Pelton turbine and shaft, and finally a hydraulic section (blue). The bond graph representation is developed in accordance with equation (5.1) for the hydraulic part, equation (5.5) for the Pelton turbine and equation (5.6) and equation (5.7) for the electromechanical part.

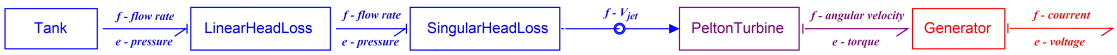

Figure 5.6 – Hydro-electric system representation: word-bond graph

The detailed model is given in Fig. 5.7. Besides allowing the power transfer representation between each element, the energy direction is also shown explicitly. The model is realized step by step by adding each element of the system respecting energy exchange and conservation. We can choose at each step the level of detail for the model, depending on modelling assumptions. At most, it is possible to analyse properties of the dynamical model, such as comparing dynamics between different parts (level modelling) or properties of the model (controllability/observability... level control properties).

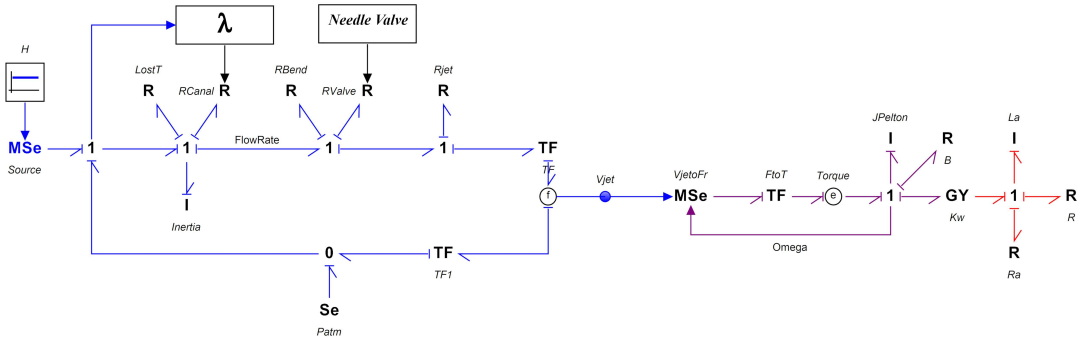

Figure 5.7 – Hydro-electric bond graph representation

We proceed some simulations that are presented in the next section. Since this model is a non-linear one, the classical structural analysis on bond graph model is not implemented at the moment. The first objective is to check the validity of the model with simulations.

5.3.2 Mathematical description

In order to describe the hydraulic system, some classical analytical equations from different physical domains can be written, [White, 2011].

The flow of an incompressible fluid through the pipe is described by unsteady Bernoulli equation along a streamline between point 1 and 3, neglecting flow velocity in the tank, [Idel'cik, 1986]. It is written in the Eq. (5.1).

$$\rho g H = \rho L \frac{d\,v_2}{dt} + \frac{1}{2}\rho v_3^2 + \lambda \frac{L}{D_c}\rho \frac{v_2^2}{2} + K_l p \tag{5.1}$$

ρ is the volumetric mass density, g is gravity, the height of water level is H, L represents the pipe length, D_c is the pipe diameter, v_2 and v_3 are the flow velocities in the points 2 and 3

respectively (see Fig. 5.5) and finally K_lp represents the total loss of pressure head cause by singularities through the pipe and valve.

Equation (5.1) is solved to determine the velocity at the point 3 ($v_3 = v_{jet}$-stream velocity). Then, the continuity equation (5.2) is applied and after equation. (5.1) is rewriting in (5.3). The parameters S_2 and S_3 correspond to the cross-sectional area of the pipe and the cross-sectional area of the convergent nozzle respectively, [Idel'cik, 1986].

$$v_2 = v_{jet}\frac{S_3}{S_2} \tag{5.2}$$

$$\frac{d\,v_jet}{dt} = \frac{gHS_2}{LS_3} - v_{jet}^2\left(\frac{1+(\frac{S_3}{S_2})^2(\lambda\frac{L}{D_c}+K_{lp})}{2L\frac{S_3}{S_2}}\right) \tag{5.3}$$

The final expression to determine v_{jet} is given in (5.4)

$$v_3 = \sqrt{\frac{b}{a}\left(\frac{\exp^{2\sqrt{a\cdot b}t}-1}{1+\exp^{2\sqrt{abt}}}\right)} \tag{5.4}$$

where $a = \frac{1+\left(\frac{S_3}{S_2}\right)^2(\lambda\frac{L}{D_c}+K_{lp})}{2L\frac{S_3}{S_2}}$ and $b = \frac{gHS_2}{LS_3}$.

Now, by analysing the energy conversion between the hydraulic energy and the mechanic energy, it is possible to find the relative force from the Pelton turbine wheel when a stream with certain velocity (v_{jet}) is applied on its buckets, [Zhang, 2016, White, 2011]. The absolute velocity at the inlet of the wheel corresponds to v_{jet}. The relative velocity can be defined as $\omega_1 = v_{jet} - u$ from the typical velocity triangle shown in the Fig. 5.8. $\omega_1 = \omega_2$ is the impeller turbine rotational velocity and u is defined as inlet tangential bucket velocity.

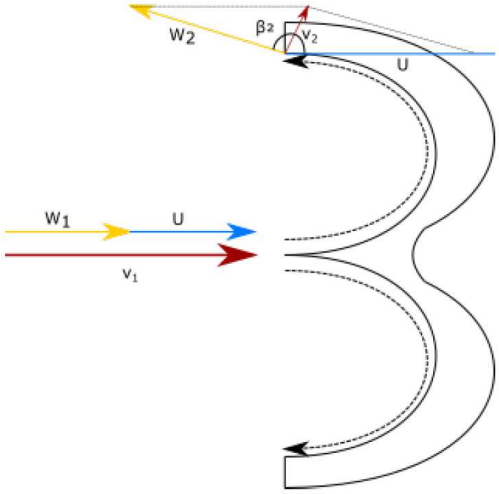

Figure 5.8 – Triangle of velocities for an individual bucket

The turbine force relation on the Pelton turbine obtained from the Newton's second law is defined in equation (5.5).

$$F_r = \rho Q_v (v_{jet} - \omega R)(1 - \cos\beta_2) \tag{5.5}$$

Q_v is the volume flow and R is the impeller radius of the turbine. From F_r, it is possible to obtain the torque from the Pelton turbine as $\tau_{pelton} = F_r\, R$. The relation between the Pelton turbine and the DC generator are given in the next equations divided in mechanical (5.6) and electric part (5.7), where I is defined as the moment of inertia, B is the friction coefficient in the mechanical part, L_a is the generator's inductance, R_a is the electric resistance, k_g is the generator constant and, V_i and i_a as the voltage and current generated respectively.

$$I\frac{d\omega}{dt} + B\omega = \tau_{pelton} - \tau_{generator} \tag{5.6}$$

$$L_a\frac{di_a}{dt} + R_a i_a + k_g\omega = V_i \tag{5.7}$$

5.3.3 Simulations

The parameters selected for this simulation are listed in the table 5.1. Other parameters are choosing during the simulation.

Element	Symbol	Value
Atmospheric pressure	P_{atm}	101 325 Pa
Density	ρ	1000 kg m^{-3}
Dynamic viscosity	μ	1×10^{-3} Pa s
Height	H	50m
Pipe length	L	50m
Pipe Diameter	D_c	0.3 m
Jet outlet diameter	D_{jet}	0.1 m
Convergent (pressure loss coefficient)	K_{conv}	0.5
Elbow (pressure loss coefficient)	K_{coude}	1.13
Tank (pressure loss coefficient)	$K_{reservoir}$	0.5
Pelton turbine diameter	D_r	2m
Pelton turbine Mass	M	5000kg
Friction of pelton turbine	B	22.025×10^{-3} N m s rad^{-1}
Resistance	R_a	$22.3 \times 10^{-3}\ \omega$
Inductance	L_a	0.2×10^{-3} H
Electromotive force constant	k_g	9.5×10^{-3} N m A^{-1}
Load Resistance	R_l	4.498 80 Ω

Table 5.1 – Parameters for the Pelton Turbine Simulation.

In Fig. 5.9, the pressures actuating on the hydraulic part are shown, including the atmospheric pressure.

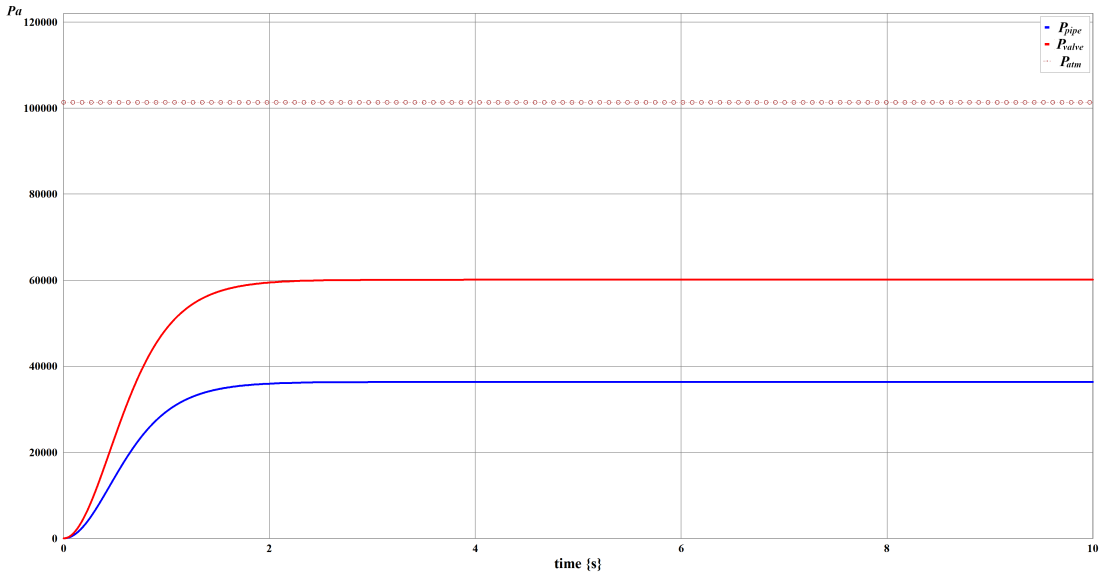

Figure 5.9 – Pressures in the hydraulic part.

The output velocity for the water from the nozzle in presented in the Fig. 5.10.

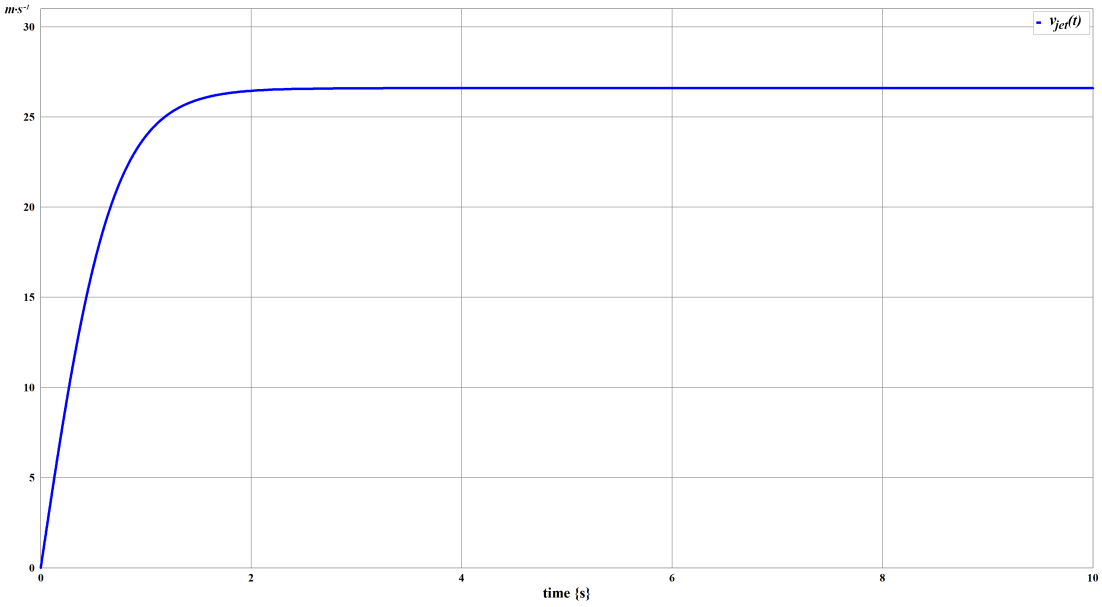

Figure 5.10 – The jet output speed v_{jet}.

When the jet is interacting with the buckets of the Pelton turbine, the angular velocity (ω) is obtained (Fig. 5.11) and the torque of the Pelton turbine is computed (Fig. 5.12).

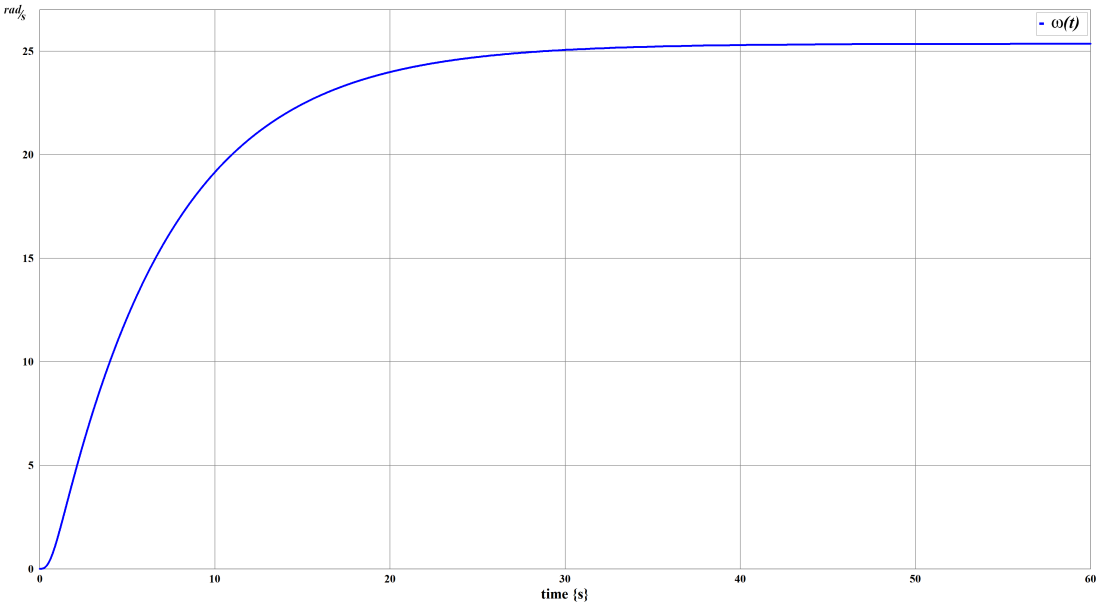

Figure 5.11 – Angular velocity of the Pelton turbine.

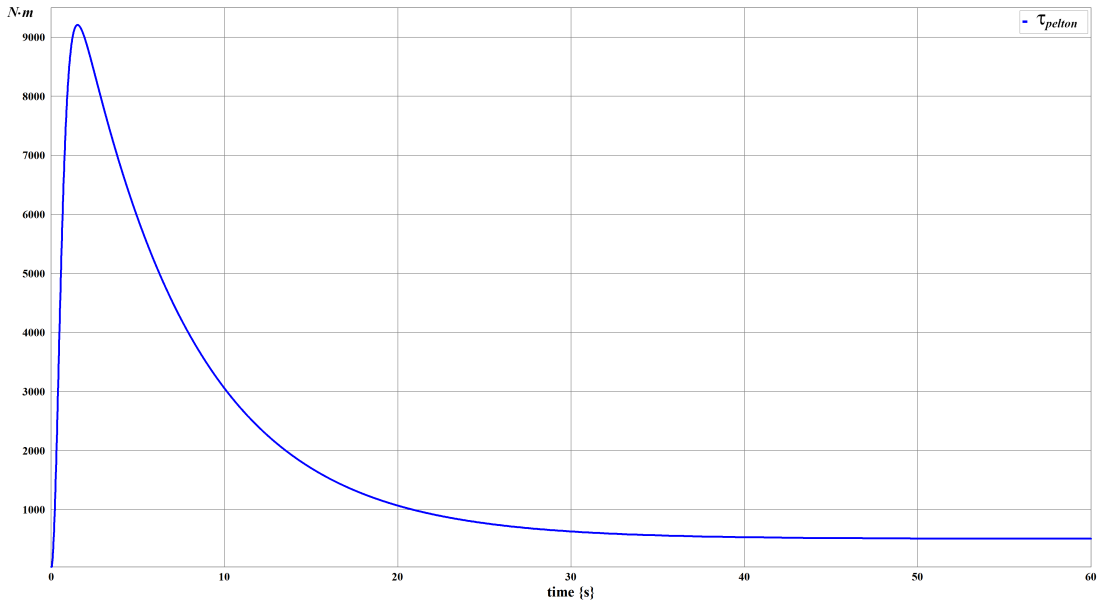

Figure 5.12 – Torque in the mechanical part of Pelton turbine.

The electric variables actuating on the load as voltage and current are shown in Fig. 5.13.

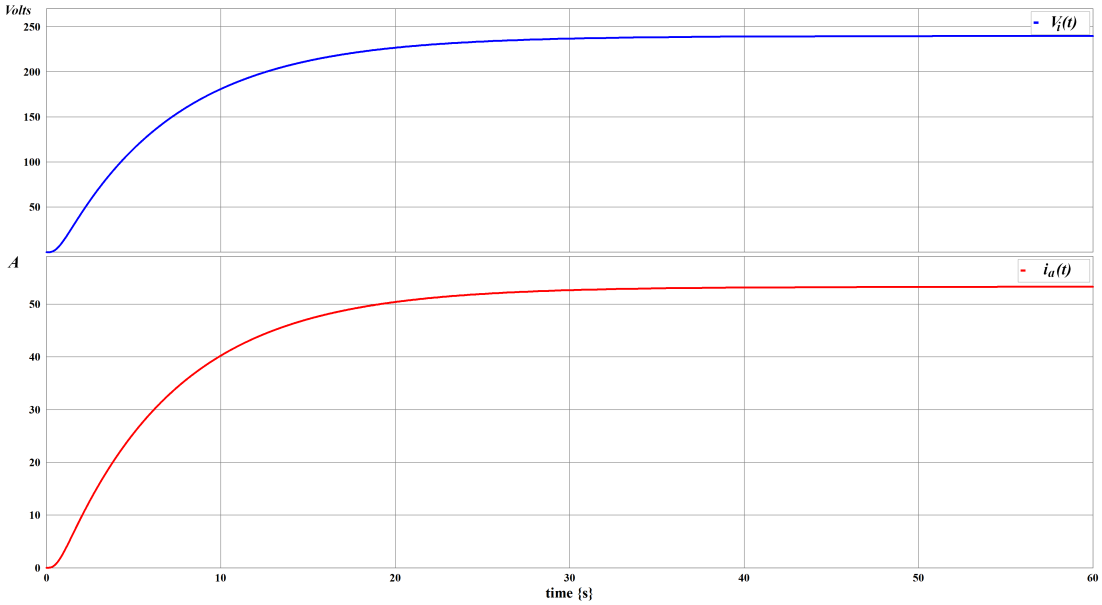

Figure 5.13 – Voltage and current applied to the Load.

5.4 Conclusion

This project is actually in its first version and we implemented simulations from the bond graph model. The project will be developed in a real version, *i.e.*, a real plant application. The different control strategies as those mentioned in this research work could be applied in a next work in order to increase the efficiency of the plant and prevent different perturbations (*e.g.*, pressure losses, frictions, cavitation). Nevertheless, we must first validate the model and simple control strategies. We aim at doing this part during the end of the thesis.

This project also presents the opportunity to apply the control methodology presented in this work with an extension to MIMO non-linear systems.

This model can serve as a basis for studying other renewable energy sources because the structure presented has the possibility to be rewritten easily following the context, as claimed when using an integrated approach.

General Conclusion and Perspectives

This thesis is concerned with aspects involved in designing and implementing controllers and observers for linear systems subject to disturbances. This includes also a comparative study of design methodologies from analysis of the model up to the synthesis of the controller and of the observer as a new approach based on the bond graph representation and on the concept of state variables derivatives. We spoke of Derivative State Feedback and Unknown Input Observer (explicitly based on the state variables derivatives). This conclusion summarizes firstly the research effort presented in the thesis. We thus conclude with some remarks about the use of state variables derivatives and with open questions.

The thesis started with a comparison of three fundamentally different existing methodologies for control systems subject to disturbance, namely PID, state feedback control, and Derivative State Feedback control, all applied to a torsion bar system used as the case study in this thesis. We include some theoretical bases about model properties (finite and infinite structure) that are key aspects when synthesizing the control law in the state space domain. The bond graph model as the control laws are validated in this chapter.

The architecture for the UIO bond graph based is presented in chapter 2. It is one of the main theoretical contributions of the thesis. This UIO is compared with some other well-known observers which for some of them give also very good results, ***but*** the main point, from our point of view, is that the theoretical framework used for our UIO-BG is that it is very close to the framework used for the Disturbance Rejection Problem, from analysis to synthesis. It is based on the structural properties of the bond graph model.

In chapter 3, we compared the performances of three approaches (DOBC, ADRC, DSF-BG) for the Disturbance Rejection Problem on the model of the Torsion Bar system with simulations. We prove the efficiency of the Derivative State Feedback control law and the methodology from analysis to synthesis in order to obtain the control law. We took the opportunity to refine and clarify our framework for the solving the Input-Output Decoupling Problem with a Derivative State Feedback control law type. It is the second theoretical contribution of our work. The potential development of this approach is an interesting issue not only when classical solutions to the Input-Output decoupling problem don't exist, but also in order to solve simultaneously the two problems. Other possibilities like using invariant subspaces defined in the geometric approach could be explored too.

We proved the effectiveness of the Derivative State Feedback control strategy in chapter 4, by applying it from a practical point of view on the real Torsion-Bar system. Results are analysed and compared with the two other control strategies (DOBC and ADRC). One main advantage of the approach is that it can be considered as included in an integrated approach where estimation and control are analysed identically as well as synthesized, graphically, structurally or from a mathematical point of view. Since the unknown variables are perfectly estimated whatever they may be, the UIO could be as well exploited for solving other similar problems, FDI, parameter estimation...

In chapter 5, a hydroelectric power plant is described as a new case study. Some simulations are carried out in order to validate the integrated approach as well as the model. This project is developed in the Fluid Mechanics Laboratory in Ecole Centrale de Lille, and we aim to apply our results step by step on a simplified plant.

To end up, we would aim to prove that the combined proposed DSF-UIO with BG is an innovative solution in the future to facilitate the renewable energy sources integration and to improve their performances. We would aim to highlight two points:

- **Derivative state variables**: Two main statements can be highlighted: firstly, the state variables of a bond graph model are "energy" variables, thus their derivates are power variables that are commonly used as state variables in the literature. Secondly, derivative state variables are estimated from the bond graph model (BG-estimation) without applying any derivation since they are directly measured on the bond graph model. These two points were crucial in our decision to choose this approach.

- **Structural analysis - integrated approach**: From analysis to design, it is possible to extract information from the bond graph model with a structural point of view due to two main features: causality and graphical representation. The bond graph representation allows us to harness the potential of the integrated approach when solving the different problems (Disturbance Rejection and Estimation)

Based on the results obtained in this thesis, the continuing work toward the studied problems in this research area can be described as following:

- **Energy consumption**: In many recent papers, it is claimed that energy consumption is lower when using a Derivative State Feedback control law instead of a classical state feedback control law. We have to check this point. Up to now, it was not possible to bring to light a substantial difference.

- **Impulsive modes**: for each problem, Disturbance Rejection with Derivative State Feedback control law, and Unknown Input Observer-Bond Graph based, the nature of the infinite modes of the Controlled/Observed model must be clarified. As a matter of fact, impulsive modes emerge. Concerning these impulsive modes, from a theoretical point of view, they introduce discontinuity in the state trajectory and thus unbounded values of the control law, [Verghese et al., 1981]. Indeed, an impulsive mode can cause a jump at time $t = 0$ for some state variables and thus impulses for the control law for some initial conditions. Even

if values can change strongly and rapidly, the effectiveness of the approach is proved in this thesis work with application of this control type applied to a real Torsion-Bar system. We agree that a theoretical study of impulsive modes and of its effects with a good framework is essential. It will give as a potential problem for future works.

- **Finite modes**: One challenge is also to clarify the link between the stability property of the controlled/observed system with its finite structure, particularly the link between the set of invariant zeros of the different submodels and the composition of the set of fixed modes associated to the Derivative State Feedback controller/observer. As for the classical problems of Disturbance Rejection and Input-Output decoupling with a state feedback control law, the set of fixed modes is not easy to bring out. We also have to clarify this point, may be with a joint analysis of some invariant subspaces (geometric approach).

Bibliography

[Åmström and Hägglund, 1995] Åmström, K. and Hägglund, T. (1995). *PID Controllers: Theory, Design, and Tuning*. 2nd edition.

[Abdelaziz, 2008] Abdelaziz, T. H. S. (2008). Robust pole assignment for linear time-invariant systems using state-derivative feedback. *Proc. IMechE, Journal of Systems and Control Engineering*, 223:187–199.

[Abdelaziz and Valážek, 2004] Abdelaziz, T. H. S. and Valážek, M. (2004). Pole-placement for SISO linear systems by state-derivative feedback. *IEE Proceedings - Control Theory and Applications*, 151:377–385.

[Abdelaziz and Valážek, 2005] Abdelaziz, T. H. S. and Valážek, M. (2005). Direct algorithm for pole placement by state-derivative feedback for multi-input linear systems - nonsingular case. *Kybernetika*, 41(5):637–660.

[Al-Alaoui, 1993] Al-Alaoui, M. (1993). Novel digital integrator and differentiator. *Electronics Letters*, 29(4):376–378.

[Al-Bayati and Skaf, 2010] Al-Bayati, A. H. and Skaf, Z. (2010). A comparative study of linear observers applied to a dc servo motor. In *Proceedings of the 2010 International Conference on Modelling, Identification and Control*, pages 785–790.

[Albertos et al., 2015] Albertos, P., García, P., Gao, Z., and Liu, T. (2015). Disturbance rejection in process control. *Proceeding of the 11th World Congress on Intelligent Control and Automation, Shenyang, China, June 29 - July 4 2014*.

[Armentano, 1985] Armentano, V. A. (1985). Exact disturbance decoupling by a proportional-derivative state feedback law. In *Proc. of 24th Conference on Decition and Control, Ft. Lauderdale, Florida, U.S.*, pages 533–538.

[Bakhshande and Söffker, 2015] Bakhshande, F. and Söffker, D. (2015). Proportional-integral-observer: A brief survey with special attention to the actual methods using acc benchmark. *IFAC-PapersOnLine*, 48(1):532 – 537. 8th Vienna International Conference on Mathematical Modelling.

[Balakrishnan and Verghese, 2012] Balakrishnan, H. and Verghese, G. C. (2012). 6.02 introduction to eecs ii digital communication systems. *Digital Communication Systems*. OpenCourseWare.

[Baldini et al., 2018] Baldini, A., Felicetti, R., Freddi, A., Longhi, S., and Monteriù, A. (2018). Fault-tolerant disturbance observer based control for altitude and attitude tracking of a quadrotor. In *2018 26th Mediterranean Conference on Control and Automation (MED)*, pages 1–6.

[Bartolini et al., 2000] Bartolini, G., Pisano, A., and Usai, E. (2000). First and second derivative estimation by sliding mode technique. *Journal of Signal Processing*.

[Basile and Marro, 1973] Basile, G. and Marro, G. (1973). A new characterization of some structural properties of linear systems: Unknown-input observability, invertibility and functional controllability. *International Journal of Control*, 17(5):931–943.

[Basile and Marro, 1992] Basile, G. and Marro, G. (1992). *Controlled and Conditioned Invariants in Linear System Theory*. Prentice Hall, Inc.

[Bhattacharyya, 1978] Bhattacharyya, S. P. (1978). Observer design for linear systems with unknown inputs. *IEEE Transactions on Automatic Control*, 23:483–484.

[Bonilla Estrada and Malabre, 2000] Bonilla Estrada, M. and Malabre, M. (2000). Proportional and derivative state-feedback decoupling of linear systems. *IEEE Transactions on Automatic Control*, 45:730–733.

[Borutzky and Dauphin-Tanguy, 2004] Borutzky, W. and Dauphin-Tanguy, G. (2004). Incremental bond graph approach to the derivation of state equations for robustness study. *Simulation Modelling Practice and Theory*, 12:41–60.

[Borutzky and Granda, 2002] Borutzky, W. and Granda, J. (2002). Bond graph based frequency domain sensitivity analysis of multidisciplinary systems. *Proceedings of the Institution of Mechanical Engineers. Part I-Journal of Systems and Control Engineering*, 216:85–99.

[Boukhobza et al., 2007] Boukhobza, T., Hamelin, F., and Martinez-Martinez, S. (2007). State and input observability for structured linear systems: A graph-theoretic approach. *Automatica*, 43:1204–1210.

[Bourlès, 2010] Bourlès, H. (2010). *Linear Systems*. ISTE Ltd and John Wiley & Sons, Inc.

[Bourlès and Marinescu, 2011] Bourlès, H. and Marinescu, B. (2011). *Linear Time-Varying Systems: Algebraic-Analytic Approach*. Springer-Verlag, LNCIS 410.

[Brunovsky, 1970] Brunovsky, P. (1970). A classification for linear controllable systems. *Kybernetika*, 6:173–187.

[Burden and Faires, 2011] Burden, R. L. and Faires, J. D. (2011). *Numerical Analysis*. Richard Stratton, editor, ninth edition. Boston, U.S.

[Burger, 2011] Burger, M. (2011). *Disturbance Rejection using Conditional Integrators*. Thesis for the degree of philosophiae doctor.

[Cardim et al., 2007] Cardim, R., Teixeira, M. C. M., Assunção, E., and Covacic, M. R. (2007). Design of state-derivative feedback controllers using a state feedback control design. In 3rd IFAC Symposium on System Structure and Control, editors, *IFAC Proceedings Volumes*, volume 40, pages 22–27. Elsevier.

[Carlsson et al., 1991] Carlsson, B., Ahlen, A., and Sternad, M. (1991). Optimal differentaition based on stochastic signal models. *IEEE Transactions on Signal Processing*, 39(2):341–353.

[Chang et al., 1991] Chang, F. R., Fang, C. H., and Wang, C. H. (1991). Doubly coprime matrix-fraction representations using proportional and derivative feedback concepts in generalized state-space systems. *IEEE Transactions on Automatic Control*, 36:1193–1195.

[Chen, 1998] Chen, C.-T. (1998). *Linear System Theory and Design*. Oxford University Press, Inc., New York, NY, USA, 3rd edition.

[Chen and Seborg, 2002] Chen, D. and Seborg, D. E. (2002). Pi/pid controller design based on direct synthesis and disturbance rejection. *Industrial and Engineering Chemistry Research*, 41(19):4807–4822.

[Chen et al., 2011] Chen, W., Khan, A., Abid, M., and Ding, S. (2011). Integrated design of observer based fault detection for a class of uncertain nonlinear systems. *Int. J. of Applied Mathematics and Computer Sciences*, 21 (3):423–430.

[Chen et al., 2016] Chen, W., Yang, J., Guo, L., and Li, S. (2016). Disturbance-observer-based control and related methods—an overview. *IEEE Transactions on Industrial Electronics*, 63(2):1083–1095.

[Chen, 2004] Chen, W.-H. (2004). Disturbance observer based control for nonlinear systems. *IEEE/ASME Transactions on Mechatronics*, 9(4):706–710.

[Cheng et al., 2015] Cheng, S., Wei, Y., Liang, S., Zhang, K., and Liang, Q. (2015). Rejection and tracking sinusoidal signals based on state-derivative feedback. In *2015 34th Chinese Control Conference (CCC)*, pages 23–29.

[Chitour, 2002] Chitour, Y. (2002). Time-varying high-gain observers for numerical differentiation. *IEEE Transactions on Automatic Control*, 47(9):1565–1569.

[Cobb, 1984] Cobb, D. (1984). Controllability, observability, and duality in singular systems. *IEEE Transactions on Automatic Control*, 29 (12):1076–1082.

[Cominos and Munro, 2002] Cominos, P. and Munro, N. (2002). PID controllers: recent tunings methods and design to specification. *IEE Proceedings-Control Theory Applications*, 149(1).

[Commault and Dion, 1982] Commault, C. and Dion, J. M. (1982). Structure at infinity of linear multivariable systems : a geometric approach. *IEEE Transactions on Automatic control*, 27:693–696.

[Coob, 1984] Coob, D. (1984). Controllability, observability, and duality in singular systems. *IEEE Transactions on Automatic Control*, vol29:1076–1082.

[Cui et al., 2018] Cui, J., Zeng, S., Ren, Y., Chen, X., and Gao, Z. (2018). On the robustness and reliability in the pose deformation system of mobile robots. *IEEE Access*, 6:29747–29756.

[Daafouz et al., 2006] Daafouz, J., Fliess, M., and Millerioux, G. (2006). Une approche intrinséque des observateurs linéaires à entrées inconnues. *CIFA'2006, Bordeaux, France*.

[Dabroom and Khalil, 1997] Dabroom, A. and Khalil, H. (1997). Numerical differentiation using high-gain observers. In *Proceedings of the 36th IEEE Conference on Decision and Control*, volume 5, pages 4790–4795. San Diego, California USA.

[Dabroom and Khalil, 1999] Dabroom, A. M. and Khalil, H. K. (1999). Discrete-time implementation of high-gain observers for numerical differentiation. *International Journal of Control*, 72(17):1523–1537.

[Darouach, 2009] Darouach, M. (2009). Complements to full order observer design for linear systems with unknown inputs. *Applied Mathematics Letters*, 22:1107–1111.

[Darouach et al., 1994] Darouach, M., Zazadinski, M., and Xu, S. (1994). Full-order observers for linear systems with unknown inputs. *IEEE Transactions on Automatic Control*, 39:606–609.

[Dauphin-Tanguy, 2000] Dauphin-Tanguy, G. (2000). *Les Bond Graphs*. Hermes Science, Paris.

[Descusse and Dion, 1982] Descusse, J. and Dion, J. M. (1982). On the structure at infinity of linear square decoupled systems. *IEEE Transactions on Automatic Control*, 27:971–974.

[Dion and Commault, 1993] Dion, J. and Commault, C. (1993). Feedback decoupling of structured systems. *IEEE Transactions on Automatic Control*, 38:1132–1135.

[Dion and Commault, 1982] Dion, J. M. and Commault, C. (1982). Smith-McMillan factorizations at infinity of rational matrix functions and their control interpretation. *System & Control Letters*, 1:312–320.

[Diop et al., 1994] Diop, S., Grizzle, J., Moraal, P., and Stefanopoulou, A. (1994). Interpolation and numerical differentiation for observer design. In *American Control Conference*, volume 2, pages 1329–1333.

[Djeziri et al., 2006] Djeziri, M. A., Merzouki, R., Ould-Bouamama, B., and Dauphin-Tanguy, G. (2006). Fault detection of backlash phenomenon in mechatronic system with parameter uncertainties using bond graph approach. *International Conference on Mechatronics and Automation*, pages 600–605. Luoyang, China.

[Djeziri et al., 2007] Djeziri, M. A., Merzouki, R., Ould-Bouamama, B., and Dauphin-Tanguy, G. (2007). Bond graph model based for robust fault diagnosis. *Proceedings of the 2007 American Control Conference*, pages 3017–3022. New York, NY, US.

[Duan et al., 2005] Duan, Y. F., Ni, Y. Q., and Ko, J. M. (2005). State-derivative feedback control of cable vibration using semiactive magnetorheological dampers. *Computer-Aided Civil and Infranstructure Engineering*, 20:431–449.

[Edwards and Spurgeon, 1996] Edwards, C. and Spurgeon, S. K. (1996). Robust output tracking using a sliding-mode controller/ observer scheme. *International Journal of Control*, 64(5):967–983.

[Estrada and Malabre, 1997] Estrada, M. B. and Malabre, M. (1997). On the decoupling of linear systems using proportional and derivative state feedback. In *Proceedings of the 36th Conference on Decision and Control, San Diego, CA, US*, pages 1439–1440.

[Fahmy and O'Reilly, 1989] Fahmy, M. M. and O'Reilly, J. (1989). Parametric eigenstructure assignment for continuous-time descriptor systems. *International Journal of Control*, 49(1):129–143.

[Falb and Wolovich, 1967] Falb, P. L. and Wolovich, W. A. (1967). On the decoupling of multivariable systems. *Preprints JACC, Philadelphia*, pages 791–796.

[Fliess, 1990] Fliess, M. (1990). Some basic structural properties of generalized linear systems. *Systems & Control Letters*, 15:391–396.

[Floquet and Barbot, 2006] Floquet, T. and Barbot, J. P. (2006). *Advances in variable structure and sliding mode control*, chapter A canonical form for the design of unknown input sliding mode observers, pages 271–292. Springer.

[Gao, 2014] Gao, Z. (2014). On the centrality of disturbance rejection in automatic control. *ISA Transactions*, 53(4):850 – 857. Disturbance Estimation and Mitigation.

[Gilbert, 1969] Gilbert, E. G. (1969). The decoupling of multivariable systems by state feedback. *SIAM Journal of Control and Optimization*, 7:50–63.

[Glover and Doyle, 1988] Glover, K. and Doyle, J. C. (1988). State-space formulae for all stabilizing controllers that satisfy an h_{inf}-norm bound and relations to relations to risk sensitivity. *Systems & Control Letters*, 11(3):167 – 172.

[Gonzalez et al., 2018] Gonzalez, J., Jimenez, J., and Sueur, C. (2018). Comparison of control strategies for a real bar system in the presence of disturbances: a bond graph approach. In *International Conference on "Bond Graph Modeling" ICBGM'2018*, Bordeaux, France.

[Gonzalez and Sueur, 2018a] Gonzalez, J. and Sueur, C. (2018a). Bond graph approach for disturbance rejection with derivative state feedback. In *11th International Conference on "Integrated Modeling and Analysis in Applied Control and Automation" IMAACA'18, part of I3M'2018 "International Multidisciplinary Modeling and Simulation Multiconference"*, Budapest, Hungary.

[Gonzalez and Sueur, 2017] Gonzalez, J. A. and Sueur, C. (2017). Unknown input observer for `MIMO` systems with stability. In Bruzzone, Dauphin-Tanguy, and Junco, editors, *Proc. of the 10th Int. Conf. IMAACA, Barcelona, Spain*, pages 1–8.

[Gonzalez and Sueur, 2018b] Gonzalez, J. A. and Sueur, C. (2018b). Unknown input observer with stability: A structural analysis approach in bond graph. *European Journal of Control*, 41:25–43.

[Gonzalez, Joel and Sueur, Christophe, 2019] Gonzalez, Joel and Sueur, Christophe (2019). Comparison of disturbance rejection with derivative state feedback and active disturbance rejection control: Case study. In *International Conference on Control, Decision and Information Technologies (CODIT'19)*, Paris, France.

[Griewank and Walther, 2008] Griewank, A. and Walther, A. (2008). *Evaluating Derivatives: Principles and Techniques of Algorithmic Differentiation*. Other Titles in Applied Mathematics. SIAM, second edition. Philadelphia, U.S.

[Guidorzi and Marro, 1971] Guidorzi, R. and Marro, G. (1971). On Wonham stabilizability condition in the synthesis of observers for unknown-input systems. *IEEE Trans. Automat. Control*, 16:499–500.

[Guo and Jin, 2013] Guo, B. and Jin, F. (2013). The active disturbance rejection and sliding mode control approach to the stabilization of the euler–bernoulli beam equation with boundary input disturbance. *Automatica*, 49(9):2911–2918.

[Guo et al., 2016] Guo, B., Wu, Z., and Zhou, H. (2016). Active disturbance rejection control approach to output-feedback stabilization of a class of uncertain nonlinear systems subject to stochastic disturbance. *IEEE Transactions on Automatic Control*, 61(6):1613–1618.

[Guo and Zhao, 2016] Guo, B.-Z. and Zhao, Z. (2016). *Active Disturbance Rejection Control for Nonlinear Systems: An Introduction*. Wiley.

[Habibi et al., 2019] Habibi, H., Howard, I., and Simani, S. (2019). Reliability improvement of wind turbine power generation using model-based fault detection and fault tolerant control: A review. *Renewable Energy*, 135:877 – 896.

[Han, 2009] Han, J. (2009). From pid to active disturbance rejection control. *IEEE Transactions on Industrial Electronics*, 56(3):900–906.

[Hautus, 1979] Hautus, M. L. J. (1979). (A-B)-invariant and stability subspaces: a frequency domain description with applications. *Memorandum COSOR*, 7915. 1979.

[Hautus, 1980] Hautus, M. L. J. (1980). (a,b)-invariant and stability subspaces, a frequency domain description. *Automatica*, 16:703–707.

[Hautus, 1983] Hautus, M. L. J. (1983). Strong detectability and observers. *Linear Algebra and its Applications*, 50:353–368.

[Hidayat et al., 2011] Hidayat, Z., Babuska, R., De Schutter, B., and Núñez, A. (2011). Observers for linear distributed-parameter systems: A survey. In *2011 IEEE International Symposium on Robotic and Sensors Environments (ROSE)*, pages 166–171.

[Hou and Muller, 1992] Hou, M. and Muller, P. (1992). Design of observers for linear systems with unknown inputs. *IEEE Trans. Automat. Control*, 37:871–875.

[Huang and Messner, 1998] Huang, Y. and Messner, W. (1998). A novel disturbance observer design for magnetic hard drive servo system with a rotary actuator. *IEEE Transactions on Magnetics*, 34(4):1892–1894.

[Icart et al., 1989] Icart, S., Lafay, J., and Malabre, M. (1989). A unified study of the fixed modes of systems decoupled via regular static state feedback. *In Proc. Joint Conf: New Trends in System Theory, Genoa - Italy*, Birkhauser, Boston:425–432.

[Idel'cik, 1986] Idel'cik, I. (1986). *Mémento des pertes de charge*. Collection de la Direction des Études et Recherches d'Électricité de France. Eyrolles,EDF.

[IRENA, 2017] IRENA (2017). Rethinking energy 2017: Accelerating the global energy transformation. *The International Renewable Energy Agency - ISBN 978-92-95111-06-6*.

[IRENA, 2019a] IRENA (2019a). Global energy transformation: A roadmap to 2050. *The International Renewable Energy Agency - ISBN 978-92-9260-121-8*.

[IRENA, 2019b] IRENA (2019b). Renewable energy statistics 2019. *The International Renewable Energy Agency - ISBN 978-92-9260-137-9*.

[IRENA, 2019c] IRENA (2019c). Renewable power generation costs in 2018. *The International Renewable Energy Agency - ISBN 978-92-9260-126-3*.

[Ishikawa and Tomizuka, 1998] Ishikawa, J. and Tomizuka, M. (1998). Pivot friction compensation using an accelerometer and a disturbance observer for hard disk drives. *IEEE/ASME Transactions on Mechatronics*, 3(3):194–201.

[Kailath, 1980] Kailath, T. (1980). *Linear Systems*. Prentince Hall, Englewood-Cliff, N.J.

[Kalman et al., 1969] Kalman, R. E., Falb, P. L., and Arbib, M. A. (1969). *Topics in Mathematical System Theory*. McGraw-Hill, New York.

[Kalsi et al., 2010] Kalsi, K., Lian, J., Hui, S., and Zak, S. (2010). Sliding-mode observers for systems with unknown inputs: A high-gain approach. *Automatica*, 46:347–353.

[Kam and Dauphin-Tanguy, 2005] Kam, C. S. and Dauphin-Tanguy, G. (2005). Bond graph models of structured parameter uncertainties. *Journal of the Franklin Institute*, 342:379–399.

[Karnopp, 1979] Karnopp, D. (1979). Bond graphs in control: Physical state variables and observers. *Journal of The Franklin Institute*, 308(3):221–234.

[Karnopp et al., 1975] Karnopp, D. C., Margolis, D. L., and Rosenberg, R. C. (1975). *System dynamics: a unified approach*. A. Wiley - interscience publications. John Wiley & Sons, 2 edition.

[Kawamura et al., 1988] Kawamura, S., Miyazaki, F., and Arimoto, S. (1988). Is a local linear PD feedback control law effective for trajectory tracking of robot motion? In *Proc. 1988 IEEE International Conference on Robotics and Automation.*, pages 1335–1340.

[Kempf and Kobayashi, 1999] Kempf, C. J. and Kobayashi, S. (1999). Disturbance observer and feedforward design for a high-speed direct-drive positioning table. *IEEE Transactions on Control Systems Technology*, 7(5):513–526.

[Kim et al., 2015] Kim, S., Kwon, W., Ban, J., and Won, S. (2015). Decentralized H_∞ control of large-scale descriptor systems using proportional-plus-derivative state feedback. In *15th International Conference on Control, Automation and Systems (ICCAS), Busan, South Korea*, pages 1572–1576.

[Kleijn, 2008] Kleijn, I. C. (2008). *Torsion Bar 1.0 Reference Manual*.

[Kleijn, 2013] Kleijn, I. C. (2013). *20-sim 4C Reference Manual*.

[Korosi and Veselý, 2018] Korosi, L. and Veselý, V. (2018). Novel approach to robust pi controller design with state derivative feedback for linear uncertain systems. In *2018 19th International Carpathian Control Conference (ICCC)*, pages 488–491.

[Koussiouris, 1980] Koussiouris, T. (1980). A frequency domain approach to the block decoupling problem ii: pole assignment while block decoupling a minimal system by state feedback and a non singular input transformation and the observability of the block decoupled system. *Int. Journal of Control*, 32:443–464.

[Krohling, 1997] Krohling, R. (1997). Design of pid controller for disturbance rejection: a genetic optimization approach. In *Second International Conference On Genetic Algorithms In Engineering Systems: Innovations And Applications*, pages 498–503.

[Kudva et al., 1980] Kudva, P., Viswanadham, N., and Ramakrishna, A. (1980). Observers for linear systems with unknown inputs. *IEEE Trans. Automat. Control*, 25:113–115.

[Kwak et al., 2002] Kwak, S.-K., Washington, G., and Yedavalli, R. K. (2002). Acceleration feedback-based active and passive vibration control of landing gear components. *Journal of Aerospace Engineering*, 15:1–9.

[Le, 1992] Le, V. X. (1992). Synthesis of proportional-plus-derivative feedbacks for descriptor systems. *IEEE Transactions on Automatic Control*, 37:672–675.

[Levant, 1998] Levant, A. (1998). Robust exact differentiation via sliding mode technique. *Automatica*, 34(3):379–384.

[Levant, 2003] Levant, A. (2003). Higher order sliding modes, differentiation and output feedback control. *International Journal of Control*, 76(9):924–941.

[Lewis and Symons, 1991] Lewis, F. L. and Symons, V. L. (1991). A geometric theory for derivative feedback. *IEEE Transactions on Automatic Control*, 36:1111–1116.

[Li et al., 2014] Li, S., Yang, J., Chen, W.-H., and Chen, X. (2014). *Disturbance Observer-Based Control: Methods and Applications*. CRC Press, 1st edition edition.

[Luenberger, 1971] Luenberger, D. (1971). An introduction to observers. *IEEE Transactions on Automatic Control*, Vol. AC-16, No. 6:596–602.

[Macfarlane and Karcanias, 1976] Macfarlane, A. G. J. and Karcanias, N. (1976). Poles and zeros of linear multivariable systems: a survey of the algebraic, geometric and complex-variable theory. *International Journal of Control*, 24(1):33–74.

[Malabre and Martínez-García, 1993] Malabre, M. and Martínez-García, J. C. (1993). The modified disturbance rejection problem with stability: A structural approach. *Second European Control Conference, ECC'93, Goningen, The Netherlands*, 2:1119 – 1124.

[Martínez-García et al., 1995] Martínez-García, J. C., Malabre, M., Dion, J.-M., and Commault, C. (1995). Condensed structural solutions to the disturbance rejection and decoupling problems with stability. *3rd European Control Conference, ECC'95, Rome, Italy*, 3b:2545 – 2550.

[Martínez-García et al., 1993] Martínez-García, J. C., Malabre, M., and Rabah, R. (1993). The partial non interacting problem: Structural and geometric solutions. *Kybernetika*, 30(6):645–658.

[Mayr, 1970] Mayr, O. (1970). *The Origins of Feedback Control*. MIT Press, Cambridge, MA, USA.

[Mboup et al., 2007] Mboup, M., Join, C., and Fliess, M. (2007). A revised look at numerical differentiation with an application to nonlinear feedback control. *The 15th Mediterranean Conference on Control and Automation - MED'2007*.

[Mehdi, 2010] Mehdi, D. (2010). *Dérivation numérique: synthèse, application et intégration*. PhD thesis, Ecole Centrale de Lyon.

[Miklosovic and Gao, 2004] Miklosovic, R. and Gao, Z. (2004). A robust two-degree-of-freedom control design technique and its practical application. In *Conference Record of the 2004 IEEE Industry Applications Conference, 2004. 39th IAS Annual Meeting.*, volume 3, pages 1495–1502 vol.3.

[Miller and Mukunden, 1982] Miller, B. J. and Mukunden, R. (1982). On designing reduced-order observers for linear time-invariant systems subject to unknown inputs. *Internat. J. Control*, 35:183–188.

[Mita et al., 1998] Mita, T., Hirata, M., Murata, K., and Zhang, H. (1998). h_∞ control versus disturbance-observer-based control. *IEEE Transactions on Industrial Electronics*, 45(3):488–495.

[Morari and Manfred, 1989] Morari, M. and Manfred, E. (1989). *Robust process control*. Prentice Hall, Englewood Cliffs, New Jersey.

[Moreira et al., 2010] Moreira, M. R., Júnior, E. I. M., Esteves, T. T., Teixeira, M. C. M., Cardim, R., Assunção, E., and Faria, F. A. (2010). Stabilizability and disturbance rejection with state-derivative feedback. *Mathematical Problems in Engineering,Hindawi Publishing Corporation*, 2010:12 pages.

[Morgan, 1964] Morgan, B. (1964). The synthesis of linear multivariable systems by state variable feedback. *Proc.1964 JACC, Stanford, California*, pages 446–465.

[Morse, 1973] Morse, A. S. (1973). Structural invariants of linear multivariable systems. *SIAM J. Control*, 11:446–465.

[Morse and Wonham, 1973] Morse, A. S. and Wonham, W. (1973). Status of noninteracting controls. *IEEE Trans. Auto. Contr.*, AC-11:568–581.

[Niemann et al., 1995] Niemann, H. H., Stoustrup, J., Shafai, B., and Beal, S. (1995). Ltr design of proportional-integral observers. *International Journal of Robust and Non linear Control*, 5:671–693.

[Nikiforuk and Tamura, 1988] Nikiforuk, P. and Tamura, K. (1988). Design of a disturbance accommodating adaptive control system and its application to a dc-servo motor system with coulomb friction. *Journal of Dynamic Systems, Measurement, and Control*, 110 (4):343–349.

[Ortego Sampedro, 2013] Ortego Sampedro, E. (2013). Etude d'un systeme hydropneumatique de stockage d'energie utilisant une pompe/turbine rotodynamique.

[Paynter, 1960] Paynter, H. M. (1960). *Analysis design of engineering systems*. MIT Press, Cambridge, Massachusetts.

[Pei and Shyu, 1989] Pei, S. and Shyu, J. (1989). Design of fir hilbert transformers and differentaitors by eigenfilter. *IEEE Transaction on Acousticc, Speech, and Signal Processing*, Vol. 37(No. 11):pp. 1457–1461.

[Pichardo-Almarza et al., 2005] Pichardo-Almarza, C., Rahmani, A., Dauphin-Tanguy, G., and Delgado, M. (2005). Proportional–integral observer for systems modelled by bond graphs. *Simulation Modelling Practice and Theory*, 13(3):179 – 211.

[Radke and Zhiqiang Gao, 2006] Radke, A. and Zhiqiang Gao (2006). A survey of state and disturbance observers for practitioners. In *2006 American Control Conference*, page 6 pp.

[Ratolojanahary et al., 2019] Ratolojanahary, N., Gonzalez, J., Dupont, P., Lainé, A., Neu, T., Guyomarc'H, D., and Sueur, C. (2019). Approach of dynamic modelling of a hydraulic system. In *Proceedings of 5th International Conference. Which models for extreme situations and crisis management? SimHydro 2019*, Nice, France.

[Reithmeier and Leitmann, 2003] Reithmeier, E. and Leitmann, G. (2003). Robust vibration control of dynamical systems based on the derivative of the state. *Archive of Applied Mechanics*, 72(11):856–864.

[REN21, 2019] REN21 (2019). Renewables 2019 global status report.

[Riachy and Fliess, 2011] Riachy, S. and Fliess, M. (2011). High-order sliding modes and intelligent pid controllers: first steps toward a practical comparison. *IFAC Proceedings*, 44 (1):10982–10987.

[Rosenberg and Karnopp, 1983] Rosenberg, R. and Karnopp, D. (1983). *Introduction to physical system dynamics*. McGraw Hill.

[Rosenbrock, 1970] Rosenbrock, H. (1970). *State space and multivariable theory*. Nelson, London, England.

[Schrader and Sain, 1989] Schrader, C. B. and Sain, M. K. (1989). Research on system zeros: a survey. *International Journal of Control*, 50(4):1407–1433.

[Seshagiri and Khalil, 2005] Seshagiri, S. and Khalil, H. (2005). Robust output feedback regulation of minimum-phase nonlinear systems using conditional integrators. *Automatica*, 41(1):43–54.

[Singh and Khalil, 2005] Singh, A. and Khalil, H. (2005). Regulation of nonlinear systems using conditional integrators. international journal of robust and nonlinear control. *International Journal of Robust and Nonlinear Control*, 15(8):339–362.

[Sueur, 2016] Sueur, C. (2016). Disturbance rejection with derivative state feedback. In *9th International Conference on Integrated Modeling and Analysis in Applied Control and Automation, IMAACA'16, Larnaca, Cyprus*.

[Sueur and Dauphin-Tanguy, 1991] Sueur, C. and Dauphin-Tanguy, G. (1991). Bond-graph approach for structural analysis of MIMO linear systems. *Journal of the Franklin Institute*, 328:55–70.

[Sueur and Dauphin-Tanguy, 1992] Sueur, C. and Dauphin-Tanguy, G. (1992). *Poles and zeros of multivariable linear systems: a bond graph approach.*, pages 211–228. Bond Graph for Engineers (P.C. Breedveld and G. Dauphin-Tanguy) Elsevier Science Publisher B. V.

[Swonder and Swonder, 1971] Swonder, S. C. and Swonder, D. D. (1971). Feedback estimation systems and the separation principle of stochastic control. *IEEE Transactions on Automatic Control*, 16(4):350–354.

[Tang et al., 2018] Tang, T., Niu, S., Chen, X., and Qi, B. (2018). Disturbance observer-based control of tip-tilt mirror for mitigating telescope vibrations. *IEEE Transactions on Instrumentation and Measurement*, pages 1–7.

[Tarasov et al., 2013] Tarasov, E., Gahlouz, I., Sueur, C., and Ould-Bouamama, B. (2013). State and unknown input observer: analysis and design. *7th IMAACA'13, part of 10th I3M2013, Athens, Greece, September 25-27*.

[Tarasov et al., 2014a] Tarasov, E., Sueur, C., and Ould-Bouamama, B. (2014a). UI0 approach for estimation of non linear components behavior. *53rd IEEE Conference on Decision and Control, CDC'14, Los Angeles, California, USA,December 15-17*.

[Tarasov et al., 2014b] Tarasov, E., Sueur, C., Ould-Bouamama, B., and Dauphin-Tanguy, G. (2014b). Flat control of a torsion bar with unknown input estimation. *Multi-Conference on Systems and Control, IEEE MSC'2014, Antibes, France, October 08-10*.

[Tavakoli et al., 2005] Tavakoli, S., Griffin, I., and Fleming, P. J. (2005). Robust pi controller for load disturbance rejection and setpoint regulation. In *Proceedings of 2005 IEEE Conference on Control Applications, 2005. CCA 2005.*, pages 1015–1020.

[Tidke et al., 2018] Tidke, A., Sonawane, P., Savakhande, V. B., Chewale, M. A., and Wanjari, R. A. (2018). Disturbance rejection pid controller optimized using genetic algorithm for time delay systems. In *2018 International Conference on Control, Power, Communication and Computing Technologies (ICCPCCT)*, pages 245–249.

[Tong and Yang, 2011] Tong, S. and Yang, G. (2011). Observer-based fault-tolerant control against sensor failures for fuzzy systems with time delays. *Int. J. of Applied Mathematics and Computer Sciences*, 21 (4):617–628.

[Trentelman et al., 2001] Trentelman, H. L., Stoorvogel, A. A., and Hautus, M. (2001). *Control theory for linear systems*. London, UK: Springer.

[Verghese, 1978] Verghese, G. C. (1978). Infinite frequency behaviour in generalized dynamical systems. *PhD Thesis, Stanford University,*. 1978.

[Verghese and Kailath, 1979] Verghese, G. C. and Kailath, T. (1979). Impulsive behavior in dynamical systems, structure and significance. In *Proc. 4th Int. Symp. Marh. Theory, Networks Syst.*

[Verghese et al., 1981] Verghese, G. C., Levy, B. C., and Kailath, T. (1981). A generalized state-space for singular systems. *IEEE Transactions on Automatic Control*, vol. AC-26:811–831.

[Visioli and Zhong, 2011] Visioli, A. and Zhong, Q.-C. (2011). *Disturbance Observer-based Control*, pages 195–212. Springer London, London.

[Vrančić et al., 2004] Vrančić, D., Strmčnik, S., and Kocijan, J. (2004). Improving disturbance rejection of pi controllers by means of the magnitude optimum method. *ISA Transactions*, 43(1):73 – 84.

[Wang et al., 2018] Wang, B., Shen, Z., Liu, H., and Hu, J. (2018). Linear adrc direct current control of gridconnected inverter with lcl filter for both active damping and grid voltage induced current distortion suppression. *IET Power Electronics*.

[Wang et al., 2017] Wang, C., Quan, L., Zhang, S., Meng, H., and Lan, Y. (2017). Reduced-order model based active disturbance rejection control of hydraulic servo system with singular value perturbation theory. *ISA Transactions*, 67:455 – 465.

[White, 2011] White, F. M. (2011). *Fluid Mechanics*. Mcgraw-Hill series in mechanical engineering, 7th edition.

[Wicher, 2018] Wicher, B. (2018). Adrc load position controller for two mass system with elastic joint and backlash. In *2018 23rd International Conference on Methods Models in Automation Robotics (MMAR)*, pages 333–338.

[Wicher and Nowopolski, 2017] Wicher, B. and Nowopolski, K. (2017). Model of adrc speed control system for complex mechanical object with backlash. In *2017 22nd International Conference on Methods and Models in Automation and Robotics (MMAR)*, pages 379–383.

[WilliamsII and Lawrence, 2007] WilliamsII, R. L. and Lawrence, D. A. (2007). *Linear Space-State Control Systems*. John Wiley and Sons, Inc.

[Wonham, 1985] Wonham, W. M. (1985). *Linear multivariable control : a geometric approach*. Springer Science+Business Media New York, 3rd ed. edition.

[Wonham and Morse, 1970] Wonham, W. M. and Morse, A. (1970). Decoupling and pole assignment in linear multivariable systems: a geometric approach. *SIAM Journal of Control and Optimization*, 8:1–18.

[Xu et al., 2012] Xu, D., Jiang, B., and Shi, P. (2012). Nonlinear actuator fault estimation observer: an inverse system approach via a T – S fuzzy model. *Int. J. Appl. Math. Comput. Sci.*, 22(1):183–196.

[Xue et al., 2015] Xue, W., Bai, W., Yang, S., Song, K., Huang, Y., and Xie, H. (2015). Adrc with adaptive extended state observer and its application to air–fuel ratio control in gasoline engines. *IEEE Transactions on Industrial Electronics*, 62(9):5847–5857.

[Yang et al., 2013] Yang, D., Tarasov, E., Sueur, C., and Ould-Bouamama, B. (2013). New unknown input observer for control design: a bond graph approach. *SSSC-IFAC'2013, Grenoble, France*.

[Yip and Sincovec, 1981] Yip, E. L. and Sincovec, R. F. (1981). Solvability, controllability, and observability of continuous descriptor systems. *IEEE Transactions on Automatic Control*, Vol. 26:702–707.

[Zhang, 2016] Zhang, Z. (2016). *Pelton Turbines*. Springer International Publishing.

[Zhao and Gao, 2010] Zhao, S. and Gao, Z. (2010). An active disturbance rejection based approach to vibration suppression in two-inertia systems. In *Proceedings of the 2010 American Control Conference*, pages 1520–1525.

[Zhao and Guo, 2016] Zhao, Z.-L. and Guo, B.-Z. (2016). Active disturbance rejection control approach to stabilization of lower triangular systems with uncertainty. *International Journal of Robust and Nonlinear Control*, 26(11):2314–2337.

Appendix A

Finite and Infinite Structures

A.1 Finite and infinite structures

Consider an invertible square model $\Sigma(C,A,B,F)$ described by the state space representation (A.1).

$$\begin{cases} \dot{x}(t) = Ax(t) + Bu(t) + Fd(t) \\ y(t) = Cx(t) \end{cases} \tag{A.1}$$

The infinite structure of the multivariable linear model $\Sigma(C,A,B)$ is characterized by different integer sets: $\{n_i'\}$ is the set of infinite zero orders of the global model $\Sigma(C,A,B)$ and $\{n_i\}$ is the set of row infinite zero orders of the row sub-systems $\Sigma(C_i,A,B)$. The infinite structure is well defined in case of LTI models with a transfer matrix representation or with a graphical representation (structured approach). The row infinite zero order n_i verifies condition $n_i = \min\left\{k | C_i A^{(k-1)} B \neq 0\right\}$. n_i is equal to the number of derivations of the output variable $y_i(t)$ necessary for at least one of the input variables to appear explicitly. The global infinite zero orders are equal to the minimal number of derivations of each output variable necessary so that the input variables appear explicitly and independently in the equations. The infinite structure is also pointed out with the Smith-McMillan form at infinity of the transfer matrix [Bourlès, 2010, Dion and Commault, 1982].

A similar study can be proposed for model $\Sigma(C,A,F)$. In order to differentiate the infinite structures of models $\Sigma(C,A,B)$ and $\Sigma(C,A,F)$, the row infinite zero orders of model $\Sigma(C,A,B)$ **will be denoted as** $\{n_{ci}\}$ and the row infinite zero orders of model $\Sigma(C,A,F)$ **will be denoted as** $\{n_{pi}\}$.

The finite structure of a linear model $\Sigma(C,A,B)$ is characterized by different polynomial matrices. The invariant zeros (transmission zeros for controllable/observable models) of model $\Sigma(C,A,B)$ are the zeros of the system matrix defined in equation (A.2). n_{IZ}, the number of invariant zeros of model $\Sigma(C,A,B)$ is equal to $n_{IZ} = n - \Sigma n_{ci}'$. In a similar manner, the finite structure of model $\Sigma(C,A,F)$ can be highlighted.

$$S(s) = \begin{pmatrix} sI - A & -B \\ C & 0 \end{pmatrix} \tag{A.2}$$

System $\Sigma(C,A,B)$ is state controllable iff matrix $[sI - A \ -B]$ does not contain any zero, and observable iff matrix $[sI - A^t \ C^t]^t$ doesn't contain any zero. Otherwise, zeros are called input (output) decoupling zeros (respectively) [Rosenbrock, 1970].

A.2 Finite and infinite structures of bond graph models

Causality and causal paths are useful for the study of properties, such as controllability, observability and systems poles/zeros [Sueur and Dauphin-Tanguy, 1992, Boukhobza et al., 2007]. State space and transfer representations can be directly written from a bond graph model, thus properties of these mathematical representations can be derived before any calculus with a causal analysis. Bond graph models with integral causality assignment (BGI) can be used to determine reachability conditions and the number of invariant zeros by studying the infinite structure. The rank of the controllability matrix is derived from bond graph models with derivative causality (BGD). A Linear Time-Invariant (LTI) Bond Graph (BG) model is controllable if and only if the two following conditions are verified (see [Sueur and Dauphin-Tanguy, 1991]): first, there is a causal path between each dynamical element and one of the input sources and secondly each dynamical element can have a derivative causality assignment in the bond graph model with a preferential derivative causality assignment (with a possible duality of input sources). The observability property can be studied in a similar way, but with output detectors. Systems invariant zeros are poles of inverse systems. Inverse systems can be constructed by bond graph models with bi-causality (BGB) which are thus useful for the determination of invariant zeros. The concept of causal path is used for the study of the infinite structure of the model. The causal path length between an input source and an output detector in the bond graph model is equal to the number of dynamical elements met in the path. Two paths are different if they have no dynamical element in common. The order of the infinite zero n_{ci} for the row sub-system $\Sigma(C_i,A,B)$ is equal to the length of the shortest causal path between the i^{th} output detector y_i and the set of input sources. The global infinite structure is defined with the concepts of different causal paths. The orders of the infinite zeros of a global invertible linear bond graph model are calculated according to equation (A.3), where l_k is the smallest sum of the lengths of the k different input-output causal paths.

$$\begin{cases} n'_{c1} = l_1 \\ n'_{ck} = l_k - l_{k-1} \end{cases} \tag{A.3}$$

The number of invariant zeros is determined by the infinite structure of the Bond Graph model with Integral causality (BGI) model. The number of invariant zeros associated to a controllable, observable, invertible and square bond graph model is equal to $n - \sum n'_{ci}$.

Appendix B

Pole Placement: Unknown Input Observer (UIO)

B.1 Proof of proposition 3: Pole placement for matrix N_{CL_r}

Pole placement for matrix N_{CL_r} is equivalent to pole placement for system $\Sigma(CA^{r-1}, N_{OL})$. The observability property of this system must be studied, and particularly the rank of the observability matrix which is equal to the number of poles which can be assigned. The n rows of the observability matrix of system $\Sigma(CA^{r-1}, N_{OL})$ are

$$CA^{r-1}\ ,\ CA^{r-1}\cdot N_{OL}\ ,\ \cdots\ ,\ CA^{r-1}\cdot N_{OL}^{n-1}\ .$$

Each row is calculated.

$$\begin{array}{l} CA^{r-1} \\ CA^{r-1}(N_{OL}) = (CA^{r-1})(A^{-1} - A^{-1}F(CA^{-1}F)^{-1}CA^{-1}) = CA^{r-2} \\ CA^{r-1}(N_{OL})^2 = CA^{r-3} \\ \quad \vdots \\ CA^{r-1}(N_{OL})^{r-2} = CA \\ CA^{r-1}(N_{OL})^{r-1} = C \\ CA^{r-1}(N_{OL})^{r} = 0 \\ \quad \vdots \\ CA^{r-1}(N_{OL})^{n-1} = 0 \end{array} \tag{B.1}$$

The rank of this observability matrix is r because model $\Sigma(C,A)$ is observable and the non null rows calculated in (B.1) are thus linearly independent. This proved that r poles can be assigned in equation (2.15) and that the observer has $n-r$ fixed poles.

B.2 Proof of proposition 4: Fixed modes of the estimation error, SISO case

First, the observability property of model $\Sigma(CA^{r-1},N_{OL})$ is studied. The non-observable poles are the roots of the invariant polynomials obtained from the Smith Form of matrix $N(s)$ defined in (B.2). With matrix CA^{r-1}, only r modes of matrix N_{OL} can be assigned, because the rank of the observability matrix of system $\Sigma(CA^{r-1},N_{OL})$ is equal to r. The rank of matrix (B.2) is less than r for some values of s, that are the non-observable modes. This rank is equal to r with $s=0$. Thus, the null modes (if any) of $\Sigma(CA^{r-1},N_{OL})$ are observable modes.

$$N(s)=\begin{bmatrix} sI-N_{OL} \\ CA^{r-1} \end{bmatrix} \tag{B.2}$$

The fixed poles of the state estimation error defined in (2.15) are thus the $n-r$ non-observable poles of model $\Sigma(CA^{r-1},N_{OL})$. Now, some equivalent transformations are proposed for the Smith Matrix $S(s)$ of system $\Sigma(C,A,F)$ defined in (B.3).

$$S(s)=\begin{bmatrix} sI-A & -F \\ C & 0 \end{bmatrix} \tag{B.3}$$

$$S(s)\sim\begin{bmatrix} sA^{-1}-I & -A^{-1}F \\ C & 0 \end{bmatrix}\sim\begin{bmatrix} sA^{-1}-I & -A^{-1}F \\ C+sCA^{-1}-C & -CA^{-1}F \end{bmatrix} \tag{B.4}$$

$$\sim\begin{bmatrix} sA^{-1}-I & A^{-1}F(CA^{-1}F)^{-1} \\ sCA^{-1} & I \end{bmatrix} \tag{B.5}$$

$$\sim\begin{bmatrix} sA^{-1}-I-A^{-1}F(CA^{-1}F)^{-1}(-sCA^{-1}) & 0 \\ sCA^{-1} & I \end{bmatrix} \tag{B.6}$$

$$\sim\begin{bmatrix} sN_{OL}-I & 0 \\ 0 & I \end{bmatrix} \tag{B.7}$$

Since $det\,(p_oI-N_{OL})=p_o^n\det\left(I-\frac{N_{OL}}{p_o}\right)$, with $s=\left(\frac{1}{p_o}\right)$ it comes

$$\det(p_oI-N_{OL})=(-1)^n s^{-n}\det(sN_{OL}-I)$$

which is a polynomial of degree n with variable p_o and degree $-n$ with variable s. But, $\det(S(s))$ is a polynomial of degree $n-r$, thus from a simple mathematical analysis it is proved that the polynomial $\det(p_oI-N_{OL})$ has r null roots and that the roots of the polynomial $\det(sN_{OL}-I)$ are the inverse of the non null roots of polynomial $\det(p_oI-N_{OL})$ since $\left(p_o=\frac{1}{s}\right)$. In that case the non null poles of matrix N_{OL} are the inverses of the invariant zeros of model $\Sigma(C,A,F)$.

The non-observable modes of system $\Sigma(CA^{r-1},N_{OL})$ are thus all the inverse of the invariant zeros of system $\Sigma(C,A,F)$. They are the fixed modes of the state estimation error equation.

B.3 Proof proposition 8: fixed modes of the estimation error, non square model

The fixed poles of the state estimation error defined in (2.24) are the non observable poles of model $\Sigma\left(\begin{bmatrix} C_1A^{n_{p1}-1} \\ \bar{C}_1 \end{bmatrix}, N_{OL}\right)$. The non observable poles are the roots of the invariant polynomials obtained from the *Smith form* of matrix $N(s)$ defined in (B.8). With matrix $C_1A^{n_1-1}$, the n_1 null modes of matrix N_{OL} can be assigned (see proof of the SISO case). The goal is to emphasize the number of modes which can be assigned with matrix $\bar{C}_1$.

$$N(s) = \begin{pmatrix} sI - N_{OL} \\ C_1A^{n_{p1}-1} \\ \bar{C}_1 \end{pmatrix} \tag{B.8}$$

Now, some equivalent transformations are proposed for the Smith matrix $S(s)$ of system $\Sigma(C,A,F)$ defined in (B.9).

$$S(s) = \begin{pmatrix} (sI - A) & -F \\ C_1 & 0 \\ \bar{C}_1 & 0 \end{pmatrix} \tag{B.9}$$

$$S(s) \sim \begin{pmatrix} (sA^{-1} - I) & -A^{-1}F \\ C_1 & 0 \\ \bar{C}_1 & 0 \end{pmatrix} \tag{B.10}$$

$$\sim \begin{pmatrix} (sA^{-1} - I) & -A^{-1}F \\ C_1 + (sC_1A^{-1} - C_1) & -C_1A^{-1}F \\ \bar{C}_1 & 0 \end{pmatrix} \tag{B.11}$$

$$\sim \begin{pmatrix} (sA^{-1} - I) & A^{-1}F\left[C_1A^{-1}F\right]^{-1} \\ sC_1A^{-1} & I \\ \bar{C}_1 & 0 \end{pmatrix} \tag{B.12}$$

$$\sim \begin{pmatrix} (sA^{-1} - I) - A^{-1}F\left[C_1A^{-1}F\right]^{-1} - sC_1A^{-1} & 0 \\ sC_1A^{-1} & I \\ \bar{C}_1 & 0 \end{pmatrix} \tag{B.13}$$

$$\sim \begin{pmatrix} sN_{OL} - I & 0 \\ 0 & I \\ \bar{C}_1 & 0 \end{pmatrix} \sim \begin{pmatrix} sN_{OL} - I & 0 \\ \bar{C}_1 & 0 \\ 0 & I \end{pmatrix} \tag{B.14}$$

The roots of $det(sN_{OL} - I)$ are the $n - n_{p1}$ inverse of the non null poles of matrix N_{OL}. From equations (B.9) and (B.14), the non observable modes of $\Sigma(\bar{C}_1, N_{OL})$ are thus all the inverse of the invariant zeros of system $\Sigma(C,A,F)$. Since only the null poles of matrix N_{OL} can be placed

with matrix $C_1A^{n_{p1}-1}$, the non observable poles of system $\Sigma\left(\left[\begin{array}{c} C_1A^{n_{p1}-1} \\ \bar{C}_1 \end{array}\right], N_{OL}\right)$ are thus the inverse of the invariant zeros of $\Sigma(C,A,F)$. They are the fixed modes of the state estimation error equation.

B.4 Proof proposition 9: Necessary Condition for Pole Placement, MIMO case with $p = q = 2$

Consider the matrix product,

$$N_{CL} \cdot F = \left(A^{-1} - A^{-1}F\left(CA^{-1}F\right)^{-1}CA^{-1}\right)F - K\left[\begin{array}{c} C_1A^{n_{p1}-1} \\ C_2A^{n_{p2}-1} \end{array}\right]F = -K\Omega\ .$$

Suppose that matrix Ω which is equivalent to a decoupling matrix in control theory, is not invertible. in that case, $\{n_{p1}, n_{p2}\} \neq \{n'_{p1}, n'_{p2}\}$, *i.e.*, the row infinite structure of system $\Sigma(C,A,F)$ is different of its global infinite structure. The rank of matrix $N_{CL} \cdot F$ is equal to 1, thus matrix N_{CL} is not invertible and the observer cannot be synthesized.

B.5 Proof proposition 10 and 11: Fixed Poles for the MIMO case, with $p = q = 2$

Matrix N_{CL} in this MIMO square problem is written as

$$N_{CL} = A^{-1} - A^{-1}F(CA^{-1}F)^{-1}CA^{-1} - K\left[\begin{array}{c} C_1A^{n_{p1}-1} \\ C_2A^{n_{p2}-1} \end{array}\right].$$

Pole placement is thus studied with the observability property of system $\Sigma\left(\left[\begin{array}{c} C_1A^{n_{p1}-1} \\ C_2A^{n_{p2}-1} \end{array}\right], N_{OL}\right)$. The rows of the observability matrix of this system are calculated, firstly with the row matrix $C_1A^{n_{p1}-1}$.

$$\begin{array}{l} C_1A^{n_{p1}-1} \\ C_1A^{n_{p1}-1}N_{OL} = C_1A^{n_{p1}-1}(A^{-1} - A^{-1}F(CA^{-1}F)^{-1}CA^{-1}) = C_1A^{n_{p1}-2} \\ C_1A^{n_{p1}-1}(N_{OL})^2 = C_1A^{n_{p1}-3} \\ \vdots \\ C_1A^{n_{p1}-1}(N_{OL})^{n_{p1}-2} = C_1A \\ C_1A^{n_{p1}-1}(N_{OL})^{n_{p1}-1} = C_1 \\ C_1A^{n_{p1}-1}(N_{OL})^{n_{p1}} = 0 \\ \vdots \\ C_1A^{n_{p1}-1}(N_{OL})^{n-1} = 0 \end{array} \qquad \text{(B.15)}$$

The same result is obtained with the row matrix $C_2A^{n_{p2}-1}$, and the non null rows of the observability matrix of system $\Sigma\left(\begin{bmatrix} C_1A^{n_{p1}-1} \\ C_2A^{n_{p2}-1} \end{bmatrix}, N_{OL}\right)$ are thus:

$$[C_1^t, (C_1A)^t, \cdots, (C_1A^{n_{p1}-1})^t, C_2^t, (C_2A)^t, \cdots, (C_2A^{n_{p2}-1})^t]^t \ .$$

The *Rank* of this matrix is equal to $n_{p1}+n_{p2}$ because model $\Sigma(C,A,F)$ is observable and for each output variable, the observability index is greater or equal to the row infinite zero order. The non null rows of the observability matrix of system $\Sigma\left(\begin{bmatrix} C_1A^{n_{p1}-1} \\ C_2A^{n_{p2}-1} \end{bmatrix}, N_{OL}\right)$ are thus one part of the independent rows of the observability matrix of system $\Sigma(C,A)$.

B.6 Proof proposition 13: Fixed Poles for the MIMO case, with a null invariant zero

Matrix N_{CL} in this MIMO problem is in equation (2.35). Pole placement is studied with the observability property of system $\Sigma\left(\begin{bmatrix} C_1A^{n_{p1}-1} \\ C_2A^{n_{p2}-1} \end{bmatrix}, N_{OL}\right)$, because the number of modes which can be assigned is equal to the rank of this observability matrix. The rows of the observability matrix of this system are calculated, firstly with the row matrix $C_1A^{n_{p1}-1}$ associated with the null invariant zero, then with matrix matrix $C_2A^{n_{p2}-1}$.

$$\begin{array}{ll}
C_1A^{n_{p1}-1} & \\
C_1A^{n_{p1}-1} & N_{OL} = C_1A^{n_{p1}-1}\left(A^{-1} - A^{-1}F\begin{bmatrix} C_1A^{-2}F \\ C_2A^{-1}F \end{bmatrix}^{-1}\begin{bmatrix} C_1A^{-2} \\ C_2A^{-1} \end{bmatrix}\right) = C_1A^{n_{p1}-2} \\
C_1A^{n_1-1} & (N_{OL})^2 = C_1A^{(n_{p1}-3)} \\
\vdots & \\
C_1A^{n_{p1}-1} & (N_{OL})^{n_{p1}-2} = C_1A \\
C_1A^{n_{p1}-1} & (N_{OL})^{n_{p1}-1} = C_1 \\
C_1A^{n_{p1}-1} & (N_{OL})^{n_{p1}} = C_1A^{-1} \\
C_1A^{n_{p1}-1} & (N_{OL})^{n_{p1}+1} = 0 \\
\vdots & \\
C_1A^{n_{p1}-1} & (N_{OL})^{n-1} = 0
\end{array} \tag{B.16}$$

A similar result is obtained for the row matrix $C_2A^{n_{p2}-1}$, but the expression $C_2A^{n_{p2}-1}(N_{OL})^{n_{p2}} = 0$. Therefore, the non null rows of the observability matrix of system $\Sigma\left(\begin{bmatrix} C_1A^{n_{p1}-1} \\ C_2A^{n_{p2}-1} \end{bmatrix}, N_{OL}\right)$ are thus:

$$[(C_1A^{-1})^t, C_1^t, (C_1A)^t, \cdots, (C_1A^{n_{p1}-1})^t, C_2^t, (C_2A)^t, \cdots, (C_2A^{n_{p2}-1})^t]^t \ .$$

The rank of this matrix is equal to $n_{p1}+n_{p2}+1$ because model $\Sigma(C,A,F)$ is observable and for each output variable, the observability index is greater or equal to the row infinite zero order. The non null rows of the observability matrix of system $\Sigma\left(\begin{bmatrix} C_1A^{n_{p1}-1} \\ C_2A^{n_{p2}-1} \end{bmatrix}, N_{OL}\right)$ are thus one part of the independent rows of the observability matrix of system $\Sigma(C,A)$. This rank can also be studied with the invariant subspaces defined in the geometric approach.

Contents

ESTIMATION AND CONTROL OF DYNAMICAL SYSTEMS WITH UNKNOWN INPUTS TOWARD RENEWABLE SOURCES

Abstract

Nowadays, industrial processes must be efficient, particularly at the production level and/or energy consumption.
This research work aims at improving the process efficiency by analysing the influences of disturbances on their behaviour, from the conception phase to the synthesis of controller/observer, in an integrated approach.
The disturbance rejection problem is first introduced as well as different control laws allowing attenuate/reject these disturbances. The Torsion-Bar (T-B) system is presented. It will be used as case study all along this research work. A control law based on the concept of derivative state variable is presented and validated while applied as disturbance rejection on the T-B system.
In order to reject the disturbance, different physical variables must be estimated, such as state variables, derivative state variables as disturbance variables. An unknown input observer based on the bond graph representation is recalled and extended in the multivariable case. It is the first theoretical contribution of this work. As for the synthesis of control laws, an integrated approach is developed.
We thus compare the efficiency of different so-called « modern control laws » for the disturbance rejection problems by simulation with the T-B system example. We analyse the efficiency of our approach. One extension to the Input-Output decoupling problem allows us to extend the disturbance rejection problem to other control law type in an integrated approach. At least, these techniques are applied on the real T-B system and compared. We validate our approach.
Since this work aims at analysing and developing efficient control laws for industrial processes, a simplified model of a hydroelectric plant is developed, in order to apply our results. A simplified bond graph model is validated with simulations. It will be used as a basis for the control of a plant. We are working with researchers of the fluid mechanic lab for developing a first plant.

Keywords: disturbance rejection, bond graph, derivative state feedback, unknown input observer, pole placement, structural approach, torsion-bar system, pelton turbine.

ESTIMATION ET CONTRÔLE DES SYSTÈMES DYNAMIQUES À ENTRÉES INCONNUES ET ENERGIES RENOUVELABLES

Résumé

De nos jours, les processus industriels se doivent d'être efficaces, en particulier au niveau de leur production et/ou consommation énergétique.
Ce travail de recherche vise à améliorer l'efficacité des processus en analysant l'influence des perturbations sur leur comportement, de la phase de conception à la synthèse des contrôleurs/observateurs, ceci dans une approche intégrée.
Le problème du Rejet de Perturbation est d'abord introduit ainsi que différents types de contrôles permettant d'atténuer et/ou rejeter ces perturbations. Le système de Barre de Torsion est présenté. Il va servir de cas d'étude tout au long du travail de recherche. Une loi de commande basée sur le concept d'état dérivé est présentée et ensuite validée avec comme application le rejet de perturbation appliqué à la barre de torsion.
Afin d'effectuer le rejet de perturbation, il est nécessaire d'estimer les grandeurs physiques utilisées dans les différentes expressions de loi de commande, en particulier les variables d'état, leurs dérivées ainsi que les variables de perturbation. Un observateur à entrées inconnues basé sur la représentation Bond Graph est rappelé et ensuite étendu au cas multi-variable. C'est la première contribution théorique de ce travail de recherche. Une démarche intégrée est proposée, semblable à celle exploitée pour la synthèse de lois de commande.
Nous comparons ensuite l'efficacité de différentes techniques de commandes dites « modernes » pour le rejet de perturbation par simulation sur le système barre de torsion et analysons ainsi l'efficacité de la technique proposée. Une extension théorique au problème du découplage entrée-sortie nous permet de généraliser le problème du rejet de perturbation à d'autres types de contrôle dans une même démarche intégrée d'analyse et de synthèse. Enfin, ces techniques sont exploitées et analysées sur le système réel. Nous validons ainsi expérimentalement nos résultats.

Comme ce travail vise à analyser et développer des techniques performantes de commande pour les processus industriels, un modèle très simplifié de centrale hydroélectrique est développé afin d'appliquer les résultats de nos travaux. Un modèle Bond Graph simplifié est validé par simulation. Il va servir de base pour le pilotage d'une centrale. Une première expérimentation est en cours avec des chercheurs du laboratoire de mécanique des fluides.

Mots clés : rejet de perturbations, bond graph, retour d'état dérivé, observateur à entrées inconnues, placement de pôles, approche structurelle, système de barre de torsion, turbine pelton.

Centre de Recherche en Informatique, Signal et Automatique de Lille
Université Lille 1 – Bâtiment M3 extension – Avenue Carl Gauss – 59655 Villeneuve-D'Ascq Cedex – FRANCE –